Design Decision Making for Market Systems and Environmental Policy with Vehicle Design Applications

Ching-Shin Shiau

Submitted in Partial Fulfillment of the Requirements for
the Degree of
Doctor of Philosophy

in

Mechanical Engineering

Carnegie Mellon University
Pittsburgh, Pennsylvania

May 2010

ACKNOWLEDGEMENTS

I feel that my PhD study was a long but also short journey. I feel it was long because the whole process took years' dedication. I feel it was short because the first day I arrived in Pittsburgh and got lost was just like yesterday.

This dissertation could not be completed without the support and advice from many people. This first on my thank list is my advisor, Jeremy Michalek, and committee members, Chris Hendrickson, Jonathan Cagan and Baohong Sun. I want to thank Jeremy for offering me this unique research opportunity and for his continuous guidance in the past years. It has been a lot of fun doing research and exploring new problems together. I would like to thank Chris for generously sharing his insight and knowledge. Chris is also the person pointing me the most important thing to do when sometimes I get entangled in my multi-tasking. I would like to thank Jon for asking big picture questions to my research, which makes me re-think about the implications of the study. I would like to thank Baohong for her crucial suggestions about market modeling and demand estimation from a marketing researcher's perspective. I am truly grateful for their help and comments.

I want to thank the faculty and students in the CMU Green Design Institute, MUSES Project Group and xEV Group: Lester Lave, Jay Apt, Mike Griffin, Scott Matthew, Jay Whitacre, Chris Weber, Costa Samaras, Paulina Jaramillo, Matthew Kocoloski, Christine Costello and Scott Peterson. I have had the benefits from the discussions and knowledge sharing in the meetings. I want to thank the members in Design Decisions Laboratory: Surya, Aida, Nikhil, Elizabeth, Orkun, Varun and Camilo, the members in Professor Cagan's group: Seth, Ian, Lindsay and Kate, and the members in Professor McGaughey's group: Eric, Ming Young and John. These years that we worked under the same roof of Hamerschlag Hall were wonderful.

I want to thank my beloved wife Hsiao-Tzu (Lisa). Without her encouragement and support, I would never come to the U.S. to pursue my degree. Finally, I want to gratefully thank my family – my parents, my parents-in-law, my brother-in-law Hsiao-Tang (Stephen), my sister I-Ling and my brother Nai-Jen. Though they are thousands miles away, they have been the best support in my life.

This research was supported in part by the National Science Foundation Material Use, Science, Engineering and Society (MUSES) program, the National Science Foundation CAREER Award, the CMU CIT Dean Fellowship, the Liang Ji-Dian Fellowship, and grants from Ford Motor Company and Toyota Motor Corporation. The supports from these programs and organizations are acknowledged.

ABSTRACT

DESIGN DECISION MAKING FOR MARKET SYSTEMS AND ENVIRONMENTAL POLICY WITH VEHICLE DESIGN APPLICATIONS

by

Ching-Shin Shiau

Chair: Jeremy J. Michalek

The goal of design decision making is to create products to satisfy functional requirements and meet consumer preferences in order to succeed in the marketplace. Using only engineering objectives and constraints may be insufficient to fully describe product performance as market and social objectives are involved in design decisions. This dissertation attempts to address three broad questions at the interface of engineering design, market systems, and public policy in an effort to provide insight for designers, consumers, and policy-makers.

The first question, "*How does market competition affect product design decisions?*" is addressed in a game-theoretic framework. Methodology is proposed to account for competitor price reactions to a new product entrant, and the study results indicate that ignoring competitors' pricing reactions can cause profit overestimation and impede the market performance of a new product design. Furthermore, mathematical analysis shows that consumer preference heterogeneity as a critical factor coupling engineering design and strategic market planning under long-run design competition.

The second question, "*What are the economic and environmental implications of plug-in hybrid electric vehicles (PHEVs)?*" is addressed through vehicle performance simulation, driver

behavior characterization, and life cycle assessment. The results indicate charging between distances matters – PHEVs with small battery packs and short electric travel distances can outperform ordinary hybrid vehicles and large PHEVs if drivers charge frequently. PHEV design and allocation for various social objectives, including minimum petroleum consumption, life cycle costs and greenhouse gas emissions, are analyzed using an optimization framework. The study suggests that alternative PHEV designs are needed for different social targets, carbon allowance policy may have marginal impact to PHEV design under current US grid mix, and the subsidy on battery capacity can be less effective than that on all-electric range because recently developed battery technology allows maximum energy use in the batteries.

The third question addressed is "*How does public policy affect vehicle design in a competitive market?*" A model integrating vehicle design, oligopolistic market competition, and Corporative Average Fuel Economy (CAFE) regulations is presented to analyze automakers' design decisions. A distinctive pattern is identified in firms' vehicle design responses to fuel economy standards at market equilibrium. The results imply that automakers may fail to improve their vehicle fuel economy when a high CAFE standard is imposed. Through a case study of powertrain design incorporating the estimates of recent automotive market data and fuel-efficiency technology options, it is shown that fuel economy design responses are more sensitive to gasoline prices than CAFE policy.

TABLE OF CONTENTS

LIST OF TABLES

LIST OF FIGURES

LIST OF ABBREVIATIONS

AARA	American Recovery and Reinvestment Act of 2009
AER	All Electric Range
BTS	Bureau of Transportation Statistics
CAFE	Corporate Average Fuel Economy
CARB	California Air Resources Board
CV	Conventional Vehicle
DOD	Battery Depth of Discharge
DOE	US Department of Energy
DOT	US Department of Transportation
EIA	US Energy Information Administration
EISA	Energy Independence and Security Act of 2007
EPA	US Environmental Protection Agency
EPCA	Energy Policy and Conservation Act of 1975
EPRI	Electric Power Research Institute
FOC	First-Order Condition
GHG	Greenhouse Gas
HEV	Hybrid Electrical Vehicle
HWFET	EPA Highway Fuel Economy Test
IIA	Independence from Irrelevant Alternatives
IID	Independent and Identically-Distributed
KKT	Karush-Kuhn-Tucker condition
LCA	Life Cycle Assessment
MINLP	Mixed-Integer Nonlinear Programming
MPEC	Mathematical Programs with Equilibrium Constraints
MPG	Miles Per Gallon
NHTS	National Household Travel Survey
NHTSA	National Highway Traffic Safety Administration
NLP	Nonlinear Programming
PHEV	Plug-in Hybrid Electrical Vehicle
PSAT	Powertrain System Analysis Toolkit
SOC	Battery State of Charge
UDDS	EPA Urban Dynamometer Driving Schedule
VMT	Vehicle Mileage Travelled

CHAPTER 1. INTRODUCTION

1.1 Background

Design decision making is a complex task, especially when multiple stakeholders' concerns are involved. Designers have to go beyond engineering focus and consider other disciplines to meet different stakeholders' demand and requirements. For example, the result of vehicle design decisions is a combination of performance requirements, consumer preferences, and governmental regulations. In order to avoid suboptimal decisions and make products succeed in the market, integrated studies to examine the implications across design, market and policy domains are needed.

The research scope of this dissertation is illustrated in Figure 1.1, where the three circles represent the fundamental research regions: (1) product design, (2) market systems, and (3) public policy. This study focuses at the interfaces of the three regions, and the goal of this study is to characterize the influence of market factors and governmental policy to product design decisions and examine the potential implications. The three textboxes connecting to the crossover areas I, II and III in Figure 1.1 define the primary research topics in this thesis. The section and chapter numbers indicate where the research questions and answers are proposed.

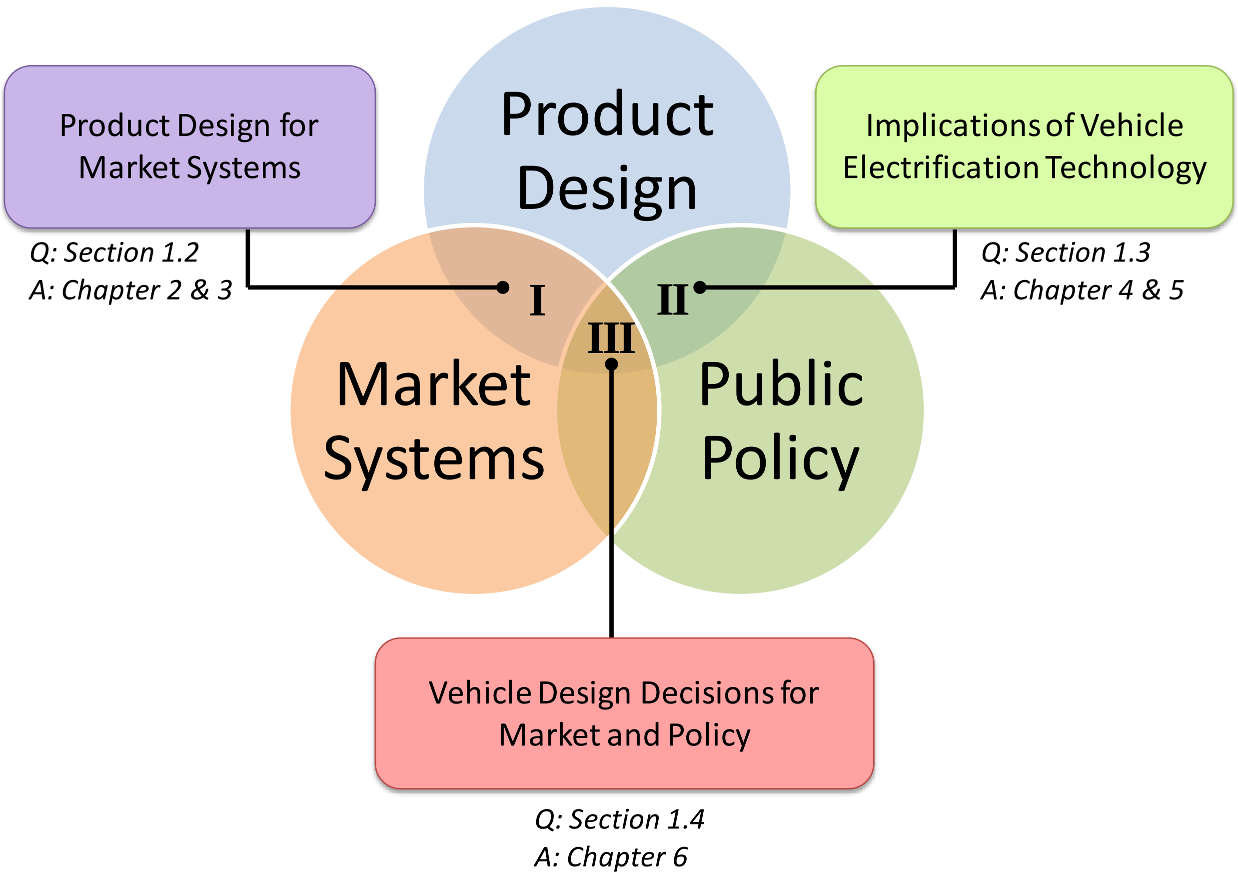

Figure 1.1 Overview of dissertation research scope

Area I is the crossover between product design and market systems. Research in this region generally focuses how various market factors affect product profitability and design decisions. This research category is defined as *Product Design for Market Systems* (Michalek, 2008). This dissertation concentrates on analyzing the influence of demand modeling and market competition to design decisions. The motivation and the corresponding research question are presented in Section 1.2.

Area II is the crossover between product design and policy. The particular research topic defined in this dissertation is *Implications of Vehicle Electrification Technology*, and the goal is to evaluate the potential benefits of electrified vehicles and bring useful suggestions to designers and policy makers. More specifically, this dissertation focuses on the economic and environmental assessment of plug-in hybrid vehicle technology. The research scope and question are detailed in Section 1.3.

Area III is the crossover of design, market and policy. The specific research topic defined for this section is *Vehicle Design Decisions for Market and Policy*. Under this broad scope, this dissertation confines the research direction to a problem of vehicle powertrain design, oligopolistic competition and fuel efficiency standards, and the research statement is elaborated in Section 1.4.

Research in the overlapping area between market systems and public policy can be found in the economic and policy literature, where the main focus is to obtain policy implications by conducting economic or econometric analyses, such as regression model, market simulation, etc. These studies usually do not have direct implications about product design, but they provide the useful fundamentals for connecting design, market and policy systems.

1.2 Product Design for Market Systems

The goal of design for market systems is to integrate social and economic science into product design processes and help designers make successful design decisions in the marketplace (Michalek, 2008). One key market aspect considered by designers in their decision making is consumer preference (Michalek, 2005). In the perspective of design theory and methodology, researchers have developed various tools, such as Quality Function Deployment (QFD) and Value Opportunity Analysis (VOA), to evaluate design concepts on customer requirements and engineering performance (Ullman, 1992; Cagan and Vogel, 2002; Dieter and Schmidt, 2008). In perspective of design automation, many studies to integrate quantitative demand model into design decision making have been conducted (Wassenaar and Chen, 2003; Luo et al., 2005;

Michalek et al., 2005; Wassenaar et al., 2005; Besharati et al., 2006; Lewis et al., 2006; Michalek et al., 2006; Williams et al., 2008; Orsborn et al., 2009). These works provide methodologies for designers to integrate consumer preference components into their product design decisions. Compared to above studies, this dissertation has an alternative focus - market competition. It is another crucial market factor that can affect product design, but has been limitedly discussed in the design community. This leads to the first research question in this thesis:

How does market competition affect product design decisions?

Two types of market competition, *short-run* and *long-run* competition, are distinguished by their definitions in economics. Table 1.1 shows the assumptions for the two competition types with regard to commodity and differentiated products. For commodities, firms compete on price or quantity because product attribute is essentially homogenous. The short-run commodity competition assumes that production technology is not changed in a relative short period of time, and marginal cost is fixed. In contrast, the long-run commodity competition accounts for firms' production technology changes over a longer timeframe, and thus lower marginal costs can occur (Stockman, 1996). For differentiated products, they compete not only on prices but also characteristics (product attributes). It is known that market competition can increase the firms' incentives to differentiate their product for avoiding pure price competition (Berry, 1992; Mazzeo, 2002). Differentiating product features through design decisions is what designers most concern, and therefore this study concentrates on the competition of differentiated products.

Table 1.1 Definitions for short- and long-run market competition

	Commodity	**Differentiated Product**
Short-Run	No change in production technology	**Price Competition** Competitors change prices only but no design and technology changes occur
Long-Run	New production technology occurs	**Design and Price Competition** Product price, design and technology changes occur in the market

The distinction between short- and long-run competition of differentiated product can be recognized by the occurrence of design and technology changes, as shown in Table 1.1. The technology change here may include innovative engineering design for creating new product features and new production technology for unit cost reduction. Within the scope of differentiated product competition, three classes are further defined: (1) Class I: design with no market competition – competitors are assumed fixed or nonexistent; (2) Class II: design with short-run competition – the design attributes of competitor products are fixed, but that competitors will adjust prices in response to a new entrant; (3) Class III: design with long-run competition – this scenario represents competition over a sufficiently long time period that all firms in the market are able to redesign their products as well as set new prices competitively. The flows of design decision, market reaction, and market outcome of these three classes are illustrated in Figure 1.2.

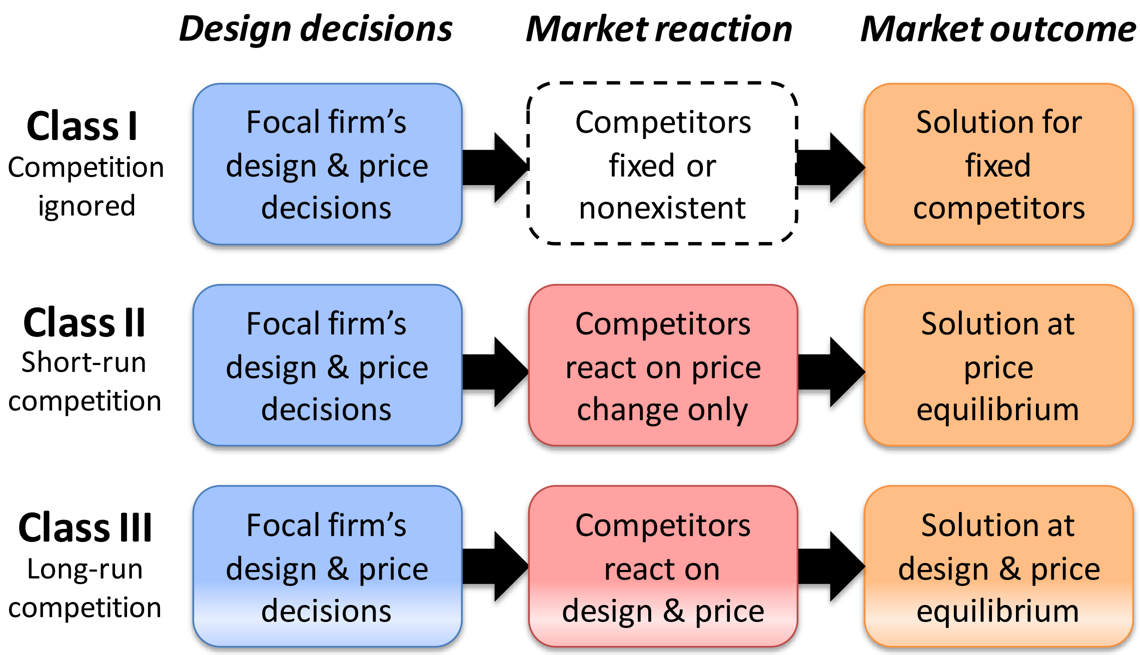

Figure 1.2 Classifications of design problems with differentiated product competition

While most design research in the literature belong to Class I (competition ignored), this study focuses on the Class II and III problems because market competition might affect product performance in the marketplace and thus product design decisions. In Chapter 2, an efficient optimization approach to solve Class II problems is proposed, and multiple case studies are solved using the method for demonstration. In Chapter 3, an investigation is carried out to examine the influence of consumer preference heterogeneity and channel structure in Class III design problems.

The study results show that market competition can affect optimal product design decisions. Specifically, traditional optimization approaches ignoring market competition could result in profit overestimation and deter the market performance of the product optimized. The study also demonstrates that modeling consumer heterogeneity is critical in a product design problem of long-run product competition – treating consumer taste variations as negligible noise makes design decisions disengaged from market systems. In addition to these findings, the solution approaches presented in the two chapters provide useful tools for designers to perform product design optimization with accounting for competitors' pricing reactions in the market.

1.3 Implications of Vehicle Electrification Technology

Developing new vehicle technology is automobile industry's response to consumer preferences (e.g. fuel economy and safety) and public concerns (e.g. foreign oil dependency and global warming) (MacLean and Lave, 2003). Among several potential vehicle technologies to address the above issues, plug-in hybrid electric vehicles (PHEVs) have been considered as a promisingly near-term approach to reduce lifecycle greenhouse gas (GHG) emissions and petroleum consumption in the U.S. transportation sector. A PHEV functions by using large rechargeable storage batteries that utilize electricity from the electrical grid and provide a portion of the propulsion energy (Romm, 2006; EPRI, 2007; Samaras and Meisterling, 2008; Bradley and Frank, 2009). Since approximately 60% of U.S. passenger vehicle miles are traveled by vehicles driving less than 30 miles per day (BTS, 2003), PHEVs may be able to displace a large portion of gasoline consumption with electricity. Several automobile manufacturers have announced plans to produce PHEVs commercially in the future, including General Motors' Chevrolet Volt (Bunkley, 2008) and Toyota's plug-in version of the Prius (Toyota, 2009). However, many factors may affect the potential benefits of PHEVs, such as battery technology (Duvall, 2004; Pesaran et al., 2007; Lemoine, 2008), source of electrical grid (Samaras and Meisterling, 2008; Sioshansi and Denholm, 2009), driving behaviors (Gonder et al., 2007; Moawad et al., 2009), etc. These uncertainties form the second research question in this dissertation:

What are the design and policy implications of plug-in hybrid technology?

Chapter 4 and 5 are dedicated to seek possible answers to this question. In Chapter 4, an analysis for the impacts of battery weight and driving distance between charges to PHEV performances is presented by comparing several PHEV designs to ordinary hybrid vehicles and conventional gasoline vehicles. The study in Chapter 5 takes a step further by posing a PHEV design optimization model with accounting for U.S. drivers' daily driving patterns and battery degradation. The investigation results show that PHEVs have implications in reducing petroleum consumption, life cycle cost and GHG emissions if PHEV designs are optimized to the corresponding social objectives, while the effect of allocating vehicles to the right drivers with various daily driving distances becomes secondary. Specifically, PHEVs with small to medium battery capacity can have lower average life cycle cost than conventional gasoline vehicles and ordinary hybrid vehicles (e.g. Toyota Prius) if drivers charge their plug-in vehicles frequently. A series of sensitivity analyses show that the economic performances of PHEVs are directly affected by battery cost, fuel price and electricity price. Imposing high carbon allowance price would not improve the cost competency of PHEVs unless the regional grid mix has large portion of renewable (low carbon intensity) energy source. Another important finding is that new lithium ion battery technology allows vehicle designers to maximize usable energy in the battery pack without shortening the battery life significantly; limiting usable energy window in the battery design may cause suboptimal design and hinder the expected benefits of PHEVs.

1.4 Vehicle Design Decisions for Market and Policy

Governmental policy and regulations are initiated to address public concerns. While designers often concentrate on product performance and profitability during product design,

design decisions do have policy implications (Michalek et al., 2004). For example, U.S. automakers' vehicle designs are affected by safety requirements (NHTSA, 2006), emission standards (EPA, 2007), and fuel economy regulations (EPA, 2007). Regulatory factors may enter design problems in the form of additional constraints, penalty costs or new objectives. When product design is under the influences of both market factors and governmental regulations, the implications in design decisions ought to be examined by integrated study of design, market and policy.

Particularly, this dissertation study focuses on the interaction between vehicle designs and fuel efficiency standards. This direction is motivated by the recent changes in the Corporate Average Fuel Economy (CAFE) standards (NHTSA, 2006) due to the requirements in the Energy Independence and Security Act (EISA) (US Congress, 2007). The CAFE regulations state that automobile manufacturers are required to maintain a fleet average fuel economy above a specified standard set for a vehicle fleet, i.e. passenger car or light truck. If the criterion is not followed, manufacturers would be penalized based on the total fleet sales and the mpg (miles per gallon) falling behind the standard. Recently, higher fuel efficiency standards have been proposed separately by the U.S. federal agency (NHTSA, 2009), California state government (CARB, 2004) and European Union (European Parliament, 2008). All these policies have shown a trend on increasing fuel economy standards. This leads to third research question in this dissertation:

How does CAFE policy affect vehicle design decisions in a competitive market?

Chapter 6 is dedicated to answer this question by conducting a structural analysis for observing the vehicle design changes as different levels of CAFE standards are imposed. The impacts of fuel economy standard, inflated CAFE penalty, and gasoline price are tested in a case study of automaker vehicle design, which comprises of vehicle simulation, fuel-saving technology and recent automotive demand estimates. The study results show that automakers' vehicle design decisions for profit maximization under generic demand model and various levels of CAFE standards follow a unique pattern: Vehicle design responses do not always bind with CAFE regulations; vehicle designs become disengaged when the fuel efficiency threshold is too low or high. The results also show that CAFE penalty parameter (per vehicle per mpg violated) plays a distinct role in affecting firm's design decisions; i.e. when automakers fail to response to high CAFE standards, increasing penalty may be an alternative tool to improve fleet fuel economy. The sensitivity analysis on gasoline price variation indicates that firms' vehicle designs are more sensitive to fuel cost than CAFE standards.

While the research path of this dissertation study does not necessarily follow the sequence of above topics, the center is always product design decision making. The purpose of this dissertation research is not to create a do-it-all model to solve all problems, but to understand their fundamental structure, to pose practical solution strategies, and to perform case studies for reaching useful implications.

CHAPTER 2. PRODUCT DESIGN FOR PRICE COMPETITION

This chapter focuses on product design for price competition – the Class II problem described in Section 1.2. Prior approaches in the literature have ignored competitor reactions to a new product entrant. Under a game-theoretic framework, this chapter proposes an optimization framework for finding optimal product design solutions on competitors' pricing reactions in the market. The approach is tested with three product design case studies from the marketing and engineering design literature. The results show that new product design under Stackelberg and Nash equilibrium cases are superior to ignoring competitor reactions. The solution outcome implies that a product that would perform well in current market may perform poorly in the market that the new product will create. The efficiency, convergence stability, and ease of implementation of the proposed approach enables practical implementation for new product design problems in competitive market systems. The content in this chapter is based on the publication by Shiau and Michalek (2009).

2.1 Literature Review

Table 2.1 lists prior studies for price competition in product design and distinguishes them by solution approach, demand model type, equilibrium type, case studies, and presence of design constraints. The solution approach is the method used for finding the design solution under price competition. The demand model type specifies the market demand function formulation. Equilibrium type distinguishes Nash and Stackelberg models (Fudenberg and Tirole, 1991): Nash equilibrium refers to a point at which no firm can achieve higher profit by unilaterally selecting any decision other than the equilibrium decision. The Stackelberg case, also known as the leader-follower model, assumes that the leader is able to predict the responses of followers, in contrast with the Nash model, which assumes that each firm only observes competitor responses. The Stackelberg case is appropriate for cases where one player is able to "move first," and the introduction of a new product entrant is a case where the firm could exploit this first-move advantage. The penultimate column in Table 2.1 identifies whether the model incorporates design constraints representative of tradeoffs typically present in engineering design.

Table 2.1 Literature on new product design optimization under price competition

Literature	**Solution approach**	**Price equilibrium**	**Demand model**	**Design constraints**	**Case study**
Choi et al. (1990)	Iterative variational inequality algorithm	Stackelberg	Ideal point logit	Yes	Pain reliever
Horsky and Nelson (1992)	Discrete selection from FOC solutions	Nash	Logit	No	Automobile
Rhim and Cooper (2005)	Two-stage genetic algorithm	Nash	Ideal point logit	No	Liquid detergents
Lou et al. (2007)	Discrete selection and iterative optimization	Nash	HB* mixed logit	No	Angle grinder
This study	One-step NLP/MINLP with Lagrangian FOC	Nash/ Stackelberg	Logit and latent class models	Yes	Pain reliever Weight scale Power grinder

*HB: Hierarchical Bayes

Choi et al. (1990) (henceforth CDH) proposed an algorithm for solving the new product design problem under price competition while treating the new product entrant as Stackelberg leader. They tested the method on a pain reliever example with ingredient levels as decision variables and an ideal point logit demand model with linear price utility. The study applied the variational inequality relaxation algorithm (Harker, 1984) to solve the follower Nash price equilibria. In Section 2.3, we use CDH's problem as a case study and show that the method can have convergence difficulties, and as a result the Stackelberg solution found by their algorithm was not fully converged.

In contrast to the continuous decision variables used by CDH, other prior approaches restrict attention to discrete decision variables that reflect product attributes observed by consumers, as opposed to design variables controlled by designers under technical tradeoffs. We refer to the focus on product attributes as product positioning, in contrast to product design. These prior product positioning problems assume that all combinations of discrete variables are feasible, thus no additional constraint functions are considered. Horsky and Nelson (1992) used historic automobile market data to construct a logit demand model and cost function using four product attribute decision variables. With five levels for each of their four variables, they applied exhaustive enumeration to solve for equilibrium prices of all 625 possible new product entrant combinations using first-order condition (FOC) equations. Rhim and Cooper (2005) used a two-stage method incorporating genetic algorithms and FOCs to find Nash solutions for new product positioning problems. The model allows multiple new product entries to target different user market segments. The product in the study is liquid detergent with two attributes. Lou et al. (2007) conducted a study for optimal new product positioning of a handheld angle grinder under Nash price competition in a manufacturer-retailer channel structure . There are six product attributes with various levels in the problem, resulting in 72 possible combinations. Similar to the study by Horsky and Nelson (1992), they used a discrete selection method, but the design candidates were pre-screened to a smaller number in order to avoid full exhaustive enumeration, and the profits of a few final candidates at Nash price equilibrium were calculated through a sequential iterative optimization approach. Prior approaches to product design and positioning under price competition suffer from inefficient computation and convergence issues due to iterative strategies to identify equilibria and combinatorial limitations of discrete attribute models.

We propose an alternative approach to find optimal design and equilibrium competition solutions without iterative optimization of each firm. Our approach poses a nonlinear programming (NLP) or mixed-integer nonlinear programming (MINLP) formulation for new product profit maximization with respect to prices and design variables subject to first-order necessary conditions for the Nash price equilibrium of competitors. We examine three case studies from the literature and show that accounting for competitor price competition can result in different optimal design decisions than those determined under the assumption that competitors will remain fixed. The approach is well-suited to engineering design optimization problems, requiring little additional complexity and offering greater efficiency and convergence stability than prior methods, particularly for the highly-constrained problems in engineering design.

The remainder of this chapter is organized as follows: In Section 2.2, we explain the detailed formulation of the proposed approach with Nash and Stackelberg competition models, and we introduce a modified Lagrangian formulation to accommodate cases with variable bounds. In Section 2.3, we demonstrate the proposed approach by solving three product design examples from the literature, and we conclude in Section 2.4.

2.2 Proposed Methodology

For a new product design problem under short-run competition, there are three sets of decision variables to be determined – new product design variables, new product price, and prices of competitor products. In the following sections, we describe the proposed product design optimization models under Nash and Stackelberg strategies incorporating the FOC equation for unconstrained prices. We then examine the special cases where prices are constrained and develop a Lagrangian extension for this case (the basic concept of the Lagrangian FOC method is described in Appendix A). The major assumptions for the proposed approaches are: (1) Focal firm will design a set of differentiated products that will enter a market with existing products sold by competitors; (2) competitors are Nash price setters for profit maximization with fixed products; (3) competitor product attributes and costs are known; and (4) price is continuous, and each firm's profit function is differentiable with respect to its corresponding price.

2.2.1 Profit Maximization under the Nash Model

The necessary condition for unconstrained Nash price equilibrium can be expressed using FOC $\partial\Pi_k/\partial p_j = 0$ for product j produced by firm k (Friedman, 1986). For short-run Nash competition, new product design variables, new product price, and competitors' prices follow the Nash framework, which forms three sets of simultaneous equations. If there are no additional constraints on design variables and prices, the formulation is given by:

$$
\begin{aligned}
&\frac{\partial \Pi_k}{\partial \mathbf{x}_j} = \mathbf{0};\ \frac{\partial \Pi_k}{\partial p_j} = 0;\ \frac{\partial \Pi_{k'}}{\partial p_{j'}} = 0 \\
&\text{where } \Pi_k = \sum_{j \in J_k} q_j \left(p_j - c_j \right);\ \Pi_{k'} = \sum_{j \in J_{k'}} q_{j'} \left(p_{j'} - c_{j'} \right) \\
&\qquad q_j = Q s_j;\ s_j = f_{\mathrm{S}}\left(p_j, \mathbf{z}_j, p_{\hat{j}}, \mathbf{z}_{\hat{j}}\ \forall \hat{j} \neq j \right) \\
&\qquad q_{j'} = Q s_{j'};\ s_{j'} = f_{\mathrm{S}}\left(p_{j'}, \mathbf{z}_{j'}, p_{\hat{j}'}, \mathbf{z}_{\hat{j}'}\ \forall \hat{j}' \neq j' \right) \\
&\qquad \mathbf{z}_j = f_{\mathrm{Z}}\left(\mathbf{x}_j \right);\ c_j = f_{\mathrm{C}}\left(\mathbf{x}_j, q_j \right) \\
&\qquad \forall j \in J_k;\ \forall j' \in J_{k'};\ \forall k' \in K \setminus k
\end{aligned}
\tag{2.1}
$$

where Π_k is the net profit of all new products J_k from firm k and $\Pi_{k'}$ is the net profit sum of the products of firm k'. Each new product j has design vector $\mathbf{x}_j$, attribute vector $\mathbf{z}_j$ (as a function of the design $\mathbf{z}_j=f_{\mathrm{Z}}(\mathbf{x}_j)$), price p_j, unit cost c_j (as a function of the design and product volume

$c_j=f_C(\mathbf{x}_j,q_j)$), predicted market share s_j (as a function of the attributes and prices of all products $s_j=f_S(p_j,\mathbf{z}_j,p_{\bar{j}},\mathbf{z}_{\bar{j}}\ \forall\bar{j}\neq j)$) and predicted demand q_j. The total size of the market is Q. Each competitor $k'\in K\backslash k$ has price decisions $p_{j'}$ with fixed design attributes $\mathbf{z}_{j'}$ for all its products $\forall j'\in J_{k'}$. In the simultaneous equation set, the $\partial\Pi_k/\partial\mathbf{x}_j$ and $\partial\Pi_k/\partial p_j$ represent the FOCs of the Nash design and price decisions of the new product, and $\partial\Pi_{k'}/\partial p_{j'}$ is the FOC for the price decisions of competitor products.

While Eq. (2.1) presents the fundamental structure of Nash equation set, it does not account for design constraints and price bounds. Constraints on design variables are typical in engineering design problems. Bounds on price may be imposed by manufacturer, retailer, consumer, or government policies, and they may also be used to indicate model domain bounds. To account for these cases, we propose a generalized formulation incorporating Lagrange multipliers into Eq. (2.1) and present it in an NLP form:

$$\begin{aligned}
&\text{Maxmize } \Pi_k=\sum_{j\in J_k} q_j\left(p_j-c_j\right)\\
&\text{with repsect to } \mathbf{x}_j, p_j, \boldsymbol{\lambda}_j, \boldsymbol{\mu}_j, \bar{\boldsymbol{\mu}}_j, p_{j'}, \bar{\boldsymbol{\mu}}_{j'}\\
&\text{subject to } \frac{\partial L_k}{\partial \mathbf{x}_j}=\mathbf{0};\ \frac{\partial L_k}{\partial p_j}=0;\ \frac{\partial L_{k'}}{\partial p_{j'}}=0\\
&\mathbf{h}\left(\mathbf{x}_j\right)=\mathbf{0};\ \mathbf{g}\left(\mathbf{x}_j\right)\le\mathbf{0};\ \boldsymbol{\mu}_j\ge\mathbf{0};\ -\boldsymbol{\mu}_j^T\mathbf{g}\left(\mathbf{x}_j\right)\le t\\
&\bar{\mathbf{g}}\left(p_j\right)\le\mathbf{0};\ \bar{\boldsymbol{\mu}}_j\ge\mathbf{0};\ -\bar{\boldsymbol{\mu}}_j^T\bar{\mathbf{g}}\left(p_j\right)\le t\\
&\bar{\mathbf{g}}\left(p_{j'}\right)\le\mathbf{0};\ \bar{\boldsymbol{\mu}}_{j'}\ge\mathbf{0};\ -\bar{\boldsymbol{\mu}}_{j'}^T\bar{\mathbf{g}}\left(p_{j'}\right)\le t\\
&\text{where}\\
&\quad L_k=\Pi_k+\sum_{j\in J_k}\left(\boldsymbol{\lambda}_j^T\mathbf{h}\left(\mathbf{x}_j\right)+\boldsymbol{\mu}_j^T\mathbf{g}\left(\mathbf{x}_j\right)+\bar{\boldsymbol{\mu}}_j^T\bar{\mathbf{g}}\left(p_j\right)\right);\\
&\quad L_{k'}=\Pi_{k'}+\sum_{j'\in J_{k'}}\left(\bar{\boldsymbol{\mu}}_{j'}^T\bar{\mathbf{g}}\left(p_{j'}\right)\right);\ \Pi_{k'}=\sum_{j\in J_{k'}} q_{j'}\left(p_{j'}-c_{j'}\right);
\end{aligned}\tag{2.2}$$

$$
\begin{aligned}
& q_j = Qs_j;\ s_j = f_{\mathrm{S}}\left(p_j, \mathbf{z}_j, p_{\hat{j}}, \mathbf{z}_{\hat{j}}\ \forall \hat{j} \neq j\right); \\
& q_{j'} = Qs_{j'};\ s_{j'} = f_{\mathrm{S}}\left(p_{j'}, \mathbf{z}_{j'}, p_{\hat{j}'}, \mathbf{z}_{\hat{j}'}\ \forall \hat{j}' \neq j'\right); \\
& \mathbf{z}_j = f_{\mathrm{Z}}\left(\mathbf{x}_j\right);\ c_j = f_{\mathrm{C}}\left(\mathbf{x}_j, q_j\right) \\
& \forall j \in J_k;\ \forall j' \in J_{k'};\ \forall k' \in K \setminus k
\end{aligned}
$$

In above formulation, $\boldsymbol{\lambda}$, $\boldsymbol{\mu}$, and $\overline{\boldsymbol{\mu}}$ are the Lagrange multiplier vectors for the design equality constants $\mathbf{h}$, design inequality constraints $\mathbf{g}$, and price bounds $\overline{\mathbf{g}}$, respectively. Eq. (2.2) determines the profit-maximizing new product design $\mathbf{x}_j$ and price p_j that are in Nash equilibrium with competitor prices $p_{j'}$, $\forall j' \in J_{k'}$, $\forall k' \in K \setminus k$. The objective function[1] is the total profit Π_k of firm k. The equality and inequality constraints, $\mathbf{h}(\mathbf{x}_j)$ and $\mathbf{g}(\mathbf{x}_j)$, define the feasible domain of the engineering design, and the inequality constraint $\mathbf{g}(p_j)$ accounts for the price bounds. The FOCs of Lagrangian equations with additional inequality constraints represent the Karush-Kuhn-Tucker (KKT) necessary condition of Nash equilibrium for regular points (Bazaraa and Shetty, 1979). Such formulation has been known as mathematical programs with equilibrium constraints (MPECs) (Lou et al., 1996). Since MPECs do not satisfy constraint qualifications, it can induce numerical instability in convergence (Ye et al., 1997; Scheel and Scholtes, 2000). For resolving the issue, various algorithms and reformulation approaches have been proposed (Lou et al., 1996; Anitescu, 2000; Ralph and Wright, 2004). In this study, we follow a regularization scheme presented by Ralph and Wright (2004) and introduce a positive relaxation parameter t into the KKT complementary slackness conditions. The regularized NLP formulation can avoid the constraint qualification failures of MPECs and result in strong stationarity and second-order sufficient condition near a local solution of the MPEC (Ralph and Wright, 2004). The competitors' prices obtained from Eq. (2.2) are solutions based on necessary conditions. If the

[1] Note that the objective function of the NLP form is not needed to identify points that satisfy Nash necessary conditions; however, in practice including the objective of producer k can help to also enforce (local) sufficiency conditions for producer k. Sufficiency for competitors must be determined post hoc (Appendix A).

profit function is non-concave, the solutions need to be tested with Nash definition (Eq. (A.1) in Appendix A) verifying sufficient conditions: We take the FOC solution and optimize each individual firm's profit with respect to its own pricing decisions while holding other firms' decisions fixed. If no higher profit is found throughout the test, the price solutions are Nash prices.

2.2.2 Profit Maximization under the Stackelberg Model

For the proposed Stackelberg competition model, it is assumed that the new product enters the market as a leader, while other competitors react as followers. Followers observe others' price decisions, including the new product price, as exogenous variables and compete with one another to reach a Nash price equilibrium. The new product leader is able to predict its followers' Nash price settings within its optimization, giving it an advantage. The formulation using a Stackelberg model can be expressed in the following NLP from:

$$
\begin{aligned}
&\text{maximize } \Pi_k = \sum_{j\in J_k} q_j \left(p_j - c_j \right) \\
&\text{with respect to } \mathbf{x}_j, p_j, p_{j'}, \bar{\boldsymbol{\mu}}_{j'} \\
&\text{subject to } \mathbf{h}\left(\mathbf{x}_j\right) = \mathbf{0};\ \mathbf{g}\left(\mathbf{x}_j\right) \le \mathbf{0};\ \bar{\mathbf{g}}\left(p_j\right) \le \mathbf{0}; \\
&\quad \frac{\partial L_{k'}}{\partial p_{j'}} = 0;\ \bar{\mathbf{g}}\left(p_{j'}\right) \le \mathbf{0};\ \bar{\boldsymbol{\mu}}_{j'} \ge \mathbf{0};\ -\bar{\boldsymbol{\mu}}_{j'}^T \bar{\mathbf{g}}\left(p_{j'}\right) \le t; \\
&\text{where } \ L_{k'} = \Pi_{k'} + \sum_{j'\in J_{k'}} \left(\bar{\boldsymbol{\mu}}_{j'}^T \bar{\mathbf{g}}\left(p_{j'}\right)\right);\ \Pi_{k'} = \sum_{j\in J_{k'}} q_{j'} \left(p_{j'} - c_{j'} \right) \\
&\quad q_j = Qs_j;\ s_j = f_{\mathrm{S}}\left(p_j, \mathbf{z}_j, p_{\hat{j}}, \mathbf{z}_{\hat{j}}\ \forall \hat{j} \ne j \right) \\
&\quad q_{j'} = Qs_{j'};\ s_{j'} = f_{\mathrm{S}}\left(p_{j'}, \mathbf{z}_{j'}, p_{\hat{j}'}, \mathbf{z}_{\hat{j}'}\ \forall \hat{j}' \ne j' \right) \\
&\quad \mathbf{z}_j = f_{\mathrm{Z}}\left(\mathbf{x}_j\right);\ c_j = f_{\mathrm{C}}\left(\mathbf{x}_j, q_j\right) \\
&\forall j \in J_k;\ \forall j' \in J_{k'};\ \forall k' \in K \setminus k
\end{aligned}
\tag{2.3}
$$

Nash sufficiency conditions for followers must be verified post hoc as before. Comparing Eq. (2.3) to Eq. (2.2), the Stackelberg case relaxes the constraint requiring the focal firm to be in Nash equilibrium. Stated as a relaxation, it is clear that the focal firm's profit will be at least as large under the Stackelberg as under the Nash model.[2]

Compared to the solution approaches in literature, the proposed methods have significant advantages in several aspects. First, the approach is able to solve the problem in a single step if a unique design solution with price equilibrium exists.[3] Second, since the approaches employ FOC equations to find equilibrium prices, the convergence of the whole formulation is faster and more stable than prior approaches that use iteration loops. Third, the formulations can be solved using commercially-available NLP solvers with minimum additional programming effort. When discrete design variables exist, the NLP model becomes a MINLP problem. However, the price equilibrium constraints remain in the continuous domain, and MINLP solvers can be used to solve Eq. (2.3) (Viswanathan and Grossmann, 1990; Tawarmalani and Sahinidis, 2004; Bonami et al., 2008). MPEC problems with discrete-constraints have been studied in the literature (Labbe et al., 1998; de la Torre et al., 2007; Scaparra and Church, 2008), but we do not pursue them here.

2.2.3 Evaluation

In order to compare profitability of the new product design arrived at under different modeling assumptions, we define three profit terms:

(1) *Model-estimated profit*: Profit of the design and price solution to a particular game model, i.e. fixed, Nash or Stackelberg, as estimated by that model.

[2] CDH (1990) used a duopoly game to prove that a Stackelberg leader strategy can always receive at least as high a payoff as a Nash strategy if a Stackelberg equilibrium exists.

[3] For the cases of multiple local optima and price equilibria, multi-start can be implemented to identify solutions.

(2) *Competitor-reacted profit*: Profit of the design and price solution to a particular game model via post-hoc computation of competitor price equilibrium. The profit represents the market performance of a particular design and pricing solution if competitors adjust prices in response to the new entrant. Competitor-reacted profit is equal to model-estimated profit for the new product using Nash and Stackelberg strategies, but if the new entrant is optimized while assuming fixed competitors, the difference between model-estimated and competitor-reacted profit measures the impact of ignoring competitor's price adjusting reactions.

(3) *Price-equilibrium profit*: Profit of the design solution as estimated via post-hoc computation of price equilibrium of all firms (including the new entrant). The equilibrium profit represents the profit that a particular design solution would realize if all firms adjust prices in response to the new entrant and reach a market equilibrium. Equilibrium profit is equal to model-estimated profit for the new product design using Nash and Stackelberg strategies, but if the new entrant is optimized while assuming fixed competitors, the difference between model-estimated and price-equilibrium profit measures the impact of ignoring competitors' price reactions on the *design* of the product, assuming that poor pricing choices can be corrected in the marketplace after product launch.

2.3 Case Studies

We examine three product design case studies from the literature to test the proposed approach and examine the improvement that Stackelberg and Nash strategies can make with respect to the methods that ignore competitive reactions. Each case study involves different product characteristics, utility functions, demand models, variable types, and design constraints.

For each case, we solve the problem using the traditional fixed competitor assumption and compare to Nash and Stackelberg competition approaches. We also compare the computational efficiency and convergence of the proposed methods with the relaxation methods.

2.3.1 Case study 1: Pain Reliever

The pain reliever problem was introduced by CDH (Choi et al., 1990): Price and product attributes of a new pain reliever product are to be determined for maximizing profit in the presence of fourteen existing competitor products in the market. This new product design case study is a product positioning problem, and thus the attributes of a product are identical to its design decision variables (**z**=**x**). Each product has four attributes of pharmaceutical ingredient weight (unit in mg), including aspirin z_1, aspirin substitute z_2, caffeine z_3 and additional ingredients z_4. The product specifications[4] and initial prices of competitor products are listed in Table 2.2. There are two highlights in CDH's model. First, the product H is assumed a generic brand, which has a fixed price of \$1.99. The generic brand does not participate in the price competition. Second, there are five products, A, C, I, K and L, with identical product attributes and costs.

The demand model is an ideal point model with observable utility v, given by:

$$v_{ij} = -\left(\sum_{n=1}^{N} \beta_i \left(z_{nj} - \theta_{in} \right)^2 + \bar{\beta}_i p_j + b_i \right) \quad \forall i, j \tag{2.4}$$

[4] The values of aspirin substitute are the weighted combination of acetaminophen and ibuprofen. The numbers are not provided in CDH's paper (Choi et al., 1990). We obtained the attribute data from the mixed complementarity programming library (MCPLIB) (Dirkse and Ferris, 1995) and verified with original author. The data of consumer preference weightings (30 individuals) are also included in that library.

Table 2.2 Specifications of existing pain reliever products in the market

Product	Aspirin (mg) z_1	Aspirin sub. (mg) z_2	Caffeine (mg) z_3	Additional ingredients (mg) z_4	Cost ($) c	Initial price ($) p
A	0	500	0	0	$4.00	$6.99
B	400	0	32	0	$1.33	$3.97
C	0	500	0	0	$4.00	$5.29
D	325	0	0	150	$1.28	$3.29
E	325	0	0	0	$0.98	$2.69
F	324	0	0	100	$1.17	$3.89
G	421	0	32	75	$1.54	$5.31
H	500	0	0	100	$1.70	$1.99
I	0	500	0	0	$4.00	$5.75
J	250	250	65	0	$3.01	$4.99
K	0	500	0	0	$4.00	$7.59
L	0	500	0	0	$4.00	$4.99
M	0	325	0	0	$2.60	$3.69
N	227	194	0	75	$2.38	$4.99
Cost	0.3	0.8	0.4	0.2	cost unit: $/100mg	

where z_{nj} is the value of product attribute n on product j, θ_{in} is consumer i's desired value for attribute n, β_i is consumer i's sensitivity of utility to deviation from the ideal point, $\overline{\beta}_i$ is consumer i's sensitivity of utility to price, and b_i is a constant utility term estimated from consumer i. In this model, product attributes that deviate from ideal attributes cause reduced utility, which is less preferred by consumers. Under the standard assumption that utility u_{ij} is partly observable v_{ij} and partly unobservable ε_{ij} so that $u_{ij}=v_{ij}+\varepsilon_{ij}$, and that the unobservable term ε_{ij} is an independent and identically-distributed (IID) random variable with a standard Gumbel distribution (Train, 2003), the resulting choice probability is defined in logit form with an outside good of utility $v_{i0}=0$:

$$s_{ij} = \frac{\exp\left(\chi v_{ij}\right)}{1+\sum_{j'\in J}\exp\left(\chi v_{ij'}\right)} \quad \forall i, j \tag{2.5}$$

The weighting coefficient χ is arbitrarily given by χ=3, given by CDH. The profit function is:

$$\Pi_j = q_j\left(p_j - c_j\right) = \left(Q\frac{1}{I}\sum_{i=1}^{I} s_{ij}\right)\left(p_j - c_j\right) \quad \forall j \tag{2.6}$$

In this problem, the market demand and profit are based on a simulated market size of 30 consumers. The FOC equation for the price is (detailed derivation in Appendix B.1):

$$\frac{\partial \Pi_j}{\partial p_j} = \sum_{i=1}^{I} s_{ij}\left[1 - \chi\bar{\beta}_i\left(p_j - c_j\right)\left(1 - s_{ij}\right)\right] = 0 \quad \forall j \tag{2.7}$$

Two constraint functions on the new product design are given by the ingredient weight limitations (Choi et al., 1990):

$$\begin{aligned} g_1 &= 325 - z_{1j} - z_{2j} \leq 0 \\ g_2 &= z_{1j} + z_{2j} - 500 \leq 0 \end{aligned} \tag{2.8}$$

By applying the above equations into the Nash and Stackelberg formulations (Eq. (2.2) and Eq. (2.3)), the model was solved using the sequential quadratic programming (SQP) NLP solver in the Matlab Optimization Toolbox. The solutions to the pain reliever problem with fixed competitors, Nash, and Stackelberg strategies are presented in Table 2.3, with CDH's Stackelberg solution shown in the last column. Several interesting observations are found from the results. First, the fixed-competitor solution has overestimated profit and market share predictions by presuming that competitors will not act. As shown in Figure 2.1, when competitors are allowed to react by altering prices under Nash competition, the competitor-reacted profit shows a significant profit reduction from estimated. Second, the competitor-reacted profit and price-equilibrium profit are nearly identical (to significant digits). The equilibrium profit from the fixed competitor case is lower than the Nash and Stackelberg cases, implying that the attribute decisions determined by assuming fixed competitors are suboptimal, even if the new entrant's price is adjusted optimally in response to market competition. Third, we found the solution under the Stackelberg model has a different design and price point, resulting in slightly higher profit than the Nash solutions[5], which supports the claim that Stackelberg is a better approach when promoting new product development (Choi et al., 1990). Fourth, we found that CDH's Stackelberg solution is not fully converged since the Nash sufficient-condition test (Eq. (A.1)) shows that the competitors (followers) are able to find alternative price decisions that result in higher profits. In other words, the follower prices do not reach a Nash equilibrium in their solutions and fail the Nash best response definition. Moreover, the competitor-reacted profit has a significant gap from CDH's model-estimated profit, which again shows the solution is not a stable equilibrium. The fixed-competitor strategy has the worst performance when market competition is present, while Stackelberg leads to a higher profit than Nash, and the competitor-reacted profit upon CDH's solution does not reach the true Stackelberg equilibrium due to incomplete convergence. As a result, CDH's suboptimal Stackelberg design solutions overestimate the profit and have a lower equilibrium profit than the true Stackelberg profit solved by our proposed method.[6] Overall, the proposed methods using Nash and Stackelberg strategies result in an equilibrium profit 1.2% and 1.5% higher than the fixed competitor case, respectively, and prevent the suboptimal design decisions.

[5] CDH (Choi et al., 1990) compared their Stackelberg solution to the optimal new product solution with competitors fixed at Nash prices (suboptimal solution) and concluded Stackelberg resulted in higher profit. However, the comparison for the two strategies should base on fully converged equilibrium solutions.

[6] We use multi-start to search for all stationary points in the feasible domain and perform post hoc Nash best response verification (Eq. (A.1)). We found only one unique Stackelberg solution.

Table 2.3 New product design and pricing equilibrium solutions for the pain reliever problem

		Fixed competitor	Nash	Stackelberg	CDH solution
New product design and price	$x_1 = z_1$	124.0	102.7	101.5	102.1
	$x_2 = z_2$	201.0	222.3	223.5	222.9
	$x_3 = z_3$	0	0	0	0
	$x_4 = z_4$	0	0	0	0
	Price	$3.74	$3.85	$3.74	$3.77
	Cost	$1.98	$2.09	$2.09	$2.38
Strategy-estimated profit		$8.60 (16.3%)	$7.78 (14.7%)	$7.80 (15.7%)	$8.16 (16.1%)
Competitor-reacted profit		$7.68 (14.5%)	$7.78 (14.7%)	$7.80 (15.7%)	$7.80 (15.5%)
Price-equilibrium profit		$7.68 (14.5%)	$7.78 (14.7%)	$7.80 (15.7%)	$7.80 (15.7%)
Price, market share%, profit of competitors at price equilibrium	A	$6.25, 3.55%, $2.39	$6.27, 3.45%, $2.35	$6.29, 3.41%, $2.34	$6.29, 3.41%, $2.34
	B	$2.26, 6.15%, $1.71	$2.26, 6.18%, $1.73	$2.26, 6.16%, $1.72	$2.26, 6.16%, $1.72
	C	$6.25, 3.55%, $2.39	$6.27, 3.45%, $2.35	$6.29, 3.41%, $2.34	$6.29, 3.41%, $2.34
	D	$2.27, 7.73%, $2.31	$2.28, 7.78%, $2.34	$2.28, 7.73%, $2.32	$2.28, 7.73%, $2.32
	E	$1.97, 11.4%, $3.39	$1.97, 11.5%, $3.42	$1.97, 11.3%, $3.39	$1.97, 11.3%, $3.39
	F	$2.18, 9.10%, $2.75	$2.18, 9.16%, $2.78	$2.19, 9.08%, $2.76	$2.19, 9.08%, $2.76
	G	$2.47, 4.60%, $1.28	$2.47, 4.63%, $1.29	$2.47, 4.62%, $1.29	$2.47, 4.62%, $1.29
	H	$1.99, 7.52%, $0.65	$1.99, 7.57%, $0.66	$1.99, 7.56%, $0.66	$1.99, 7.56%, $0.66
	I	$6.25, 3.55%, $2.39	$6.27, 3.45%, $2.35	$6.29, 3.41%, $2.34	$6.29, 3.41%, $2.34
	J	$4.76, 3.37%, $1.77	$4.76, 3.36%, $1.76	$4.77, 3.29%, $1.74	$4.77, 3.29%, $1.74
	K	$6.25, 3.55%, $2.39	$6.27, 3.45%, $2.35	$6.29, 3.41%, $2.34	$6.29, 3.41%, $2.34
	L	$6.25, 3.55%, $2.39	$6.27, 3.45%, $2.35	$6.29, 3.41%, $2.34	$6.29, 3.41%, $2.34
	M	$4.29, 11.4%, $5.80	$4.26, 11.5%, $5.70	$4.26, 11.2%, $5.59	$4.27, 11.2%, $5.60
	N	$3.90, 6.36%, $2.90	$3.93, 6.33%, $2.93	$3.95, 6.11%, $2.88	$3.95, 6.11%, $2.88

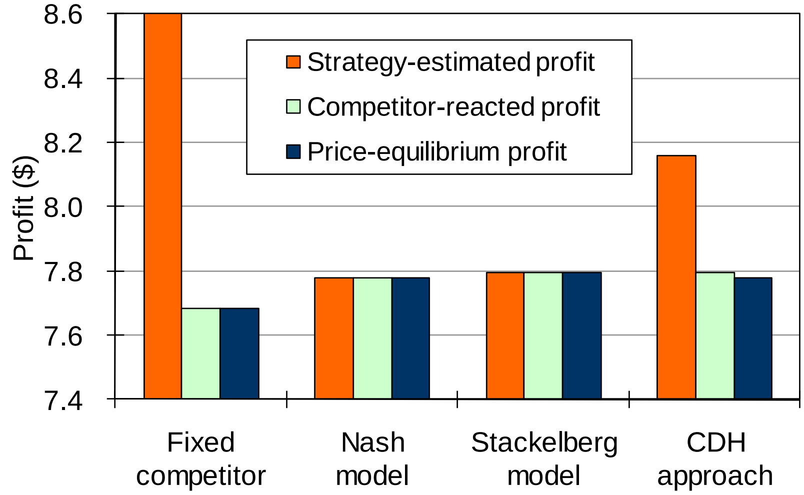

Figure 2.1 Comparison of four strategies for the pain reliever problem

We further compare the computational time and solution error of the proposed method with two other approaches, the relaxation parallel method (the CDH method) (Harker, 1984; Choi et al., 1990; Nagurney, 1993) and the relaxation serial method (sequential iterative optimization method) (Nagurney, 1993; Michalek et al., 2004). We use infinity norm: $\delta=|\mathbf{Z}^{*}-\mathbf{Z}|_{\infty}$ to define solution error, where $\mathbf{Z}^{*}$ is the target solution vector, including prices and new product design attributes, and $\mathbf{Z}$ is the solution vector found by each algorithm.[7] The benchmarking results are shown in Figure 2.2.[8] For the Nash case, while the two relaxation methods have difficulty to reach a solution with error less than 10^{-6}, the proposed approach is able to find more accurate solutions with relatively shorter computational time. For the Stackelberg case, the proposed formulation shows a surpassing performance on both computational time and solution error.

[7] The elements in the $\mathbf{Z}^{*}$ and $\mathbf{Z}$ vectors are dimensionless and normalized to upper and lower bounds of each variable. $\mathbf{Z}^{*}$ is obtained by using the proposed method with a convergence tolerance 10^{-16}.

[8] The computer system setup comprises of OS: Windows XP; CPU: Intel Core2 2.83Hz; RAM: 2.0 Gbyte; and solver: active-set SQP algorithm in Matlab R2008a.

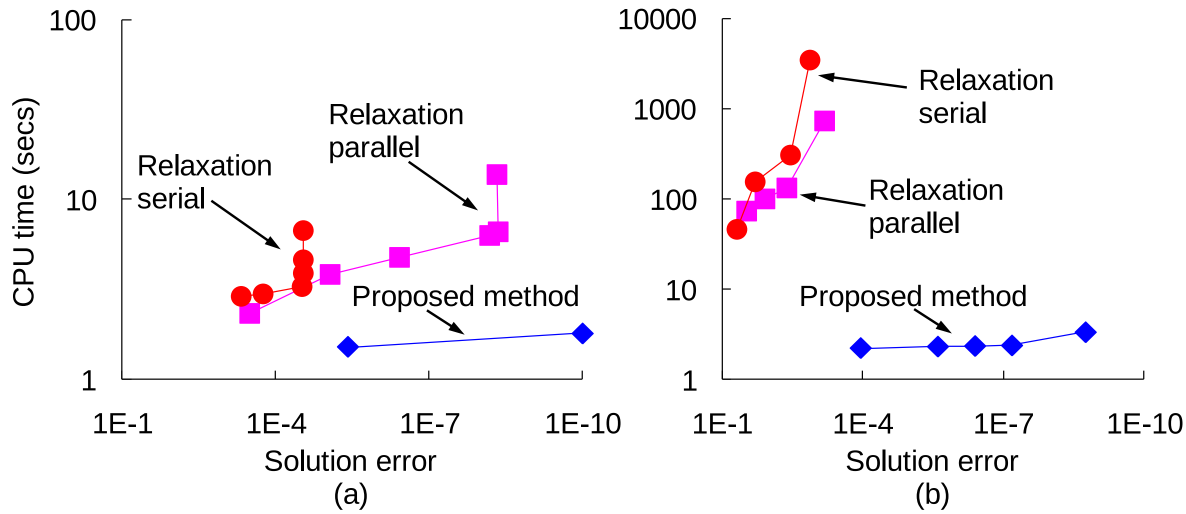

Figure 2.2 Computational time versus solution error for the painkiller problem (a) Nash case; (b) Stackelberg case

2.3.2 Case study 2: Weight Scale

The weight scale case study was introduced by Michalek and co-workers (Michalek et al., 2005; 2006). Compared to the first case study, this model has more complicated engineering design constraints and product attributes with a higher-order nonlinear equations. There are 14 design variables x_1-x_{14}, 13 fixed design parameters y_1-y_{13}, where the detailed definitions are listed in Table 2.4. The five product attributes z_1-z_5 and engineering constraint functions g_1-g_8 are shown in Table 2.5 as functions of the design variables. Table 2.6 presents the part-worth utility of the latent class model presented in (Michalek, 2005). There are 7 market segments, where the no-choice utility in each segment is fixed at zero during estimation.

Table 2.4 Design variables, parameters and constraint functions in the weight scale problem

	Description	Unit	Upper/lower bounds
x_1	Length from base to force on long lever	in.	[0.125, 36]
x_2	Length from force to spring on long lever	in.	[0.125, 36]
x_3	Length from base to force on short lever	in.	[0.125, 24]
x_4	Length from force to joint on short lever	in.	[0.125, 24]
x_5	Length from force to joint on long lever	in.	[0.125, 36]
x_6	Spring constant	lb/in	[1, 200]
x_7	Distance from base edge to spring	in.	[0.5, 12]
x_8	Length of rack	in.	[1, 36]
x_9	Pitch diameter of pinion	in.	[0.25, 24]
x_{10}	Length of pivot horizontal arm	in.	[0.5, 1.9]
x_{11}	Length of pivot vertical arm	in.	[0.5, 1.9]
x_{12}	Dial diameter	in.	[9, 13]
x_{13}	Cover length	in.	[9, 13]
x_{14}	Cover width	in.	[9, 13]
y_1	Gap between base and cover	in.	0.30
y_2	Min. distance between spring and base	in.	0.50
y_3	Internal thickness of scale	in.	1.90
y_4	Minimum pinion pitch diameter	in.	0.25
y_5	Length of window	in.	3.0
y_6	Width of window	in.	2.0
y_7	Distance from top of cover to window	in.	1.13
y_8	Number of lbs measured per tick mark	lb	1.0
y_9	Horizontal dist. spring to pivot	in.	1.10
y_{10}	Length of tick mark plus gap to number	in.	0.31
y_{11}	Number of lbs that number spans	lb	16
y_{12}	Aspect ratio of number (length/width)	-	1.29
y_{13}	Min. allow lever dist. base to centerline	in.	4.0

Table 2.5 Attribute and constraint functions in the weight scale problem

Design attribute functions	Engineering design constraint functions
$z_1 = \dfrac{4\pi x_6 x_9 x_{10}\left(x_1+x_2\right)\left(x_3+x_4\right)}{x_{11}\left(x_1\left(x_3+x_4\right)+x_3\left(x_1+x_5\right)\right)}$	$g_1: x_{12}-\left(x_{14}-2y\right)_1 \le 0$ $g_2: x_{12}-\left(x_{13}-2y_1-x_7-y_9\right)\le 0$
$z_2 = x_{13}x_{14}^{-1}$	$g_3: \left(x_4+x_5\right)-\left(x_{13}-2y_1\right)\le 0$
$z_3 = x_{13}x_{14}$	$g_4: x_5-x_2 \le 0$
$z_4 = \pi x_{12} z_1^{-1}$	$g_5: x_7+y_9+x_{11}+x_8-\left(x_{13}-2y_1\right)\le 0$
$z_5 = \dfrac{\left(2\tan\left(\pi y_{11} z_1^{-1}\right)\right)\left(0.5x_{12}-y_{10}\right)}{\left(1+2y_{12}^{-1}\tan\left(\pi y_{11} z_1^{-1}\right)\right)}$	$g_6: \left(x_{13}-2y_1\right)-\left(0.5x_{12}+y_7\right)-x_7-y_9-x_{10}-x_8 \le 0$ $g_7: \left(x_1+x_2\right)^2-\left(x_{13}-2y_1-x_7\right)^2-0.25\left(x_{14}-2y_1\right)^2 \le 0$
	$g_8: \left(x_{13}-2y_1-x_7\right)^2+y_{13}^2-\left(x_1+x_2\right)^2 \le 0$

Table 2.6 Part-worths in the latent class model of the weight scale problem

Attribute	Level	Market Segment 1	2	3	4	5	6	7
Weight Capacity z_1 (lb)	200	-1.34	-0.60	-0.38	-0.34	-0.92	-0.70	-1.19
	250	-0.36	-0.11	0.03	0.34	0.50	0.02	0.55
	300	0.06	0.21	0.08	0.70	0.37	0.04	0.34
	350	-0.21	0.05	-0.14	0.70	0.57	-0.09	-0.20
	400	-0.13	-0.15	0.20	0.51	0.55	-0.12	-0.19
Aspect Ratio z_2	0.75	-0.79	0.20	-0.04	0.44	0.10	-0.18	-1.40
	0.88	0.07	0.70	0.15	0.50	0.32	0.23	-0.62
	1	0.38	0.79	0.20	0.55	0.51	0.29	-0.02
	1.14	-0.09	-0.07	0.12	0.54	0.16	-0.10	0.57
	1.33	-1.34	-1.73	-0.56	-0.08	0.09	-0.89	0.39
Platform Area z_3 (in.^{2})	100	0.01	-0.45	0.19	0.36	0.17	0.45	-0.45
	110	-0.04	-0.21	-0.02	0.28	0.09	0.10	-0.49
	120	-0.41	-0.03	0.00	0.50	0.05	-0.05	-0.01
	130	-0.68	0.10	-0.12	0.46	0.30	-0.48	0.00
	140	-0.86	0.00	-0.27	0.31	0.45	-0.87	0.25
Gap size z_4 (in.)	2/32	-1.56	-0.55	-3.49	0.18	0.32	-0.39	-0.06
	3/32	-0.89	-0.21	-0.65	0.39	0.28	-0.15	-0.08
	4/32	-0.07	0.22	0.92	0.66	0.22	0.15	-0.13
	5/32	0.18	-0.02	1.48	0.49	0.00	-0.13	-0.28
	6/32	0.37	-0.03	1.56	0.20	0.23	-0.33	-0.14
Number size z_5 (in.)	0.75	-0.96	-1.20	-0.73	-0.35	-0.40	-1.24	-1.13
	1	-0.44	-0.51	-0.18	0.15	0.17	-0.72	-0.26
	1.25	0.12	0.34	0.25	0.58	0.22	0.17	0.07
	1.5	-0.30	0.32	0.21	0.72	0.60	0.48	0.17
	1.75	-0.39	0.47	0.24	0.81	0.48	0.46	0.46
Price p	$10	0.47	0.13	0.43	0.70	3.19	1.64	0.24
	$15	-0.08	0.13	0.41	0.64	1.92	1.28	0.19
	$20	-0.22	0.02	0.03	0.52	0.40	0.36	0.03
	$25	-0.79	-0.02	-0.29	0.25	-1.48	-1.12	-0.34
	$30	-1.35	-0.86	-0.79	-0.20	-2.97	-3.02	-0.81
Outside good		0	0	0	0	0	0	0
Segment size		7.1%	19.2%	14.2%	19.8%	13.6%	15.8%	10.3%

The discrete part-worths are interpolated by using fourth-order polynomials, and the utility is expressed as a continuous function ψ. Thus the observable utility of product j in market segment m is given by:

$$v_{mj} = \bar{\psi}_{mj}\left(p_j\right) + \sum_{n=1}^{5} \psi_{mnj}\left(z_{nj}\right) \tag{2.9}$$

where $\bar{\psi}_{mj}$ is the price utility polynomial and ψ_{mnj} is utility polynomial for attribute n for product j in segment m. The logit choice probability of product j in segment m is:

$$s_{mj} = \frac{\exp(v_{mj})}{\exp(v_{m0}) + \sum_{j' \in J} \exp(v_{mj'})} \quad \forall j \tag{2.10}$$

with outside good utility v_{m0}=0. The profit function of product j is given by:

$$\Pi_j = \sum_{m=1}^{M} Q_m s_{mj} \left(p_j - c_j \right) - c^{\mathrm{F}} \quad \forall j \tag{2.11}$$

The segment market size Q_m is calculated by multiplying the total market size, 5×10^6 units, by the corresponding market size ratio listed in bottom row of Table 2.6. The unit cost c_j is \$3.00, and the fixed investment cost c^{F} is one million dollars (Michalek et al., 2005). The FOC equation for Nash price equilibrium under the latent class model is (detailed derivations in Appendix B.2):

$$\frac{\partial \Pi_j}{\partial p_j} = \sum_{m=1}^{M} Q_m s_{mj} \left[\frac{\partial \bar{\psi}_{mj}}{\partial p_j} \left(1 - s_{mj}\right)\left(p_j - c_j \right) + 1 \right] = 0 \quad \forall j \tag{2.12}$$

Table 2.7 shows the specifications of four competing products, C1, R2, S3 and T4, in the market, where each product has a unique combination of product characteristics. We used Matlab SQP active-set solver with multistart and found multiple solutions that satisfy FOCs. After verifying post-hoc with the Nash definition (Eq. (A.1)), the unique market equilibrium was identified. The optimal price and attribute solutions under the fixed competitors, Nash, and Stackelberg cases are shown in Table 2.8. The fixed competitor case produces a distinct design solution from the other two, while Nash and Stackelberg cases have similar design attributes but significantly different price decisions. The design variables vary arbitrarily within the space of feasible designs that produce optimal attributes in this model. The design variables vary arbitrarily within the space of feasible designs that produce optimal attributes in this model.

Table 2.7 Specifications of weight scale competitors

Product	Weight capacity z_1	Aspect ratio z_2	Platform area z_3	Gap size z_4	Number size z_5	Price p
C1	350	1.02	120	0.188	1.40	$29.99
R2	250	0.86	105	0.094	1.25	$19.99
S3	280	0.89	136	0.156	1.70	$25.95
T4	320	1.06	115	0.125	1.15	$22.95

Table 2.8 New product design solutions for the weight scale problem

		Fixed competitor	Nash	Stackelberg
New product design and price	z_1	258	261	260
	z_2	1.046	1.038	1.039
	z_3	132	140	140
	z_4	0.117	0.119	0.119
	z_5	1.350	1.383	1.386
	Price	$18.24	$17.14	$15.87
Strategy-estimated Profit		$24.0M (33.8%)	$13.8M (21.0%)	$13.9M (23.2%)
Competitor-reacted Profit		$13.5M (19.0%)	$13.8M (21.0%)	$13.9M (23.2%)
Price-equilibrium Profit		$13.7M (21.2%)	$13.8M (21.0%)	$13.9M (23.2%)
Price, market share%, profit of competitors at price equilibrium	C1	$16.96, 21.3%, $13.8M	$17.26, 21.3%, $14.2M	$17.13, 20.7%, $13.7M
	R2	$15.00, 14.6%, $7.75M	$14.84, 14.7%, $7.70M	$15.11, 14.2%, $7.60M
	S3	$17.54, 20.2%, $13.7M	$16.99, 20.2%, $13.1M	$17.81, 19.6%, $13.5M
	T4	$17.69, 16.7%, $11.2M	$18.13, 16.8%, $11.7M	$17.93, 16.3%, $11.1M
Share of no-choice		6.1%	6.1%	6.0%

Similar to the observations in the first case study, the fixed competitor assumption gives the highest model-estimated profit, but the competitor-reacted and price-equilibrium profits demonstrate that the prediction is overestimated when market competition is taken into account. Figure 2.3 compares the competitor-reacted profits of different approaches graphically. The price-equilibrium profit is 1.6% higher than competitor-reacted profit, which implies that suboptimal pricing is a significant component of the competitor-reacted profit loss in the fixed competitor case, but suboptimal design is a larger component. The Stackelberg approach leads to a higher expected profit than Nash. The Nash and Stackelberg approaches are able to produce 1.1% and 3.4% higher competitor-reacted profits, and 1.3% and 1.8% higher price-equilibrium profit than the fixed competitor case. In this case, the new product Stackelberg leader has the lowest price, but the approach is able to gain the highest market share and profit. This case study again demonstrates that incorporating price competition in product design can not only avoid overestimation of profitability, but also help designer make the best strategic design decisions.

The computational benchmarking for this problem between the proposed method and the relaxation methods is shown in Figure 2.4. For the Nash case, the relaxation methods cannot reach a solution with an error less than 10^{-2}. In the same amount of computational time, the proposed Nash formulation finds the solutions with significantly higher accuracy. For the Stackelberg case, the relaxation methods fail to converge, whereas the proposed Stackelberg formulation reaches the solutions in relatively short computational time. These results once again show the limitation of algorithms using iterative optimizations for handling an engineering design problem with higher-order nonlinearity and complexity.

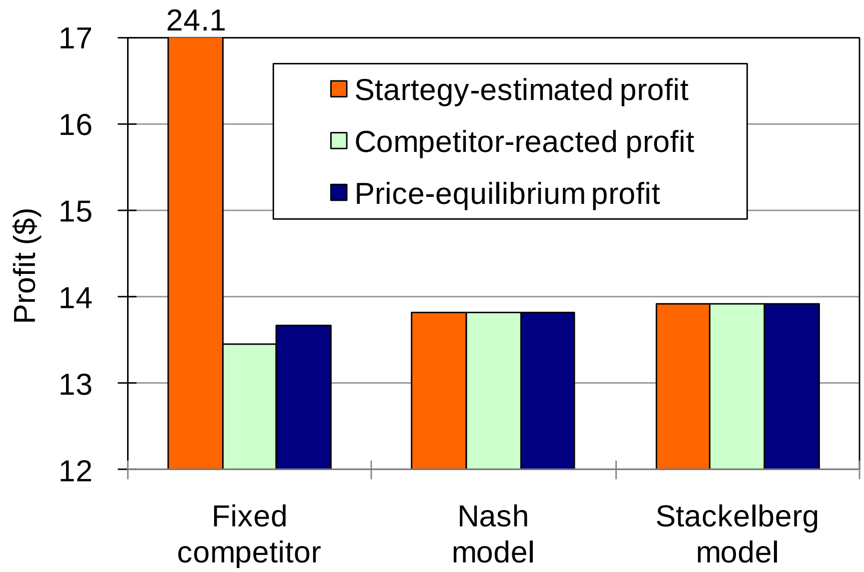

Figure 2.3 Competitor-reacted profits under various strategies for the weight scale design problem

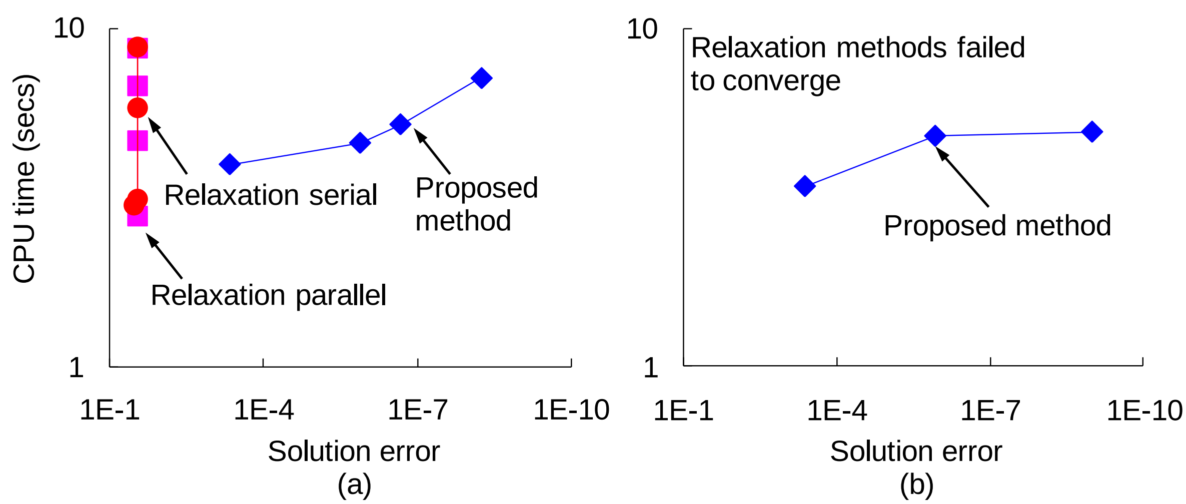

Figure 2.4 Computational time versus solution error for the weight scale problem: (a) Nash case; (b) Stackelberg case

2.3.3 Case study 3: Angle Grinder

The angle grinder case study determines the optimal attributes and price of a hand held power grinder (Luo et al., 2005; Besharati et al., 2006; Luo et al., 2007; Williams et al., 2008). The market demand model is a latent class model[9] with four market segments and six discrete attributes, including price (3 levels: $79, $99 and $129), current rating (3 levels: 6, 9 and 12 amps), product life (3 levels: 80, 110 and 150 hours), switch type (4 levels: paddle, top slider, side slider and trigger) and girth type (2 levels: small and large). The part-worth utilities of product attributes and price at each level (Besharati et al., 2006) are shown in Table 2.9. Since the new product design variables are identical to the product attributes, we categorize this case study as a product positioning problem (**z** = **x**).

Table 2.9 Conjoint part-worths in the angle grinder latent class model

		Market segment			
Attribute	Level	1	2	3	4
Price p	$79	-0.11	-0.09	0.005	-0.02
	$99	-0.89	-1.15	1.92	-0.24
	$129	1.00	1.25	-1.92	0.26
Brand z_1	New	-0.55	0.45	2.21	-0.17
	A	0.18	1.06	-2.37	-0.20
	B	0.83	0.11	-1.59	1.15
	C	-0.47	-1.63	1.74	-0.79
Current rating z_2	6 amps	1.25	0.45	-1.48	-0.46
	9 amps	0.13	-1.42	-0.65	-2.38
	12 amps	-1.39	0.97	2.13	2.84
Product life z_3	80 hrs	-0.86	-0.13	-4.72	0.80
	110 hrs	1.34	-0.47	-5.83	0.74
	150 hrs	-0.47	0.60	10.5	-1.55
Switch type z_4	Paddle	0.43	0.30	-3.29	-0.65
	Top slider	-1.02	-0.65	-3.05	0.42
	Side slider	2.39	-0.07	2.46	0.56
	Trigger	-1.81	0.43	3.87	-0.33
Girth size z_5	Small	1.51	0.72	1.51	0.41
	Large	-1.51	-0.72	-1.51	-0.41
No-purchase		-0.02	-0.02	-0.02	-0.02
Segment size		37.8%	24.8%	12.1%	25.3%

[9] The original demand model was presented in latent class model with four market segments (Luo et al., 2005; Besharati et al., 2006; Williams et al., 2008). The same market data were then estimated using hierarchical Bayesian method with mixed logit model (Luo et al., 2007).

The major difference of this case study from the previous two cases is its discrete decision variables. In order to derive analytical expressions for price utility, we interpolate the discrete price part-worths into the underlying continuous space using polynomial $\bar{\psi}$. Therefore, the observable utility component for product *j* in market segment *m* is given by:

$$v_{mj} = \bar{\psi}_{mj} + \sum_{d=1}^{D_n} w_{mnd} z_{ndj} \tag{2.13}$$

where *m* is the market segment index, $\bar{\psi}_{mj}$ is the interpolated price utility for market segment *m* as function of price p_j, w_{mnd} is the part-worth utility at level *d* of attribute *n* in market segment *m*, and z_{ndj} is a binary indicator variable that is equal to 1 if product *j* contains attribute *n* at level *d* and 0 otherwise. Further, *M* is the number of segments and D_n is the number of levels for attribute *n*. The price utility function in each segment is fit through the discrete levels with a quadratic function $\bar{\psi}_{mj} = \bar{a}_{2m}p^2_j + \bar{a}_{1m}p_j + \bar{a}_{0m}$, where $\bar{a}_{2m}$, $\bar{a}_{1m}$ and $\bar{a}_{0m}$ are coefficients determined via ordinary least squares regression. The four resulting price utility curves are plotted in Figure 2.5. It can be seen that the price responses in each segment are not monotonically decreasing when price increases within the range of \$75-\$130. This implies that the data will predict an unusual increase in demand with increasing price in segments 1, 2, and 4, providing incentive for firms to charge high prices. The share of choices s_{mj} and profit Π_j are given by Eq. (2.10) and Eq. (2.11), respectively. The FOC equation for the Nash price equilibrium (detailed derivations in Appendix B.2) is

$$\frac{\partial \Pi_j}{\partial p_j} = \sum_{m=1}^{M} Q_m s_{mj} \left[\left(2\bar{a}_{2m} p_j + \bar{a}_{1m} \right) \left(1 - s_{mj} \right) \left(p_j - c_j \right) + 1 \right] = 0 \quad \forall j \tag{2.14}$$

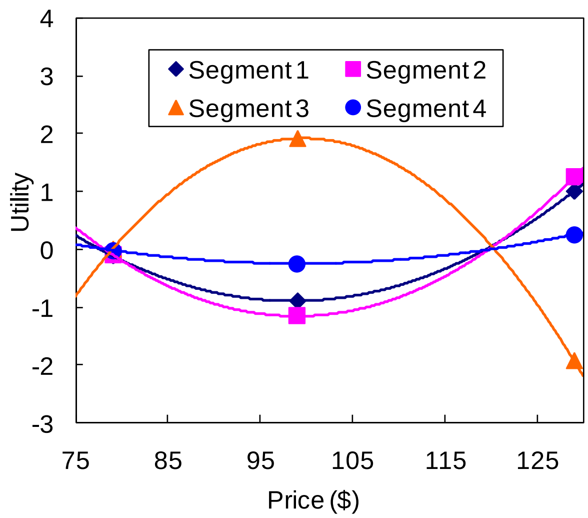

Figure 2.5 Price part-worth fitting functions for the angle grinder demand model

Based on the available price part-worth utility in the demand model, we confine the price decisions within a range of the survey data ($\overline{g}_1$: $75-p_j \leq 0$; $\overline{g}_2$: $p_j-130 \leq 0$) since unbounded price in this model will encourage firms toward infinite prices and result in no equilibrium solution. Furthermore, the specifications of competing products in the market are shown in Table 2.10. The estimated costs of product X, Y and Z are \$68.15, \$100.94 and \$49.58, respectively (Luo et al., 2007), and the new product cost is assumed \$75, independently of the design. The total market size is 9×10^6 units.

Because of the existence of both discrete design attributes and continuous price variables, Eq. (2.2) is not valid for Nash solutions. On the other hand, the Stackelberg formulation of this problem using only price FOC equation (Eq. (2.14)) can form a MINLP model without difficulty. The formulation is solved by using MINLP solver GAMS/Bonmin (Bonami et al., 2008) (CPU time: 0.086 secs). The optimal solutions are shown in Table 2.11. For the fixed competition case, it can be seen that the new product price reaches the modeling upper bound. We find that the new product and product Y dominate the market with relatively high shares and profits, while product X and Z have low market shares. For the Stackelberg case, the design attributes and price of the new product are identical to the fixed competitor case, but it can be seen that all competitors revised their price decisions in response to the new entrant to increase profitability. As a result, all prices reached the upper bound ($130) of the demand model, and the estimated market shares and profits of product X, Y and Z are higher than the fixed competitor case[10].

Table 2.10 Specifications of existing angle grinder products in the market

Product brand z_1	Current rating z_2	Product life z_3	Switch type z_4	Girth size z_5	Price p
X	9 amps	110 hrs	Side slider	Large	$99
Y	12 amps	150 hrs	Paddle	Small	$129
Z	6 amps	80 hrs	Paddle	Small	$79

Table 2.11 Optimal new product solutions for fixed and Stackelberg cases

		Fixed competitor	Stackelberg
New product design and price	x_1=z_1	12 amps	12 amps
	x_2=z_2	110 hours	110 hours
	x_3=z_3	Side slider switch	Side slider switch
	x_4=z_4	Small girth	Small girth
	price	$130	$130
Strategy-estimated profit		$299M (60.3%)	$244M (49.3%)
Competitor-reacted profit		$244M (49.3%)	$244M (49.3%)
Price-equilibrium profit		$244M (49.3%)	$244M (49.3%)
Price, market share%, profit of competitors	X	$99, 1.9%, $5.0M	$130, 10.0%, $56M
	Y	$129, 34.4%, $87M	$130, 34.0%, $89M
	Z	$79, 2.4%, $6.0M	$130, 6.0%, $43M
Share of no-choice		0.9%	0.7%

In the case, price bounds were added because finite price equilibrium solutions do not exist within the domain of the demand model's trusted region (i.e.: the region based on interpolation of measured survey or past purchase data). For example, in a general sense, increasing price induces decreasing utility, holding all other factors constant. However, some

[10] We do not compare computational cost or test the CDH method in this case because active price bounds make price solutions trivial.

consumers may assume, within some range, that products with higher prices have higher quality or better non-visible characteristics (Plassmann et al., 2008). A model built on such data will predict that higher prices result in greater demand, and thus higher profit if no other tradeoff exists. As a result, no price equilibrium exists within the measurable price range, and extrapolation leads to infinite prices.

There are several useful observations for this case study. First, we demonstrate that a product design and price competition problem containing discrete variables can be solved by a MINLP solver without exhaustive search or heuristic selection used in prior methods (Horsky and Nelson, 1992; Rhim and Cooper, 2005). Second, the fixed competitor model has significantly overestimated predicted profit by 22.5%. Third, this special case demonstrates the influence of concavity to the existence of equilibrium solutions. Due to the unique price utility responses, the individual profit function is not concave with respect to its price variable. Thus it is expected that a price equilibrium may not exist in the interior decision space but only boundary equilibrium exists (Friedman, 1986). Finally, product Y dominates market segments 2 and 3, while the new product is designed to dominate segments 1 and 4, which are the two biggest segments (Table 2.12). In a heterogeneous market, design and pricing decisions are often coupled, and the best solution depends on the positioning of competitors; therefore, accounting for competitor reactions can be critical to successfully locating new products in the market. Furthermore, without applying an upper bound to price, we find that all price decisions diverge, and no finite price equilibrium solution exists. As we can see in Figure 2.5, extrapolating the price utility curves of segments 1, 2, and 4 results in higher utility for higher prices. Applying an upper bound creates finite equilibria, but the bound activity clearly suggests that the data do not support the solution. This model is problematic for the optimization application, and results suggest that more data should be collected beyond the existing range in order to measure the eventually-decreasing utility associated with increased price. It is also possible in this case that survey respondents inferred high quality from high prices in the survey, since they tend to see such correlations in the marketplace; however, conjoint results should not exhibit these trends if respondents correctly treat all attributes not shown as equal across all profiles.

Table 2.12 Market shares in each segment at boundary equilibrium

Market segment	1	2	3	4	Total
	37.8%	24.8%	12.1%	25.3%	100%
A	25.6%	0.9%	0%	0.2%	10.0%
B	5.1%	70.8%	99.8%	10.0%	34.0%
C	13.1%	3.6%	0%	0.6%	6.0%
New product	**55.6%**	**23.6%**	**0.1%**	**88.5%**	**49.3%**
No-purchase	0.6%	1.1%	0.1%	0.8%	0.7%

2.4 Conclusions

Prior profit maximization methods in engineering design ignore competitive reactions in market systems. We propose an approach to solve the new product design problems for profit maximization while accounting for competitive reactions under Nash and Stackelberg price competition. Based on the theory of mathematical programs with equilibrium constraints, our approach accounts for competitive reactions through inclusion of equilibrium conditions as constraints in the optimization framework. This approach requires little additional complexity and offers greater efficiency and convergence stability than prior methods. Because the equilibrium conditions are set only with respect to competitor pricing decisions, it is not necessary to know competitor cost structures or internal competitor product engineering details, and the equilibrium conditions can be added to any existing product design profit optimization problem.

We show that failing to account for competitive reactions can result in suboptimal design and pricing solutions, and significant overestimation of expected market performance. Application of the method to three case studies from the literature exhibits its ability to handle problems of interest in the engineering domain. The case study results indicate that the Stackelberg approach is most preferred because of the capability to generate higher profits than Nash by anticipating competitor reactions. Both Nash and Stackelberg approaches can avoid overestimation of market performance and potentially poor product design positioning resulting from the common fixed-competitor model.

CHAPTER 3. PRODUCT DESIGN FOR MARKET SYSTEMS

This chapter focuses on the design problems of long-term market competition with price and design changes – the Class III problem defined in Section 1.2. Specifically, we examine how profit-maximizing designs are influenced by two structural factors in market systems: (1) the structure of manufacturer-retailer interactions and (2) the structure of heterogeneity in consumer preference modeling. A game-theoretic model with all manufacturers and retailers as decision-makers is proposed, and corresponding general equilibrium equations for each channel scenario are presented in the following sections. The investigation in this chapter aims to answer the following questions:

(1) *How does consumer preference heterogeneity affect optimal product design?* The use of the standard logit model, where differences among consumer utility functions are modeled as random noise, is compared to the random-coefficient mixed logit model, where the structure of consumer preference heterogeneity is modeled directly. The resulting effects on optimal design decisions are examined accordingly.

(2) *How do channel structures affect optimal product design?* Research in marketing and management science has shown that channel structures have a significant effect on optimal pricing decisions; the effect of channel structures on optimal design decisions is examined.

A case study of vehicle design is presented to demonstrate the analytical observations found during the investigation. The content in this chapter is based on the publication by Shiau and Michalek (2009).

3.1 Literature Review

Methods for profit maximization in design require the designer to model not only physical and technical attributes of the product, but also to predict cost and demand resulting from design decisions. To do this, researchers have drawn upon quantitative methods from marketing and econometrics to model consumer choice as a function of the design's attributes using survey data or past purchase data. While econometricians have used these models more commonly for *estimation*, to understand the structure of preferences in the marketplace, engineers have used these models for *prediction* to simulate market demand and optimize products for profitability (Li and Azarm, 2000; Wassenaar and Chen, 2003; Michalek et al., 2005; Michalek et al., 2006). In contrast to the active research on demand modeling in design optimization, there has been only limited attention paid to the role of *market competition* in product design. Some studies have used game-theoretic models to simulate competition (and cooperation) among engineering design decision-makers (Lewis and Mistree, 1998), but models that address the role of market competition among firms in product design are limited. Based on the three classifications (Class I, II and III) in Figure 1.2, Table 3.1 further identifies the prior product design literature using random utility discrete choice models for consumer choice simulation using two additional dimensions, (1) manufacturers, and (2) retailers. On the manufacturer dimension, Class I models treat the focal manufacturer as the only decision maker, where competitors are either not present or they are treated as fixed entities that will not react to the presence of a new design entrant. Class II models assume that competitors will respond to a new design entrant by adjusting pricing strategy, but competitor designs will remain fixed. Class III models assume that competitors will respond by both repricing and redesigning their products. Most prior studies do not account for the presence of retailers, instead assuming that manufacturers sell directly to consumers. When the retailer is taken into account, the model is said to incorporate the product's distribution channel structure (Coughlan, 2001; Ingene and Parry, 2004). Studies that account for retailers either assume the retailer to impose an exogenously-determined fixed margin over the manufacturer's wholesale price, or the retailer is treated a decision maker who will set margin in order to maximize profit.

Table 3.1 Literature on product design optimization using random utility discrete choice models

			Retailer		
	Class	**Competitors**	None	Fixed	Decide margin
Manufacturer	**I**	None	Wassenaar et al. (2003) Michalek et al. (2005) Michalek et al. (2006)	–	–
		Fixed	Besharati et al. (2006)	Williams et al. (2008)	–
	II	Decide price	Choi et al. (1990) **Chapter 2**	–	Luo et al. (2008)
	III	Decide price and design	Choi et al. (1992) Choi & Desarbo (1993) Michalek et al. (2004)	–	**This Chapter**

Class I models are most common in the profit maximization design literature. These approaches take the perspective of a single firm and assume there are no other decision-makers. Most models have taken the firm to be a monopolist in the product class with no competition other than the outside good (i.e., the no-purchase or no-choice option), so that consumers are modeled to either buy from the firm or not buy at all (Wassenaar and Chen, 2003; Michalek et al., 2005; Besharati et al., 2006; Michalek et al., 2006; Williams et al., 2008). Besharati et al. (2006) included static competitor products and proposed an approach to generate optimal robust-design sets considering utility variations in both the new design and competing products. Williams et al. (2008) also included fixed competitors and went further to incorporate retailer decisions in their model. Rather than model the retailer as a margin-setting profit maximizer, they assume a fixed margin and predict the channel acceptance rate, i.e., the probability that a retailer will agree to sell the new product through its distribution, which depends on the manufacturer's decisions of product attributes, wholesale price, and slotting allowance paid to the retailer. The primary limitation of class I methods is that they ignore competitor reactions. In differentiated oligopoly markets, competitors can be expected to react to a new product entry by changing prices in the short term and by changing designs in the long term. Thus, models that ignore competitor reactions will tend to overestimate profitability of a new entrant according to the findings in Chapter 2.

Class II models assume that competitor designs are fixed but attempt to account for competitor pricing reactions using game theory (Friedman, 1986). Since the time needed to design and deploy a new product is substantial for many product classes, most firms are not able to change their product designs in the short term, but pricing decisions can be changed rapidly. Thus, class II formulations may be a good description of short-term firm behavior for many product classes. Choi et al. (1990) posed a solution approach for class II problem using iterative price optimization of competitors. The results in Chapter 2 show that ignoring competitor reactions can result in significant overestimation of profits and suboptimal design variables. Lou et al. (2007) applied a different approach: They first performed product selection by combining discrete product attributes to reduce the optimal candidates to a manageable number. Then the optimal price and design solution are determined by exhaustive enumeration to find the alternative with the highest profit at price equilibrium with fixed competitor product attributes.

Class III models assume that firms are able to change both prices and product designs in reaction to a new product entry. As the lead time of new product development becomes shorter due to advancements in computer-aided design (CAD), computer-aided engineering (CAE), concurrent engineering, rapid prototyping, flexible manufacturing, supply chain management, and streamlined processes, it may be overly restrictive to assume that competitor product lines will remain fixed. Assuming consistent consumer preferences and rapid technology implementation, Class III formulations search for combinations of design and pricing decisions that are in equilibrium, therefore product design variables and price must be solved simultaneously. Choi et al. (1992) extended their previous short-run price competition framework (Choi et al., 1990) to find Nash solutions in a long-run product repositioning problem using an iterative approach. Choi and Desarbo (1993) proposed a framework using nonlinear integer programming with a sequential iterative process to identify Nash equilibria for discrete product attribute selection. Michalek et al. (2004) proposed a vehicle design problem with multiple automobile manufacturers competing on vehicle design and price under alternative government policy scenarios.

Channel structure models have been used widely in management and marketing science to model manufacturer-retailer, manufacturer-manufacturer, and retailer-retailer interactions in a competitive market. These studies focus on price competition and treat design as fixed. Jeuland and Shugan (1983) introduced a bilateral channel structure model with two separate manufacturer-retailer channels competing in the market. Later McGuire and Staelin (1983) proposed a model with two competing manufacturers selling products through a company store[11] and a franchised retailer[12]. Choi (1991) presented a channel structure model for a common retailer[13], systematically defining several game rules to describe the interactions between

[11] A company store (also called factory store) is a retail store owned by a specific manufacturer, so that wholesale price and retail price are equal. Such a channel configuration is also referred to as vertical integration (McGuire and Staelin, 1983).

[12] A franchised retailer (also called exclusive store) is a retail store owned by a private company that sells products from only one manufacturer.

[13] A common retailer is a retailer who sells products produced by multiple manufacturers.

manufacturers and retailers based on the concepts of Nash and Stackelberg (leader-follower) games. Lee and Staelin (1997) extended Choi's single common retailer framework to include multiple common retailers. While these prior approaches used simple linear or nonlinear demand functions, Besanko et al. (1998) incorporated the logit demand function into Choi's common retailer model (Harker and Choi, 1991), and Sudhir (2001) extended Besanko's work by deriving an array of analytical equilibrium equations using various profit maximization strategies under both vertical Nash and manufacturer Stackelberg game rules.[14]

This study attempts to fill a gap in the prior literature by posing a class III formulation under alternative channel structures and examining the impact of each structure on design and pricing decisions. The remainder of this chapter proceeds as follows: In Section 3.2, we derive equations for an integrated model of design and pricing equilibrium under alternative channel structures and demand heterogeneity, and we examine the structure of the results, posing several propositions on the role of heterogeneity in competitive design. In Section 3.3, a vehicle design example is implemented to demonstrate our methodology and test the degree to which channel structure and demand heterogeneity influence optimal design in a practical example, and conclusions are made in Section 3.4.

3.2 Methodology

We develop our methodology by first posing models for consumer choice and channel structures, then deriving equilibrium conditions for firm competition in each case, and finally examining implications of the results. Following the prior literature, our modeling assumptions include: (1) the market is described as a non-cooperative oligopolistic game with complete

[14] Vertical Nash, first defined by Choi (Harker and Choi, 1991), is the Nash competition scenario between manufacturer and retailer players. Similarly, a manufacturer Stackelberg game treats manufacturer players as Stackelberg leaders and retailer players as Stackelberg followers.

information (Fudenberg and Tirole, 1991) and a fixed number of firms (no entry and exit) (Tirole, 1988); (2) manufacturers and retailers (if they exist) are Nash price setters for profit maximization; (3) firms are generic with identical decision-spaces, no technological change, identical cost structures, no differences in intellectual property rights, and negligible brand effects; (4) market demand is described by a random-utility discrete-choice model with time invariant consumer preference coefficients; and (5) price and design decision variables are continuous, and each firm's profit function is differentiable.

3.2.1 Consumer Choice Model

Market equilibrium conditions for profit maximizing firms depend upon consumer choice behavior. We adopt the random utility discrete choice model, which is ubiquitous in marketing and econometrics (Greene, 2003) and has seen recent application in engineering design (Wassenaar and Chen, 2003; Michalek et al., 2005; Besharati et al., 2006; Michalek et al., 2006). Random utility models presume that each consumer i gains some utility $u_{ij} \in \Re$ from each product alternative j. Consumers are taken as rational, selecting the alternative that provides the highest utility, but each consumer's utility is only partly observable. Specifically, the utility is expressed as $u_{ij} = v_{ij} + \varepsilon_{ij}$ where v_{ij} is the observable component and ε_{ij} is the unobservable component. The observable term v_{ij} is a function of the observable parameters of a choice scenario: in this case, the attributes $\mathbf{z}_j$ and price p_j of each product j, so that $v_{ij} = v(p_j,\mathbf{z}_j,\boldsymbol{\beta}_i)$, where $\boldsymbol{\beta}_i$ is a vector of coefficients specific to individual i. The product attributes $\mathbf{z}_j$ are functions of the design variables $\mathbf{x}_j$ for each product, therefore $\mathbf{z}_j=\mathbf{z}(\mathbf{x}_j)$. By assuming the error term ε_{ij} follows the standard IID Gumbel distribution $f_\varepsilon(\varepsilon)=\exp(-\exp(-\varepsilon))$, which is close to Gaussian but more convenient, the probability s_{ij} of consumer i choosing product j is given by the logit model (Train, 2003):

$$s_{ij} = \frac{\exp\left(v_{ij}\right)}{\exp\left(v_0\right) + \sum_{k \in K} \sum_{j' \in J_k} \exp\left(v_{ij'}\right)} \tag{3.1}$$

where K is the set of manufacturers, J_k is the set of products sold by manufacturer k, and the utility of the outside good v_0 represents the utility value of the individual choosing none of the alternatives in the choice set. To obtain the total share of choices, we can integrate over consumers i. If $f_\beta(\boldsymbol{\beta})$ represents the joint probability density function of $\boldsymbol{\beta}$ coefficients across the consumer population i, and $s_{j|\boldsymbol{\beta}}$ is s_{ij} calculated conditional on $\boldsymbol{\beta}_i = \boldsymbol{\beta}$ (i.e.: $v_{ij} = v(p_j, \mathbf{z}_j, \boldsymbol{\beta})$), then the *share of choices* for product j (the probability of a randomly selected individual choosing product j) is:

$$s_j = \int s_{j|\boldsymbol{\beta}} f_\beta(\boldsymbol{\beta}) d\boldsymbol{\beta} \tag{3.2}$$

The integral form of Eq. (3.2) is called the *mixed logit* or *random coefficients model* (Train, 2003). The mixed logit model has been demonstrated to be capable of approximating any random utility discrete choice model (McFadden and Train, 2000). In practical applications, the mixed logit choice probability is approximated using numerical simulation by taking a finite number of draws from the distribution $f_\beta(\boldsymbol{\beta})$ (Train, 2003):

$$\hat{s}_j = \frac{1}{R}\sum_{r=1}^{R} s_{rj} = \frac{1}{R}\sum_{r=1}^{R} \frac{\exp\left(v_{rj}\right)}{\exp\left(v_0\right) + \sum_{k \in K} \sum_{j' \in J_k} \exp\left(v_{rj'}\right)} \tag{3.3}$$

where R is the number of random draws, s_{rj} is the logit choice probability for product j in the r-th draw, and v_{rj} is the corresponding simulated observable utility. The random coefficients of the mixed logit model are able to account for systematic taste variations, i.e.: heterogeneity, across individuals.

The standard logit model, also known specifically as the *multinomial logit model* when more than two choice alternatives are present, is a special case where the coefficients $\boldsymbol{\beta}$ are taken as deterministic, aggregate parameters during estimation, and variation across consumers is accounted for only in the unobservable error term ε. When heterogeneity of consumer preferences is negligible, the logit model may be sufficient for estimation while requiring less data and offering lower complexity and computational cost. When heterogeneity is significant, the mixed logit model is capable of capturing the structure of heterogeneity. For these reasons, both logit and mixed logit models are compared in this study.

3.2.2 Channel Structures

Figure 3.1 shows the vertical price interaction paths of four distribution channels with different retailer types, where w is the manufacturer's wholesale price and p is the retail price. The four channel scenarios are:

(1) *Company store* (CS): A company store sells only products from a single manufacturer, and the retail prices are directly controlled by the corresponding manufacturer (w=p) (McGuire and Staelin, 1983). There is no vertical interaction between a manufacturer and its company-owned retailer because of integration.

(2) *Franchised retailer* (FR): A franchised store is privately-owned but has a contract with the corresponding manufacturer. It sells only the products produced by the specific manufacturer. However, the manufacturer does not control retail prices directly, and the retailer is able to determine its own margins (McGuire and Staelin, 1983).

(3) *Single common retailer* (SCR): A common retailer sells mixed products from all available manufacturers, and it has control of its margins (Harker and Choi, 1991). The SCR case represents a powerful retailer dominating a regional market with no other equal-powered competitors in the region.

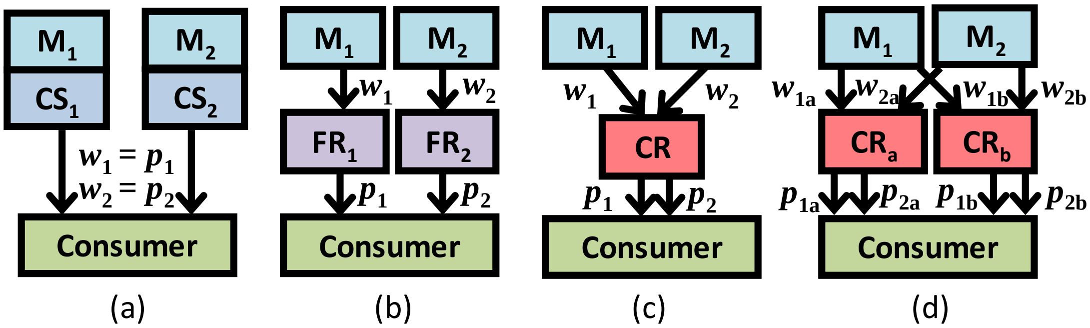

Figure 3.1 Channel structure scenarios: (a) Company Store, (b) Franchised Retailer, (c) Single Common Retailer, and (d) Multiple Common Retailers

(4) *Multiple common retailers* (MCR): This scenario represents more than one medium-sized retailer in the regional market (Lee and Staelin, 1997). These common retailers compete with one another for pursuing maximum profits.

Manufacturer and retailer profit depend on demand q_j, which can be predicted by multiplying the total size of the market Q by the share of choices s_j taken by product j, so that $q_j=Qs_j$. We consider the product cost in two components, (1) the variable manufacturing cost c_j per unit product, which is a function of the design $\mathbf{x}_j$, and (2) the total fixed investment cost c^{F}_j, so that total cost for product j is $q_j c_j(\mathbf{x}_j) + c^{\mathrm{F}}_j$. We derive first the general multiple common retailer case with a set of retailers $t \in T$ and then examine alternative channel structures as special cases. The profit function for manufacturer k is a sum over the retailers T and the set of products J_k:

$$\Pi_k^{\mathrm{M}} = \left[\sum_{t \in T} \sum_{j \in J_k} q_{jt} \left(w_{jt} - c_j \right) - c_j^{\mathrm{F}} \right] \tag{3.4}$$

where w_{jt} is the wholesale price of product j when sold to retailer t.[15] The manufacturer profit functions for the other three channel structure scenarios can be simplified from Eq. (3.4) by

[15] We assume manufacturers can offer different wholesale prices to different retailers.

removing the retailer index t, as shown in . The profit function for retailer t in the MCR scenario is given by:

$$\Pi_t^{\mathrm{R}} = \sum_{k \in K} \sum_{j \in J_k} q_{jt} \left(p_{jt} - w_{jt} \right) = \sum_{k \in K} \sum_{j \in J_k} q_{jt} m_{jt} \tag{3.5}$$

where m_{jt} is retailer t's margin for product j. The SCR scenario is a special case of MCR with a unique t. In the FR scenario, the profit function of a franchised store can be simplified from Eq. (3.5) by indexing each retailer with its corresponding manufacturer k and limiting the product category to the corresponding manufacturer source. For the CS scenario, the company store has no retail profit. The manufacturer and retailer profit formulations for the four channel structure scenarios are listed in Table 3.2.

Table 3.2 Manufacturer and retailer profit functions

Channel Structure	**Manufacturer profit**	**Retailer profit**
Company Store (CS)	$\Pi_k^{\mathrm{M}} = \left[\sum_{j \in J_k} q_j \left(w_j - c_j \right) \right] - c_j^{\mathrm{F}}$	–
Franchised Retailer (FR)	$\Pi_k^{\mathrm{M}} = \left[\sum_{j \in J_k} q_j \left(w_j - c_j \right) \right] - c_j^{\mathrm{F}}$	$\Pi_k^{\mathrm{R}} = \sum_{j \in J_k} q_j m_j$
Single Common Retailer (SCR)	$\Pi_k^{\mathrm{M}} = \left[\sum_{j \in J_k} q_j \left(w_j - c_j \right) \right] - c_j^{\mathrm{F}}$	$\Pi^{\mathrm{R}} = \sum_{k \in K} \sum_{j \in J_k} q_j m_j$
Multiple Common Retailers (MCR)	$\Pi_k^{\mathrm{M}} = \left[\sum_{t \in T} \sum_{j \in J_k} q_{jt} \left(w_{jt} - c_{jt} \right) \right] - c_{jt}^{\mathrm{F}}$	$\Pi_t^{\mathrm{R}} = \sum_{k \in K} \sum_{j \in J_k} q_{jt} m_{jt}$

3.2.3 Equilibrium Conditions

When we consider channel structures in a game-theoretic framework, manufacturers and retailers are both players (decision makers) in the game. The strategy (decisions) of a manufacturer includes wholesale price w and product design variables $\mathbf{x}$, and the strategy of a retailer is retail margin *m*. Choi defines this game as a *vertical Nash* game for price competition (Harker and Choi, 1991). We extend the model by including design competition. As shown in Figure 3.2, the manufacturer makes wholesale price and design decisions to maximize its profit based on the retail margin observed. Accordingly manufacturer profit is calculated as a function of wholesale price, cost, and market demand, which is a function of retail prices. The retailer makes its retail margin decision independently from manufacturer decisions (except in the CS case). Each retailer observes manufacturer wholesale prices and product attributes, as well as any competitor retailer prices. At market equilibrium, no manufacturer or retailer can reach higher profit by changing decisions unilaterally. For a vertical Nash game, each channel member (either manufacturer or retailer) is assumed to act non-cooperatively.

The FOC necessary conditions for the vertical Nash game produce a system of nonlinear equations (one equation for each unknown) given by:

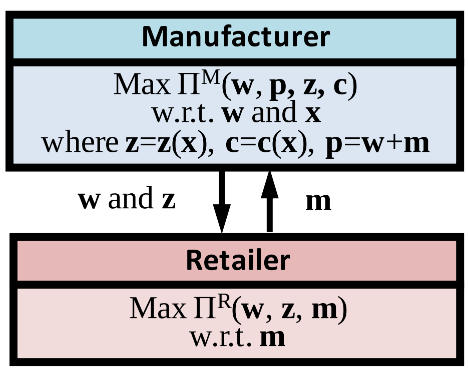

Figure 3.2 Interaction between manufacturer and retailer in the vertical Nash game

$$
\begin{aligned}
&\frac{\partial \Pi_k^{\mathrm{M}}}{\partial w_{jt}} = f_{\mathrm{w}}\left(\mathbf{x}_j, w_{jt}, m_{jt}; \forall j,t\right) = 0 \quad \forall k,t,\, j \in J_k \\
&\frac{\partial \Pi_k^{\mathrm{M}}}{\partial \mathbf{x}_j} = \mathbf{f}_{\mathrm{x}}\left(\mathbf{x}_j, w_{jt}, m_{jt}; \forall j,t\right) = \mathbf{0} \quad \forall k,\, j \in J_k \\
&\frac{\partial \Pi_t^{\mathrm{R}}}{\partial m_{jt}} = f_{\mathrm{m}}\left(\mathbf{x}_j, w_{jt}, m_{jt}; \forall j,t\right) = 0 \quad \forall k,t,\, j \in J_k
\end{aligned}
\tag{3.6}
$$

where t is replaced by k in the FR case. These FOC conditions are necessary but not sufficient. Hence, any candidate FOC solution must be checked to see if it a Nash equilibrium (Eq. (A.1)) by globally optimizing each player post hoc while holding all other players constant at the FOC solution.[16] Similar to finding the optimal solution in a general optimization problem, the existence and uniqueness of an equilibrium solution in a market competition problem depends on the equations describing the model (Friedman, 1986). For the logit demand model specifically, Anderson et al. (1992) demonstrated that a strictly quasi-concave profit function results in a unique Nash price equilibrium. However, when design variables are included, the logit profit function may become non-concave, and multiple local optima may exist (Hanson and Martin, 1996). Therefore, convergence properties and the existence and uniqueness of equilibria are problem dependent. In our case study, necessary conditions in each case revealed either a unique solution or a small set of solutions that were easy to check post hoc to identify the unique Nash equilibrium. To obtain the FOC equation sets for all channel structure scenarios, we first derive the FOCs with respect to manufacturer's wholesale price and design, and then retailer's margin.

[16] The FOC approach is more efficient than the sequential iteration method used in Michalek *et al.* (2004). The sequential iteration method requires iterative solution of a series of NLP problems for each manufacturer until Nash equilibrium is reached, while the FOC approach is a single step NLP execution for a local solution. The differences between two algorithms are discussed by Shiau and Michalek (Shiau and Michalek, 2007).

Wholesale Price: The wholesale price FOC equation is taken for each manufacturer k with respect to the wholesale price that manufacturer sets for each of its products $j \in J_k$ to sell to each retailer t. Under the mixed logit demand, the Nash necessary condition equation is:[17]

$$\frac{\partial \Pi_k^{\mathrm{M}}}{\partial w_{jt}} = \int_{\boldsymbol{\beta}} s_{jt|\boldsymbol{\beta}} \left(\frac{\partial v_{jt|\boldsymbol{\beta}}}{\partial p_{jt}} \left(\left(w_{jt} - c_j \right) - \sum_{j' \in J_k} \sum_{t' \in T} s_{j't'|\boldsymbol{\beta}} \left(w_{j't'} - c_{j'} \right) \right) + 1 \right) f_{\beta}(\boldsymbol{\beta}) d\boldsymbol{\beta} = 0 \qquad \forall t, k, j \in J_k \tag{3.7}$$

where $s_{jt|\boldsymbol{\beta}}$ is shorthand for the share of choices predicted by the logit model, given $\boldsymbol{\beta}$: in this case $\exp(v(p_{jt},\mathbf{z}_j,\boldsymbol{\beta}))[\exp(v_0) + \Sigma_k \Sigma_{t'} \Sigma_{j' \in Jk} \exp(v(p_{jt'},\mathbf{z}_{j'},\boldsymbol{\beta}))]^{-1}$, following Eq. (3.1). In the case of a single common retailer and a single product per manufacturer under standard logit, the integral in Eq. (3.7) collapses and the expression can be further simplified and rearranged as:

$$w_j = c_j + \left(-\frac{\partial v_j}{\partial p_j} \left(1 - s_j \right) \right)^{-1} \quad \forall j \in J_k \tag{3.8}$$

Eq. (3.8) illustrates that wholesale price at equilibrium is comprised of product cost plus a manufacturer margin, which is determined by the sensitivity of consumer observable utility to price and the corresponding share of choices. The same result was obtained by Besanko et al. (1998) in the case of price only (with no design decisions).

Design: For the case of an unconstrained design space, the design variable FOC equations for MCR are obtained similarly by setting the derivative of the manufacturer profit function with respect to each design variable to zero. Without loss of generality, we assume all designs are carried by all retailers (potentially with q=0):

[17] The detailed derivations of all FOC equations for the MCR scenario are shown in the supplemental document that is available by contacting the authors.

$$\frac{\partial \prod_k}{\partial \mathbf{x}_j} = \int_{\boldsymbol{\beta}} \sum_{t \in T} \left[\left(\frac{\partial v_{jt|\boldsymbol{\beta}}}{\partial \mathbf{z}_j} \frac{\partial \mathbf{z}_j}{\partial \mathbf{x}_j} \right) \left(s_{jt|\boldsymbol{\beta}} \left(w_{jt} - c_j \right) - \left(\sum_{\bar{t} \in T} s_{j\bar{t}|\boldsymbol{\beta}} \right) \right. \right.$$
$$\left. \left. \sum_{j' \in J_k} s_{j't|\boldsymbol{\beta}} \left(w_{j't} - c_{j'} \right) \right) - \frac{\partial c_j}{\partial \mathbf{x}_j} \right] f_\beta(\boldsymbol{\beta}) d\boldsymbol{\beta} = 0 \tag{3.9}$$
$$\forall k, t, j \in J_k$$

When equality constraints $\mathbf{h}(\mathbf{x})=\mathbf{0}$ and inequality constraints $\mathbf{g}(\mathbf{x})\leq\mathbf{0}$ exist in the design domain, additional constraint handling in needed. To account for constraints, we implement the Lagrangian FOC method (Appendix A) and re-formulate Eq. (3.9) as:

$$\frac{\partial L_k}{\partial \mathbf{x}_j} = \int_{\boldsymbol{\beta}} \sum_{t \in T} \left[\left(\frac{\partial v_{jt|\boldsymbol{\beta}}}{\partial \mathbf{z}_j} \frac{\partial \mathbf{z}_j}{\partial \mathbf{x}_j} \right) \left(s_{jt|\boldsymbol{\beta}} \left(w_{jt} - c_j \right) - \left(\sum_{\bar{t} \in T} s_{j\bar{t}|\boldsymbol{\beta}} \right) \left(\sum_{j' \in J_k} s_{j't|\boldsymbol{\beta}} \left(w_{j't} - c_{j'} \right) \right) - \frac{\partial c_j}{\partial \mathbf{x}_j} \right] f_\beta(\boldsymbol{\beta}) d\boldsymbol{\beta}$$
$$- \boldsymbol{\lambda}_j^T \frac{\partial \mathbf{h}_j}{\partial \mathbf{x}_j} - \boldsymbol{\mu}_j^T \frac{\partial \mathbf{g}_j}{\partial \mathbf{x}_j} = \mathbf{0} \quad \forall k, t, j \in J_k \tag{3.10}$$
$$\boldsymbol{\mu}_j{}^T \mathbf{g}\left(\mathbf{x}_j\right) = 0; \quad \boldsymbol{\mu}_j \geq \mathbf{0}; \quad \mathbf{h}\left(\mathbf{x}_j\right) = \mathbf{0}; \quad \mathbf{g}\left(\mathbf{x}_j\right) \leq \mathbf{0}$$

where $\boldsymbol{\lambda}_j$ and $\boldsymbol{\mu}_j$ are Lagrange multiplier vectors for product j. The formulation of Eq. (3.10) corresponds to the Karush-Kuhn-Tucker (KKT) necessary conditions for optimality of a constrained NLP (Papalambros and Wilde, 2000).

Retailer Margin: The retailer margin FOC equation for the MCR case is taken for each retailer with respect to its margin. The condition for a common retailer t under mixed logit demand is:

$$\frac{\partial \Pi_t^{\mathrm{R}}}{\partial m_{jt}} = \int_{\boldsymbol{\beta}} s_{jt|\boldsymbol{\beta}} \left[\frac{\partial v_{jt|\boldsymbol{\beta}}}{\partial p_{jt}} \left(m_{jt} - \sum_{k' \in K} \sum_{j' \in J_{k'}} s_{j't|\boldsymbol{\beta}} m_{j't} \right) + 1 \right]$$
$$f_\beta(\boldsymbol{\beta}) d\boldsymbol{\beta} = 0 \quad \forall k, t, j \in J_k \tag{3.11}$$

In the case of a single product per manufacturer and a single common retailer under logit demand, Eq. (3.11) can be simplified and rearranged as:

$$m_j = \frac{1}{1-s_j}\left[\left(-\frac{\partial v_j}{\partial p_j}\right)^{-1} + \sum_{k\in K}\sum_{\substack{j'\in J_k \\ j'\neq j}} s_{j'} m_{j'}\right] \forall j \in J_k \tag{3.12}$$

Combining Eq. (3.8) and Eq. (3.12), the retail price of product *j* selling through common retailer *t* satisfies:

$$p_j = w_j + m_j = c_j + \left[\frac{1}{1-s_j}\left(-\frac{\partial v_j}{\partial p_j}\right)^{-1}\right] + \frac{1}{1-s_j}\left[\left(-\frac{\partial v_j}{\partial p_j}\right)^{-1} + \sum_{k\in K}\sum_{\substack{j'\in J_k \\ j'\neq j}} s_{j'} m_{j'}\right] \ \forall j \in J_k \tag{3.13}$$

Equation (3.13) illustrates that retailer price at market equilibrium is composed of manufacturing cost, manufacturer margin, and retailer margin. From the general FOC equations for the MCR case under mixed logit demand, the equations for the other three cases can be obtained through simplifications. The equations for 4 channel scenarios are listed in Table 3.3. The FOC equations under the standard logit can by obtained by collapsing the integrals in the mixed logit equations for a single point $\boldsymbol{\beta}$. The results for logit produce closed form expressions and provide intuition, while the mixed logit model accommodates heterogeneity by modeling its structure directly. Equilibrium solutions can be obtained by solving the system equations in Table 3.3 using the Lagrangian FOC method presented in Appendix A.

3.2.4 Analytics Observations

We now examine several useful observations about equilibrium conditions under the standard logit case when the utility function *v* is linear in price. The linear price assumption is important because models with nonlinear utility for price may contain interaction terms that imply consumers' sensitivity to price varies with the value of other attributes, thus coupling price to attributes. However, if interaction terms are negligible, as is most commonly assumed, then the standard main-effects logit model has utility linear in price, and consumers make choices via typical compensatory tradeoffs between price and other attributes. The first two propositions show that manufacturers and retailers set identical margins for all products.

Table 3.3 FOC equations for mixed logit model and different channel structures

Company Store (CS)	$\frac{\partial \Pi_k^{\mathrm{M}}}{\partial w_j} = \int_{\boldsymbol{\beta}} s_{j\mid\boldsymbol{\beta}} \left[\frac{\partial v_{j\mid\boldsymbol{\beta}}}{\partial p_j} \left(\left(w_j - c_j\right) - \sum_{j' \in J_k} s_{j'\mid\boldsymbol{\beta}} \left(w_{j'} - c_{j'}\right) \right) + 1 \right] f_\beta(\boldsymbol{\beta}) d\boldsymbol{\beta} = 0$ $\frac{\partial \Pi_k^{\mathrm{M}}}{\partial \mathbf{x}_j} = \int_{\boldsymbol{\beta}} s_{jt\mid\boldsymbol{\beta}} \left[\left(\frac{\partial v_{j\mid\boldsymbol{\beta}}}{\partial \mathbf{z}_j} \frac{\partial \mathbf{z}_j}{\partial \mathbf{x}_j} \right) \left(\left(w_j - c_j\right) - \sum_{j' \in J_k} s_{j'\mid\boldsymbol{\beta}} \left(w_{j'} - c_{j'}\right) \right) - \frac{\partial c_j}{\partial \mathbf{x}_j} \right] f_\beta(\boldsymbol{\beta}) d\boldsymbol{\beta} = \mathbf{0}$ $\forall k, j \in J_k$
Franchised Retailer (FR)	$\frac{\partial \Pi_k^{\mathrm{M}}}{\partial w_j} = \int_{\boldsymbol{\beta}} s_{j\mid\boldsymbol{\beta}} \left[\frac{\partial v_{j\mid\boldsymbol{\beta}}}{\partial p_j} \left(\left(w_j - c_j\right) - \sum_{j' \in J_k} s_{j'\mid\boldsymbol{\beta}} \left(w_{j'} - c_{j'}\right) \right) + 1 \right] f_\beta(\boldsymbol{\beta}) d\boldsymbol{\beta} = 0$ $\frac{\partial \Pi_k^{\mathrm{M}}}{\partial \mathbf{x}_j} = \int_{\boldsymbol{\beta}} s_{jt\mid\boldsymbol{\beta}} \left[\left(\frac{\partial v_{j\mid\boldsymbol{\beta}}}{\partial \mathbf{z}_j} \frac{\partial \mathbf{z}_j}{\partial \mathbf{x}_j} \right) \left(\left(w_j - c_j\right) - \sum_{j' \in J_k} s_{j'\mid\boldsymbol{\beta}} \left(w_{j'} - c_{j'}\right) \right) - \frac{\partial c_j}{\partial \mathbf{x}_j} \right] f_\beta(\boldsymbol{\beta}) d\boldsymbol{\beta} = \mathbf{0}$ $\frac{\partial \Pi^{\mathrm{R}}}{\partial m_j} = \int_{\boldsymbol{\beta}} s_{j\mid\boldsymbol{\beta}} \left[\frac{\partial v_{j\mid\boldsymbol{\beta}}}{\partial p_j} \left(m_j - \sum_{j' \in J_k} s_{j'\mid\boldsymbol{\beta}} m_{j'} \right) + 1 \right] f_\beta(\boldsymbol{\beta}) d\boldsymbol{\beta} = 0$ $\forall k, j \in J_k$
Single Common Retailer (SCR)	$\frac{\partial \Pi_k^{\mathrm{M}}}{\partial w_j} = \int_{\boldsymbol{\beta}} s_{j\mid\boldsymbol{\beta}} \left[\frac{\partial v_{j\mid\boldsymbol{\beta}}}{\partial p_j} \left(\left(w_j - c_j\right) - \sum_{j' \in J_k} s_{j'\mid\boldsymbol{\beta}} \left(w_{j'} - c_{j'}\right) \right) + 1 \right] f_\beta(\boldsymbol{\beta}) d\boldsymbol{\beta} = 0$ $\frac{\partial \Pi_k^{\mathrm{M}}}{\partial \mathbf{x}_j} = \int_{\boldsymbol{\beta}} s_{jt\mid\boldsymbol{\beta}} \left[\left(\frac{\partial v_{j\mid\boldsymbol{\beta}}}{\partial \mathbf{z}_j} \frac{\partial \mathbf{z}_j}{\partial \mathbf{x}_j} \right) \left(\left(w_j - c_j\right) - \sum_{j' \in J_k} s_{j'\mid\boldsymbol{\beta}} \left(w_{j'} - c_{j'}\right) \right) - \frac{\partial c_j}{\partial \mathbf{x}_j} \right] f_\beta(\boldsymbol{\beta}) d\boldsymbol{\beta} = \mathbf{0}$ $\frac{\partial \Pi^{\mathrm{R}}}{\partial m_j} = \int_{\boldsymbol{\beta}} s_{j\mid\boldsymbol{\beta}} \left[\frac{\partial v_{j\mid\boldsymbol{\beta}}}{\partial p_j} \left(m_j - \sum_{k' \in K} \sum_{j' \in J_{k'}} s_{j'\mid\boldsymbol{\beta}} m_{j'} \right) + 1 \right] f_\beta(\boldsymbol{\beta}) d\boldsymbol{\beta} = 0$ $\forall k, j \in J_k$
Multiple Common Retailers (MCR)	$\frac{\partial \Pi_k^{\mathrm{M}}}{\partial w_{jt}} = \int_{\boldsymbol{\beta}} s_{jt\mid\boldsymbol{\beta}} \left[\frac{\partial v_{jt\mid\boldsymbol{\beta}}}{\partial p_{jt}} \left(\left(w_{jt} - c_j\right) - \sum_{j' \in J_k} \sum_{t' \in T} s_{j't'\mid\boldsymbol{\beta}} \left(w_{j't'} - c_{j'}\right) \right) + 1 \right] f_\beta(\boldsymbol{\beta}) d\boldsymbol{\beta} = 0$ $\frac{\partial \Pi_k^{\mathrm{M}}}{\partial \mathbf{x}_j} = \int_{\boldsymbol{\beta}} \sum_{t \in T} \left[\left(\frac{\partial v_{jt\mid\boldsymbol{\beta}}}{\partial \mathbf{z}_j} \frac{\partial \mathbf{z}_j}{\partial \mathbf{x}_j} \right) \left(s_{jt\mid\boldsymbol{\beta}} \left(w_{jt} - c_j\right) - \left(\sum_{\bar{t} \in T} s_{j\bar{t}\mid\boldsymbol{\beta}} \right) \sum_{j' \in J_k} s_{j't\mid\boldsymbol{\beta}} \left(w_{j't} - c_{j'}\right) \right) - s_{jt\mid\boldsymbol{\beta}} \frac{\partial c_j}{\partial \mathbf{x}_j} \right] f_\beta(\boldsymbol{\beta}) d\boldsymbol{\beta} = \mathbf{0}$ $\frac{\partial \Pi_t^{\mathrm{R}}}{\partial m_{jt}} = \int_{\boldsymbol{\beta}} s_{jt\mid\boldsymbol{\beta}} \left[\frac{\partial v_{jt\mid\boldsymbol{\beta}}}{\partial p_{jt}} \left(m_{jt} - \sum_{k' \in K} \sum_{j' \in J_{k'}} s_{j't\mid\boldsymbol{\beta}} m_{j't} \right) + 1 \right] f_\beta(\boldsymbol{\beta}) d\boldsymbol{\beta} = 0$ $\forall t, k, j \in J_k$

Proposition 1: *In the logit case with utility linear in price, the Nash equilibrium requires that each manufacturer has equal margins for all its products.*

Proof: From the wholesale price FOC equation for the general MCR case under the logit model, the equation can be rearranged to:

$$w_{jt}-c_j=-\left(\frac{\partial v_{jt}}{\partial p_{jt}}\right)^{-1}+\sum_{j'\in J_k}\sum_{t'\in T}s_{j't'}\left(w_{j't'}-c_{j'}\right)\qquad \forall j\in J_k \tag{3.14}$$

For the case where v_j is linear in price, $\partial v_j/\partial p_j = \beta_p$, and the right hand side of the equation is identical for all $j\in J_k$. Therefore, each product produced by manufacturer k has the identical manufacturing margins $w_{jt}-c_j$. This result holds for the other channel types, which are special cases of Eq. (3.14).

Proposition 2: *In the logit case with utility linear in price, the Nash equilibrium requires that retail margins are equal for all products and all retailers.*

Proof: From the retail margin FOC equation for the general MCR case under the logit model, the retail margin of product *j* selling at retailer *t* is:

$$m_{jt}=-\left(\frac{\partial v_{jt}}{\partial p_{jt}}\right)^{-1}+\sum_{k'\in K}\sum_{j'\in J_{k'}}s_{j'}m_{j't}\qquad \forall j\in J_k \tag{3.15}$$

For the case where v_j is linear in price, $\partial v_j/\partial p_j = \beta_p$, and the right hand side of the equation is identical for all products sold by retailer *t* or any other retailer. Therefore, the retail margins of all products are equal. This result holds for the other channel types (FR and SCR), which are special cases of Eq. (3.15).

The third proposition shows that design is independent of pricing and competition under the linear logit model. This implies that design can successfully be undertaken independently when consumers are homogeneous (or, more precisely, when variation among consumers is taken as

IID random noise in the logit model). However, heterogeneity couples the problems, making necessary joint consideration of design with pricing and competition.

Proposition 3: *In the logit case with utility linear in price, the Nash equilibrium requires that all designs satisfy a system of equations that is independent of price and competitor designs. When this system of equations has a unique solution, it implies that (a) all designs are identical across all producers and (b) the optimal design is independent of price, competition, and channel structure.*

Proof: By substituting Eq. (3.14) from Proposition 1 into Eq. (3.9) for the general MCR case under the logit model (integral removed), we obtain a simplified equilibrium equation:

$$\left(\sum_{t\in T} s_{jt}\right)\left(-\left(\frac{\partial v_{jt}}{\partial p_{jt}}\right)^{-1}\frac{\partial v_{jt}}{\partial \mathbf{x}_j}-\frac{\partial c_j}{\partial \mathbf{x}_j}\right)=\mathbf{0} \tag{3.16}$$

Because $s > 0$ (for all finite values of the decision variables), for the case where v_j is linear in price, $\partial v_j/\partial p_j = \beta_\mathrm{p}$, the function can be presented as:

$$\frac{\partial v_{jt}}{\partial \mathbf{z}_j}\frac{\partial \mathbf{z}_j}{\partial \mathbf{x}_j}+\beta_\mathrm{p}\frac{\partial c_j}{\partial \mathbf{x}_j}=\mathbf{0} \quad \forall t\in T\mathbf{,}\ j\in J_k \tag{3.17}$$

Satisfaction of this system of equations is a necessary condition for a Nash equilibrium. If Eq. (3.17) has a unique solution and if a Nash equilibrium exists, then Eq. (3.17) specifies the equilibrium design. Implication (a) follows from noting that Eq. (3.17) is identical for each j and is independent of all other $j'\neq j$.[18] Implication (b) follows from noting that Eq. (3.17) is independent of p_j, $p_{j'}$, $\mathbf{x}_{j'}$ $\forall j'\neq j$. In other words, the equilibrium design can be calculated as a function of consumer utility functions and manufacturer cost functions without regard to price or

[18] Note also that for the special case of traditional profit maximization of a product line for a single producer with fixed competitors (outside good) and no retail structure (CS case), this implies that under logit linear in price all products in the line will be identical at the optimum.

competitor decisions, and design is decoupled from the game. While we do not derive conditions under which Eq. (3.17) has a unique solution, we observe that in practical applications Eq. (3.17) typically has a unique solution or a small finite number of candidate solutions that can be checked post hoc for satisfaction of the Nash definition.

The final two propositions show the necessity of incorporating an outside good to establish finite equilibria in the case of a manufacturer or retailer monopoly.

Proposition 4: *In the logit case with utility linear in price and a monopolist manufacturer, an outside good is required for existence of a finite Nash equilibrium.*

Proof: Considering a single manufacturer with multiple common retailers (MCR case), the outside good market share $s_0 = 1-\Sigma_{j\in J}\,\Sigma_{t\in T}\,s_{jt}$. For the case where v_j is linear in price, $\partial v_j/\partial p_j=\beta_\mathrm{p}$. Following Proposition 1 and substituting the s_0 expression into the MCR wholesale price FOC equation in Table 3 with the integral collapsed, the manufacturing margin solution at equilibrium becomes a function of s_0:

$$w_{jt}-c_j=-\left(\frac{\partial v_{jt}}{\partial p_{jt}}\right)^{-1}\left(1-\sum_{j'\in J}\sum_{t'\in T}s_{j't'}\right)^{-1}=\frac{-1}{\beta_\mathrm{p}s_0} \qquad \forall t\in T,\, j\in J \tag{3.18}$$

When the outside good is not included in the demand model, s_0=0, and Eq. (3.18) is undefined, implying no finite solution. This result holds true for all four channel types.

Proposition 5: *In the logit case with utility linear in price and a monopolist retailer, an outside good is required for existence of a finite Nash equilibrium.*

Proof: In the SCR case, the market share of the outside good $s_0=1-\Sigma_{k\in K}\Sigma_{j\in Jk}s_j$. With utility linear in price, $\partial v_j/\partial p_j=\beta_\mathrm{p}$. Following Proposition 2 and substituting the s_0 expression into the MCR retail margin FOC equation in Table 3 with the integral collapsed, the retail margin solution at equilibrium becomes a function of s_0:

$$m_j = -\left(\frac{\partial v_{jt}}{\partial p_{jt}}\right)^{-1}\left(1 - \sum_{k' \in K}\sum_{j' \in J_{k'}} s_{j'}\right)^{-1} = \frac{-1}{\beta_{\mathrm{p}} s_0} \quad \forall j \in J_k \tag{3.19}$$

When the outside good is not included in the demand model (s_0 = 0) and Eq. (3.19) becomes undefined, implying no finite solution. Since the retail price is decided by the single common retailer's profit maximization behavior, the absence of an outside good implies that consumers have no other choice and must purchase one of the products from the retailer. For the estimation studies of the single common retailer pricing behavior in the marketing science literature, the outside good is usually included in the logit choice model to represent the consumer's no-purchase choice (Besanko et al., 1998; Sudhir, 2001).

3.3 Case Study: Vehicle Design

Theoretical results show that the design is decoupled from competition and channel structures for the logit model. However, it does not necessarily follow that designs will differ substantially at equilibrium under alternative channel structures for representative problems in the engineering design domain when heterogeneity is present. To demonstrate the methodology and test the sensitivity of design solutions to channel structure, we adopt the vehicle design model proposed by Michalek et al. (2004), which integrated engineering simulations of vehicle performance with logit models of consumer choice to study vehicle design of profit seeking firms in competition under the CS channel structure.

Following the vehicle design model in (Michalek et al., 2004), we take the firm's decision variables[19] to be the relative size of the vehicle's engine x_1, final drive ratio x_2, and wholesale price w. We examine only the default small car equipped with a SI-102 spark-ignition engine (base engine power 102 kW) and use the ADVISOR-2004 vehicle simulator (AVL, 2004) to simulate performance data. Specifically, two attributes, gas mileage z_1 and required time to accelerate from 0-60mph z_2, are simulated as a function of x_1 and x_2. To calculate z_1, two EPA regulated drive cycles, for city (Federal Test Procedure, FTP) and highway (Highway Fuel Economy Test, HWFET) driving, were simulated, with z_1 = 1/(0.55/city+0.45/highway) (EPA, 2004). The acceleration performance is calculated through simulated full throttle acceleration. To simplify calculations, simulation points were taken over a range of variable values, and curve-fitting was used to create a meta-model for each $z_1(x_1,x_2) = 2.34x_1^2-6.72x_2^2-0.81x_1x_2-16.0x_1+11.2x_2+38.6$ and $z_2(x_1,x_2) = 2.22\cdot\exp(-1.85x_1+2.25)+4.39x_2^2-10.6x_2+12.2$. Over the points in the sample, the curves deviate from simulator predictions by no more than 0.3 mpg and 0.7 seconds. Each design variable has associated lower and upper bounds: $1.0\leq x_1\leq 3.0$ and $0.8\leq x_2\leq 1.3$. The cost function, built from a regression on engine sales data (Michalek et al., 2004), is given by $c^V=7500+670.5\cdot\exp(0.643x_1)$.

The logit model utility form was adopted from a study by Boyd and Mellman (1980), where $v_j = \beta_p p_j + 100\beta_1/z_{1j} + 60\beta_2/z_{2j}$, and β_p, β_1 and β_2 are the coefficients of each attribute. The study provided the coefficients for both logit and mixed logit models. For aggregate logit, $\beta_p = -2.84\times10^{-4}$, $\beta_1 = -0.339$ and $\beta_2 = 0.375$. For mixed logit, each beta coefficient is taken as following an independent lognormal distribution. The random coefficients are given by $\boldsymbol{\beta}=\exp(\boldsymbol{\eta}+\boldsymbol{\Phi}\boldsymbol{\sigma})$, where $\boldsymbol{\Phi}$ is the standard normal distribution and $\boldsymbol{\eta}$ and $\boldsymbol{\sigma}$ are the lognormal

[19] We assume that automotive manufacturers are capable of adjusting engine power and final drive gear ratio on their existing engines and gearboxes without complete re-design from scratch. Therefore automakers compete on both vehicle design and price in a static timeframe.

parameters[20]. The parameters for the three vehicle attributes are $\eta_p = -7.94$, $\eta_1 = -1.28$, $\eta_2 = -1.75$, $\sigma_p = 1.18$, $\sigma_1 = 0.001$ and $\sigma_2 = 1.34$. The means of $\boldsymbol{\beta}$ are thus -7.15×10^{-4}, -0.278 and 0.426, respectively. Compared to the logit coefficients, the mean mixed logit preferences are more sensitive to price and acceleration time, but less sensitive to fuel economy. It is noted that the logit and mixed logit preference coefficients do not represent unique market characteristics, but only different demand modeling approximations. The histograms in Figure 3.3 show the approximated shape of the lognormal distribution for each coefficient using 1000 random draws (R=1000). The standard deviations of the mixed logit coefficients in the normal space, 1.24×10^{-3}, 2.78×10^{-4} and 0.956, disclose that consumer taste variation for acceleration performance is relatively larger than the other two attributes. The distribution of the fuel economy coefficient is the most concentrated among three attributes because of its small deviation value.

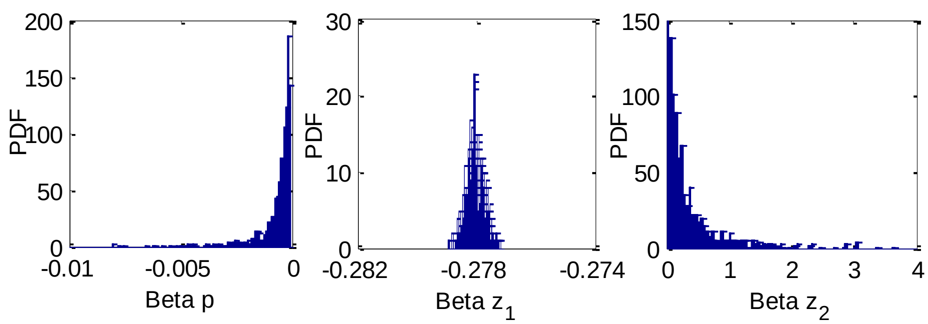

Figure 3.3 Distributions of consumer preference coefficients in the mixed logit model

[20] The mean and standard deviation of a lognormal distribution are $\exp(\eta+\sigma^2/2)$ and $[(\exp(\sigma^2)-1)\cdot\exp(2\eta+\sigma^2)]^{1/2}$ respectively.

Further, we assume the outside good utility v_0 is equal to zero throughout the case study in order to avoid the monopoly pricing issue revealed in Proposition 5, although estimation of the outside good was not included in the original study. In particular, if an outside good were included during the initial maximum likelihood data fitting procedure[21], we would expect the relative utility of the outside good to differ in the logit and mixed logit model fits, so attaching an arbitrary outside good utility post hoc should not be expected to yield accurate share of choices predictions for the auto market. Still, the example serves well to illustrate the structure of the problem and the method and principles outlined here. We examine the case of two manufacturers for all four scenarios and two common retailers in the MCR scenario. The total market size Q is given by 1.57×10^6 (Michalek et al., 2004). We solve the FOC equations for each scenario using the sequential quadratic programming (SQP) implementation in the Matlab Optimization Toolbox and verify that solutions are Nash by globally optimizing each player separately post hoc using a multistart loop. The results at market equilibrium under all eight scenarios are shown in Table 3.4.[22] In all cases except the mixed logit MCR case, competing firms have identical solutions to one another at equilibrium, so only the solution of one manufacturer and one retailer is reported.[23] The mixed logit MCR case results in firms selecting distinct strategies, so all solutions are reported. Specifically, the first two rows in the mixed logit MCR scenario show manufacturer M1's products sold through the two retailers R1 and R2. M1's profit is the sum of M1-R1 and M1-R2, and similarly R1's profit is the sum of M1-R1 and M2-R1.

[21] Besanko *et al.* (Besanko et al., 1998) and Sudhir (Sudhir, 2001) use zero utility as outside good in their estimations for the market data.

[22] There is no active constraint for the solutions in all cases.

[23] Under assumptions of constant marginal cost and identical fixed cost, Anderson *et al.* (Anderson et al., 1992) proved that under multinomial logit in an oligopolistic model there exists a unique and symmetric price equilibrium when the profit function is strictly quasi-concave.

Results verify that the equilibrium design is unchanged under alternative channel structures in the logit case, although wholesale price and retail price vary. This is expected since the conditions satisfy Proposition 3. In this case the optimal design is independent of the game, and the resulting wholesale prices and retail margins can be interpreted as the outcomes of pure price competition. In the CS scenario, manufacturers are the only decision makers and thus have the highest wholesale price and profit, due to the integrated retailer (profits need not be split among manufacturers and retailers). For the SCR scenario, the monopolistic retailer has the highest unit retail margin and also the highest profit because of its dominative power among channel members. Since consumers can only choose between the products offered by the retailer and the outside good, lack of price competition leads to high prices. For the FR and MCR scenarios, neither the manufacturer nor the retailer has dominative power in the market channel. However, for the same outside good, the MCR scenario is able to gain higher total market share (7.2% vs. 4.1%) and higher profits ($422M vs. $235M) than the FR. The MCR channel provides the manufacturer with higher market share than a single franchised dealer. Furthermore, we expect that the logit model will tend to overestimate demand for similar products in a competitive market because the logit's independence from irrelevant alternatives (IIA) property restricts substitution patterns and underestimates the degree to which similar (or in this case, identical) products draw market share from one another (Train, 2003). In contrast to the identical designs under the logit model, the mixed logit model results in substantially different design solutions under different channel structure scenarios. Comparing equilibrium vehicle designs between the two demand models, logit results reveal a less powerful engine design than under mixed logit, which is not unexpected since the relative scale between fuel economy and the other coefficients estimated in logit is relatively greater than the mean coefficient in mixed logit.

Table 3.4 Vehicle price and design solutions at market equilibrium

			Price and Cost					Design				Market Performance		
			Wholesale price w	**Vehicle cost** c^{V}	**Manufr. margin** $w-c^{V}$	**Retailer margin** m	**Retail price** p	**Eng. scale** x_1	**FD ratio** x_2	**MPG** z_1	**Acc. time** z_2	**Market share** s	**Manufr. profit** Π^{M}	**Retailer profit** Π^{R}
Logit	**CS**	M1 M2	\$13,168	\$9,301	\$3,867	N/A	\$13,168	1.54	1.12	22.2	7.11	9.6%	\$583M	N/A
	FR	M1 M2	\$12,947	\$9,301	\$3,646	\$3,646	\$16,593	1.54	1.12	22.2	7.11	4.1%	\$235M	\$235M
	SCR	M1 M2	\$12,941	\$9,301	\$3,640	\$16,737	\$29,678	1.54	1.12	22.2	7.11	3.9%	\$225M	\$470M
	MCR	M1-R1 M1-R2 M2-R1 M2-R2	\$13,066	\$9,301	\$3,765	\$3,765	\$16,831	1.54	1.12	22.2	7.11	3.6%	$\Pi^{M}{}_{1}=$ \$422M $\Pi^{M}{}_{2}=$ \$422M	$\Pi^{R}{}_{1}=$ \$422M $\Pi^{R}{}_{2}=$ \$422M
Mixed Logit	**CS**	M1 M2	\$17,083	\$10,167	\$6,916	N/A	\$17,083	2.15	1.16	16.9	6.26	11.9%	\$1155M	N/A
	FR	M1 M2	\$18,713	\$10,364	\$8,349	\$8,349	\$27,062	2.26	1.16	16.1	6.19	7.3%	\$952M	\$952M
	SCR	M1 M2	\$58,044	\$11,441	\$46,603	\$246,564	\$304,608	2.76	1.17	13.5	6.00	0.3%	\$255M	\$2,702M
	MCR	M1-R1	\$42,899	\$10,327	\$32,572	\$32,572	\$75,471	2.24	1.16	16.2	6.20	0.3%	$\Pi^{M}{}_{1}=$ \$1066M	$\Pi^{R}{}_{1}=$ \$1066M
		M1-R2	\$18,490	\$10,327	\$8,163	\$8,164	\$26,654					7.2%		
		M2-R1	\$18,490	\$10,327	\$8,163	\$8,164	\$26,654	2.24	1.16	16.2	6.20	7.2%	$\Pi^{M}{}_{2}=$ \$1066M	$\Pi^{R}{}_{2}=$ \$1066M
		M2-R2	\$42,899	\$10,327	\$32,572	\$32,572	\$75,471					0.3%		

The CS case results in the highest manufacturer profit and market share among the four channel types, as might be expected because there is no retailer competing with the manufacturer.[24] We also found that a smaller engine is chosen and greater fuel economy is achieved in the CS case than the other three cases. The FR case results in equal margins for manufacturers, and an intermediate design result at the market equilibrium. The SCR case shows an extreme solution with high retail margin, which results in high retail price and low market share. In this case, each manufacturer's profit is drastically reduced due to low demand, though wholesale price is increased significantly at market equilibrium. The equilibrium strategy in this case appears to target those few consumers willing to pay high price at a premium for the product when no alternative is available except the outside good. As such, the solution is sensitive to the utility of the outside good. We conducted a sensitivity analysis and found that the retail price (retail margin) is more sensitive to the utility of the outside good, while the manufacturer wholesale price is less affected.

The mixed logit MCR case presents an interesting result. The solution indicates that the best strategy for manufacturers is to offer different wholesale prices for the same product to different retailers.[25] Each common retailer's best margin decision is to set a higher margin on the high price product and lower margin on low price product. Therefore each product has a high-low price pair, causing significant market share differences. The two manufacturers and two common retailers have similar profits, and the vehicle design solutions in this case are close to the FR design solutions. This solution appears to set low prices that target the general population but also offer the *same design* at higher prices in order to target a very small segment of the

[24] In the Nash game, the number of players in game affects the price and profit at equilibrium. For example, a monopoly results in higher profit and prices than an oligopoly (Mas-Colell et al., 1995).

[25] A saddle point is found in the MCR model, which has identical solutions across manufacturers and retailers (w=\$19,275, m=\$8,990, x_1=2.22, x_2=1.16). It satisfies the first-order criterion but fails in Nash equilibrium verification.

market (0.3%) that is insensitive to price. Although the lognormal distribution insures that all consumers prefer lower prices (β_p<0), the price-insensitive consumers (with β_p≈0) will choose the higher priced product with some nonzero probability and provide high profit per consumer to the manufacturer and retailer. The particular results for the SCR and MCR cases may contain artifacts from (1) predicting consumer choice at high prices, which requires extrapolation of the utility function beyond the range of existing market data, and (2) assuming a specific distributional shape (IID lognormal) for the mixed logit utility function parameters. The high price solutions for the SCR case are not unexpected: If there existed an unregulated monopolist retailer in the automotive market, the retailer would own dominating market power to control retail price, and we expect that prices would be higher than what we observe in today's market. However, extrapolation of the utility function far beyond the data points used to fit it introduces additional uncertainty. Retail margins and prices are expected to decrease when more manufacturer and retailers are involved due to increased competition.[26]

Under the mixed logit model, the smallest engine design, which is the lowest cost design, is found in the CS case where there is no retail buffering (Gupta and Loulou, 1998) between the manufacturer and consumer. The SCR case, where a monopolist retailer creates strong buffering, results in the largest engine design. The company store is an integrated channel that takes no retailer profit, and the manufacturer gains the highest profit in this case. The franchised retailer and manufacturer have equal "power" in our case study of two manufacturers and two retailers, and each makes equal profit at equilibrium. The single common retailer has the highest retail margin due to domination of the regional market and reduced competition. The multiple common

[26] Anderson *et al.* (Anderson et al., 1992) showed that under standard logit a producer's margin is proportional to the inverse of number of producers minus one (section 7.2). Therefore, including more producers would reduce the margin and price.

retailer case presents the results of two-level competition and its optimal decisions show different price decisions for the same product design at market equilibrium.

Overall, these results verify that optimal design decisions depend on competition and channel type when heterogeneity is taken into account. Only under linear logit demand can the problem generally be reduced to pure pricing competition and independent design optimization.

3.4 Summary

We pose a game-theoretic model for determining equilibrium design and pricing decisions of profit seeking firms in competition, and we examine the influence of two factors: (1) the structure of manufacturer-retailer interactions in the market and (2) the structure of heterogeneity in consumer preference modeling. We find that the influence of these factors to firms' equilibrium design decisions is coupled: Under linear logit the optimal design can be determined independently of price and competition. However, consumer preference heterogeneity (mixed logit) couples the two problems, bringing design into the competitive game. The results from a vehicle design case study show that profit-maximizing designs can change substantially under alternative channel structures for practical problems. Thus, as consumer heterogeneity becomes increasingly important to modeling market phenomena for guiding design, it will also become more important to effectively coordinate product planning decisions with engineering design decisions.

CHAPTER 4. EVALUATION OF PHEV ECONOMIC AND ENVIRONMENTAL PERFORMANCES

Increasing concerns regarding high oil prices, fossil fuel dependency, and climate change have resulted in policymakers and the automobile industry evaluating alternative strategies for passenger transportation. Plug-in hybrid electric vehicle (PHEV) technology offers a possible approach to reducing lifecycle GHG emissions and dependency on oil by displacing propelling energy on fuel by electricity from the electrical grid (Romm, 2006; EPRI, 2007; Samaras and Meisterling, 2008; Bradley and Frank, 2009). While the U.S. transportation sector is overwhelmingly powered by petroleum, oil-fired power plants provide only about 1.6% of U.S. electricity generation (EIA, 2009). The price differential between retail electricity and gasoline could make electric-powered travel more cost competitive than gasoline, depending on the additional vehicle capital costs (Scott et al., 2007; Lemoine et al., 2008). However, the benefits of PHEVs depend on the vehicle and battery characteristics - PHEVs require large batteries for energy storage, which affect vehicle cost, weight, and performance; more batteries enable PHEVs to have longer electric travel capacity but the additional weight may deter the expected advantages of PHEVs.

This chapter presents an assessment about the economic and environmental performances of plug-in hybrid technology. PHEV simulation models are constructed to explore the impact of battery size on fuel consumption, cost, and GHG emission benefits over a range of distances between charges. The tradeoffs identified in this analysis can provide a space for vehicle manufacturers, policymakers, and the public to examine optimal decisions for PHEV design, policy and use. The content in this chapter is based on the publication by Shiau et al. (2009).

4.1 Plug-in Hybrid Systems

All PHEVs have a drivetrain that incorporates an electric motor and an internal combustion engine (ICE), and like conventional hybrid electric vehicles (HEVs) these components can be arranged in (1) *series*, (2) *parallel*, or (3) *split* configurations (Frank, 2007). In a series configuration, the engine provides electrical power through a generator to charge the battery and power the motor, and the motor provides torque to the wheels. The primary advantage of the series configuration is the ability to size the engine for average, rather than peak, energy needs and run it at its most efficient operating point. However, relatively large batteries and motors are required to satisfy peak power requirements, and efficiency losses are inherent in converting mechanical energy to electrical energy and back to mechanical energy again. In a parallel configuration, such as the Honda Civic and Accord hybrids, the engine and motor both provide torque to the wheels, and the engine charges the battery only by applying torque to the motor in reverse – there is no separate generator. Because the engine provides torque to the wheels, the battery and motor can be sized smaller, but the engine is not free to operate at its most efficient point. A split powertrain, such as the one used in the popular Toyota Prius, uses a planetary gear system power split device and a separate motor and generator to allow the engine to provide torque to the wheels and/or charge the battery through the generator, depending on use conditions. The split drivetrain has the benefits of the series and parallel systems, but it requires more components.

The hybrid drivetrain has several advantages in terms of improving vehicle efficiency. First, the additional electric motor enables the engine to operate at its most efficient load more of the time, utilizing the batteries to smooth out spikes in power demand. Second, having an additional source of power in the form of an electric motor enables designers to select smaller engine designs with higher fuel efficiency and lower torque capabilities. Third, HEV and PHEV powertrains enable energy that is otherwise lost in braking to be captured to charge the battery and enable the engine to be shut off rather than idling when the vehicle is at rest – both of which reduce energy waste during vehicle operations, especially in urban driving conditions.

We focus on the split configuration in our PHEV study because of its flexibility to perform similarly to a parallel or series drivetrain. The block diagrams in Figure 4.1 show the structure of the powertrain system in a split PHEV and its energy flow during operation. The structure of a PHEV is similar to that of an ordinary HEV, except the PHEV carries a larger battery pack and offers plug-charging capability (Frank, 2007). PHEVs store energy from the electrical grid (produced from a variety of energy sources at power plants) to partially offset gasoline use for propulsion. The system has two energy storage devices – a fuel tank for gasoline and a battery pack for electricity – and three power generation devices – an internal combustion engine, a traction motor and a control motor. The traction motor has higher power output than the control motor and delivers major electrical energy to propel the vehicle. The smaller control motor assists the engine to operate near its optimal efficiency range and balances torque and speed requirements. The power from the engine and motors is coupled by a planetary gear set and then delivered to the wheels. There are two different energy flow paths: electricity energy flow and gasoline energy flow. All electricity flow is bidirectional because the two motors can function as generators.

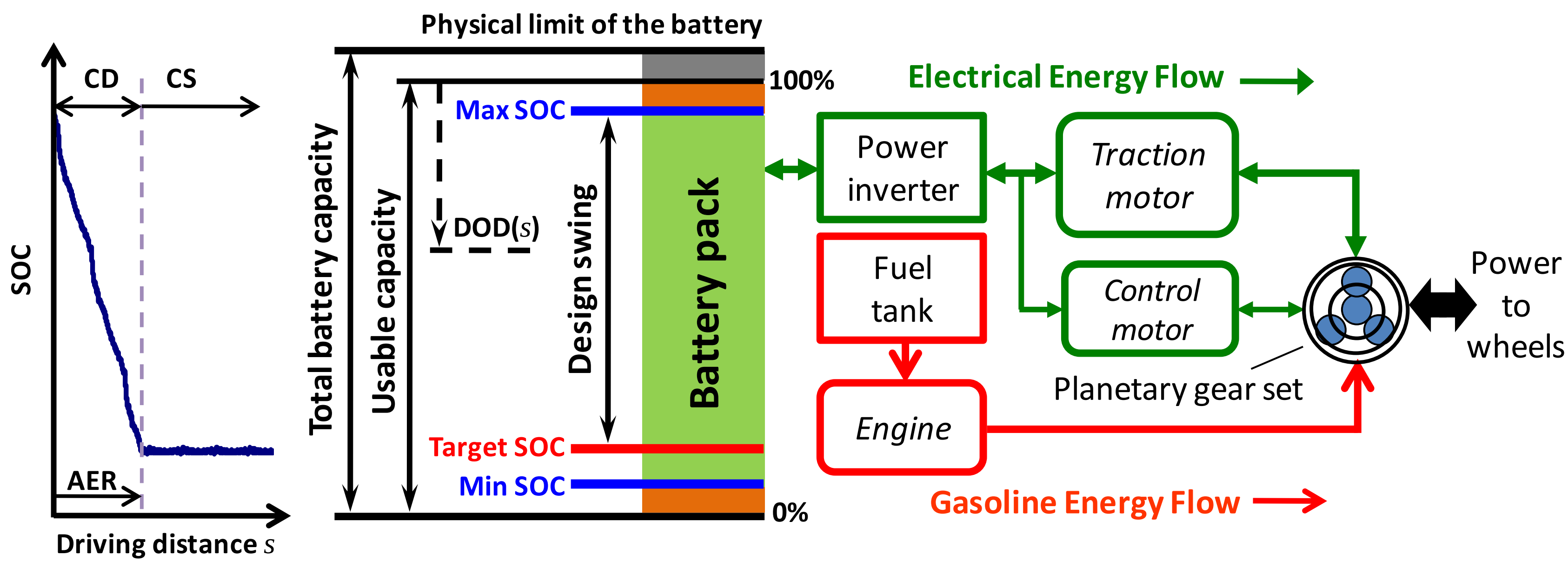

Figure 4.1 Energy flow in a PHEV with a split powertrain system

The battery of a PHEV, which can be recharged using conventional electrical outlets, would allow the vehicle to drive for a limited range using energy from the electricity grid. A fully charged PHEV operates in *charge-depleting mode* (CD mode) until the battery is depleted to a target state of charge (SOC), at which point the vehicle switches to *charge-sustaining mode* (CS mode), using the engine to maintain the target SOC. A PHEV can be further categorized as (1) *all-electric* or (2) *blended*, depending on its energy management strategy in the charge-depleting state (Bradley and Frank, 2009). An all-electric PHEV functions as a pure electric vehicle (EV) in CD mode, using only electrical energy from the battery for propulsion and disabling any engine operation. Blended PHEVs invoke a strategy where the motor provides primary power in charge-depleting mode, but the engine is used as needed to provide additional power. In the charge-sustaining state, all PHEVs operate similarly to a standard HEV, using the engine to maintain the target battery SOC.

Since the performance of blended PHEV can vary widely based on a broad range of control strategy parameters, for simplicity and fair comparisons we restrict attention to all-electric PHEVs, which disables engine operation in CD mode and draws propulsion energy entirely from the battery until it reaches a target SOC, as shown in Figure 4.1. The distance that a PHEV can travel on electricity alone with a fully charged battery is called its *all-electric range* (AER)[27]. Once the driving distance reaches the AER and the battery is depleted to the target SOC, the PHEV switches to operate in CS mode, and the gasoline engine provides energy to propel the vehicle and maintain battery charge near the target SOC. In CS mode, the PHEV operates similar to an ordinary HEV.

[27] AER is defined as energy-equivalent electric propulsion distance for blended mode PHEVs, but we consider only all-electric PHEVs here (Markel et al., 2006).

The battery diagram in Figure 4.1 presents several definitions relevant to battery capacity. Total battery capacity is determined by the physical charge limits of the battery. Since manufacturing variability implies that every battery cell has a different physical charge limit, battery manufacturers often define 100% SOC at a more controllable level under the upper limit. The capacity window between 0% and 100% defines the usable capacity of the battery. Maximum, target, and minimum SOC are further determined by hybrid vehicle designers based on their design application. We define the capacity window between maximum and target SOC as design swing, and the ratio of discharged capacity to the usable capacity as depth of discharge (DOD), where DOD is a function of driving distance *s*. We further define state of energy (SOE) as the percent of energy remaining in the battery: SOE = energy remaining / energy capacity. If the battery voltage is constant with SOC, then SOC and SOE are equivalent; however, we use SOE in our model to account for voltage variation and focus on the quantity of interest.

4.2 Effects of Battery Weight on PHEVs

Since PHEVs rely on large storage batteries for any economic or environmental benefits relative to traditional hybrids and ICE vehicles, the characteristics and design issues associated with PHEV batteries play an important role in the potential adoption of PHEVs. Consumer acceptance and adoption will mainly depend on battery cost, operating cost, power and performance, battery cycle and calendar life, and safety, among other characteristics. Overviews of the current state of battery technology for PHEV applications as well as future goals are provided in (Burke, 2007; Kalhammer et al., 2007; Karden et al., 2007; Axsen et al., 2008). The two current dominant battery technologies considered likely candidates for PHEV applications are nickel-metal hydride (NiMH) and lithium-ion (Li-ion) batteries. NiMH batteries have performed well and have proven reliable in existing hybrids vehicles (Kalhammer et al., 2007).

However, their relatively low energy density (Wh/liter) and specific energy (Wh/kg) implies large, heavy batteries for extended electric travel. Li-ion batteries have higher energy density and specific energy and are benefiting from increased technological advancement, but concerns regarding calendar life, and safety (internal corrosion and high environment temperatures could cause Li-ion batteries to combust) (Karden et al., 2007). Another issue is that both batteries self-discharge more rapidly at high temperature, which reduces charge capacity and battery life (Axsen et al., 2008). In spite of the technical difficulties to be overcome, Li-ion batteries have been widely evaluated for their great potential as PHEV energy storage devices (Burke, 2007; Kalhammer et al., 2007; Karden et al., 2007; Axsen et al., 2008), thus we focus on Li-ion batteries in this study.

The energy required to produce the raw materials and manufacture the Li-ion battery have been estimated to account for approximately 2-5% of the life cycle GHG emissions from a PHEV, which is relatively small if the original battery can last the life of the vehicle (Samaras and Meisterling, 2008). During vehicle operation, the battery mass in PHEVs is large enough to affect fuel economy and acceleration. Due to data constraints, previous studies evaluating the GHG benefits of PHEVs assumed that the additional weight of potentially large storage batteries did not affect the gasoline fuel economy or the electrical requirements for propulsion. Zervas and Lazarou (2008) presented relationships between ICE vehicle weight and CO_2 emissions and argued that exploring weight thresholds for passengers cars in the European Union could help reduce GHGs from passenger transportation. Furthermore, a preliminary regression estimation of the impact of weight and power on traditional hybrids found that weight decreases hybrid fuel economy (Reynolds and Kandlikar, 2007). Hence, technical sensitivity analysis is warranted to explore the impact of additional battery and potential structural weight on fuel consumption, greenhouse gas emissions, and operating costs of PHEVs.

Conventional vehicles (CVs) that hold more fuel can travel farther without refueling. Similarly, PHEVs with larger battery capacity can travel farther on electricity before drawing on liquid fuel. However, batteries have a considerably lower specific energy than liquid fuel: When a vehicle is filled with 10 gallons (38 liters) of gasoline, it contains approximately 360 kWh of energy embodied in the fuel. The vehicle weighs an additional 28 kg, and it gradually loses those that weight as the fuel is combusted in the engine. In contrast, a PHEV battery pack may contain 3-30 kWh and weigh 30-300 kg plus the additional vehicle structural weight required to carry these batteries, and the vehicle must carry this weight even after the battery is depleted. Additional battery weight decreases the attainable efficiency in miles per kWh in CD-mode as well as miles per gallon in CS mode (once the battery is depleted to its lower target SOC). Thus, while increased battery capacity extends AER, it decreases efficiency in both CD and CS modes.

Because extra battery weight may require additional structural support in the vehicle body and chassis, we investigate the effects of additional weight needed to support each additional kg of battery and impose a parameter called the *structural weight multiplier*. Via informal discussions with several automakers, we estimate that this multiplier is typically around +1x (one kg of additional structural weight required per kg of battery) with a range of +0x (no additional weight required) to +2x (two kg of additional structural weight required per kg of battery). The requirement for the additional structural weight is dependent on the vehicle type and its design. For example, if a vehicle base structure is optimized for light weight, then adding batteries may require additional structural elements to support the weight of batteries and the additional weight of the structure itself will call for more structural support. On the other hand, if a vehicle is weight-constrained by other considerations, such as crash-test performance or hauling capacity, the vehicle may require only limited structural weight to support the added batteries. We assume that one kg of additional structural weight is required for each kg added to the vehicle (+1x case) as our base case, and we investigate the +0x and +2x cases for the purpose of sensitivity analysis. We also account for the weight of larger electric motors required to maintain target performance characteristics in heavier vehicles. Particularly we size the motor of each vehicle such that it can perform 0-60 miles per hour (mph) acceleration in a time comparable to the general vehicle specification (10-10.5 seconds) when the vehicle is in CS mode.

4.3 Method

4.3.1 PHEV Simulation

We use the U.S. Department of Energy Powertrain System Analysis Toolkit (PSAT) vehicle physics simulator (Argonne National Laboratory, 2008) to model and examine design tradeoffs between battery capacity and PHEV benefits. PSAT is a forward-looking vehicle simulator, meaning it models the driver as a control system that attempts to follow a target driving cycle of defined vehicle speed at every time step by actuating the accelerator and brake pedals. For the PHEV simulations in our study, we used the model year 2004 Toyota Prius as a baseline for engine, body and powertrain configurations.[28] Additional battery capacity was added to the base configuration in order to attain a set of AER requirements, and the electric motor was scaled to maintain acceleration characteristics at low SOC. The PSAT split hybrid control

[28] We use the default MY04 Prius configurations in the PSAT software package. The vehicle body weight is 824 kg, drag coefficient is 0.26, frontal area is 2.25 m^2, tire specification is P175/65 R14, and front/rear weight ratio is 0.6/0.4.

strategy for maximum engine efficiency was modified so that the vehicle operates in electric only CD-mode without engaging the engine until the battery reaches 35% SOC, after which time the vehicle switches to CS mode and operates like a Toyota Prius, using the split control strategy with a target SOC of 35% and SOC operating range of 30-40%.

The design variables controlled in this study are the number of battery modules and the size (power scaling factor) of the electric motor. The engine model is a 1.4 liter four-cylinder engine with a 57 kW maximum power. The base motor is a permanent magnet type with a maximum peak power of 52 kW and a weight of 40 kg including a 5kg controller. Performance map and weight characteristics of larger motors needed for the PHEV cases are predicted using a motor scaling parameter.[29] The battery model is based on a Saft Li-ion battery package, where each module is comprised of three cells in series with a specific energy adjusted to 100 Wh/kg (Kalhammer et al., 2007). The weight of each cell is 0.173 kg, and its capacity is 6 Ah with a nominal output voltage of 3.6 volts. Accounting for the weight of packaging using a factor of 1.25, the weight of one 3-cell module is 0.65 kg. The total battery size and capacity was scaled by specifying an integer number of battery modules.[30] Additional structural weight in the body and chassis required to support the weight of the battery and motor are controlled by the structural weight multiplier. In order to compare the performance of HEV to PHEVs using comparable technology and prices, we use the current Prius model as our HEV base case but replace its original NiMH battery and control strategy with the Saft Li-ion battery module and a simplified split control strategy.[31] The CV in our study is simulated by using a Honda Civic configuration in the PSAT package with an altered car body and tires to match Prius

[29] The performance map and motor and controller weight are scaled linearly with peak power.

[30] Results of PHEV simulation may vary depending on battery configuration. In this study we assume that battery modules are arranged in series for simplicity.

[31] We assume a target SOC at 55% (Kelly et al., 2002) for the base HEV, and the number of Li-ion battery modules is adjusted to match the original NiMH battery capacity of 1.3 kWh.

specifications. The engine, motor and battery configurations of the base HEV and CV are shown in the last two columns of Table 4.1.

Simulations were performed to test PHEVs with 7-, 20-, 40-, and 60-mile AERs (PHEV7, PHEV20, PHEV40 and PHEV60, respectively)[32] under three cases of structural weight multipliers +0x, +1x, and +2x. We used the EPA Urban Dynamometer Driving Schedule (UDDS) driving cycle (EPA, 1996) to measure fuel efficiency in CS mode and electricity efficiency in CD-mode in the vehicle simulations. In each test, the number of battery modules needed to reach the target AER was first determined. To compare equivalent-performance vehicles, motor size (power) was then adjusted to achieve a 0-60 mph acceleration time specification of 10 +0.5/-0.0 seconds, which is approximately the acceleration performance of a Toyota Prius. This procedure was repeated iteratively until convergence to a vehicle profile that satisfies both required AER and acceleration specifications for each case.

4.3.2 Economic and GHG Parameters

The PHEV operation costs in this study are evaluated based on an electricity charging cost of $0.11 per kWh and retail gasoline price $3.00 per gallon ($0.80 per liter), which were similar to U.S. prices in 2007 (EIA, 2008). Sensitivity to changes in energy prices is evaluated in Section 4.3.2. The total operating cost to travel a particular distance is the sum of the cost of the electricity needed to charge the battery[33] and the cost of the gasoline used. For distances less than the AER, the battery was only charged as much as needed for the trip. For distances greater than the AER, the battery was charged to the maximum SOC. Moreover, in order to calculate the vehicle cost, we estimated the vehicle base cost, excluding the Li-ion battery, using the Prius

[32] We use the notation PHEV*x* to denote a PHEV with an AER of *x* miles.
[33] We assume an 88% charging efficiency between outlet and PHEV battery (EPRI, 2007).

MSRP less its NiMH battery cost of $3,900 (Naughton, 2008), resulting in a vehicle base cost of $17,600. The base total battery capacity cost is assumed to be $1,000 per kWh (Lemoine et al., 2008), and a future low cost cases are examined in a sensitivity analysis.[34] The same base vehicle cost is used in our cost estimation for the CV, HEV and PHEV.

Life cycle GHGs are expressed in kg CO_2-equivalent (kg-CO_2-eq) with a 100-year timescale (IPCC, 2001). The GHG emissions calculations in this study assume a U.S. average grid mix of 0.730 kg of CO_2-eq emitted per kWh of electricity charged to the PHEV battery[35], and 11.34 kg of CO_2-eq per gallon of gasoline (3.0 kg CO_2-eq per liter).[36] We further assume 8,500 kg CO_2-eq per vehicle for vehicle manufacturing (excluding emissions from battery production) plus 120 kg CO2-eq for each kWh of Li-ion battery capacity produced (Samaras and Meisterling, 2008). These values represent the U.S. average life cycle emissions, including combustion and the upstream fuel cycle impacts.

4.4 Results and Discussion

The final PHEV configurations and simulation results are shown in Table 4.1, which reveal that additional weight affects required battery capacity, CD-mode electrical efficiency, CS mode gasoline fuel efficiency, operation cost per mile, and GHG emissions per mile. Greater motor power is needed to achieve baseline acceleration performance as the vehicle weight increases, although the weight of the larger motor itself is small compared to the additional battery weight. Increased weight also requires more batteries to achieve a target AER, creating a compounding effect. Further, the additional battery volume of large capacity PHEVs may cause

[34] We intend total battery capacity cost to account for the full cost implications of adding battery capacity to the vehicle, including cell, packaging, wiring, controls, assembly, and increased structural and motor requirements..

[35] We use life cycle electricity emissions at the power plant of 0.67 kg CO_2-eq per kWh (Samaras and Meisterling, 2008), and we assume a 9% power transmission and distribution loss (EIA, 2008).

[36] For gasoline, 8.81 kg CO_2-eq per gallon (2.33 kg CO2-eq per liter) is generated in combustion and 2.54 kg CO_2-eq per gallon (0.67 kg CO_2-eq per liter) is emitted in the supply chain (EPA, 2006; Wang et al., 2007).

design feasibility issues and require significantly reduced cargo area and/or elimination of the spare tire.

Based on the simulation results of CD-mode and CS-mode efficiency under fixed 0-60mph acceleration specifications, Figure 4.2 shows the net effects of increasing AER on vehicle weight, efficiency, operation cost and operation-associated GHG emissions. We found that relationships are fairly linear in this range; increasing the target AER of a given PHEV by 10 miles results in an additional ~95 kg of vehicle weight. This additional weight reduces CD-mode and CS-mode efficiencies by 0.10 mile/kWh and 0.68 mile/gal, respectively. These efficiency reductions cause an increase in vehicle operating costs of \$0.40-\$0.80 per 1000 miles in CD-mode and CS-mode, respectively, and an increase in operation-associated GHG emissions of 3.0-3.2 kg CO_2-eq per 1000 miles in CD-mode and CS-mode, respectively. The linear regression functions for the +1x structural weight case are

$$
\begin{aligned}
\eta_{\mathrm{E}} &= -0.010 s_{\mathrm{AER}} + 5.67 \\
\eta_{\mathrm{G}} &= -0.068 s_{\mathrm{AER}} + 51.7 \\
c_{\text{OP-CD}} &= 0.004 s_{\mathrm{AER}} + 2.20 \\
c_{\text{OP-CS}} &= 0.008 s_{\mathrm{AER}} + 5.79 \\
v_{\text{OP-CD}} &= 0.029 s_{\mathrm{AER}} + 14.6 \\
v_{\text{OP-CS}} &= 0.032 s_{\mathrm{AER}} + 21.9
\end{aligned}
\tag{4.1}
$$

where s_{AER} is AER in miles, η_{E} and η_{G} are the CD-mode and CS-mode efficiencies in units of miles per kWh and miles per gallon respectively, $c_{\text{OP-CD}}$ and $c_{\text{OP-CS}}$ are the operation costs per 100 mile under CD and CS mode respectively, and $v_{\text{OP-CD}}$ and $v_{\text{OP-CS}}$ are operation GHG emissions in kg CO_2-eq per 100 miles in CD- and CS-mode respectively. It should be noted that while costs and GHG emissions both increase with AER in CD and CS modes, this does not imply that total cost and emissions will increase, since PHEVs with larger AERs can travel more miles on low cost, potentially low GHG electricity. These costs and emissions associated with efficiency losses are small relative to overall PHEV operation costs and emissions. In the following sections, we examine the effect of AER and charging frequency on fuel economy, operating cost, and GHG emissions.

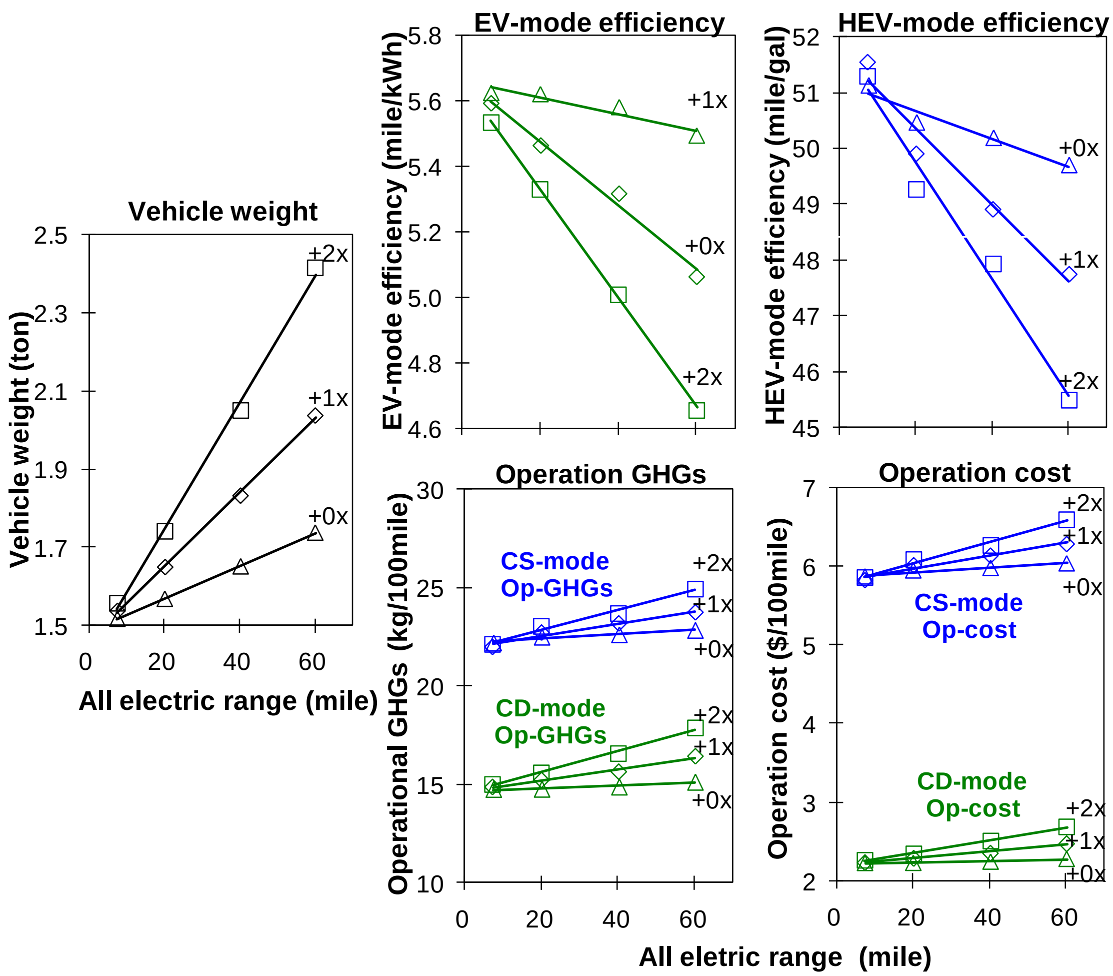

Figure 4.2 Effect of increasing target AER on PHEV operation performances

4.4.1 Operational Performance

To compare the operational performances of different vehicle configurations, we examine three PHEV characteristics: fuel consumption (i.e. fuel economy), operational costs and operational GHG emissions. Because these three performance criteria depend on the distance traveled between charges, two key quantities are needed. For a distance s traveled between charges in a vehicle with an all-electric range of s_{AER}, the distance traveled on electric in CD-mode s_{E} and the distance traveled on gasoline in CS-mode s_{G} are calculated as

$$\begin{aligned} s_{\mathrm{E}} &= \begin{cases} s & \text{if } s \le s_{\mathrm{AER}} \\ s_{\mathrm{AER}} & \text{if } s > s_{\mathrm{AER}} \end{cases} \\ s_{\mathrm{G}} &= \begin{cases} 0 & \text{if } s \le s_{\mathrm{AER}} \\ s - s_{\mathrm{AER}} & \text{if } s > s_{\mathrm{AER}} \end{cases} \end{aligned} \tag{4.2}$$

The results of fuel economy (CS-mode efficiency) in Table 4.1 indicate that as the target AER increases from 7 miles to 60 miles, the modeled urban driving fuel economy decreases 7.4% from 51.5 miles per gallon (mpg) to 47.7 mpg in the +1x base case due to increased weight. This effect is reduced under lower structural weight assumptions and amplified for larger structural weight. The average fuel consumption per mile g is calculated by

$$g = \frac{1}{s}\left(\frac{s_{\mathrm{G}}}{\eta_{\mathrm{G}}}\right) \tag{4.3}$$

where η_{G} is the fuel efficiency (mile per gallon of gasoline) in CS mode. Figure 4.3 shows the average fuel consumption for PHEVs compared to the HEV and CV. PHEVs consume no gasoline within the AER. Beyond the AER, fuel is consumed at a greater rate for heavier vehicles. The graph shows that PHEVs consume less gasoline than HEVs and CVs over the entire range of charging frequencies examined.

Table 4.1 PHEV configurations and performance results

	PHEV	Structural weight factor	+0x				+1x				+2x				HEV	CV
		Target AER (mile)	7	20	40	60	7	20	40	60	7	20	40	60		
Vehicle Design	Engine	Engine power (kW)	57	57	57	57	57	57	57	57	57	57	57	57	57	113
		Weight (kg)	114	114	114	114	114	114	114	114	114	114	114	114	114	251
	Motor	Motor power (kW)	55	57	60	65	56	61	68	77	57	65	77	93	55	
		Motor weight (kg)	37	38	40	43	37	41	45	51	38	43	51	62	37	
		Controller weight (kg)	5	5	6	6	5	6	6	7	5	6	7	9	5	
		Structural weight (kg)	0	0	0	0	3	7	12	19	7	19	38	62	0	
		Total weight (kg)	42	44	46	50	46	53	64	78	51	69	97	133	42	
	Battery	Number of modules	46	123	248	376	46	127	260	408	46	130	276	444	20	
		Number of cells	138	369	744	1128	138	381	780	1224	138	390	828	1332	60	
		Battery volume (m^3)	0.13	0.35	0.70	1.06	0.13	0.36	0.74	1.15	0.13	0.37	0.78	1.26	0.06	
		Battery capacity (kWh)	3.0	8.0	16.1	24.4	3.0	8.2	16.8	26.4	3.0	8.4	17.9	28.8	1.3	
		Battery weight (kg)	30	80	161	244	30	82	168	264	30	84	179	288	13	
		Structural weight (kg)	0	0	0	0	17	69	156	251	34	143	332	550	0	
		Total weight (kg)	30	80	161	244	47	152	324	516	64	227	511	837	13	
	Vehicle	Vehicle weight (kg)	1516	1567	1651	1737	1536	1649	1832	2037	1558	1740	2051	2414	1499	1475
Simulation Results	CD mode	Efficiency* (Wh/mile)	178	178	179	182	179	183	188	197	181	188	200	215	-	-
		Simulation AER (mile)	7.5	20.2	40.4	60.2	7.5	20.2	40.3	60.2	7.4	20.2	40.3	60.3	-	-
	CS mode	Efficiency (gal/100 mile)	1.96	1.98	1.99	2.01	1.94	2.00	2.04	2.09	1.95	2.03	2.09	2.20	1.93	3.53
		0-60 mph time (sec)	10.2	10.2	10.3	10.1	10.2	10.1	10.2	10.2	10.1	10.1	10.3	10.2	10.1	10.3
Operation Cost and GHG Emissions	Oper. cost	CD mode ($/mile)	0.022	0.022	0.022	0.023	0.022	0.023	0.024	0.025	0.023	0.023	0.025	0.027	-	-
		CS mode ($/mile)	0.059	0.059	0.060	0.060	0.058	0.060	0.061	0.063	0.058	0.061	0.063	0.066	0.058	0.106
	Oper. GHGs	CD mode (kg/mile)	0.148	0.148	0.149	0.151	0.148	0.152	0.156	0.164	0.150	0.156	0.166	0.178	-	-
		CS mode (kg/mile)	0.222	0.225	0.226	0.228	0.220	0.227	0.232	0.237	0.221	0.230	0.237	0.249	0.219	0.400

* Battery to wheels electrical efficiency is reported here. An 88% charging efficiency is used to estimate plug to wheels efficiency.

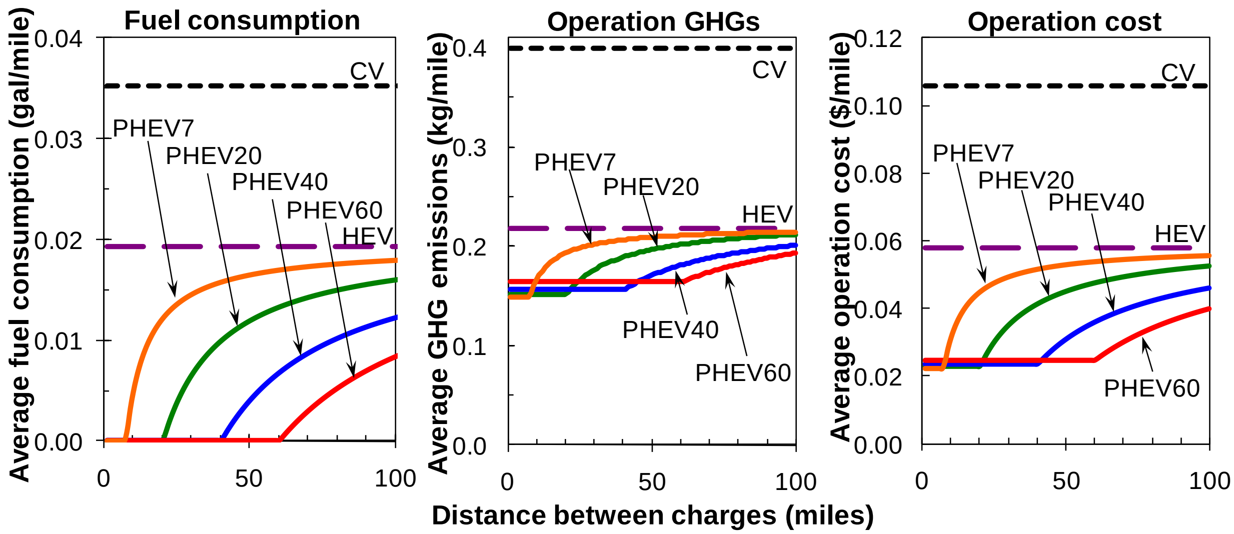

Figure 4.3 Operation-associated fuel consumption, GHG emission, and cost

The second consideration is GHG emissions, which were calculated by including combustion and supply chain emissions associated with electricity v_E = 0.730 kg CO_2-eq per kWh, battery charging efficiency η_C = 88%, and gasoline v_G = 11.34 kg CO_2-eq per gal. The average operation-associated GHG emissions per mile v_{OP} is calculated using the following equation:

$$v_{OP} = \frac{1}{s}\left(\frac{s_E}{\eta_E} \frac{v_E}{\eta_C} + \frac{s_G}{\eta_G} v_G \right) \tag{4.4}$$

Table 4.1 lists the GHG emissions per mile for each case in both CD and CS mode. The data show that the average life cycle GHG emissions associated with driving in CS mode are roughly 1.5 times those associated with CD mode. Figure 4.3 shows the average use phase GHG emissions per mile as a function of distance traveled between charges. For frequent charging, a smaller capacity PHEV minimizes operation-associated emissions. Larger capacity PHEVs are able to reduce more operational emissions for longer driving distance up to 100 miles. Generally the results show that PHEVs have significantly lower operational GHG emissions than the HEV and CV for urban driving.

The third performance characteristic is average operation cost, which represents the average consumer expense per mile associated with recharging cost and fuel expense. The average operation cost c_{OP} is calculated by:

$$c_{\mathrm{OP}} = \frac{1}{s}\left(\frac{s_{\mathrm{E}}}{\eta_{\mathrm{E}}}\frac{c_{\mathrm{E}}}{\eta_{\mathrm{C}}} + \frac{s_{\mathrm{G}}}{\eta_{\mathrm{G}}}c_{\mathrm{G}}\right) \tag{4.5}$$

where η_{E} is the electrical efficiency in CD mode, η_{C} is the battery charging efficiency, c_{E} is the cost of electricity, and c_{G} is gasoline cost. Figure 4.3 shows the average operation cost per mile for CD and CS mode under the three structural weight multiplier cases assuming c_{E} = \$0.11 per kWh, η_{C} = 88% and c_{G} = \$3.00 per gallon. Larger capacity PHEVs are heavier, thus increasing the operation cost in both CD and CS mode; however, they also extend the distance that the vehicle operates in the less-expensive CD mode. Figure 4.3 shows the average operation cost per mile as a function of distance between charges. For frequent charges, a PHEV with an AER approximately equal to the distance between charges minimizes the operation cost. Each PHEV has clear operation cost advantages when the driving distance between charges is less than or equal to its AER. Once the driving distance extends beyond the AER, the operational costs of PHEVs increase rapidly. For urban driving distances less than 100 miles, all PHEVs have lower operation costs than the HEV and CV.

4.3.2 Results and Sensitivity Analyses

In this section, we analyze the net GHG emissions and net costs by combining the values in the use (operating) phase and production (manufacturing) phase. We also conduct several sensitivity analyses on the parameters listed in Table 4.2. To account for net lifecycle GHG emissions over the vehicle life, we add the operation GHG emissions v_{OP} (Eq. (4.4)) to the emissions associated with vehicle and battery manufacturing:

$$v_{\mathrm{TOT}} = v_{\mathrm{OP}} + \frac{1}{s_{\mathrm{LIFE}}}\left(v_{\mathrm{VEH}} + v_{\mathrm{BAT}}\kappa\right) \tag{4.6}$$

where v_{VEH} = 8,500 kg CO_2-eq is the assumed life cycle GHG emissions of vehicle manufacturing excluding its battery and v_{BAT} = 120 kg CO_2-eq per kWh is the life cycle GHG emissions of batteries (Lemoine, 2008; Samaras and Meisterling, 2008). The resulting total GHG emissions for the base case and the other five scenarios are shown in Figure 4.4. It can be seen that all of the PHEVs reduce GHG emissions compared to the HEV and CV, and the PHEV7 has the lowest average GHG emissions for small trips under the average U.S. grid mix. New battery technology with a high specific energy of 140 Wh/kg (USABC, 2008) or a high SOC operating range (swing of 80%) implies reduced battery requirements, which lowers emissions associated with all PHEVs; however, general trends remain unchanged. Low-carbon electricity with average battery charging emissions of 0.218 kg CO_2-eq per kWh (0.2 kg CO_2-eq per kWh at the power plant with 9% transmission loss) would significantly lower GHG emissions from PHEVs.

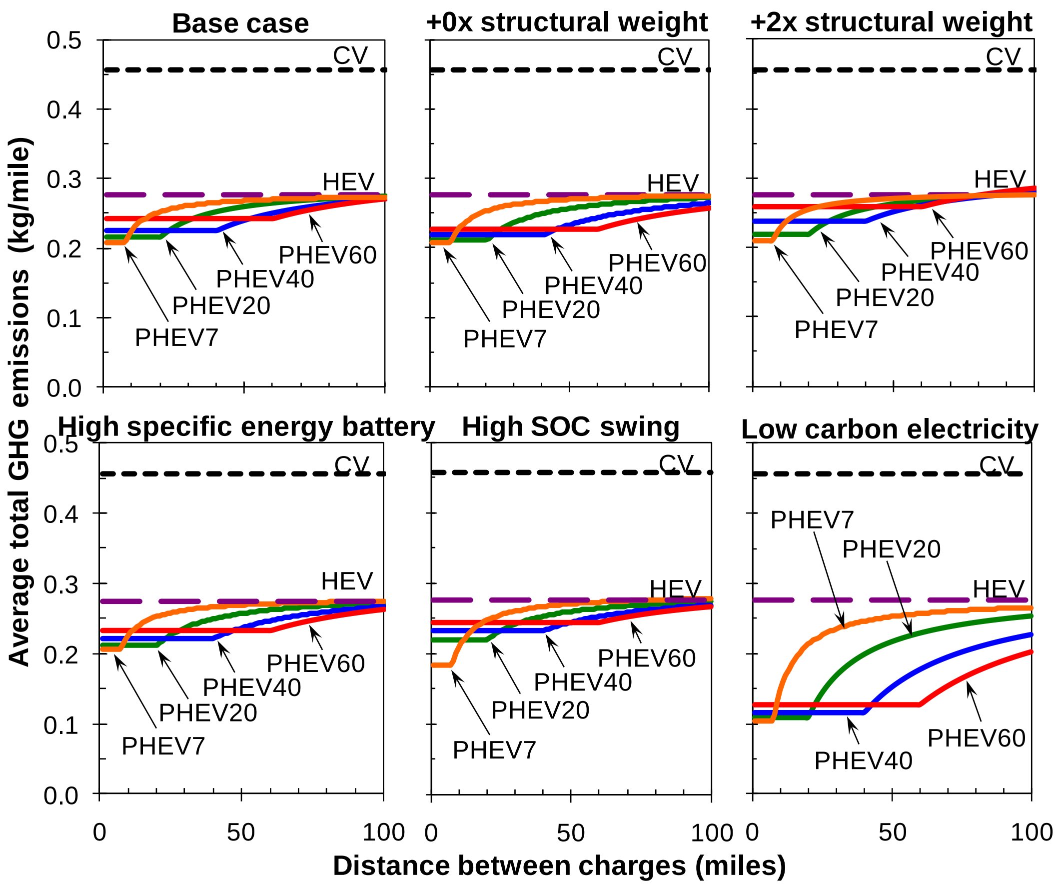

Figure 4.4 Lifetime GHGs per lifetime miles driven as a function of the distance driven between charges

Table 4.2 Parameter levels for sensitivity analyses

Sensitivity analysis parameter	Unit	Low level	**Base level**	High level
Structural weight	–	+0x	**+1x**	+2x
Discount rate	%	0	**5**	10
Gas price	$/gal	1.5	**3**	6
Battery SOC swing	%	–	**50**	80
Battery specific energy	Wh/kg	–	**100**	140
Battery replacement frequency over life	–	–	**0**	1
Electricity price	$/kWh	0.06	**0.11**	0.30
Total battery capacity cost	$/kWh	{250,500}	**1000**	–
CO_2 lifecycle emissions in electricity	kg-CO_2-eq/kWh	0.218	**0.730**	–
Carbon tax	$/ton	–	**0**	100

The net cost implications over the vehicle lifetime is calculated by considering the vehicle base cost, battery purchase price, and net present value of operation costs, battery replacement cost, and costs imposed by a potential tax on CO_2. The equation for the net present value of lifetime cost per mile is given by

$$c_{\mathrm{TOT}} = \frac{1}{s_{\mathrm{LIFE}}}\left(\left(c_{\mathrm{VEH}} + c_{\mathrm{BAT}}\kappa\right) + \sum_{n=1}^{N} \frac{\left(c_{\mathrm{OP}} + \rho v_{\mathrm{OP}}\right) s_{\mathrm{ANUL}}}{\left(1+r\right)^{n}} \right. \\ \left. + \rho\left(v_{\mathrm{VEH}} + v_{\mathrm{BAT}}\kappa\right) + \gamma \frac{c_{\mathrm{BAT}}\kappa\left(1+\rho\right)}{\left(1+r\right)^{N/2}} \right) \tag{4.7}$$

We assume that the annual vehicle miles traveled s_{ANUL} = 12,500 miles (20,000 km) (EPA, 2005), the vehicle lifetime N = 12 years, and thus vehicle lifetime mileage s_{LIFE} = 150,000 miles (240,000 km). Vehicle purchase cost includes the vehicle base cost (excluding the battery) c_{VEH} = \$17,600 plus battery cost calculated by total battery capacity cost c_{BAT} = \$1,000 per kWh multiplied by battery capacity κ, in kWh. The second term in Eq. (4.7) is net present value of operation costs c_{OP} (Eq. (4.5)) plus the carbon tax paid for operation over vehicle's lifetime. The carbon tax is estimated by tax rate ρ per kg-CO_2-eq and operational GHG emission per mile υ_{OP} (Eq. (4.4)), conservatively assuming a consumer would bear the full cost of a carbon tax imposed on producers. The net present value of annual operational costs and carbon taxes are calculated using a discount rate r. The third term is carbon tax cost for the GHG emissions of vehicle and battery manufacturing, v_{VEH} and v_{BAT}, respectively. The last term is the present value of battery replacement cost with carbon tax on the battery if a replacement occurs, where γ = 0 for no battery replacement and γ = 1 for one time replacement at half vehicle life (the 6th year). The parameters for the base case study are listed in the center column of Table 4.2, including +1x structural weight, 5% discount rate, \$3.00/gal gasoline price, 50% battery SOC swing (80-30%), battery specific energy 100 Wh/kg, no battery replacement over vehicle life, total battery capacity cost \$1000/kWh, average U.S. electricity mix, and no carbon tax (ρ = 0). The cost analysis results of the base case are shown in Figure 4.5. It can be seen that the small PHEV7 has the best economic performance for frequent charges within ~20 miles. When the driving distance between charges becomes longer, the HEV is less expensive. We also found that the PHEV20 and the CV are have similar costs, which are slightly higher than the HEV, while large capacity PHEVs have significantly higher average costs over their lifetime. The relative benefit of the HEV over the CV is based on a \$1000/kWh assumption, which is less expensive than past NiMH battery costs reported for the Prius (Naughton, 2008).

For the sensitivity analyses shown in Figure 4.5, we found that increase or decrease of structural weight does not alter the rank of vehicle cost competitiveness; however, the cost of large PHEVs is more sensitive to structural weight increases. If the battery must be replaced at half of the vehicle's life, the cost of PHEV7 and HEV are somewhat affected, but the average costs of medium and large PHEVs surge due to their high battery costs. Low gasoline prices of \$1.50/gal make PHEVs less competitive, although the small capacity PHEV7 is comparable with the HEV and CV. High prices of \$6.00/gal increase the cost-competitiveness of PHEVs and make the small capacity PHEV7 competitive for all driving distances. However, larger PHEVs are still more costly than the HEV. Low off-peak electricity prices of \$0.06/kWh make PHEVs only slightly more cost competitive, and high peak electricity prices of \$0.30/kWh make the HEV the low-cost option, although the small capacity PHEV7 remains close in cost (Cherry, 2009). Low consumer discount rates (0%) improve PHEV competitiveness and high discount rates (10%) make PHEVs less competitive, but in all cases the PHEV7 is competitive for drivers who charge frequently, and it is similar to HEV costs when charged infrequently. Total battery capacity costs of \$500/kWh further improve cost competitiveness of the PHEV7, and cheap costs of $250 per kWh would significantly increase competitiveness of PHEVs, making them similar to or less expensive than HEVs and CVs across all distances driven between charges. A battery technology with an increased SOC swing, which would allow more of the battery's physical capacity to be used in operation, would also improve PHEV competitiveness, making moderate ranged PHEVs cost competitive with the HEV and CV. A $100 tax per metric ton of GHG emissions ($0.1 per kg-$CO_2$-eq) associated with production and use would not improve PHEV competitiveness significantly under the current electricity grid mix. This result is consistent with the high carbon abatement costs for PHEVs estimated by Kammen (2008) and Lemoine (2008). However, a carbon tax combined with low-carbon electricity at current prices would improve competitiveness of PHEVs and make the PHEV7 less costly for all drivers.

4.3.3 Vehicle selection decisions

Figure 4.6 summarizes the best vehicle choice for minimizing fuel consumption, lifetime cost, or lifetime greenhouse gas emissions as a function of the distance the vehicle will be driven between charges. For short distances of less than 10 miles between charges, the PHEV7 is the robust choice for minimizing gasoline consumption, cost, and emissions. For moderate to long distances of 20-100 miles between charges, PHEVs release fewer GHG, but HEVs are generally less costly, even under a $100 carbon tax. High gas prices, improved battery technology with low cost or a high SOC swing, or low-carbon electricity combined with carbon tax policy can make PHEVs economically competitive over a wider range. However, large-capacity PHEVs are not the low cost choices under any scenario.

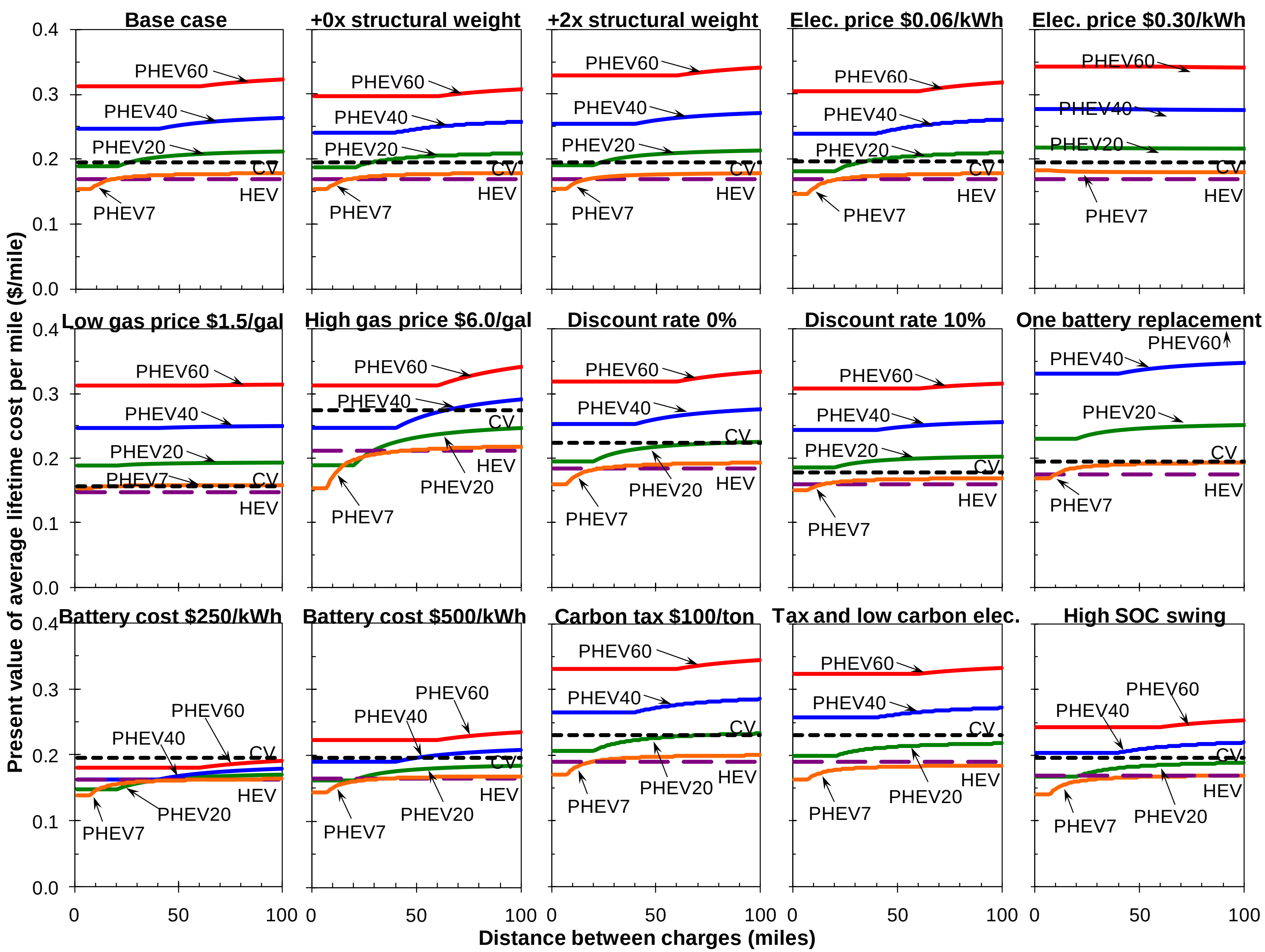

Figure 4.5 NPV of vehicle lifetime costs per lifetime miles driven as a function of the distance driven between charges

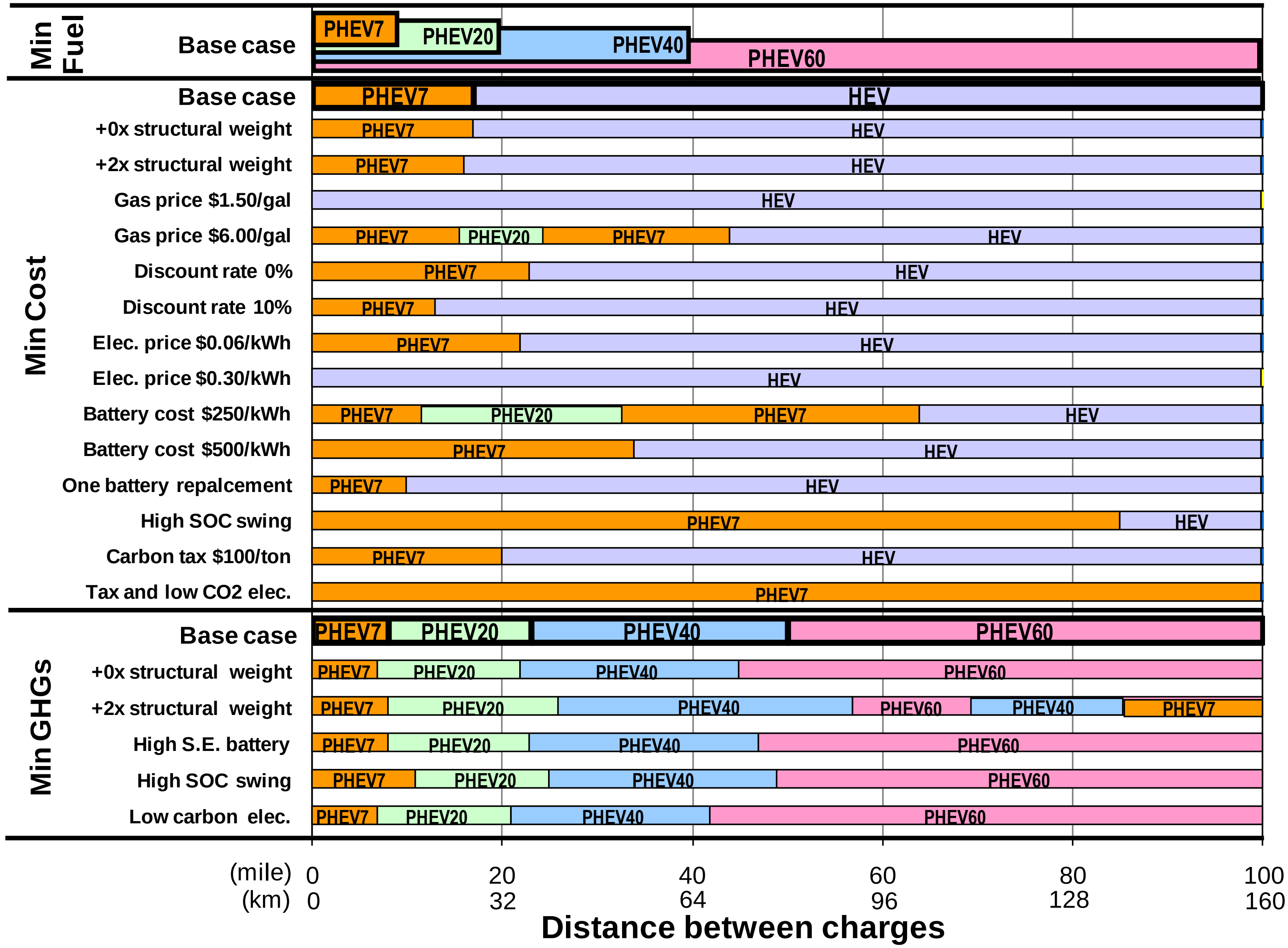

Figure 4.6 Best vehicle choice as a function of distance driven between charges

4.3.4 Vehicle Efficiency Simulation

The PSAT simulation predicts a PHEV electrical efficiency η_E of about 4.6-5.6 miles/kWh (equal to 178-215 Wh/mile) from battery to wheel, or about 4-5 miles/kWh (equal to 202-244 Wh/mile) from plug to wheel for the UDDS urban driving cycle, which are on the upper end of values previously reported in the literature. Since PHEVs have not been deployed on a large scale, uncertainty remains regarding the actual value of η_E achieved. Several factors might have influenced the η_E reported by PSAT. These include the possibility of omitted losses or loads (e.g. battery HVAC systems or other electrical loads) and our focus on an urban driving cycle. In addition to vehicle weight, driving systems and environment (temperature, terrain, vehicle hotel loads, driving characteristics) could also affect values of η_E. Given the importance of efficiency predictions in determining economic and environmental implications, more data from PHEVs operating on the road is needed to reduce uncertainty.

4.4 Summary

Our study results indicate that the impacts of battery weight on CD-mode electrical efficiency and CS-mode fuel economy are measurable, about a 10% increase in Wh/mile and an 8% increase in gallons per mile when moving from a PHEV7 to a PHEV60. This implies that the additional weight of a PHEV60 results in a 10% increase in operation-related costs and greenhouse gas emissions per mile relative to a PHEV7 for drivers who charge frequently (every 7 miles or less).

The best choice of PHEV battery capacity depends critically on the distance that the vehicle will be driven between charges. But daytime vs. nighttime charging, geographic location, and effects of marginal changes in electricity demand on the mix of energy sources could all affect implications associated with electrified transportation. Policy and planning should be employed to minimize negative impacts of PHEV adoption on the electricity grid. Our results suggest that for urban driving conditions and frequent charges every 10 miles or less, a low-capacity PHEV sized with an AER of about 7 miles would be a robust choice for minimizing gasoline consumption, cost, and greenhouse gas emissions. For distances of ~10-20 miles, the PHEV7 has the lowest lifetime cost, and the PHEV20 has lower fuel consumption and GHG emissions. For less frequent charging, every 20-100 miles, PHEVs release fewer GHGs, but HEVs have lower lifetime costs. An increase in gas price, a decrease in the cost of usable battery capacity, or a carbon tax combined with low carbon electricity generation would make PHEV less costly for a wide range of drivers. In contrast, a battery technology that increases specific energy would not affect net cost and GHG emissions significantly, and a $100 per ton carbon tax without a corresponding drop in carbon intensity of electricity generation would not make PHEVs significantly more competitive. These results suggest that research on PHEV battery technology improvements would be better targeted toward cost reduction than improvement of specific energy, and the effect of carbon taxes on the PHEV market will depend on their effect on the electricity generation mix, such as encouraging renewables, carbon capture and sequestration, and nuclear.

PHEVs perform best when the batteries are sized according to the charging patterns of the driver. Three potential complications arise when sizing PHEVs based on the number of miles that drivers travel: (1) if the variance in miles traveled per day is large, then a capacity designed for the average distance may be suboptimal; (2) it is unclear whether it is safe to assume that drivers will consistently charge their vehicles once per day – irregular charging behavior could lead to significantly longer distances between charges than the average daily distances would suggest; and conversely; (3) widespread installation of charging infrastructure in public parking places would enable charging more than once per day, enabling shorter distances between charges.

Across the scenarios examined, the small capacity PHEV outperforms larger capacity PHEVs on cost regardless of the consumer's discount rate, and the larger PHEV40 and PHEV60 do not offer the lowest lifetime cost in any scenario, although they provide GHG reductions for some drivers and the potential to shift air pollutant emissions away from population centers. The dominance of the small-capacity PHEV over larger-capacity PHEVs across the wide range of scenarios examined in this study suggests that government incentives designed to increase adoption of PHEVs may be best targeted toward adoption of small-capacity PHEVs by urban drivers who are able to charge frequently. Because nearly 50% of U.S. passenger vehicle miles are traveled by vehicles driving less than 20 miles per day (BTS, 2003; Samaras and Meisterling, 2008), there remains significant potential in targeting this subset of drivers. Since the goals of reducing cost, GHG emissions and fuel consumption are well-aligned for drivers who will charge frequently, economic interest may lead to environmental solutions for these drivers if policies promote appropriate infrastructure and initial sales. In addition to targeted financial incentives, appropriate policies could include government fleet purchases, support for public charging infrastructure, as well as consumer education and clear labeling of gasoline and electricity consumption of PHEVs.

CHAPTER 5. OPTIMAL PHEV DESIGN FOR SOCIAL OBJECTIVES

The analysis in Chapter 4 shows that PHEVs with frequent charges can drive most of their miles on electric power, even with a relatively small battery pack, while vehicles that are charged infrequently require larger battery packs to cover longer distances with electric power. This chapter extends the prior study and poses a mixed-integer nonlinear programming (MINLP) model to determine optimal vehicle design and optimal allocation of vehicles to drivers for the minimum petroleum consumption, life cycle cost and GHG emissions. With considering the factors of U.S. drivers' daily driving patterns, battery degradation and replacement, battery swing design, and battery lease-purchase scenarios, design and policy implications of the optimal vehicle allocations are examined in various sensitivity analyses. The content in this chapter is based on a paper submission in review (Shiau et al., 2010).

5.1 Model

A benevolent dictator optimization model is proposed to determine optimal vehicle type, design, and allocation for achieving social objectives of minimum life cycle cost, GHG emissions, and petroleum consumption from personal transportation.[37] Figure 5.1 shows an overview of the modeling framework. To optimize a single vehicle for minimum life cycle cost, petroleum consumption or GHG emissions over the population of drivers, we minimize the

[37] We model allocation of vehicles to drivers as a dictated assignment based on driver daily travel distance and do not model market mechanisms. As such, we find the best possible outcome for GHG emissions, which is a lower bound for market-based outcomes.

integral of the corresponding quantity per day at each driving distance $f_O(\mathbf{x},s)$ times the probability distribution of daily driving distances $f_S(s)$ in the population of drivers:

$$\begin{aligned} &\underset{\mathbf{x}}{\text{minimize}} \int_0^\infty f_O(\mathbf{x},s)\, f_S(s)\, ds \\ &\text{subject to } \mathbf{g}(\mathbf{x}) \le \mathbf{0};\ \ \mathbf{h}(\mathbf{x}) = \mathbf{0} \end{aligned} \tag{5.1}$$

where $\mathbf{x}$ is a vector of design variables that define the vehicle, s is the distance the vehicle is driven between charges, $f_O(\mathbf{x},s)$ is the value of the objective (equivalent cost, petroleum consumption, or GHG emissions) per day for vehicle design $\mathbf{x}$ with s miles driven per day, $f_S(s)$ is the probability density function for the number of miles driven per day, $\mathbf{g}(\mathbf{x})$ is a vector of inequality constraints and $\mathbf{h}(\mathbf{x})=\mathbf{0}$ is a vector of equality constraints ensuring a feasible vehicle design.

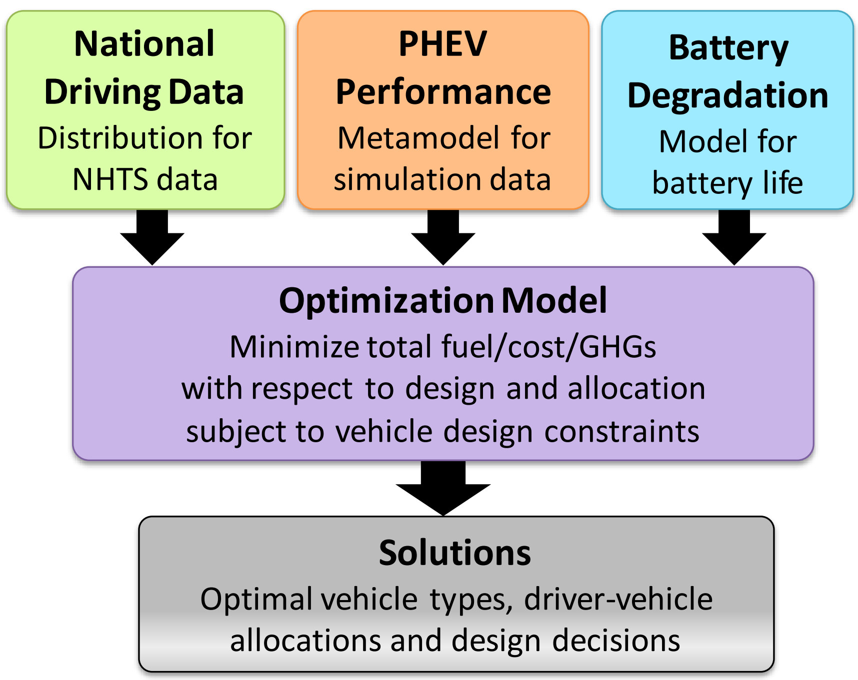

Figure 5.1 Framework of optimal PHEV design and allocation

To extend this model to the case where different drivers are assigned different vehicles based on the number of miles driven per day, we incorporate a variable s_i that defines the cutoff point such that drivers who travel less than s_i per day are assigned the vehicle defined by $\mathbf{x}_i$ and drivers who travel more than s_i per day are assigned the vehicle defined by $\mathbf{x}_{i+1}$. Extending this idea to multiple segments, the formulation for design and ordered allocation is given by

$$
\begin{aligned}
&\underset{\mathbf{x}_i, s_i \ \forall i \in \{1,\ldots,n\}}{\text{minimize}} \ \sum_{i=1}^{n} \left(\int_{s_{i-1}}^{s_i} f_{\mathrm{O}}\left(\mathbf{x}_i, s\right) f_{\mathrm{S}}\left(s\right) ds \right) \\
&\text{subject to } \mathbf{g}\left(\mathbf{x}_i\right) \le \mathbf{0};\ \mathbf{h}\left(\mathbf{x}_i\right) = \mathbf{0};\ \forall i \in \{1,\ldots,n\} \\
&\qquad\qquad s_i \ge s_{i-1};\ \forall i \in \{1,\ldots,n\} \\
&\text{where } s_0 = 0;\ s_n = \infty
\end{aligned}
\tag{5.2}
$$

In the following subsections, we first instantiate this formulation with specific models for the objective and constraint functions by specifying the distribution of miles driven per day, vehicle performance models, and the objective and constraint formulations. We then reformulate the model as a factorable, algebraic nonconvex MINLP that can be solved globally.

5.1.1 Distribution of Vehicle Miles Travelled per Day

We use daily trip data from the 2009 National Household Transportation Survey (NHTS) (BTS, 2010) to estimate the distribution of distances driven per day over the population of drivers. The survey collected data by interviewing 136,140 households across the U.S. on the mode of transportation, duration, distance and purpose of the trips taken on the survey day. We fit the weighted driving data using the exponential distribution.[38] The distribution below represents the probability density function for weighted vehicle miles traveled on the day surveyed:

[38] We excluded data entries of public transportation and also excluded drivers who traveled zero miles or more than 200 miles. We fit the distribution to the reported distance traveled on the survey day with the assumptions of (1) the survey data are representative of the population, and (2) the distance driven on the survey day is the same distance driven every day for that vehicle.

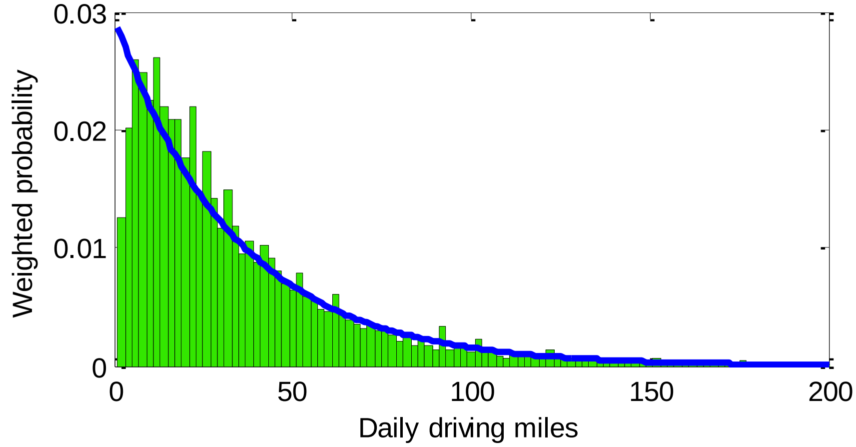

Figure 5.2. Probability density function for vehicle miles traveled per day using NHTS 2009 weighted daily trip mile data (BTS, 2010)

$$f_S(s) = \lambda e^{-\lambda s}; \quad s \geq 0 \tag{5.3}$$

The coefficient λ at maximum likelihood fit is 0.0296. Figure 5.2 shows the exponential distribution and the histogram of the surveyed daily vehicle driving miles.[39] Because we lack multiple days of data for each vehicle, we assume that a vehicle that travels s miles per day on the NHTS survey day will travel s miles every day. This assumption will produce optimistic results on the benefits of optimal allocation, since distance traveled varies over time for individual vehicles in practice.

5.1.2 Vehicle Performance Models

We carry out vehicle performance simulations using the Powertrain System Analysis Toolkit (PSAT) vehicle physical simulator developed by Argonne National Laboratory (Argonne National Laboratory, 2008). PSAT is a Matlab/Simulink forward-looking simulation package that predicts vehicle performance characteristics at both the system level (e.g. fuel consumption)

[39] The deviation between data and the exponential fit in the 0-4 mile region has little effect on results because 0-4 mile trips contribute little to the social objectives in this study (the curves in Figure 5.5(d), (e) and (f))

and the component level (e.g. engine torque and speed at each time step) over a given driving cycle using a combination of first principles and empirical component data. In our study, the body, powertrain and vehicle parameters for all PHEV and HEV simulations are based on the 2004 Toyota Prius model that uses the split powertrain system with an Atkinson engine, a permanent magnet motor, and a NiMH battery pack.[40] To account for structural weight needed to carry heavy battery packs, we include an additional 1 kg of structural weight per 1 kg of battery and motor weight. We created a comparable conventional vehicle (CV) model using a conventional powertrain and 4-cylinder engine based on the Honda Accord to account for larger engine torque and power requirements, and the parameters that define the frontal area, drag coefficient and base weight are adjusted to match the Prius for fair comparison. The detailed vehicle configuration parameters are included in Table 5.1.

Table 5.1 Vehicle configurations in simulation

Module	Property	CV	HEV	PHEV
Vehicle body & chassis	F/R weight ratio	0.6/0.4		
	Drag coefficient	0.26		
	Frontal area (m^2)	2.25		
	Tire specification	P175/65 R14		
	Body mass (kg)	824		
Engine	Power (kW)	126	57	30-60
	Mass (kg)	296	114	50-110
Motor	Power (kW)	-	52	50-110
	Mass (kg)	-	65	40-143
Battery	Number of cells	-	168	200-1000
	Mass (kg)	-	36	60-419
Electrical accessory	Average power consumption (kW)	0.8	0.8	0.8
	Net weight (kg)	1709	1520	1497-1995

[40] We use NiMH battery for HEV simulation since studies indicated that NiMH is specifically suitable for HEV technology and will be continuously used on HEVs in the future (Inderwildi et al., 2010).

For the PHEV design, the Prius engine size is scaled by the peak power output from the base engine (57 kW) using a linear scaling algorithm. Similarly, the motor is scaled from the base motor (52 kW) linearly. Both the engine and motor weights are also scaled proportionally to the peak power. We use the Saft Li-ion battery module in the PSAT package for the PHEV energy storage device. Each cell in the module weighs 0.378 kg, with a modified specific energy of 100 Wh/kg and has a battery cell energy capacity of 21.6 Wh with a nominal output voltage of 3.6 volts. The weight of each 3-cell module is 1.42 kg after accounting for a packaging factor of 1.25. The battery size and capacity are scaled by specifying the number of cells in the battery pack. We assume an 800W base electrical hotel load on the PHEV, the HEV and the CV. To estimate the performance of a PHEV, we use the standard Urban Dynamometer Driving Schedule (UDDS) driving cycle (EPA, 2007) to calculate simulated electrical efficiency (miles/kWh) in CD-mode for PHEVs, and fuel efficiency (mpg) in CS-mode for PHEVs as well as for HEVs and CVs. We also perform a simulated performance test to calculate the time required to accelerate the vehicle from 0 to 60 miles per hour (mph) in the CD-mode and in the CS mode.[41]

Because the petroleum consumption, cost, and GHG emissions per mile associated with HEVs and CVs are independent of the number of miles driven per day, we focus on PHEV design and take the HEV and CV to have fixed designs. The HEV is identical to the Prius model, which has a configuration of peak engine power 57 kW, motor power 52 kW, NiMH battery size 168 cells (1.3 kWh), fuel efficiency 60.1 miles per gallon, and 0-60 mph acceleration time 11.0 seconds. Similarly, our CV has an engine size 126 kW and fuel efficiency 29.5 miles per gallon, and 0-60 mph acceleration time 11.0 seconds. For the PHEVs, the design variables **x** consist of

[41] Our simulation results are generally optimistic for all vehicles in that they do not account for factors such as cold start, vehicle wear, improper maintenance and tire pressure, aggressive driving cycles, use of significant accessories, or terrain and weather variation.

the engine scaling factor x_1, motor scaling factor x_2, battery pack scaling factor x_3, and SOE swing x_4. In order to avoid the computationally expensive process of executing a PSAT simulation for each function evaluation in the optimization algorithm, we created a set of polynomial meta-model fits as functions of **x** for the PHEV using discrete simulation data points: (1) CD-mode electricity efficiency η_E (mile per kWh); (2) CS-mode fuel efficiency η_G (mile per gallon); (3) CD-mode 0-60 mph acceleration time t_{CD} (second); (4) CS-mode 0-60 mph acceleration time t_{CS} (second); (5) CD-mode battery energy processed per mile μ_{CD} (kWh/mile); (6) CS-mode battery energy processed per mile μ_{CS} (kWh/mile); and (7) final SOC after multiple US06 aggressive driving cycles in CS mode u_{CS} (starting at the target SOC). We evaluated the four output values using PSAT over a grid of values for the inputs x_1={30, 45, 60}/57, x_2={50, 70, 90, 110}/52, x_3={200, 400, 600, 800, 1000}/1000 and multivariate polynomial functions were fit to the data using least squares.[42] The general form of the cubic fitting function f_{m3} is defined as (the subscript 3 indicates the PHEV case, which will be discussed later).

$$\begin{aligned} f_{m3}(\mathbf{x}) = {} & a_{m1}x_1^3 + a_{m2}x_2^3 + a_{m3}x_3^3 + a_{m4}x_1^2 + a_{m5}x_1x_2^2 + a_{m6}x_1^2x_3 + a_{m7}x_1x_3^2 \\ & + a_{m8}x_2^2x_3 + a_{m9}x_2x_3^2 + a_{m10}x_1x_2x_3 + a_{m11}x_1^2 + a_{m12}x_2^2 + a_{m13}x_3^2 \\ & + a_{m14}x_1x_2 + a_{m15}x_1x_3 + a_{m16}x_2x_3 + a_{i17}x_1 + a_{m18}x_2 + a_{m19}x_3 + a_{m20} \end{aligned} \tag{5.4}$$

where the a_m terms are the coefficients for function m. The polynomial fitting coefficients for η_E, η_G, t_{CD}, t_{CS}, μ_{CD}, μ_{CS} and u_{CS} are listed in Table 5.2.[43] The maximum metamodel error among the test points is 0.1 miles/kWh, 0.1 miles/gallon, 0.5 seconds, 0.02 kWh, and 0.5% for electrical efficiency, gasoline efficiency, acceleration time, energy processed, and final SOC, respectively.

[42] SOE design swing specification (x_4) is not relevant for these performance tests.

[43] We truncated the acceleration data points greater than 13.0 seconds to improve the metamodel fit, and fit μ_{CD}, μ_{CS} and u_{CS} using quadratic terms to avoid over-fitting.

Table 5.2 Polynomial coefficients of the PHEV performance meta-model

f_{m3}	η_E	η_G	t_{CD}	t_{CS}	μ_{CD}*	μ_{CS}*	u_{CS}*
m	1	2	3	4	5	6	7
a_{m1}	0.008	2.214	1.457	3.334			
a_{m2}	0.154	1.087	-5.496	-2.266			
a_{m3}	0.353	5.578	-28.46	-20.26			
a_{m4}	-0.005	-0.815	0.913	0.414			
a_{m5}	-0.005	0.510	-0.881	-3.524			
a_{m6}	-0.025	1.562	-1.050	-0.286			
a_{m7}	0.000	2.212	-0.308	-10.11			
a_{m8}	-0.057	-0.613	2.044	1.951			
a_{m9}	-0.043	0.254	15.61	10.31			
a_{m10}	-0.016	-0.159	0.336	5.808			
a_{m11}	-0.001	-8.906	-4.634	-6.932	0.010	0.466	-0.194
a_{m12}	-0.805	-6.095	31.48	15.80	0.011	-0.008	-0.005
a_{m13}	-0.656	-15.21	34.02	39.20	0.053	-0.018	0.047
a_{m14}	0.057	0.089	1.153	7.901	0.000	-0.014	0.000
a_{m15}	0.080	-3.274	1.169	6.582	0.008	-0.038	0.011
a_{m16}	0.342	2.498	-32.06	-30.12	-0.003	0.010	-0.001
a_{m17}	-0.191	2.622	3.405	-6.734	0.097	-0.890	0.382
a_{m18}	1.189	9.285	-54.47	-26.39	0.038	0.077	0.019
a_{m19}	-0.347	5.837	9.570	-4.098	0.370	0.400	-0.077
a_{m20}	4.960	57.68	44.23	32.10	2.196	1.441	0.140

* The terms are fit with quadratic form.

5.1.3 Electric Travel and Battery Degradation

To calculate each objective function, we first define the distance driven on electric power s_E and the distance driven on gasoline s_G as a function of the vehicle's AER s_{AER} and the total distance driven per day s. Based on the same structure of Eq. (4.2), s_E and s_G are given by

$$s_E(\mathbf{x}, s) = \begin{cases} s & \text{if } s \le s_{AER} \\ s_{AER}(\mathbf{x}) & \text{if } s > s_{AER} \end{cases}$$
$$s_G(\mathbf{x}, s) = \begin{cases} 0 & \text{if } s \le s_{AER} \\ s - s_{AER}(\mathbf{x}) & \text{if } s > s_{AER} \end{cases} \tag{5.5}$$

We assume that PHEVs travelled in a distance less than the AER the battery are charged as much as needed for the trip, and the battery is fully charged for distances greater than the AER. For HEVs and CVs, there is no electrical travel; thus HEV and CV can be seen as special cases with

s_{AER} = 0, so that s_E = 0 and s_G = s. Assuming constant efficiency η_E (mile per kWh) in CD-mode, the AER of a PHEV can be calculated from the energy capacity per battery cell κ = 0.0216 kWh/cell, the (scaled) number of cells x_3, and the design swing x_4:

$$s_{\mathrm{AER}}(\mathbf{x}) = \kappa(1000x_3)x_4\eta_{\mathrm{E}} \tag{5.6}$$

We consider two distinct battery degradation models from the literature and examine their implications for PHEV design. The Rosenkranz model, which has been used in prior PHEV studies (Markel and Simpson, 2006; Simpson, 2006; Kromer and Heywood, 2009; Amjad et al., 2010; Brooker et al., 2010), views battery degradation as a function of DOD per charge cycle, as shown in Figure 5.3(a), which cannot predict additional degradation due to energy use in CS mode. In contrast, the Peterson model (2010) was constructed by cycling modern A123 $LiFePO_4$ cells under representative driving cycles (non-constant C-rate) and measuring capacity fade as a function of energy processed, including intermediate charging and discharging over the driving cycle. Results show relative energy capacity fade as a linear function of normalized energy processed, as shown in Figure 5.3(b).

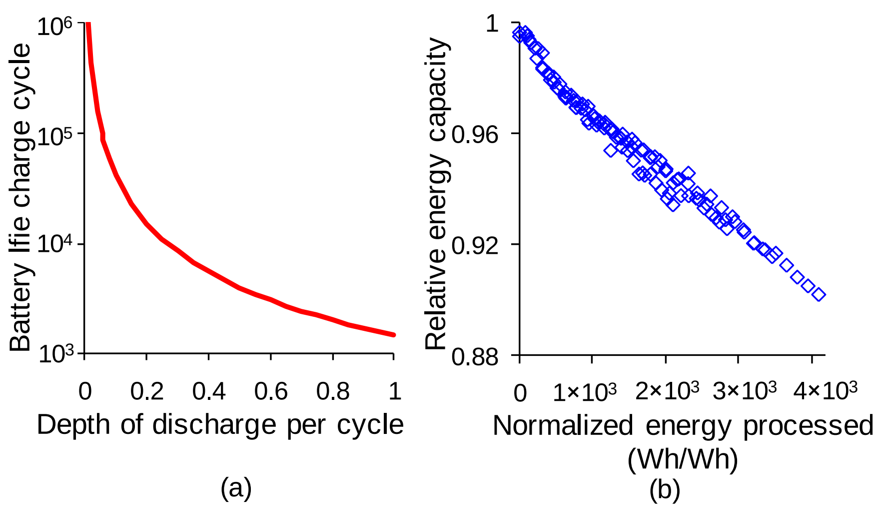

Figure 5.3 (a) Rosenkranz DOD-based degradation model; (b) Peterson energy-based degradation model

Peterson model: The daily energy processed while driving w_{DRV} and charging w_{CHG} a PHEV can be expressed as:

$$\begin{aligned} w_{\mathrm{DRV}}(\mathbf{x},s) &= \mu_{\mathrm{CD}} s_{\mathrm{E}} + \mu_{\mathrm{CS}} s_{\mathrm{G}} \\ w_{\mathrm{CHG}}(\mathbf{x},s) &= \frac{s_{\mathrm{E}}}{\eta_{\mathrm{E}}\eta_{\mathrm{B}}} \end{aligned} \tag{5.7}$$

where μ_{CD} and μ_{CS} are energy processed per mile (kWh/mile) in CD and CS mode, respectively, and battery charging efficiency η_{B} = 95% (Peterson, 2009). We assume that energy processed for daily charging is equal to net energy consumed in electrical travel per day. The relative energy capacity decrease can be calculated by the energy processed in driving and charging per cycle per cell per original cell energy capacity:

$$r_{\mathrm{P}}(\mathbf{x},s) = \frac{\alpha_{\mathrm{DRV}} w_{\mathrm{DRV}} + \alpha_{\mathrm{CHG}} w_{\mathrm{CHG}}}{1000 x_3 \kappa} \tag{5.8}$$

where $\alpha_{\mathrm{DRV}} = 3.46\times10^{-5}$ (kWh/kWh) and $\alpha_{\mathrm{CHG}} = 1.72\times10^{-5}$ (Wh/Wh) are the normalized coefficients for relative energy capacity fade (Peterson, 2009). If the battery end-of-life is defined as the point when the drop in relative energy capacity is r_{EOL}, the battery life θ_{BAT}, measured in days (or, equivalently, cycles), can be calculated as

$$\theta_{\mathrm{BAT}}(\mathbf{x},s) = \frac{r_{\mathrm{EOL}}}{r_{\mathrm{P}}} = \frac{1000 x_3 \kappa r_{\mathrm{EOL}}}{\alpha_{\mathrm{DRV}}\left(\mu_{\mathrm{CD}} s_{\mathrm{E}} + \mu_{\mathrm{CS}} s_{\mathrm{G}}\right) + \alpha_{\mathrm{CHG}} s_{\mathrm{E}} \left(\eta_{\mathrm{E}}\eta_{\mathrm{B}}\right)^{-1}} \tag{5.9}$$

The r_{EOL} criterion is defined at 20% (Peterson et al., 2010).

Rosenkranz model: To estimate battery life using the Rosenkranz model, DOD needs to be calculated first. Because we assume energy consumption is constant in CD mode, energy consumption is proportional to electric travel distance. If we define maximum SOC at 100%, the energy-based DOD δ is equal to the ratio of electric travel distance s_{E} to the maximum distance that could be traveled on total battery energy capacity:

$$\delta(\mathbf{x},s) = x_4 \frac{s_{\mathrm{E}}}{s_{\mathrm{AER}}} = \frac{s_{\mathrm{E}}}{\eta_{\mathrm{E}}(1000 x_3 \kappa)} \tag{5.10}$$

The battery life charge cycle θ_{BAT} is estimated using the degradation curve in Figure 5.3(a):

$$\theta_{\mathrm{BAT}}(\mathbf{x},s) = 1441\delta^{-1.46} = 1441\left(\frac{s_{\mathrm{E}}}{\eta_{\mathrm{E}}(1000 x_3 \kappa)}\right)^{-1.46} \tag{5.11}$$

5.1.4 Objective Functions

The three objectives, petroleum consumption, life cycle GHG emissions, and cost, are functions of vehicle design variables $\mathbf{x}$ and the distance traveled per day s. We define the functions as follows:

Petroleum consumption: The average petroleum consumed per day $f_{\mathrm{G}}(\mathbf{x},s)$ is given by

$$f_{\mathrm{G}}(\mathbf{x},s) = \frac{s_{\mathrm{G}}(\mathbf{x},s)}{\eta_{\mathrm{G}}(\mathbf{x})} \tag{5.12}$$

For the HEV and CV cases, Eq. (5.12) reduces to s/η_{G}.[44]

Lifecycle greenhouse gas emissions: The operating (use phase) GHG emissions v_{OP} represents the average GHG emissions in kg-CO_2-eq per day associated with the lifecycle of gasoline and electricity used to propel the vehicle:

$$v_{\mathrm{OP}}(\mathbf{x},s) = \frac{s_{\mathrm{E}}(\mathbf{x},s)}{\eta_{\mathrm{E}}(\mathbf{x})}\frac{v_{\mathrm{E}}}{\eta_{\mathrm{C}}} + \frac{s_{\mathrm{G}}(\mathbf{x},s)}{\eta_{\mathrm{G}}(\mathbf{x})} v_{\mathrm{G}} \tag{5.13}$$

where η_{C}=88% for battery charging efficiency (EPRI, 2007), v_{E} = 0.75 kg-CO_2-eq per kWh for electricity emissions[45], and v_{G} = 11.34 kg-CO_2-eq per gallon for gasoline life cycle emissions.

[44] Petroleum makes up less than 1.6% of the U.S. electricity grid mix (EIA, 2009), and we ignore it here.

[45] The life cycle GHG emissions of electricity is estimated based on the 2005 US average grid mixture 0.69 kg-CO_2-eq/kWh (Weber et al., 2010) with 9% transmission loss (EIA, 2008).

Total life cycle GHG emissions further includes the GHGs associated with production of the vehicle and battery. The average total lifecycle GHG emissions per day $f_V(\mathbf{x},s)$ is

$$f_V(\mathbf{x},s) = \nu_{OP}(\mathbf{x},s) + \left(\frac{\nu_{VEH}}{\theta_{VEH}(s)}\right) + \left(\frac{1000 x_3 \kappa \nu_B}{\theta_{BRPL}(\mathbf{x},s)}\right) \tag{5.14}$$

where $\theta_{VEH} = s_{LIFE}/s$ is the vehicle life in days, s_{LIFE} = 150,000 miles is the vehicle life in miles[46], θ_{BRPL} is the battery replacement effective life (defined below), ν_B = 120 kg-CO_2-eq per kWh for Li-ion battery and 230 kg-CO2-eq per kWh for NiMH battery is the life cycle GHG emissions associated with battery production, ν_{VEH} = 8,500 kg-CO_2-eq per vehicle is the life cycle GHG emissions associated with vehicle production (excluding emissions from battery production) (Samaras and Meisterling, 2008).

Battery replacement scenarios: We consider two battery replacement scenarios. The first is *battery leasing*: batteries are assumed to be replaced at the rate that they reach end of life, regardless of vehicle life. This simple and optimistic case essentially assumes that batteries can be swapped from vehicle to vehicle until they reach end of life, and $\theta_{BRPL} = \theta_{BAT}$.

The second scenario is *buy-lease*: If the battery outlasts the life of the vehicle, a single battery pack must be purchased – partial payment for batteries is not allowed, and old batteries are not placed into new vehicles. But if the vehicle outlasts the battery, battery replacement is managed by lease. In this scenario, $\theta_{BRPL} = \min(\theta_{BAT}, \theta_{VEH})$.

Equivalent annualized cost (EAC): To calculate EAC, we define a nominal discount rate r_N, an inflation rate r_I, and the real discount rate $r_R = (1+r_N)/(1+r_I) - 1$. The net present value

[46] We assume that all vehicles must be replaced every 150,000 miles, which represents the U.S. average vehicle life (EPA, 2006). This assumption may be unrealistic for vehicles driven very short or very long daily distances because other time-based factors also play a role in vehicle deterioration. However, these factors are only significant for regions of the objective function's integrand that are relatively insignificant to the integrated objective function, and they do not provide a significant source of error.

P of vehicle ownership is the sum of the cost of vehicle operation, vehicle production, and battery costs over the vehicle life:

$$P = \sum_{n=1}^{T(s)} \frac{c_{\mathrm{OP}} D}{\left(1+r_{\mathrm{R}}\right)^n} + c_{\mathrm{VEH}} + \begin{cases} \text{Buy:} & c_{\mathrm{BAT}} \\ \text{Lease:} & \displaystyle\sum_{n=1}^{T(s)} \frac{c_{\mathrm{BAT}} R\left(r_{\mathrm{N}}, B(\mathbf{x},s)\right)}{\left(1+r_{\mathrm{N}}\right)^n} \end{cases} \tag{5.15}$$

where D is driving days per year (D = 300 days in this study), T is vehicle life in years ($T(s) = \theta_{\mathrm{VEH}}/D = s_{\mathrm{LIFE}}/(sD)$), B is battery life in years ($B(\mathbf{x},s) = \theta_{\mathrm{BAT}}(\mathbf{x},s)/D$). The operating cost per day c_{OP} is the sum of the cost of electricity needed to charge the battery and the cost of gasoline consumed:

$$c_{\mathrm{OP}}\left(\mathbf{x},s\right) = \frac{s_{\mathrm{E}}\left(\mathbf{x},s\right)}{\eta_{\mathrm{E}}(\mathbf{x})} \frac{c_{\mathrm{E}}}{\eta_{\mathrm{C}}} + \frac{s_{\mathrm{G}}\left(\mathbf{x},s\right)}{\eta_{\mathrm{G}}(\mathbf{x})} c_{\mathrm{G}} \tag{5.16}$$

R is capital recovery factor. The generic expression of R as a function of discount rate r and time period N in year is

$$R\left(r,N\right) = \left(\sum_{n=1}^{N} \frac{1}{\left(1+r\right)^n} \right)^{-1} = \frac{r}{1-\left(1+r\right)^{-N}} \tag{5.17}$$

The net present value of battery leasing cost is calculated by calculating the EAC of the battery over its life B using $R(r_{\mathrm{N}}, B)$ and then summing the present value of annual battery cost over the vehicle life T. The EAC of vehicle ownership is $P \cdot R(r_{\mathrm{N}},T(s))$. We divide by D to obtain EAC per driving day:

$$\begin{aligned} f_{\mathrm{C}}\left(\mathbf{x},s\right) &= P \cdot R\left(r_{\mathrm{N}},T(s)\right) \cdot D^{-1} \\ &= c_{\mathrm{OP}} \frac{R\left(r_{\mathrm{N}},T(s)\right)}{R\left(r_{\mathrm{R}},T(s)\right)} + c_{\mathrm{VEH}} R\left(r_{\mathrm{N}},T(s)\right) D^{-1} \\ &\quad + \begin{cases} \text{Buy:} & c_{\mathrm{BAT}} R\left(r_{\mathrm{N}},T(s)\right) D^{-1} \\ \text{Lease:} & c_{\mathrm{BAT}} R\left(r_{\mathrm{N}},B(\mathbf{x},s)\right) D^{-1} \end{cases} \end{aligned} \tag{5.18}$$

The vehicle cost (excluding battery pack) c_{VEH} is the sum of vehicle base cost c_{BASE} = \$11,183, where engine cost $c_{\mathrm{ENG}}(x_1) = 17.8\times(57x_1) + 650$, motor cost $c_{\mathrm{MTR}}(x_2) = 26.6\times(52x_2) + 520$ (EPRI, 2001).[47] The battery pack cost $c_{\mathrm{BAT}} = 1000x_3\kappa c_{\mathrm{B}}$, where Li-ion battery unit cost c_{B} = \$400/kWh (for PHEV only), and NiMH battery unit cost = \$600/kWh (for HEV only) in our base case (Whitacre, 2009).[48] We use the 2008 annual average residential electricity price c_{E} = \$0.11 per kWh (EIA, 2009), and the 2008 annual average gasoline price c_{G} = \$3.30 per gallon (EIA, 2009) in our base case. For HEV and CV, $s_{\mathrm{E}} = 0$, and operating cost consists only of gasoline cost. We ignore the possibility of vehicle to grid energy arbitrage for PHEVs, since net earning potential is estimated to be low (Peterson et al., 2010), especially under a mass adoption scenario. In the base case of this study, we assume zero discounting. By applying l'Hôpital's rule, the capital recovery factor reduces to $1/N$:

$$\lim_{r\to 0}\frac{r}{1-(1+r)^{-N}} = \lim_{r\to 0}\frac{1}{N(1+r)^{-N-1}} = \frac{1}{N} \tag{5.19}$$

Thus Eq. (5.18) can be simplified to

$$\begin{aligned} f_{\mathrm{C}}(\mathbf{x},s) &= c_{\mathrm{OP}} + c_{\mathrm{VEH}}(TD)^{-1} + \begin{cases} \text{Buy: } c_{\mathrm{BAT}}(TD)^{-1} \\ \text{Lease: } c_{\mathrm{BAT}}(BD)^{-1} \end{cases} \\ &= c_{\mathrm{OP}}(\mathbf{x},s) + \frac{c_{\mathrm{VEH}}(\mathbf{x})}{\theta_{\mathrm{VEH}}(s)} + \frac{c_{\mathrm{BAT}}(\mathbf{x})}{\theta_{\mathrm{BRPL}}(\mathbf{x},s)} \end{aligned} \tag{5.20}$$

---

[47] To obtain a comparable vehicle base cost c_{BASE} (excluding engine, motor and battery) among PHEV, HEV and CV, we use the 2008 Prius manufacturer suggested retail price (MSRP) \$21,600 and subtract a 20% dealer mark-up (Lipman and Delucchi, 2006), a NiMH battery pack of \$3,250, base engine cost \$1,665 and base motor cost \$1,902 in our cost estimation. We assume 20% dealer mark-up for the Prius NiMH battery replacement cost \$3,900 (Naughton, 2008).The engine and motor costs are estimated based on size using the linear cost model from the literature (Simpson, 2006) and converted into 2008 dollars using the producer price index (BLS, 2009). The resulting vehicle base cost is c_{BASE} = \$11,183. We ignore vehicle and battery salvage value.

[48] Future battery costs are uncertain. The Li-ion battery cost \$400/kWh (Whitacre, 2009) and NiMH battery cost \$600/kWh (Duvall, 2004) are chosen to represent an optimistic but realistic estimate of near term battery costs in mass production, and we examine a range of costs in our sensitivity analysis.

The above equation has the same structure as the average lifecycle GHG function $f_V(\mathbf{x},s)$ in Eq. (5.14).

5.1.5 Constraint Functions

In order to compare apples to apples, we require that all vehicles meet a minimum acceleration constraint of 0-60 mph in less than 11 seconds. Because we have limited our scope to all-electric PHEVs, we require the acceleration constraint to be satisfied both in CD mode, using electric power alone, and in CS mode, where the gasoline engine is also used. The resulting constraints are $t_{CD}(\mathbf{x}) \leq 11$s and $t_{CS}(\mathbf{x}) \leq 11$s. Additionally, we require the gasoline engine to be large enough to provide average power for the vehicle in CS mode under an aggressive US06 driving cycle while maintaining the target SOC level in the battery. The resulting constraint is $u_{CS}(\mathbf{x}) \geq 32\%$. Finally, we impose simple bounds on the decision variables: $30/57 \leq x_1 \leq 60/57$, $50/52 \leq x_2 \leq 110/52$, $200/1000 \leq x_3 \leq 1000/1000$, $0 \leq x_4 \leq 0.8$ to avoid metamodel extrapolation. Any active simple bounds would imply a modeling limitation rather than a physical optimum. As we will later show, across all cases, of the simple bounds only the upper bounds on battery size and swing are ever active. The upper bound on battery size is reached only when minimizing petroleum consumption, since more battery is always preferred for this objective. The upper bound on swing is taken as a practical constraint since (1) SOC cannot be measured precisely, so the battery must be held safely away from the maximum physical capacity, where explosion can occur, (2) battery resistance, which is relatively flat over most of the SOC window, rises considerably near 0% SOC, causing a drop in efficiency and power output and an increase in heat generation, and (3) batteries are typically considered “dead” when their usable capacity fades to 80% of the original capacity.

5.1.6 MINLP Reformulation

The resulting model formulation (Eq. (5.2)) is comprised of integration, discrete decisions (vehicle type), and piecewise-smooth functions (with derivative discontinuities due to AER and battery life). To solve the problem globally, we pose a factorable, algebraic nonconvex MINLP reformulation that can be solved using the BARON convexification-based branch-and-reduce algorithm (Tawarmalani and Sahinidis, 2004). First, the exponential distribution form for the NHTS data fit allows the integral in Eq. (5.2) to be simplified in terms of two algebraic formulae: cumulative density function F_S:

$$\begin{aligned} F_S(s_i) &= \int_0^{s_i} f(s)ds = \int_0^{s_i} \lambda e^{-\lambda s} ds \\ &= \left[-e^{-\lambda s}\right]_0^{s_i} = 1 - e^{-\lambda s_i} \end{aligned} \tag{5.21}$$

and expected value function F_E:

$$\begin{aligned} F_E(s_i) &= \int_0^{s_i} s f_S(s) ds = \int_0^{s_i} \lambda s e^{-\lambda s} ds \\ &= \left[-s e^{-\lambda s}\right]_0^{s_i} + \int_0^{s_i} e^{-\lambda s} ds = \frac{1}{\lambda} - e^{-\lambda s_i}\left(s_i + \frac{1}{\lambda}\right) \end{aligned} \tag{5.22}$$

Thus the problem reduces to an algebraic formulation with discrete vehicle-type decisions and piecewise-smooth functions.

We next introduce four sets of binary variables to convert the problem to a twice-differentiable MINLP. The first binary variable set t_{il} identifies the vehicle type $l \in \{1,2,..,L\}$ for each segment i, where $t_{il} \in \{0,1\}$ $\forall i,l$ and $\Sigma_l t_{il} = 1$ $\forall i$. Here we consider three vehicle types $l \in \{1,2,3\}$ for CV, HEV and PHEV, respectively, and write the objective function as a binary-weighted function $\sum_l (t_l)(f(\mathrm{x}_l, s))$ where $j \in \{1,2,3\}$ and $l \in \{1,2,..,L\}$. Finally, we represent these conditions in the objective function as $\sum_j (z_{ij})(F_{ijko})$, where $z_{ij} \in \{0,1\}$, $\sum_j z_{ij} = 1$, and

$(z_{i1})(s_{\mathrm{AER}}(\mathbf{x}_i) - s_{i\text{-}1}) \leq 0$; $(z_{i2})(s_{i\text{-}1} - s_{\mathrm{AER}}(\mathbf{x}_i)) \leq 0$; $(z_{i2})(s_{\mathrm{AER}}(\mathbf{x}_i) - s_i) \leq 0$; $(z_{i3})(s_i - s_{\mathrm{AER}}(\mathbf{x}_i)) \leq 0$, $\forall i,k,o$.

The second binary variable set $z_{ij} \in \{0,1\}$ $\forall i,j$ handles one of the derivative discontinuities by identifying in which of three regions $j \in \{1,2,3\}$ on the s-axis each segment i is located, relative to s_{AER} ($\Sigma_j z_{ij} = 1$ $\forall i$).

(1) In region 1, $s_{\mathrm{AER}} \leq s_i \Rightarrow (z_{i1})(s_{\mathrm{AER}}(\mathrm{x}_i) - s_{i\text{-}1}) \leq 0$;

(2) in region 2, $s_{i\text{-}1} \leq s_{\mathrm{AER}} \leq s_i \Rightarrow (z_{i2})(s_{i\text{-}1} - s_{\mathrm{AER}}(\mathbf{x}_i)) \leq 0$ and $(z_{i2})(s_{\mathrm{AER}}(\mathbf{x}_i) - s_i) \leq 0$; and

(3) in region 3, $s_{\mathrm{AER}} \geq s_i \Rightarrow (z_{i3})(s_i - s_{\mathrm{AER}}(\mathrm{x}_i)) \leq 0$.

The integral of driver population weighted operating costs is

$$F_{i\mathrm{OC}} = \int_{s_{i-1}}^{s_i} \left(\frac{s_{\mathrm{E}}(\mathbf{x},s)}{\eta_{\mathrm{E}}(\mathbf{x})} \frac{c_{\mathrm{E}}}{\eta_{\mathrm{C}}} + \frac{s_{\mathrm{G}}(\mathbf{x},s)}{\eta_{\mathrm{G}}(\mathbf{x})} v_{\mathrm{G}} \right) f_{\mathrm{S}}(s)\, ds$$
$$= \begin{cases} j{=}1,\ s_{\mathrm{AER}} \leq s_{i-1}: \\ \quad \displaystyle\int_{s_{i-1}}^{s_i} \frac{c_{\mathrm{E}}}{\eta_{\mathrm{E}}\eta_{\mathrm{C}}} s_{\mathrm{E}} + \frac{v_{\mathrm{G}}}{\eta_{\mathrm{G}}} s_{\mathrm{G}} \lambda e^{-\lambda s} ds \\ j{=}2,\ s_{i-1} \leq s_{\mathrm{AER}} \leq s_i: \\ \quad \displaystyle\int_{s_{i-1}}^{s_{\mathrm{AER}}} \frac{c_{\mathrm{E}}}{\eta_{\mathrm{E}}\eta_{\mathrm{C}}} s_{\mathrm{E}} \lambda e^{-\lambda s} ds + \int_{s_{\mathrm{AER}}}^{s_i} \left(\frac{c_{\mathrm{E}}}{\eta_{\mathrm{E}}\eta_{\mathrm{C}}} s_{\mathrm{E}} + \frac{c_{\mathrm{G}}}{\eta_{\mathrm{G}}} s_{\mathrm{G}} \right) \lambda e^{-\lambda s} ds \\ j{=}3,\ s_i \leq s_{\mathrm{AER}}: \\ \quad \displaystyle\int_{s_{i-1}}^{s_i} \frac{c_{\mathrm{E}}}{\eta_{\mathrm{E}}\eta_{\mathrm{C}}} s_{\mathrm{E}} \lambda e^{-\lambda s} ds \end{cases} \tag{5.23}$$

With utilizing the equations of F_{S} (Eq. (5.21)) and F_{E} (Eq. (5.22)), the above integral can be expressed in sum of three analytical functions:

$$F_{i\mathrm{OC}} = \sum_{j=1}^{3} z_{ij} F_{i\mathrm{OC}j}\left(\mathbf{x}_{il}, s_{i-1}, s_i\right)$$

$$= \begin{cases} j{=}1,\ s_{\mathrm{AER}} \le s_{i-1}: \\ \quad F_{i\mathrm{OC1}} = \dfrac{c_{\mathrm{G}}}{\eta_{\mathrm{G}}}\left(F_{\mathrm{E}}\left(s_i\right) - F_{\mathrm{E}}\left(s_{i-1}\right)\right) + s_{\mathrm{AER}}\left(\dfrac{v_{\mathrm{E}}}{\eta_{\mathrm{E}}\eta_{\mathrm{C}}} - \dfrac{v_{\mathrm{G}}}{\eta_{\mathrm{G}}}\right)\left(F_{\mathrm{S}}\left(s_i\right) - F_{\mathrm{S}}\left(s_{i-1}\right)\right) \\ j{=}2,\ s_{i-1} \le s_{\mathrm{AER}} \le s_i: \\ \quad F_{i\mathrm{OG2}} = \dfrac{c_{\mathrm{E}}}{\eta_{\mathrm{E}}\eta_{\mathrm{C}}}\left(F_{\mathrm{E}}\left(s_{\mathrm{AER}}\right) - F_{\mathrm{E}}\left(s_{i-1}\right)\right) + \dfrac{v_{\mathrm{G}}}{\eta_{\mathrm{G}}}\left(F_{\mathrm{E}}\left(s_i\right) - F_{\mathrm{E}}\left(s_{\mathrm{AER}}\right)\right) \\ \qquad\qquad + s_{\mathrm{AER}}\left(\dfrac{v_{\mathrm{E}}}{\eta_{\mathrm{E}}\eta_{\mathrm{C}}} - \dfrac{v_{\mathrm{G}}}{\eta_{\mathrm{G}}}\right)\left(F_{\mathrm{S}}\left(s_i\right) - F_{\mathrm{S}}\left(s_{\mathrm{AER}}\right)\right) \\ j{=}3,\ s_i \le s_{\mathrm{AER}}: \\ \quad F_{i\mathrm{OG3}} = \dfrac{c_{\mathrm{E}}}{\eta_{\mathrm{E}}\eta_{\mathrm{C}}}\left(F_{\mathrm{E}}\left(s_i\right) - F_{\mathrm{E}}\left(s_{i-1}\right)\right) \end{cases} \tag{5.24}$$

The third binary variable set q_{io} $o \in \{1,2,3\}$ and $\Sigma_o q_{io} = 1$ $\forall i$ identifies the relative conditions between battery life θ_{BAT} and vehicle life θ_{VEH}. Here we define the battery life in vehicle mileage travelled (VMT) as s_{BAT}, which can be calculated by multiplying daily driving distance by battery life charge cycles ($s_{\mathrm{BAT}}{=}s\theta_{\mathrm{BAT}}$) with assuming one charge per day. The estimated battery life s_{BAT} using the Peterson degradation model is a non-decreasing function of s:

$$s_{\mathrm{BAT}}\left(\mathbf{x}, s\right) = s\theta_{\mathrm{BAT}} = \frac{1000 x_3 \kappa r_{\mathrm{EOL}} s}{\alpha_{\mathrm{DRV}}\left(\mu_{\mathrm{CD}} s_{\mathrm{E}} + \mu_{\mathrm{CS}} s_{\mathrm{G}}\right) + \alpha_{\mathrm{CHG}} s_{\mathrm{E}}\left(\eta_{\mathrm{E}}\eta_{\mathrm{B}}\right)^{-1}}$$

$$= \begin{cases} \dfrac{1000 x_3 \kappa r_{\mathrm{EOL}}}{\alpha_{\mathrm{DRV}}\mu_{\mathrm{CD}} + \alpha_{\mathrm{CHG}}\left(\eta_{\mathrm{E}}\eta_{\mathrm{B}}\right)^{-1}} = s_{\mathrm{BAT}}^{0} & \text{if } s \le s_{\mathrm{AER}} \\ \dfrac{1000 x_3 \kappa r_{\mathrm{EOL}}}{s^{-1} s_{\mathrm{AER}}\left(\alpha_{\mathrm{DRV}}\left(\mu_{\mathrm{CD}} - \mu_{\mathrm{CS}}\right) + \alpha_{\mathrm{CHG}}\left(\eta_{\mathrm{E}}\eta_{\mathrm{B}}\right)^{-1}\right) + \alpha_{\mathrm{DRV}}\mu_{\mathrm{CS}}} & \text{if } s > s_{\mathrm{AER}} \\ \dfrac{1000 x_3 \kappa r_{\mathrm{EOL}}}{\alpha_{\mathrm{DRV}}\mu_{\mathrm{CS}}} = s_{\mathrm{BAT}}^{\infty} & \text{if } s \to \infty \end{cases} \tag{5.25}$$

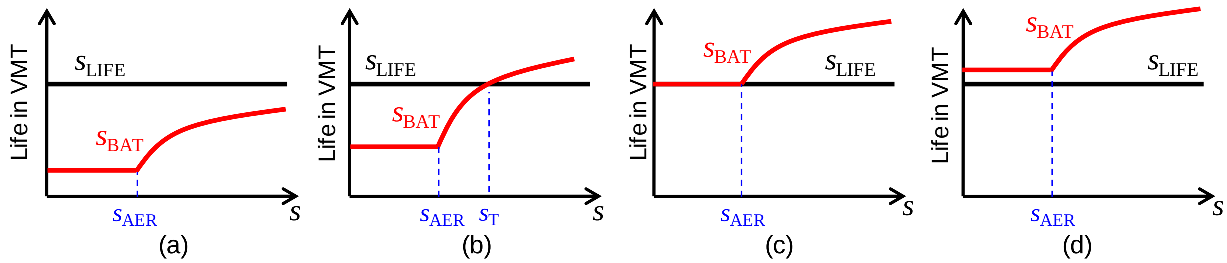

Figure 5.4 Four conditions for the battery and vehicle VMT curves

The expression for $s \rightarrow \infty$ is simplified from the conditional expression for $s > s_{\mathrm{AER}}$ by imposing $s^{-1} \rightarrow 0$. The function s_{BAT} has two unique characteristics. First, the function value is a constant when $s \leq s_{\mathrm{AER}}$. Second, when $s \geq s_{\mathrm{AER}}$, s_{BAT} is a monotonically increasing function and asymptotically approaches the life of the battery on energy processed in CS mode, which is the constant value under $s \rightarrow \infty$ condition. Because of the unique features in s_{BAT}, we are able to identify four possible relations between s_{BAT} and vehicle life s_{LIFE}:

(a) battery life $s_{\mathrm{BAT}}(\mathbf{x}, s)$ is less than vehicle life s_{LIFE} for all s;

(b) s_{BAT} curve and s_{LIFE} curve has one intersection point s_{T}, where $s_{\mathrm{LIFE}} > s_{\mathrm{BAT}}$ for $0 \leq s \leq s_{\mathrm{T}}$ and $s_{\mathrm{BAT}} > s_{\mathrm{LIFE}}$ for $s \geq s_{\mathrm{T}}$;

(c) the flat region of s_{BAT} overlaps with s_{LIFE} ($s_{\mathrm{BAT}} = s_{\mathrm{LIFE}}$) for $0 \leq s \leq s_{\mathrm{AER}}$, and $s_{\mathrm{BAT}} > s_{\mathrm{LIFE}}$ for $s \geq s_{\mathrm{T}}$; and

(d) s_{BAT} is greater than vehicle life s_{LIFE} for all s.

The four conditions are illustrated in Figure 5.4. For the condition (b) specifically, an analytical expression for s_{T} is available by solving $s_{\mathrm{LIFE}} = s_{\mathrm{BAT}}(\mathbf{x}, s_{\mathrm{T}})$:

$$s_{\mathrm{T}}(\mathbf{x}) = \frac{s_{\mathrm{LIFE}} s_{\mathrm{AER}} \left(\alpha_{\mathrm{DRV}} \left(\mu_{\mathrm{CD}} - \mu_{\mathrm{CS}} \right) + \alpha_{\mathrm{CHG}} \left(\eta_{\mathrm{E}} \eta_{\mathrm{B}} \right)^{-1} \right)}{r_{\mathrm{EOL}} \kappa \left(1000 x_3 \right) - \alpha_{\mathrm{DRV}} \mu_{\mathrm{CS}} s_{\mathrm{LIFE}}} \qquad (5.26)$$

Condition (a) occurs when the following inequality is valid:

$$s_{\mathrm{BAT}}^{\infty} \leq s_{\mathrm{LIFE}} \tag{5.27}$$

Condition (c) and (d) occur when the following inequality is valid:

$$s_{\mathrm{BAT}}^{0} \geq s_{\mathrm{LIFE}} \tag{5.28}$$

The battery replacement effective life θ_{BRPL} under buy-lease scenario is determined by $\min(\theta_{\mathrm{VEH}}, \theta_{\mathrm{BAT}})$. Therefore, three discrete cases are identified:

(1) In case 1 (o=1), $s^{\infty}{}_{\mathrm{BAT}} \leq s_{\mathrm{LIFE}}$ ($\theta_{\mathrm{BAT}} < \theta_{\mathrm{VEH}}$) $\forall s \Rightarrow (q_{i1})(\theta_{\mathrm{BAT}}(s \Rightarrow \infty) - \theta_{\mathrm{VEH}}) \leq 0$ and $\theta_{\mathrm{BRPL}}=\theta_{\mathrm{BAT}}$;

(2) for case 2 (o=2), θ_{BAT} intersects θ_{VEH} at a point $s_{\mathrm{T}} \Rightarrow (q_{i2})(\theta_{\mathrm{VEH}} - \theta_{\mathrm{BAT}}(s \Rightarrow \infty)) \leq 0$ and $(q_{i2})(\theta_{\mathrm{BAT}}(s=0) - \theta_{\mathrm{VEH}}) \leq 0$, so $\theta_{\mathrm{BRPL}} = \theta_{\mathrm{BAT}}$ for $s \leq s_{\mathrm{T}}$, $\theta_{\mathrm{BRPL}} = \theta_{\mathrm{VEH}}$ for $s \geq s_{\mathrm{T}}$; and

(3) for case 3 (o=3), $s^{0}{}_{\mathrm{BAT}} \geq s_{\mathrm{LIFE}}$ ($\theta_{\mathrm{BAT}} \geq \theta_{\mathrm{VEH}}$) $\forall s \Rightarrow (q_{i3})(\theta_{\mathrm{VEH}} - \theta_{\mathrm{BAT}}(s=0)) \leq 0$ and $\theta_{\mathrm{BRPL}} = \theta_{\mathrm{VEH}}$.

The fourth binary variable set y_{ik} identifies in which region s_{T} lies when $q_{i2} = 1$ (o=2). The three conditions $k \in \{1,2,3\}$ on the binary variable set y_{ik} are:

(1) In region 1 (k=1), $s_{\mathrm{T}}(\mathbf{x}_i) \leq s_{i\text{-}1} \Rightarrow (q_{i2})(y_{i1})(s_{\mathrm{T}}(\mathbf{x}_i) - s_{i\text{-}1}) < 0$;

(2) in region 2 (k=2), $s_{i\text{-}1} \leq s_{\mathrm{T}} \leq s_i \Rightarrow (q_{i2})(y_{i2})(s_{i\text{-}1} - s_{\mathrm{T}}(\mathbf{x}_i)) \leq 0$ and $(q_{i2})(y_{i2})(s_{\mathrm{T}}(\mathbf{x}_i) - s_i) \leq 0$; and

(3) in region 3 (k=3), $s_{\mathrm{T}}(\mathbf{x}_i) \geq s_i \Rightarrow (q_{i2})(y_{i3})(s_i - s_{\mathrm{T}}(\mathbf{x}_i)) \leq 0$.

The combinations of j, k and o result in 27 cases. For each segment i, for each of the cases $j \in \{1,2,3\}$ $k \in \{1,2,3\}$ $o \in \{1,2,3\}$, the integral in Eq. reduces to a twice-differentiable closed form factorable algebraic expression $F_{ijko}(\mathbf{x}_{il}, s_{i\text{-}1}, s_i)$. Table 5.3 presents the summary of the discrete conditions with corresponding θ_{BRPL} and the components in the total cost function. Among the o=2 cases, there are three infeasible ones because the value of s_{T} should be greater than s_{AER} when an s_{T} point exists.

Table 5.3 Discrete conditions for estimating total cost on the AER and battery life

o		j		k		θ_{BRPL}	Total cost function F_{ijko}
1	$s_{\mathrm{BAT}}^{\infty} \le s_{\mathrm{LIFE}}$	1	$s_{\mathrm{AER}} \le s_{i-1}$			θ_{BAT}	$F_{i1k1} = c_{\mathrm{VEH}} + F_{\mathrm{OC1}} + F_{\mathrm{BC1a}}$
		2	$s_{i-1} \le s_{\mathrm{AER}} \le s_i$				$F_{i2k1} = c_{\mathrm{VEH}} + \mathrm{F}_{\mathrm{OC2}} + F_{\mathrm{BC1b}}$
		3	$s_i \le s_{\mathrm{AER}}$				$F_{i3k1} = c_{\mathrm{VEH}} + \mathrm{F}_{\mathrm{OC3}} + F_{\mathrm{BC1c}}$
2	$s_{\mathrm{BAT}}^{0} \le s_{\mathrm{LIFE}} \le s_{\mathrm{BAT}}^{\infty}$	1	$s_{\mathrm{AER}} \le s_{i-1}$	1	$s_{\mathrm{T}} \le s_{i-1}$	θ_{VEH}	$F_{i112} = c_{\mathrm{VEH}} + F_{\mathrm{OC1}} + F_{\mathrm{BC3}}$
				2	$s_{i-1} \le s_{\mathrm{T}} \le s_i$	$\{\theta_{\mathrm{BAT}}, \theta_{\mathrm{VEH}}\}$	$F_{\mathrm{i}122} = c_{\mathrm{VEH}} + F_{\mathrm{OC1}} + F_{\mathrm{BC2a}}$
				3	$s_i \le s_{\mathrm{T}}$	θ_{BAT}	$F_{\mathrm{i}132} = c_{\mathrm{VEH}} + F_{\mathrm{OC1}} + F_{\mathrm{BC1a}}$
		2	$s_{i-1} \le s_{\mathrm{AER}} \le s_i$	1	$s_{\mathrm{T}} \le s_{i-1}$	Infeasible	
				2	$s_{i-1} \le s_{\mathrm{T}} \le s_i$	$\{\theta_{\mathrm{BAT}}, \theta_{\mathrm{VEH}}\}$	$F_{i222} = c_{\mathrm{VEH}} + F_{\mathrm{OC2}} + F_{\mathrm{BC2b}}$
				3	$s_i \le s_{\mathrm{T}}$	θ_{BAT}	$F_{i232} = c_{\mathrm{VEH}} + F_{\mathrm{OC2}} + F_{\mathrm{BC1b}}$
		3	$s_i \le s_{\mathrm{AER}}$	1	$s_{\mathrm{T}} \le s_{i-1}$	Infeasible	
				2	$s_{i-1} \le s_{\mathrm{T}} \le s_i$	Infeasible	
				3	$s_i \le s_{\mathrm{T}}$	θ_{BAT}	$F_{\mathrm{i}332} = c_{\mathrm{VEH}} + F_{\mathrm{OC3}} + F_{\mathrm{BC1c}}$
3	$s_{\mathrm{BAT}}^{0} \ge s_{\mathrm{LIFE}}$	1	$s_{\mathrm{AER}} \le s_{i-1}$			θ_{VEH}	$F_{i1k3} = c_{\mathrm{VEH}} + F_{\mathrm{OC1}} + F_{\mathrm{BC3}}$
		2	$s_{i-1} \le s_{\mathrm{AER}} \le s_i$				$F_{i2k3} = c_{\mathrm{VEH}} + F_{\mathrm{OC2}} + F_{\mathrm{BC3}}$
		3	$s_i \le s_{\mathrm{AER}}$				$F_{i3k3} = c_{\mathrm{VEH}} + F_{\mathrm{OC3}} + F_{\mathrm{BC3}}$

The analytical expressions of battery cost function F_{BC} for all discrete cases are

(1a) $\theta_{\mathrm{BRPL}} = \theta_{\mathrm{BAT}}$ and $s_{\mathrm{AER}} \le s_{i\text{-}1}$

$$\begin{aligned} F_{\mathrm{BC1a}} = \frac{c_{\mathrm{BAT}}}{r_{\mathrm{EOL}}} \Big[& \alpha_{\mathrm{DRV}} w_{\mathrm{CS}} \left(F_{\mathrm{E}}\left(s_i\right) - F_{\mathrm{E}}\left(s_{i-1}\right) \right) \\ & + s_{\mathrm{AER}} \left(\alpha_{\mathrm{DRV}} w_{\mathrm{CD}} + \alpha_{\mathrm{CHG}} \left(\eta_{\mathrm{E}} \eta_{\mathrm{B}} \right)^{-1} - \alpha_{\mathrm{DRV}} w_{\mathrm{CS}} \right) \left(F_{\mathrm{S}}\left(s_i\right) - F_{\mathrm{S}}\left(s_{i-1}\right) \right) \Big] \end{aligned} \tag{5.29}$$

(1b) $\theta_{\mathrm{BRPL}} = \theta_{\mathrm{BAT}}$ and $s_{i\text{-}1} \le s_{\mathrm{AER}} \le s_i$

$$\begin{aligned} F_{\mathrm{BC1b}} = \frac{c_{\mathrm{BAT}}}{r_{\mathrm{EOL}}} \Big[& \left(\alpha_{\mathrm{DRV}} \mu_{\mathrm{CD}} + \alpha_{\mathrm{CHG}} \eta_{\mathrm{E}}^{-1} \right) \left(F_{\mathrm{E}}\left(s_{\mathrm{AER}}\right) - F_{\mathrm{E}}\left(s_{i-1}\right) \right) \\ & + \alpha_{\mathrm{DRV}} \mu_{\mathrm{CS}} \left(F_{\mathrm{E}}\left(s_i\right) - F_{\mathrm{E}}\left(s_{\mathrm{AER}}\right) \right) \\ & + s_{\mathrm{AER}} \left(\alpha_{\mathrm{DRV}} \mu_{\mathrm{CD}} + \alpha_{\mathrm{CHG}} \left(\eta_{\mathrm{E}} \eta_{\mathrm{B}} \right)^{-1} - \alpha_{\mathrm{DRV}} \mu_{\mathrm{CS}} \right) \left(F_{\mathrm{S}}\left(s_i\right) - F_{\mathrm{S}}\left(s_{\mathrm{AER}}\right) \right) \Big] \end{aligned} \tag{5.30}$$

(1c) $\theta_{\text{BRPL}} = \theta_{\text{BAT}}$ and $s_i \le s_{\text{AER}}$

$$F_{\text{BC1c}} = \frac{c_{\text{BAT}}}{r_{\text{EOL}}}\left(\alpha_{\text{DRV}}\mu_{\text{CD}} + \alpha_{\text{CHG}}\left(\eta_{\text{E}}\eta_{\text{B}}\right)^{-1}\right)\left(F_{\text{E}}\left(s_i\right) - F_{\text{E}}\left(s_{i-1}\right)\right) \tag{5.31}$$

(2a) $\theta_{\text{BRPL}} = \{\theta_{\text{BAT}}, \theta_{\text{VEH}}\}$ and $s_{\text{AER}} \le s_{i\text{-}1}$

$$\begin{aligned} F_{\text{BC2a}} = \frac{c_{\text{BAT}}}{r_{\text{EOL}}}\Big[& \alpha_{\text{DRV}}\mu_{\text{CS}}\left(F_{\text{E}}\left(s_{\text{T}}\right) - F_{\text{E}}\left(s_{i-1}\right)\right) \\ & + s_{\text{AER}}\left(\alpha_{\text{DRV}}\mu_{\text{CD}} + \alpha_{\text{CHG}}\left(\eta_{\text{E}}\eta_{\text{B}}\right)^{-1} - \alpha_{\text{DRV}}\mu_{\text{CS}}\right)\left(F_{\text{S}}\left(s_{\text{T}}\right) - F_{\text{S}}\left(s_{i-1}\right)\right)\Big] \\ & + \frac{1000 x_3 \kappa c_{\text{BAT}}}{s_{\text{LIFE}}}\left(F_{\text{E}}\left(s_i\right) - F_{\text{E}}\left(s_{\text{T}}\right)\right) \end{aligned} \tag{5.32}$$

(2b) $\theta_{\text{BRPL}} = \{\theta_{\text{BAT}}, \theta_{\text{VEH}}\}$ and $s_{i\text{-}1} \le s_{\text{AER}} \le s_i$

$$\begin{aligned} F_{\text{BC2b}} = \frac{c_{\text{BAT}}}{r_{\text{EOL}}}\Big[& \left(\alpha_{\text{DRV}}\mu_{\text{CD}} + \alpha_{\text{CHG}}\eta_{\text{E}}^{-1}\right)\left(F_{\text{E}}\left(s_{\text{AER}}\right) - F_{\text{E}}\left(s_{i-1}\right)\right) \\ & + \alpha_{\text{DRV}}\mu_{\text{CS}}\left(F_{\text{E}}\left(s_{\text{T}}\right) - F_{\text{E}}\left(s_{\text{AER}}\right)\right) \\ & + s_{\text{AER}}\left(\alpha_{\text{DRV}}\mu_{\text{CD}} + \alpha_{\text{CHG}}\left(\eta_{\text{E}}\eta_{\text{B}}\right)^{-1} - \alpha_{\text{DRV}}\mu_{\text{CS}}\right)\left(F_{\text{S}}\left(s_{\text{T}}\right) - F_{\text{S}}\left(s_{\text{AER}}\right)\right)\Big] \\ & + \frac{1000 x_3 \kappa c_{\text{BAT}}}{s_{\text{LIFE}}}\left(F_{\text{E}}\left(s_i\right) - F_{\text{E}}\left(s_{\text{T}}\right)\right) \end{aligned} \tag{5.33}$$

(3) $\theta_{\text{BRPL}} = \theta_{\text{VEH}}$

$$F_{\text{BC3}} = \frac{1000 x_3 \kappa c_{\text{BAT}}}{s_{\text{LIFE}}}\left(F_{\text{E}}\left(s_i\right) - F_{\text{E}}\left(s_{i-1}\right)\right) \tag{5.34}$$

Combining the vehicle base cost function F_{VC}, operating cost F_{OC}, and battery cost function F_{BC}, the closed-form expression of the total cost function F_{ijko} for each discrete condition is available by summing three functions ($F_{ijko} = c_{\text{VEH}} + F_{\text{OC}} + F_{\text{BC}}$), as shown in the last column in Table 5.3.

Total life cycle GHG emissions: The same condition equations for the total life cycle GHG emissions can be applied by replacing the cost parameters c_{BAT}, c_{VEH}, c_{E}, and c_{G} with lifecycle emission parameters v_{BAT}, v_{VEH}, v_{E}, and v_{G}, respectively.

MINLP formulation: The complete MINLP formulation takes the form

$$
\begin{aligned}
&\underset{\substack{\mathbf{x}_{il}, t_{il}, z_{ij}, y_{ik}, q_{io}, s_i \\ \forall i \in \{1,\ldots,n\},\ \forall l,j,k,o \in \{1,2,3\}}}{\text{minimize}} \quad \sum_{i=1}^{n}\sum_{l=1}^{3}\sum_{j=1}^{3}\sum_{k=1}^{3}\sum_{o=1}^{3} t_{il} z_{ij} y_{ik} q_{io} F_{ijko}\left(\mathbf{x}_{il}, s_{i-1}, s_i\right) \\
&\text{subject to } \mathbf{x}_l^{\mathrm{LB}} \le \mathbf{x}_{il} \le \mathbf{x}_l^{\mathrm{UB}};\ t_{\mathrm{CD}} \le 11;\ t_{\mathrm{CS}} \le 11;\ u_{\mathrm{CS}} \ge 32\%; \\
&\quad \textstyle\sum_{l=1}^{3} t_{il} = 1; \quad \sum_{j=1}^{3} z_{ij} = 1; \quad \sum_{k=1}^{3} y_{ik} = 1; \quad \sum_{o=1}^{3} q_{io} = 1; \quad s_{i-1} \le s_i; \\
&\quad (z_{i1})(s_{\mathrm{AER}} - s_{i-1}) \le 0; \qquad (z_{i2})(s_{i-1} - s_{\mathrm{AER}}) \le 0; \\
&\quad (z_{i2})(s_{\mathrm{AER}} - s_i) \le 0; \qquad (z_{i3})(s_i - s_{\mathrm{AER}}) \le 0; \\
&\quad (q_{i1})\left(s_{\mathrm{BAT}}^{\infty} - s_{\mathrm{LIFE}}\right) \le 0; \qquad (q_{i2})\left(s_{\mathrm{BAT}}^{0} - s_{\mathrm{LIFE}}\right) \le 0; \\
&\quad (q_{i2})\left(s_{\mathrm{LIFE}} - s_{\mathrm{BAT}}^{\infty}\right) \le 0; \qquad (q_{i3})\left(s_{\mathrm{LIFE}} - s_{\mathrm{BAT}}^{0}\right) \le 0; \\
&\quad (q_{i2})(y_{i1})(s_{\mathrm{T}} - s_{i-1}) \le 0; \quad (q_{i2})(y_{i2})(s_{i-1} - s_{\mathrm{T}}) \le 0; \\
&\quad (q_{i2})(y_{i2})(s_{\mathrm{T}} - s_i) \le 0; \quad (q_{i2})(y_{i3})(s_i - s_{\mathrm{T}}) \le 0; \\
&\quad t_{il}, z_{ij}, y_{ik}, q_{io} \in \{0,1\}; \quad s_i \in \mathbb{R}; \quad \mathbf{x}_{il} \in \mathbb{R}^{p_l};\ \forall i \in \{1,\ldots,n\}, \forall l,j,k,o \in \{1,2,3\} \\
&\text{where } s_0 = 0;\ s_n = \infty;\ s_{\mathrm{AER}} = 10^3 t_{i3} \kappa x_3 x_4 \eta_{\mathrm{E}};\ s_{\mathrm{BAT}}^{0} = \frac{10^3 x_3 \kappa r_{\mathrm{EOL}}}{\alpha_{\mathrm{DRV}} \mu_{\mathrm{CD}} + \alpha_{\mathrm{CHG}} \eta_{\mathrm{E}}^{-1}}; \\
&\quad s_{\mathrm{BAT}}^{\infty} = \frac{10^3 x_3 \kappa r_{\mathrm{EOL}}}{\alpha_{\mathrm{DRV}} \mu_{\mathrm{CS}}};\ s_{\mathrm{T}} = \frac{s_{\mathrm{LIFE}} s_{\mathrm{AER}} \left(\alpha_{\mathrm{DRV}} \left(\mu_{\mathrm{CD}} - \mu_{\mathrm{CS}}\right) + \alpha_{\mathrm{CHG}} \eta_{\mathrm{E}}^{-1}\right)}{10^3 \kappa x_3 r_{\mathrm{EOL}} - \alpha_{\mathrm{DRV}} \mu_{\mathrm{CS}} s_{\mathrm{LIFE}}} \\
&\quad \eta_{\mathrm{E}i} = \textstyle\sum_l t_{il} f_{1l}(\mathbf{x}_{il});\ \eta_{\mathrm{G}i} = \sum_l t_{il} f_{2l}(\mathbf{x}_{il});\ t_{\mathrm{CD}i} = \sum_l t_{il} f_{3l}(\mathbf{x}_{il});\ t_{\mathrm{CS}i} = \sum_l t_{il} f_{4l}(\mathbf{x}_{il}); \\
&\quad \mu_{\mathrm{CD}i} = \textstyle\sum_l t_{il} f_{5l}(\mathbf{x}_{il});\ \mu_{\mathrm{CS}i} = \sum_l t_{il} f_{6l}(\mathbf{x}_{il});\ u_{\mathrm{CS}i} = \sum_l t_{il} f_{7l}(\mathbf{x}_{il}); \\
&\quad F_{ijko}\left(\mathbf{x}_{il},, s_{i-1}, s_i\right) = \int_{s_{i-1}}^{s_i} f_{\mathrm{O}}\left(\mathbf{x}_i, s\right) f_{\mathrm{S}}(s)\, ds
\end{aligned}
\tag{5.35}
$$

The binary variables z_{ij}, y_{ik} and q_{io} indicate the corresponding smooth regions of the objective function with respect to the AER, the battery replacement break point, and the relation between battery and vehicle life curve, respectively, and the corresponding constraints enforce matching between the binary variable region indicators and the region variables. The binary variable t_{il} represents discrete technology selection (CV, HEV, or PHEV). The functions F_{ijko} are each twice differentiable and algebraic, factorable functions, allowing use of convexification and branch-and-reduce techniques to identify global optima.

5.2 Results and Discussions

We use the Peterson battery degradation model (Eq. (5.8)), the buy-lease battery replacement scenario ($\theta_{\mathrm{BRPL}} = \min(\theta_{\mathrm{BAT}}, \theta_{\mathrm{VEH}})$) and two driver segments (n=2) as our base case and solve the MINLP model (Eq. (5.35)) using GAMS/BARON convexification-based branch-and-reduce algorithm (Tawarmalani and Sahinidis, 2004)..

5.2.1 Optimal Solutions

The optimal vehicle type, design and allocation ranges for each case are summarized in Table 5.4. The performance values of CV and HEV are included in the first two columns for comparison. To further examine the optimal solutions, we plot the following function values at the optimal solution $\mathbf{x}^*$ as a function of driving distance per day in Figure 5.5: (1) life cycle cost, GHG emissions and petroleum consumption per-mile $f_{\mathrm{O}}(\mathbf{x}^*,s)/s$; and (2) the population-weighted cost, GHG emissions and petroleum consumption per day $f_{\mathrm{O}}(\mathbf{x}^*,s)\cdot f_{\mathrm{S}}(s)$. The area under the population-weighted curve is the net objective function. In each case, we compare the CV and HEV performance with the optimal PHEV design.

The optimal solution for minimum petroleum consumption reduces to a single PHEV87 design with the maximum allowed battery size allocated to all drivers. Such a solution is expected since a large-capacity PHEV can travel long distances without using gasoline. Figure 5.5(a) shows the petroleum consumption per mile with respect to daily driving distance. No gasoline is consumed for driving distances under the AER of 87 miles. The $f_{\mathrm{F}}(\mathbf{x}^*,s)\cdot f_{\mathrm{S}}(s)$ plot in

Figure 5.5(d) illustrates that moving all drivers from the CV to a the PHEV87 reduces net petroleum consumption per person per day (the area under the curve) by 96%.

The optimal solution for minimum life cycle GHG emissions is to allocate a medium-range PHEV40 to drivers who can charge every 87 miles or less (92% of drivers and 72% of VMT per day) and allocate a longer-range PHEV25 to drivers who charge less frequently. There are two intersection points between the two PHEV GHG curves in (Figure 5.5 (b)), and the optimal single cutoff point is located at the first intersection.[49] Although the PHEV40 GHG curve surpasses the PHEV25 after 87 miles, the difference between two is almost indistinguishable, and the portion of the population driving greater than 87 miles/day is small. Assigning all drivers high-AER PHEVs can significantly reduce petroleum consumption, but there is an additional marginal benefit to assigning medium-AER PHEVs to drivers who charge frequently because reducing the number of unnecessary batteries in these vehicles reduces the emissions associated with battery production as well as the emissions associated with reduced vehicle efficiency caused by carrying heavy batteries. While the most vehicles travel short distances each day (Figure 5.2), the majority of the GHG emissions are produced by those vehicles that travel close to 25 or 45 miles/day (Figure 5.5(e)). A significant reduction in GHG emissions is achieved by allocating PHEVs to drivers rather than HEVs or CVs, and a modest additional gain is possible by segmenting the population and allocating the right PHEV to the right driver.

The minimum life cycle cost solution in the base case is to assign PHEV34s to drivers who can charge 51 miles or less (78% of drivers and 44% of VMT/day) and assign ordinary HEVs to drivers who charge less frequently. Figure 5.5(c) shows notable differences in cost trends among the two vehicles. However, when population weighting is included, the $f_C(\mathbf{x}^*,s)\cdot f_S(s)$

[49] More intersection points are needed (n>2) to identify more than two vehicle regions.

curves in Figure 5.5(f) reveals that the gap in life cycle cost between the HEV and optimized PHEVs is small. Hence we conduct a series of sensitivity analyses to examine the minimum cost solutions under various scenarios.

An important observation on the optimal PHEV designs is that the optimal battery design swing for all three objective functions is the upper bound: 80%. The degradation mechanism based on energy-processed implies that for minimum life cycle cost, GHG emissions and petroleum consumption, designers should allow the maximum possible range of the battery to be used, even though this will require battery replacement for some drivers.

Table 5.4 Optimization results for minimum fuel, petroleum, and GHG emissions objectives

Optimization Objective			**Minimum Petroleum**	**Minimum GHGs**		**Minimum Cost**	
Optimal Vehicle Set	CV	HEV	PHEV	PHEV	PHEV	PHEV	HEV
Allocation to drivers (miles/day)	0-200	0-200	0-200	0-87	87-200	0-51	51-200
AER (miles)	−	−	87	40	25	34	−
Engine power (kW)	126	57	47	47	43	46	57
Motor power (kW)	−	52	81	71	73	70	52
Number of battery cells	−	168	1000†	435	269	376	168
Battery design swing	−	−	0.8†	0.8†	0.8†	0.8†	−
Battery capacity (kWh)	−	1.3	21.6	9.4	5.8	8.1	1.3
CD-mode efficiency (miles/kWh)	−	−	5.05	5.29	5.35	5.31	−
CS-mode efficiency (mpg)	29.5	60.1	58.1	60.0	60.7	60.3	60.1
CD-mode 0-60mph time (sec)	−	−	11.0	11.0	11.0	11.0	−
CS-mode 0-60mph time (sec)	11.0	11.0	9.0	9.1	10.3	9.4	11.0
Final SOC after multi-US06 cycles	−	−	0.32	0.32	0.32	0.32	−
Petroleum (gallon per person-day)	1.12	0.55	0.04	0.18		0.32	
GHGs (kg CO_2-eq per person-day)	14.6	8.20	8.12	7.77		7.91	
Cost ($ per person-day)	6.82	5.26	6.22	5.60		5.21	
Reduction with respect to CV only	−	−	−96%	−47%		−24%	

†Variable limited by model boundary

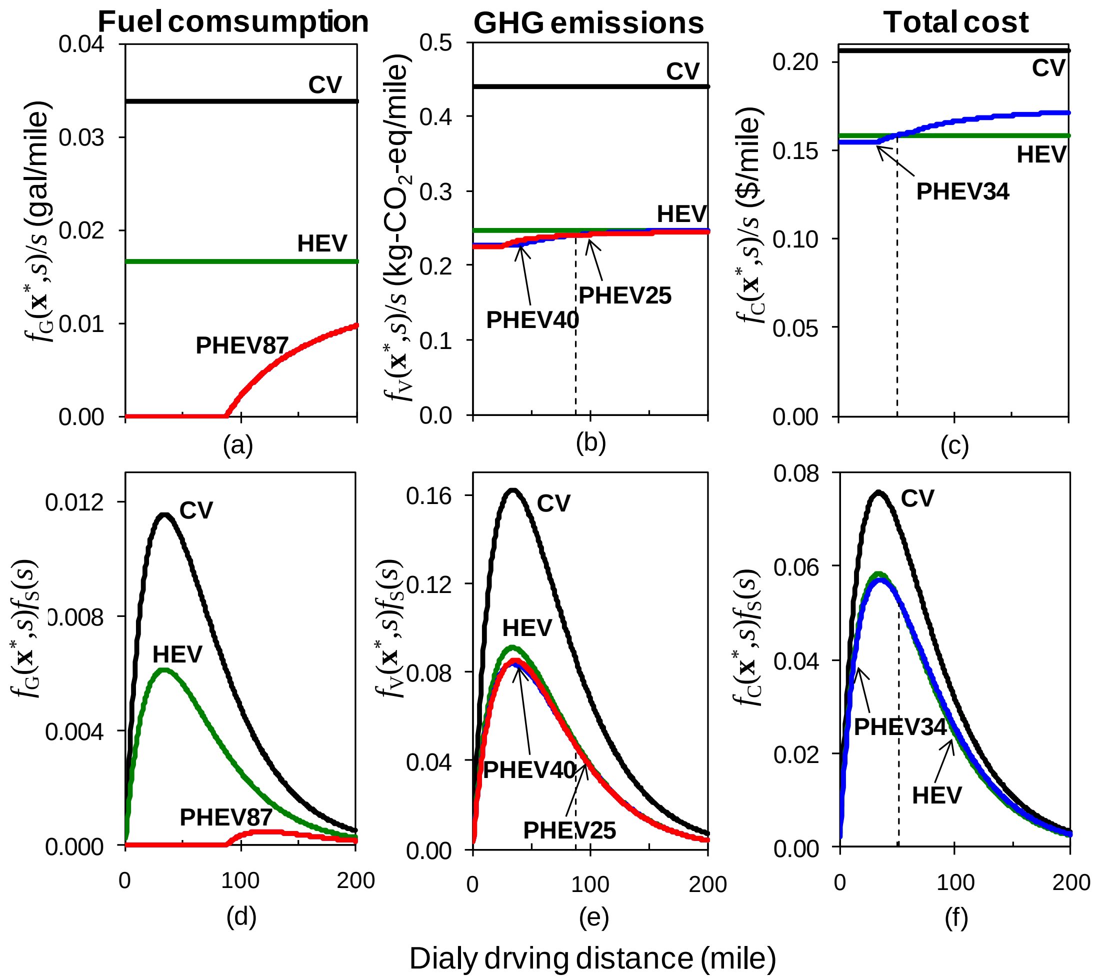

Figure 5.5 Optimal PHEV design and allocations for the base case

5.2.2 Sensitivity analyses

We conduct sensitivity analyses to examine the minimum cost solutions for various scenarios, which include (1) single-vehicle allocation model, (2) three-vehicle allocation model, (3) battery leasing scenario, (4) Rosenkranz battery degradation model, (5) low Li-ion battery cost \$250/kWh, (6) high Li-ion battery cost \$1000/kWh, (7) low NiMH battery cost at \$440/kWh, (8) high NiMH battery cost \$700/kWh, (9) low electricity price \$0.06/kWh, (10) high electricity price \$0.30/kWh, (11) low gasoline price at \$1.50 per gallon, (12) high gasoline price at \$6.0 per gallon, (13) carbon allowance price \$10 per metric ton of CO_2 equivalent (ton-CO_2-eq), (14) carbon allowance price \$100/ton-CO_2-eq, (15) nominal discount rate 5%, and (16) nominal discount rate 10%.[50] The optimal PHEV types and allocations for the sensitivity analyses are shown in Figure 5.6. The horizontal axis of the chart is percentage of population covered by the allocated vehicles. The values of percentage of VMT over the population and total cost per person per day are included for each optimal vehicle choice, and the cutoff daily mileage point is labeled where appropriate.

First, we tested sensitivity to the number of vehicle segments, examining the optimal solutions of single-vehicle and 3-vehcile allocation cases. For the single-vehicle case, ordinary HEV is the optimum choice for the entire range. The 3-vehice case shows that the range covered by PHEV34 in the base case is replaced by PHEV29 for the range of 0-33 miles and PHEV41 for the range of 33-54 miles. The allocation of HEV for longer driving distance is essentially not affected. Moreover, the minimum cost per person-day in the 3-vehicle case is only 0.2% lower than the base case, while the cost of the single-vehicle case is 1% higher. The results indicate that the two vehicle model in the base case is robust, and cases with more than three vehicles result in only minor improvements.

The battery leasing scenario does not change the optimal vehicle decisions in the base case because the optimized PHEV34 has a battery life shorter than vehicle life within 53 miles driving range, where buy-lease is equivalent to the leasing scenario ($\min(\theta_{\mathrm{BAT},}\ \theta_{\mathrm{VEH}}) = \theta_{\mathrm{BAT}}$). The Rosenkranz DOD-based degradation model, which encourages shallow swing to preserve battery life, results in a PHEV13 with 7.3 kWh battery at 32% SOE swing (a battery size equivalent to a PHEV32 with a 80% swing) for drivers below 24 miles/day and an HEV for the

[50] Among the 16 sensitivity analysis cases, the Rosenkranz and nominal discount rate cases are solved using local NLP solver with multi-start. The cost functions of these cases do not have closed-form expressions and require numerical integration.

remainder. Thus, the best use strategy for PHEV batteries depends critically on the degradation mechanism. Planned PHEVs such as the Chevrolet Volt report a battery swing of around 50% in order to maintain battery life (gm-volt.com, 2009). The Rosenkranz model is based on older battery technology, constant rate charge and discharge, and it cannot account for degradation in CS-mode. The latest data tested on modern cells with realistic driving cycles suggests that designers should consider using smaller battery packs with larger swing, even if the cost to replace the battery is accounted for.

The cases of high Li-ion battery cost, low gas price and high electricity price are not beneficial to PHEVs, and therefore the HEV is the low cost choice for all drivers in the range. The result of the low electricity price case shows that a PHEV40 has lower cost for most drivers, and the ordinary HEV remains preferable for long distance driving. Low electricity prices can be associated with off-peak charging; however, with high PHEV penetration and consequent demand for off-peak charging, off-peak rates will not remain as low. Similarly, lower battery costs or higher gasoline prices improve the economic performance PHEVs and make them cost competitive for a wide range of drivers. We also examine two additional cases with low and high HEV NiMH battery cost at $440/kWh and $700/kWh respectively (Duvall, 2004). The result indicates the HEV allocation range varies between 42-200 and 58-200 miles, but PHEV is still the low-cost choice for the drivers with short to medium daily distances.

It is worth noting that we apply 3-vehcile models for the low Li-ion battery cost and high gas price cases. The dual vehicle models result in the choice of a shorter-range PHEV for longer driving distances is counterintuitive, since we may expect high-AER PHEVs to have a cost advantage at longer driving distances. In these cases, the dual-PHEV cost curves have two intersection points, and the optimal cutoff is located at the second intersection point. The optimal solutions of 3-vehicle model allocate medium-AER PHEVs to drivers with low daily driving distances, larger-AER PHEVs to driver have medium travel distance, and lighter PHEVs for drivers who take long trips.

We examine the solution variations with two GHG allowance price levels, \$10 and \$100 per ton-CO_2-eq, by internalizing GHG emissions externalities to the cost objective function.[51] The carbon costs do not alter the vehicle design decisions significantly but extend the allocation range of PHEVs slightly. However, at lower gasoline prices (e.g.: \$3/gal), where HEVs are lower cost than PHEVs for all drivers, the GHG allowance price can be sufficient to bring PHEVs into a minimum cost solution. The take-away is that if Li-ion battery costs can be brought down to the \$400/kWh range, net life cycle costs are competitive, and while a GHG price can help encourage PHEV adoption, it is not the main driver.

The last two sensitivity analysis cases consider nominal discount rates r_N = 5% and 10% with an inflation rate r_I = 3%, the average from 2003-2008 (US Bureau of Labor Statistics, 2010). A higher discount rate makes PHEVs less attractive relative to HEVs and CVs because the vehicle purchase cost paid upfront is higher, and fuel cost savings occur in the future. At a 5% discount rate, CV is the optimal choice for drivers who travel less than 2.4 miles per day. The optimal PHEV is a smaller 23-mile AER and covers 58% rather than 78% of the population on PHEV34s in the base case. At a 10% discount rate, PHEVs are not part of the least-cost solution, and HEV is the least cost alternative for 94% of population and 99% of VMT. It should be noted that the ranges covered by CV in these cases have lower population and VMT coverage than that in practice because the weighted frequencies in 0-4 miles are less than the ones in exponential

[51] An externality cost study by the National Research Council estimated the range of environmental damage costs of carbon emissions as \$10 to \$100 per ton-CO_2-eq, with a middle estimate of \$30 (NRC, 2009). We examine the \$10/ton and \$100/ton cases, which also covers the 2020 carbon allowance prices of \$20-\$93/ton projected from the Waxman-Markey bill by the Department of Energy (EIA, 2009).

fitting (Figure 3). At $400/kWh li-ion pack costs, PHEVs are part of the least cost solution for discount rates below 7%. At a 10% nominal discount rate, PHEVs are part of the least cost solution for battery pack prices below $300/kWh.

5.3 Conclusions

We construct an optimization model to determine optimal vehicle design and allocation of conventional, hybrid, and plug-in hybrid vehicles to drivers in order to minimize net daily cost, petroleum consumption, and GHG emissions. We reformulate the model as a twice-differentiable factorable algebraic nonconvex MINLP that can be solved globally using convexification with a branch-and-reduce algorithm implemented in GAMS/BARON.

We find that (1) minimum petroleum consumption is achieved by assigning large capacity PHEVs to all drivers; (2) minimum life cycle GHG emissions are achieved by assigning medium-range PHEV40s to drivers who travel less than 87 miles/day (92% of drivers and 74% of VMT/day) and PHEV25s to drivers who travel further; and (3) minimum life cycle cost is achieved in our base case by assigning medium-range PHEV34s to drivers who travel less than 51 miles/day (78% of drivers and 45% of VMT/day) and HEVs to drivers who travel further. Optimal allocation of vehicles to drivers appears to be of second-order importance for net social cost and GHG emissions compared to an overall shift from CVs to HEVs or PHEVs. Additionally, life cycle costs of HEVs and PHEVs are comparable, particularly for drivers who charge frequently, and the least-cost solution is sensitive to the discount rate and the price of gasoline, electricity, and batteries.

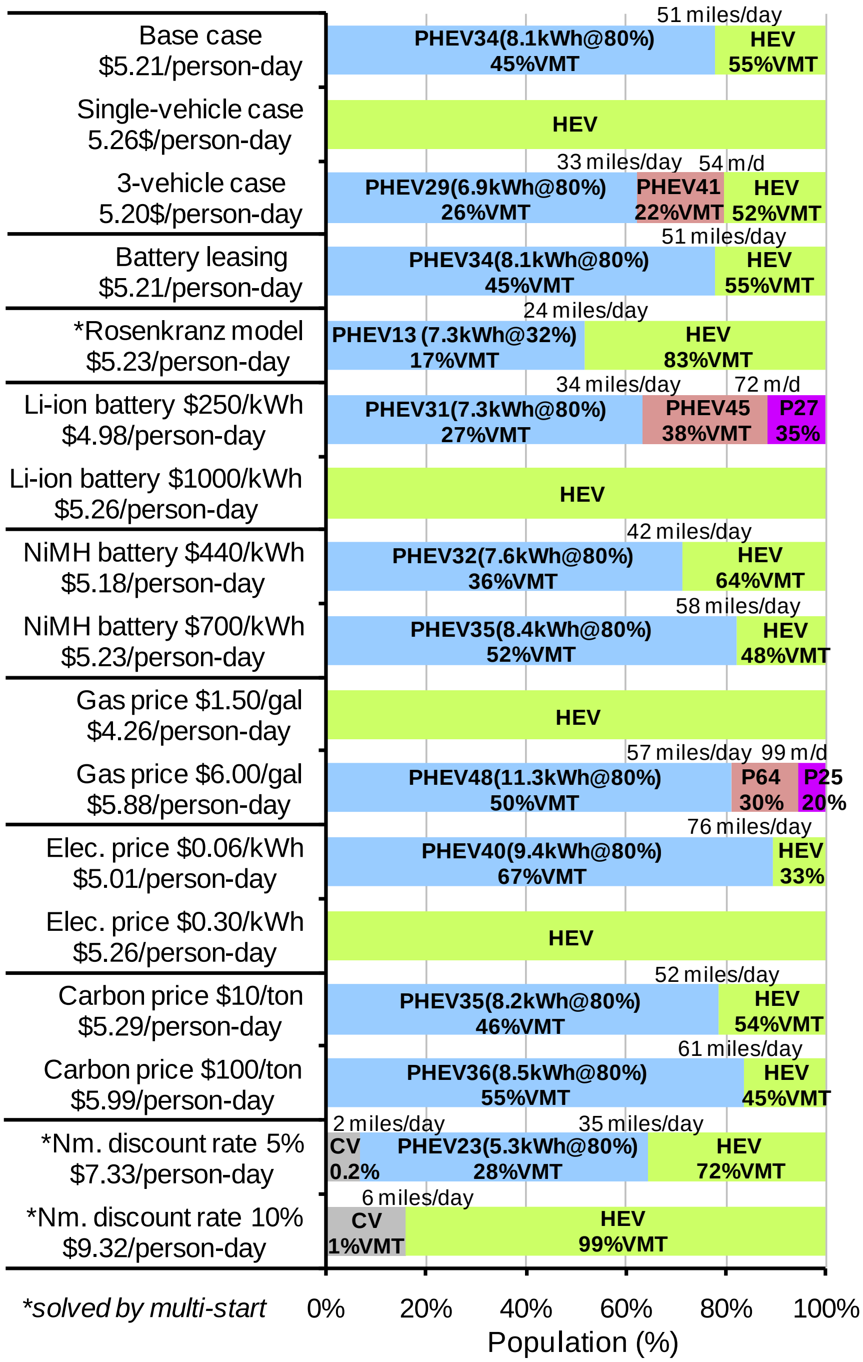

Figure 5.6 Optimal vehicle allocations for various scenarios. The base case assumes the buy-lease battery replacement scenario, the Peterson battery degradation model, \$400/kWh Li-ion battery cost, \$600/kWh NiMH battery cost, \$3.30/gal gasoline, \$0.11/kWh electricity, \$0/ton CO2-eq allowance price, and zero discounting

Relative to our base case of \$3.30/gal gasoline, \$0.11/kWh electricity, \$400/kWh Li-ion batteries, \$600/kWh NiMH batteries, and 0% discount rate PHEVs are part of the least-cost solution for gas prices above \$3.03/gal, electricity prices below \$0.14/kWh, battery prices below \$460/kWh or nominal discount rates below 7%. Carbon allowance prices have marginal impact on optimal PHEV design or penetration, even at \$100/ton. For example, when driven 34 miles per day, an HEV has life cycle emissions about 0.2 kg CO_2-eq/day greater than the PHEV34. A \$100/ton allowance price translates to a \$0.02/day penalty for the HEV relative to the PHEV35, which is about 0.4% of the equivalent daily cost of each vehicle. With the current average U.S. grid mix the relative incentive is small, even at high allowance prices. Decarbonization of the electricity grid is needed for allowance prices to be significant in PHEV competitiveness.

Using modern battery degradation models based on energy-processed in place of older DOD-based degradation models, we find that life cycle cost, GHG emissions and petroleum consumption are minimized by utilizing the maximum battery swing (80% in our model) and offering drivers a corresponding longer AER. This contrasts with current practice of restricting swing to values below 50% to improve battery life. Our results suggest that PHEV designers should optimally utilize full battery capacity and replace batteries as needed, rather than design unused battery capacity into the vehicle with the corresponding weight and cost implications. Allowing up to 80% swing rather than restricting swing to 50% reduces life cycle cost of PHEVs by 1%, GHGs by 2% and petroleum consumption by 65% in our model. Because cost implications are relatively small, other factors, such as logistics, customer satisfaction, and incentives, may play a significant role in determining battery swing in PHEV design. Current incentives for PHEVs, such as those outlined in the American Recovery and Reinvestment Act (US Congress, 2008), provide subsidies based on battery size, rather than usable battery capacity or all-electric range. This creates a disincentive to increase swing because achieving a particular AER with a larger battery pack at lower swing will earn more incentives than achieving the same AER with a smaller battery pack at higher swing. This implies that PHEV subsidies would likely be better tied to PHEV AER, rather than total battery capacity.

CHAPTER 6. STRUCTURAL ANALYSIS OF VEHICLE DESIGN UNDER CAFE POLICY

This chapter presents a structural analysis of automaker responses to generic CAFE policies in long-run oligopolistic equilibrium with considering vehicles as differentiated products – a Class III problem with CAFE penalty imposed into firm's profit function. The analysis shows that under general cost, demand, and performance functions, single-product profit maximizing firm responses to CAFE standards follow a distinct pattern: Firms ignore CAFE when the standard is low, treat CAFE as a vehicle design constraint for moderate standards, and violate CAFE when the standard is high. Further, the point and extent of first violation depends upon the penalty for violation, and the corresponding vehicle design is independent of further standard increases. Thus, increasing CAFE standards will eventually have no further impact on vehicle design if the penalty for violation is not also increased.

A case study is implemented by incorporating vehicle physics simulation, vehicle manufacturing and technology-cost models, and a mixed logit demand model to examine equilibrium powertrain design and price decisions for a fixed vehicle body. Results indicate that equilibrium vehicle design is not bound by current CAFE standards, and vehicle design decisions are directly determined by market competition and consumer preferences. Sensitivity analysis shows that firms' design responses are more sensitive to variation in fuel prices than to CAFE standards, within the examined ranges. The content in this chapter is based on the publication by Shiau et al. (Shiau et al., 2009).

6.1 Introduction

When people drive vehicles, they generate negative externalities that impact society, including among them are congestion, national security implications and environmental impact, such as GHG emissions that contribute to global warming (Porter, 1999; NRC, 2009). While economists generally advocate Pigovian taxes to efficiently correct for these negative externalities (Lesser et al., 1997; Kolstad, 2000), the vast majority of the U.S. public and lawmakers object to increased gasoline taxes (Uri and Boyd, 1989; Chernick and Reschovsky, 1997; Hammar et al., 2004; Decker and Wohar, 2007), and the government has instead relied on mandated restrictions for the average characteristics of vehicles sold by automakers. Among such policies are (1) the CAFE standards in the U.S., which penalize automakers whose sales-weighted average of fleet fuel economy drops below a government-determined standard, and (2) similar policies in California and in Europe that set standards on average fleet CO_2 emissions per mile. Rather than addressing driving patterns or fuel consumption directly, these policies create incentives for automakers to produce more efficient fleets. However, vehicle design responses to government policies are complicated by tradeoffs in available technology, consumer preferences, and competition in the marketplace. Integrated analysis is required to understand and predict vehicle design responses to transportation policies.

6.1.1 Background of CAFE

The CAFE standard regulates the average fuel economy of new vehicles sold in the United States. It requires the fleet-wide sales-weighted average fuel economy of automobiles sold by each manufacturer to achieve a prescribed standard. Manufacturers that do not achieve the CAFE standard are penalized based on their annual vehicle sales and fuel economy shortfalls. The origin of CAFE regulation can be traced to the 1973 oil crisis, when soaring crude oil prices drew the government and public's attention to the inefficiency of automobiles. The Energy Policy and Conservation Act (EPCA) of 1975 established separate CAFE standards for passenger cars and light trucks (US Congress, 1975). The executive responsibilities for implementing CAFE policy are distributed between the Environmental Protection Agency (EPA, 2007) and the National Highway Traffic Safety Administration under the Department of Transportation (DOT) (NHTSA, 2006). EPA is responsible for determining the test procedures for measuring vehicle fuel economy (and emissions) and calculating the CAFE for automobile manufacturers (EPA, 2007). NHTSA is in charge of establishing, amending and enforcing fuel economy standards and regulations. In addition to the fuel economy criterion, NHTSA is also authorized to determine the financial penalty for violating the CAFE standard. The initial penalty value set in 1978 was $5.00 per vehicle per 0.1 mpg ($50 per mpg). In 1997, NHTSA raised the penalty to $5.50 per vehicle per 0.1 mpg ($55 per mpg) (GAO, 1990).[52] The penalty has not been changed since then and has not been adjusted for inflation. Figure 6.1 shows the historical change of CAFE standards and average vehicle fuel efficiency. Note that during the 1990s combined fuel economy decreased even as the fuel economy in the separate car and truck categories increased due to consumers switching from cars to light trucks. As of December 2007, the total collected fines on CAFE violations reached $772 million, not adjusting for inflation (NHTSA, 2009). Historically, only European automobile manufacturers have paid CAFE fines, while Japanese automakers have consistently exceeded the regulatory standard and U.S. automakers have made it a policy to treat the CAFE standard as a constraint, using the CAFE credit system when necessary to avoid paying penalties.[53]

[52] NHTSA has the authority to raise CAFE penalties to $10 per 0.1 mpg ($100 per mpg) (GAO, 2007).

[53] CAFE regulation allows automakers to earn credits for exceeding fuel economy standards in one year and apply them to the prior or subsequent three model years to neutralize the violation penalty (NHTSA, 2006).

In 2007, Congress passed the Energy Independence and Security Act of 2007 (EISA), which increased the target fleet-wide average fuel economy standard to 35 mpg in 2020 with combining cars and light trucks into a single category (US Congress, 2007). The act is the first legislation since the 1974 EPCA that directly regulates U.S. fleet fuel economy. The legislation also requires NHTSA to annually reform the separate fuel economy standards for cars and light trucks in order to achieve the joint 2020 goal of 35 mpg. In April 2008, NHTSA initiated an attribute-based CAFE proposal by using vehicle footprint to determine the 2011-2015 standards (NHTSA, 2008). In April 2009, NHTSA announced the formal 2011 CAFE standards 30.2 mpg and 24.1 mpg for cars and light trucks respectively (combined 27.3 mpg) (NHTSA, 2009), which are slightly lower than the values in the 2008 proposal.

The announcement delivered two important messages. First, NHTSA will reform and adjust their regulation decisions every year based on the status of national fleet average and technology feasibility. The dash lines in show that unreformed and predicted standards for 2011-2020. Second, the significant jump in car fuel economy standard means that CAFE standards will catch up to the national fleet average, which has exceeded the standard substantially in recent years while the regulation has merely served as a lower-bound requirement in past 10 years. In May 2009, President Obama announced a higher fuel economy regulatory target, combined 35.5 mpg by 2016 to be implemented as a CO2 regulation by the EPA (The While House, 2009), which aggressively exceeds the 2020 35 mpg target set by EISA.

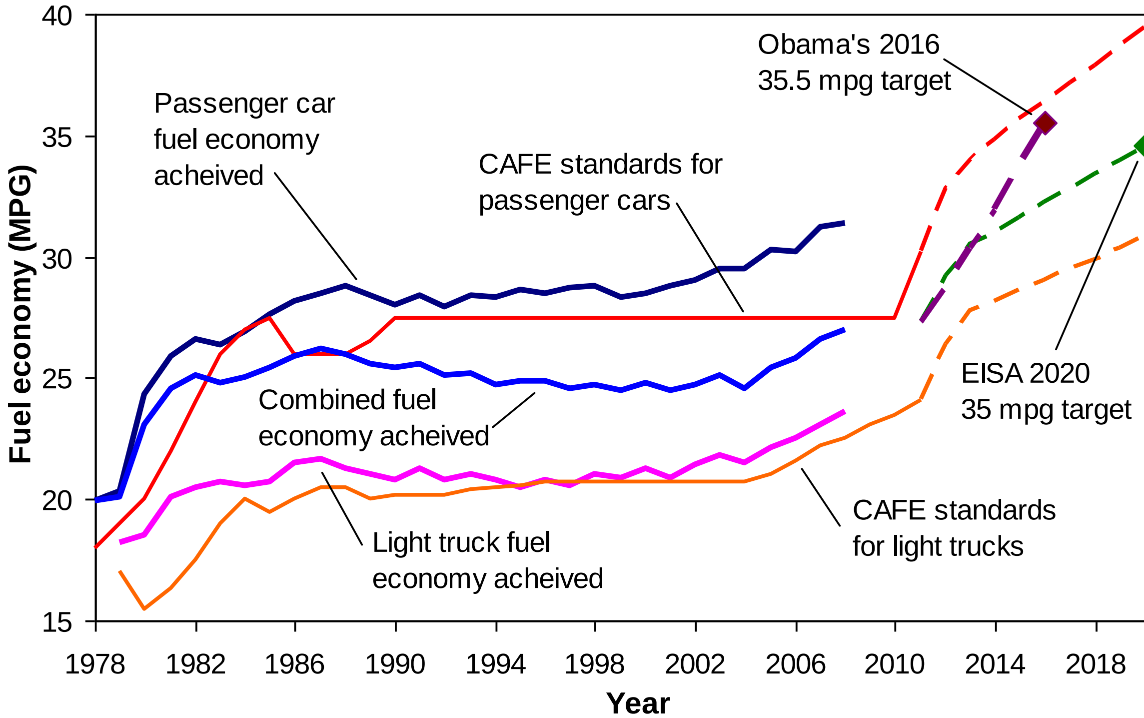

Figure 6.1 Historical and prospective changes of CAFE standards and average fuel economy records of U.S. passenger cars and light trucks

6.1.2 Carbon Dioxide Emission Regulations

Carbon dioxide (CO_2) emission standards that are measured on a fleet average per-mile basis can be seen as structurally equivalent policies to CAFE for regulating automobile fuel efficiency, since technology is not available on the market to separate and store CO_2 emissions from vehicles. The estimated CO_2 emissions per gallon of gasoline burned are roughly 8,788 grams (EPA, 2005), without including CO_2 emissions arising from the petroleum supply chain. We review the two most well-known standards, the European Union CO_2 emission standard and the California CO_2 emission standards.

The European carbon dioxide standards were issued by the European Commission (1995) to establish a voluntary CO_2 emission standard for automobile manufacturers selling vehicles in Europe as a response to the Kyoto Protocol (1997), which requires 8% reduction of greenhouse gas emissions in all economic sectors relative to 1990 levels by 2008-2012. Expecting automobile manufacturers to improve vehicle emissions voluntarily, the 1995 regulation defined an intermediate target of 140 g/km by 2008-2009 and an ultimate target of 120 g/km for 2012. However, it was found that automakers had not been reducing vehicle CO_2 emissions effectively, making the 2012 target less likely to be reached (European Parliament, 2005). Hence in 2007, the European Commission issued a proposal for a new regulation to replace the originally voluntary target with a mandatory standard of 130 g/km (European Commission, 2007). In December 2008, after automakers cited infeasibility of regulatory targets in the 2007 proposal, a resolution was made by European Commission for changing the firm 130 g/km target into gradually adaptive standards; 65% of automaker's fleet reaches the 130 g/km requirement in 2012, 75% in 2013, 85% in 2014 and 100% in 2015 (European Parliament, 2008). Moreover, a new long-term target is set to 95 g/km in 2020. The resolution also revealed the step-size penalty structure of the regulation.[54]

The California greenhouse gas emission proposal set CO_2 emission requirements for new vehicles sold in California (CARB, 2004). The program required a CO_2 emission standard of 323 g/mile (201 g/km) for the model year 2009 with annual reductions to 205 g/mile (127 g/km) for the model year 2016. The program did not define a direct penalty parameter for the automotive manufacturers who violate the standards. Instead, the law implements a credit and debit system to monitor each manufacturer's annual average fleet CO_2 emission. If emission debits are not neutralized within five years, the manufacturer is issued a civil penalty according to the Health and Safety Code (CA Code, 2008). The California CO_2 standards were rejected by

[54] The resolution proposed €5 for the first gram/km over the target, €15 for the second g/km over the target, €25 for the third g/km over the target and €95 for the fourth g/km and subsequent. After 2019, any violation will be €95 per g/km (European Parliament, 2008).

Bush administration in 2007 since the standards are stricter than federal regulations. In June 2009, the Obama administration granted a waiver for California's request beginning from model year 2009 (EPA, 2009).

Figure 6.2 shows the future CAFE standards, including the Obama administration's 2009 new proposal (Broder, 2009), and the two CO_2 emission regulatory standards for passenger cars. European emission standards are close to California emission levels, whereas the U.S. CAFE regulation is the weakest criterion.[55] However, the three regulations have similar slopes for equivalent annual carbon emission reductions. The common mechanism of the three regulations is to set increasing standards for vehicle characteristics (fuel consumption or emissions) and expect automobile manufacturers to respond with revised vehicle lines and pricing strategies that achieve the standards. We propose an integrated structural analysis to understand and predict vehicle design responses to transportation policies.

The remaining sections in this chapter proceed as follows: Section 6.2 reviews the relevant literature on analysis of CAFE policy; Section 6.3 introduces the proposed model and analysis of vehicle design responses to CAFE policy; Section 6.4 presents a case study using vehicle simulation models and a mixed logit demand model from the literature; and finally, Section 6.5 discusses conclusions and policy implications.

[55] Note that European standards are based on a different fleet composition from the car and light fleets in the U.S. Moreover, European standards use a different test cycle to measure vehicle fuel efficiency.

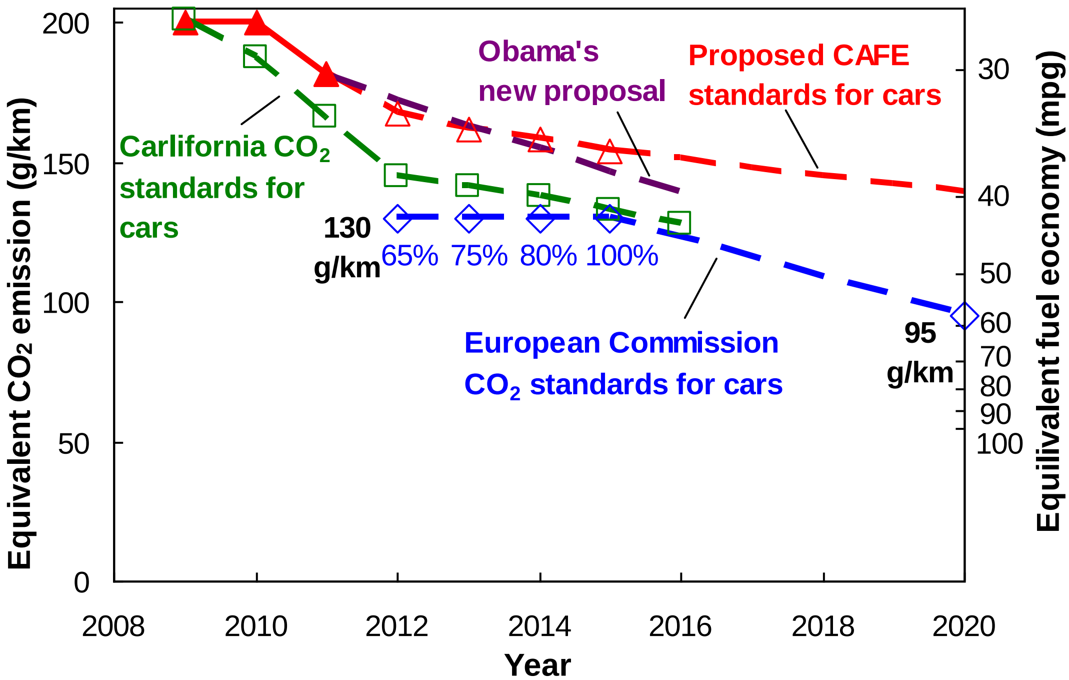

Figure 6.2 Comparison of three fuel efficiency regulations for passenger cars

6.2 Review of Literature on CAFE Impacts

Studies of CAFE effects follow two primary branches: econometric estimation and economic modeling. Econometric estimation studies use automobile sales data to examine the past impacts of CAFE policy on fuel economy (Crandall et al., 1986; Godek, 1997; Goldberg, 1998; Espey and Nair, 2005; Small and Van Dender, 2007) or on vehicle safety (Crandall et al., 1986; Crandall and Graham, 1989; Yun, 2002; Ahmad and Greene, 2005). In contrast, economic modeling studies draw on economic theory to simulate hypothetical manufacturer decision-making in response to CAFE or other policies with the aim to predict automaker responses to alternative regulation scenarios and understand structural policy implications.

The literature on economic modeling of CAFE policy can be categorized along two major dimensions where vehicles are viewed either as commodities or as differentiated products. If firms view vehicles as commodities, they control only price or production volume, while firms with differentiated products also control vehicle design attributes, such as fuel economy or performance. If consumers view vehicles as commodities, they react only to price; however, consumers of differentiated products also react to vehicle attributes, such as fuel economy or performance. Table 6.1 summarizes the prior literature with respect to this categorization.

Several studies treat vehicles entirely as commodities: Kaowa (1983) and Biller and Swann (2006) examine a single firm, using linear models of demand and treating the CAFE standard as a constraint. Kleit (1990) posed a model with two vehicle commodities (small car and large car) and examined perfect competition and oligopoly models by taking firms as price takers or price setters, respectively. Kleit argues that CAFE policy is not only inefficient, but also counterproductive by encouraging drivers to drive more in response to the reduced operation costs of higher fuel efficiency vehicles (the rebound effect). He argues for elimination of CAFE in favor of Pigovian gasoline taxes; however, Gerard and Lave argue that CAFE is potentially an effective complement to gasoline taxes (Gerard and Lave, 2003; Gerard and Lave, 2004).

Table 6.1 Literature categorization on firm decision and CAFE regulation modeling

			Demand modeling	
			Commodities Demand as a function of price only	**Differentiated** Demand as a function of price and attributes
Market structure	**Commodities** No design change (Short run)	Single firm optimization	Kwoka (1983) Biller & Swann (2006)	–
		Perfect competition	Kleit (1990)	–
		Oligopolistic competition	Kleit (1990)	–
	Differentiated Design change considered (Long run)	Industry-wide optimization	–	Greene & Hopson (2003)
		Perfect competition	Kleit (2004) Fischer et al. (2007)	–
		Oligopolistic competition	Austin & Dinan (2005) Jacobsen (2008)	Michalek et al. (2004) **This Chapter**

The remaining studies view vehicles as differentiated from the manufacturer's perspective and account for long run vehicle design changes made by firms in response to CAFE policy. Using technology-cost and technology-demand models[56] from a prior study (Greene and DeCicco, 2000), Greene and Hopson (2003) constructed a nonlinear programming framework using an industry-wide net value of fuel economy improvement as the objective function and treating the CAFE standard as a constraint. Kleit (2004) adopted Greene and Hopson's technology-cost model to extend his previous study (Kleit, 1990) to include manufacturer fuel economy responses to CAFE standard increases under perfect competition using a price-elasticity demand matrix based on General Motors conjoint analysis data with multiple market segments. Kleit assumes that firms must pay for increased fuel efficiency, but changes in fuel economy do not affect demand. The study concluded that a 3.0 mpg increase in the CAFE standard can be replaced by an 11 cent gasoline tax to save the same amount of gasoline annually at only one-fourteenth of the social welfare cost. Adopting Kleit's (2004) demand elasticity model, Austin and Dinan (2005) modeled manufacturer pricing and fuel economy improvement decisions treating CAFE as a constraint. Jacobsen (2008) identifies and models the heterogeneous responses of different manufacturer groups to the CAFE regulation; domestic automakers bind with CAFE standards, but foreign manufacturers treat the regulations as inactive lower bounds or associated taxes. His market equilibrium simulation also shows that gasoline taxes would be much cheaper than CAFE in welfare cost even if technologies for fuel efficiency improvement in response to CAFE regulation are taken into account. Fischer et al. (2007) found that the efficiency and benefits of tightening CAFE standards are difficult to quantify, but they recommend that fuel economy standards should be raised gradually over time.

[56] Greene and DeCicco (2000) created the cost-technology model via regression of retail price increases for technologies that offer fuel efficiency improvements. Similarly, they estimated the market penetration of fuel economy technology using regression on market data.

Finally, Michalek et al. (2004) conducted a numerical study of firm responses to CAFE standards accounting for logit consumer responses to vehicle fuel economy, performance, and price. They modeled firms as players in a Nash equilibrium who decide engine size and price in response to CAFE policy, and they used physics simulators to model performance, fuel economy and cost complications of engine size. They argue that CAFE standards can result in greater fuel economy improvements at lower cost to the manufacturer; however, they did not account for government revenue generated.

The bulk of prior studies treat vehicles as commodities to consumers; however, there exists a rich literature on econometric measurement of consumer responses to (differentiated) vehicle attributes (Boyd and Mellman, 1980; Train, 1980; Bunch et al., 1993; Berry et al., 1995; Goldberg, 1995; Brownstone and Train, 1999; Brownstone et al., 2000; McFadden and Train, 2000; Sudhir, 2001; Berry et al., 2004; Choo and Mokhtarian, 2004; Train and Winston, 2007). We argue that vehicles are not commodities, and accounting for consumer preferences and technical capabilities is important to understanding firm responses to CAFE. As such, we follow Greene and Hopson (2003) and Michalek et al. (2004) in viewing the vehicle as a differentiated product from the perspective of the firm and the consumer, where firms control vehicle design variables and consumers react to vehicle attributes as well as price. While Greene and Hopson (2003) and Michalek et al. (2004) provide specific numerical analyses, we instead develop a general structural analysis of long run oligopoly Nash responses (Tirole, 1988) to CAFE policy under general assumptions for cost functions, technical tradeoffs, and consumer demand, and we identify a distinct pattern in Nash responses to CAFE. We then instantiate the model with specific data and examine policy implications.

6.3 Model

We define firm k's profit function as

$$\Pi_k = \left(\sum_{j \in J_k} q_j \left(p_j - c_j \right) - c_{\mathrm{I}} \right) - \left(\rho \delta \left(z_{\mathrm{F}k}^{\mathrm{AVG}} \right) \sum_{j \in J_k} q_j \right) \tag{6.1}$$

where p_j, q_j and c_j are the price, demand and variable cost, respectively, of vehicle j; J_k is the set of vehicle models produced by firm k; c_{I} is a fixed investment cost per vehicle model; ρ is the penalty for CAFE violation in dollars per vehicle per mpg[57]; $\delta(\cdot)$ is the CAFE violation function; and $z_{\mathrm{F}k}^{\mathrm{AVG}}$ is the CAFE achieved by firm k. According to NHTSA's CAFE formulation definition, the fleet-wide average fuel economy for manufacturer k (cars and light trucks are currently calculated separately) is[58]

$$z_{\mathrm{F}k}^{\mathrm{AVG}} = \frac{\sum_{j \in J_k} q_j}{\sum_{j \in J_k} \frac{q_j}{z_{\mathrm{F}j}}} \tag{6.2}$$

The function δ is defined as

$$\delta\left(z_{\mathrm{F}k}^{\mathrm{AVG}}, \kappa \right) = \begin{cases} 0 & \text{if } z_{\mathrm{F}k}^{\mathrm{AVG}} > \kappa \quad \text{(case 1)} \\ 0 & \text{if } z_{\mathrm{F}k}^{\mathrm{AVG}} = \kappa \quad \text{(case 2)} \\ \kappa - z_{\mathrm{F}k}^{\mathrm{AVG}} & \text{if } z_{\mathrm{F}k}^{\mathrm{AVG}} < \kappa \quad \text{(case 3)} \end{cases} \tag{6.3}$$

where κ is the CAFE standard. We take the fuel economy $z_{\mathrm{F}j}$ and variable cost c_j of each vehicle j to each be a function of a vector of vehicle design variables $\mathbf{x}_j$, so that $z_{\mathrm{F}j} = f_{\mathrm{F}}(\mathbf{x}_j)$ and $c_j = f_{\mathrm{C}}(\mathbf{x}_j)$. We further take the demand q_j for each vehicle j to be a function of the design $\mathbf{x}_{j'}$ and price $p_{j'}$ of all vehicles j' in the market, so that $q_j = f_{\mathrm{Q}}(p_{j'}, \mathbf{x}_{j'}; \forall j' \in J)$. Finally, we assume that each firm sets

[57] We ignore violation cost other than the government fee, such as public relations and litigation costs.
[58] We examine only the basic CAFE penalty structure here and leave study of attribute-based standards and year to year credits for future study.

the price p_j and design $\mathbf{x}_j$ of its vehicle, and the investment cost c_I and policy parameters κ and ρ are taken as exogenous.

The three cases in Eq. (6.3) are classified by the relationship between fleet fuel economy design decisions and the CAFE fuel economy standard: In case 1 the fleet fuel economy surpasses the standard ($z_\mathrm{F}>\kappa$); in case 2 the fleet fuel economy matches the standard ($z_\mathrm{F}=\kappa$); and in case 3 the fleet fuel economy violates the standard ($z_\mathrm{F}<\kappa$). The derivative of δ with respect to firm's average fuel economy is

$$\frac{\partial \delta}{\partial z_{\mathrm{F}k}^{\mathrm{AVG}}} = \begin{cases} 0 & \text{if } z_{\mathrm{F}k}^{\mathrm{AVG}} > \kappa \quad \text{(case 1)} \\ \text{undefined} & \text{if } z_{\mathrm{F}k}^{\mathrm{AVG}} = \kappa \quad \text{(case 2)} \\ -1 & \text{if } z_{\mathrm{F}k}^{\mathrm{AVG}} < \kappa \quad \text{(case 3)} \end{cases} \tag{6.4}$$

The function δ has continuity, but its derivative is discontinuous at $z_{\mathrm{F}k}{}^{\mathrm{AVG}} = \kappa$. Figure 6.3 illustrates the conditions in Eq. (6.3) and Eq. (6.4).

In the long-run scenario, manufacturers alter price and vehicle design under competition and CAFE policy. We consider price and vehicle design as endogenous, while the CAFE standard and penalty are applied to the competitive market as exogenous variables. We assume the market is described by Nash equilibrium, where all manufacturers compete non-cooperatively in an oligopoly market (Fudenberg and Tirole, 1991). Also, for simplicity and to facilitate closed-form solutions each manufacturer is assumed to produce a single vehicle model only. We examine FOCs for Nash equilibrium in each of the three cases below.

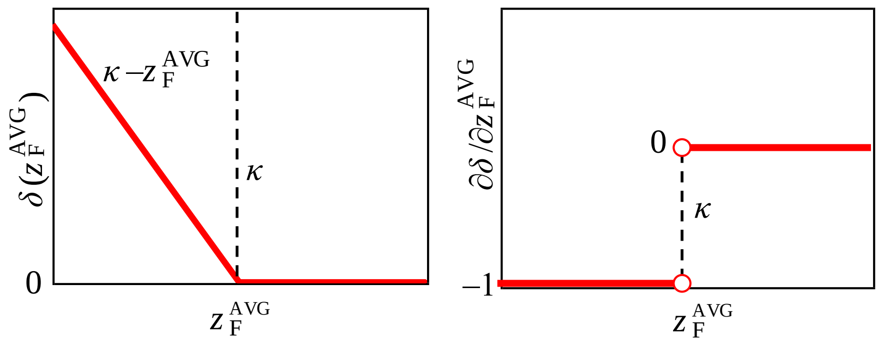

Figure 6.3 Fuel economy deviation function and its derivative

Case 1: Vehicle gas mileage surpasses the CAFE standard: In this case the first order condition with respect to price p_j from Eq. (6.1) is

$$\frac{\partial \Pi_k}{\partial p_j} = \frac{\partial q_j}{\partial p_j}\left(p_j - c_j\right) + q_j = 0 \tag{6.5}$$

Therefore, the price at market equilibrium can be expressed as:

$$p_j = c_j + q_j \left(-\frac{\partial q_j}{\partial p_j}\right)^{-1} \tag{6.6}$$

Here the equilibrium price is comprised of vehicle cost plus manufacturer markup, where the markup depends on total demand (itself a function of price) and the price elasticity. Assuming that the design variable space is unconstrained[59], the first order condition with respect to the design variables $\mathbf{x}_j$ is

$$\frac{\partial \Pi_k}{\partial \mathbf{x}_j} = \frac{\partial q_j}{\partial \mathbf{x}_j}\left(p_j - c_j\right) - q_j \frac{\partial c_j}{\partial \mathbf{x}_j} = \mathbf{0} \tag{6.7}$$

Inserting Eq.(6.6) and assuming positive demand, the equation is simplified as

[59] If design constraints are present, Lagrangian formulation should applied to the system equations, such as (Eq. (3.10)).

$$\frac{\partial q_j}{\partial \mathbf{x}_j}\left(\frac{\partial q_j}{\partial p_j}\right)^{-1}+\frac{\partial c_j}{\partial \mathbf{x}_j}=\mathbf{0} \tag{6.8}$$

Here the equilibrium design is a balance between the marginal cost of a design change and the marginal price that can be charged for the design change without changing demand.

Case 2: Vehicle design gas mileage is equal to the CAFE standard: In this case the FOC condition for price is the same as Eq. (6.6). Since vehicle fuel economy equals the CAFE standard in this case, the design solution satisfies the design function:

$$f_{\mathrm{F}}\left(\mathbf{x}_j\right)=\kappa \tag{6.9}$$

If the function has an inverse, then $\mathbf{x}_j = f_{\mathrm{F}}^{-1}(\kappa)$.

Case 3: Vehicle design gas mileage violates the CAFE standard: In this case the first order condition with respect to price p_j is

$$\frac{\partial \Pi_k}{\partial p_j}=\frac{\partial q_j}{\partial p_j}\left(p_j-c_j\right)+q_j-\rho\delta\left(z_{\mathrm{F}j}\right)\frac{\partial q_j}{\partial p_j}=0 \tag{6.10}$$

The price solution becomes

$$p_j=c_j+q_j\left(-\frac{\partial q_j}{\partial p_j}\right)^{-1}+\rho\delta\left(z_{\mathrm{F}j}\right) \tag{6.11}$$

Here the equilibrium price is comprised of vehicle cost, manufacturer markup and the CAFE penalty per vehicle. The manufacturer markup depends on demand and the price elasticity, and the CAFE penalty is passed to the consumer. The first order condition with respect to the design variable vector (again assuming no constraints) $\mathbf{x}_j$ is

$$\frac{\partial \Pi_k}{\partial \mathbf{x}_j}=\frac{\partial q_j}{\partial \mathbf{x}_j}\left(p_j-c_j-\rho\delta_j\right)+q_j\left(\rho\frac{\partial z_{\mathrm{F}j}}{\partial \mathbf{x}_j}-\frac{\partial c_j}{\partial \mathbf{x}_j}\right)=\mathbf{0} \tag{6.12}$$

Plugging in Eq. (11), the equation is simplified to

$$\frac{\partial q_j}{\partial \mathbf{x}_j}\left(\frac{\partial q_j}{\partial p_j}\right)^{-1}+\left(\frac{\partial c_j}{\partial \mathbf{x}_j}-\rho\frac{\partial z_{\mathrm{F}j}}{\partial \mathbf{x}_j}\right)=\mathbf{0} \tag{6.13}$$

Here the equilibrium design is a balance between the marginal cost of a design change due to direct cost and regulation cost and the marginal price that can be charged for the design change without changing demand.

The FOC equations for Nash pricing and design solutions for representing each firm's decisions are summarized in Table 6.2. For each case, the fuel economy of vehicle design shows different characteristics and variable dependencies. For case 1 the vehicle design is independent of CAFE parameters; for case 2 vehicle design has a fuel economy equal to the CAFE standard κ; and for case 3 vehicle price and design are functions of the CAFE penalty ρ, but not the CAFE standard κ. So $z_{\mathrm{F}j}$ is independent of κ in case 1 and case 3. For any given f_{F}, f_{C}, f_{Q}, and ρ such that $z_{\mathrm{F}j}^{***} > z_{\mathrm{F}j}^{*}$, which is the case for practical markets, at most two adjacent cases will have equilibrium conditions that are consistent with case assumptions for a given κ.

Table 6.2 First-order conditions for Nash equilibrium under CAFE regulations

Condition	Case 1 $z_{\mathrm{F}}(\mathrm{x}_j) > \kappa$	Case 2 $z_{\mathrm{F}}(\mathrm{x}_j) = \kappa$	Case 3 $z_{\mathrm{F}}(\mathrm{x}_j) < \kappa$
δ_j	0	0	$\kappa - z_{\mathrm{F}j}$
$\partial\delta_i/\partial z_{\mathrm{F}j}$	0	Undefined	−1
Price	$p_j = c_j + q_j\left(-\frac{\partial q_j}{\partial p_j}\right)^{-1}$	$p_j = c_j + q_j\left(-\frac{\partial q_j}{\partial p_j}\right)^{-1}$	$p_j = c_j + q_j\left(-\frac{\partial q_j}{\partial p_j}\right)^{-1} + \rho\delta_j$
Design	$\frac{\partial q_j}{\partial \mathbf{x}_j}\left(\frac{\partial q_j}{\partial p_j}\right)^{-1}+\frac{\partial c_j}{\partial \mathbf{x}_j}=\mathbf{0}$	$\mathbf{x}_j : f_{\mathrm{F}}(\mathbf{x}_j)=\kappa$	$\frac{\partial q_j}{\partial \mathbf{x}_j}\left(\frac{\partial q_j}{\partial p_j}\right)^{-1}+\left(\frac{\partial c_j}{\partial \mathbf{x}_j}-\rho\frac{\partial z_{\mathrm{F}j}}{\partial \mathbf{x}_j}\right)=\mathbf{0}$
Fuel economy	$z_{\mathrm{F}j}^{*}$ depends on $f_{\mathrm{F}}, f_{\mathrm{C}}, f_{\mathrm{Q}}$	$z_{\mathrm{F}j}^{**}$ depends on κ	$z_{\mathrm{F}j}^{***}$ depends on $f_{\mathrm{F}}, f_{\mathrm{C}}, f_{\mathrm{Q}}, \rho$

When a unique oligopolistic symmetric market equilibrium exists, Figure 6.4 shows Nash vehicle fuel economy responses z_{Fj} as a function of the CAFE standard κ under a fixed penalty ρ, which forms three regions. Case 1 and case 3 are independent of κ, so they appear as horizontal lines. Case 2 follows the 45° line passing through (0,0). Case 1 is valid for $z_{Fj}^{*} < \kappa$, and case 3 is valid for $z_{Fj}^{***} > \kappa$. Case 2 is valid for all κ such that $\exists \mathbf{x}_j : f_F(\mathbf{x}_j) = \kappa$. However, because case 2 is a border case for case 1 and case 3, it is not an equilibrium solution to the relaxed problem where z_{Fj} is not restricted to κ, and we consider case 2 only when the other two cases are invalid. Therefore, case 1 is valid for $\kappa < z_{Fj}^{*}$, case 3 is valid for $\kappa > z_{Fj}^{***}$, and case 2 is valid for $z_{Fj}^{*} < \kappa < z_{Fj}^{***}$. For the three regions, the policy implications are:

Region 1: Low CAFE standards do not affect firms' design decision, and fuel economy and pricing decisions are determined by oligopolistic competition directly.

Region 2: Moderate CAFE standards result in fuel economy responses that follow the standard exactly.

Region 3: High CAFE standards result in fuel economy responses that violate the standard, and firms ignore further increases in the standard, instead transferring the regulation penalty cost to consumers in the retail price. The point of first violation and the resulting fuel economy response depends on the penalty for violation.

These results imply that the performance of CAFE standards is affected by both the fuel economy criteria and the penalty: Setting too high a standard without a corresponding increase in violation penalties will result in firms ignoring further increases and passing costs on to consumers. Moreover, the difference between the solution equation set of case 1 and case 3 suggests that the width of region 2 ($z_{Fj}^{***} - z_{Fj}^{*}$) is a function of the CAFE penalty ρ and the marginal change in fuel economy with respect to the design variables ($\partial z_F / \partial \mathbf{x}$).

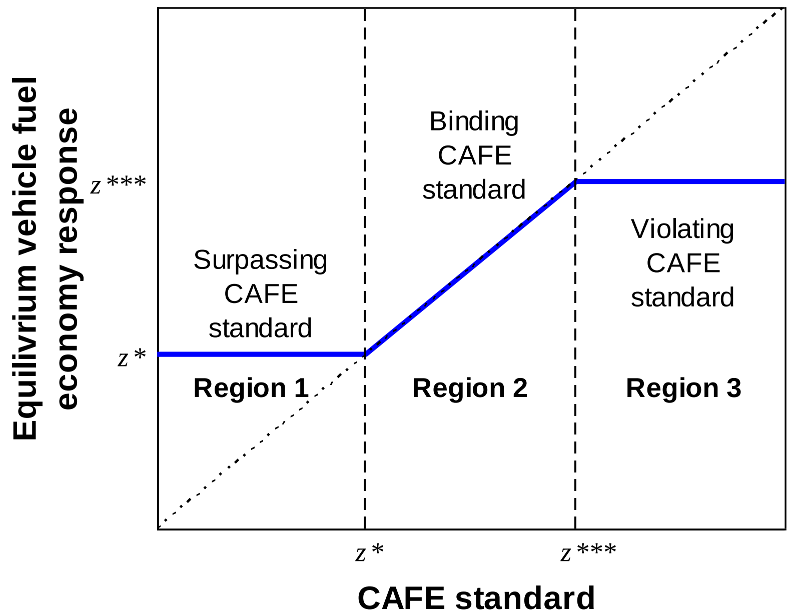

Figure 6.4 Three regions of fuel economy design responses

6.4 Case Study

We next examine a case study by using automotive market data, vehicle performance simulation, costs and fuel economy technology from the literature. In the following subsections, we detail our manufacturer design decision model and market demand model, results and sensitivity analyses.

6.4.1 Supply Side Modeling

We consider a midsize car equipped with a gasoline engine in our supply side modeling. The vehicle design decision is represented by two design variables, an engine scaling variable x_E and a technology implementation x_T. The former determines the size and power of engine, and the latter represents implementation of fuel-saving technologies. We use the vehicle physics simulator ADVISOR-2004 (AVL, 2004) [60] to evaluate fuel economy with the standard EPA city driving cycle (FTP) and highway driving cycle (HWFET). The combined fuel economy is then calculated by the harmonic mean of 55% city and 45% highway (EPA, 2007). A meta-model is established over the fuel economy simulation data as a function of the engine scaling variable x_{E}, as shown in Figure 6.5. Thus vehicle j's fuel consumption $z_{\mathrm{C}j}$ (gallon per mile), fuel economy $z_{\mathrm{F}j}$ (mile per gallon) and power-to-weight ratio $z_{\mathrm{H}j}$ (horsepower per 100 lbs) can be defined as functions of $x_{\mathrm{E}j}$ and $x_{\mathrm{T}j}$:[61]

$$\begin{aligned} z_{\mathrm{C}j} &= \left(a_{\mathrm{F2}} x_{\mathrm{E}j}^2 + a_{\mathrm{F1}} x_{\mathrm{E}j} + a_{\mathrm{F0}}\right)^{-1}\left(1 - x_{\mathrm{T}j}\right) \\ z_{\mathrm{H}j} &= a_{\mathrm{H2}} x_{\mathrm{E}j}^2 + a_{\mathrm{H1}} x_{\mathrm{E}j} + a_{\mathrm{H0}} \\ z_{\mathrm{F}j} &= z_{\mathrm{C}j}^{-1} \end{aligned} \tag{6.14}$$

The meta-model coefficients are a_{F2}=4.90, a_{F1}=–24.7, a_{F0}=48.8, a_{H2}=–0.44, a_{H1}=3.87, and a_{H0}=0.12. The vehicle cost model comprises the vehicle base cost c_{B}, engine cost c_{E} and fuel-saving technology cost c_{T} so that $c_j = c_{\mathrm{B}} + c_{\mathrm{E}j} + c_{\mathrm{T}j}$. The engine cost is modeled as an exponential function $c_{\mathrm{E}}=b_1\exp(b_2 b_{\mathrm{M}} x_{\mathrm{E}j})$ (Michalek et al., 2004). According to the technology options and cost data in NHTSA's report (NHTSA, 2008), we construct a technology-cost model by combining various fuel economy improvement technologies[62], as shown in Figure 6.6. The thick and dashed curves represents the upper and lower estimates respectively, where the technology cost function is given by $c_{\mathrm{T}j} = b_3 x^2_{\mathrm{T}j} + b_4 x_{\mathrm{T}j}$. With all costs converted into year 2007 dollars using consumer price index (BLS, 2008), the coefficients of the vehicle manufacturing cost function are b_{M}= 95 (base engine power 95 kW), c_{B} = 7836, b_1= 701, b_2 = 0.0063. The coefficients for the technology

---

[60] The configurations of the vehicle in ADVISOR are mid-size car body, 95kW spark-ignition engine (SI95) with engine power scale ranging from 0.8 to 2.0, and an empirical automatic 4-speed transmission module (TX-AUTO4-4L60E) with default control strategies.

[61] We assume that implementation of fuel-saving technology does not affect engine horsepower.

[62] NHTSA's analysis report points out that synergy or dissynergy (overlapping effectiveness) can exist when implementing multiple fuel-saving technologies into a vehicle (NHTSA, 2008). For instance, when 5-speed auto-transmission is used with variable valve timing with coupled cam phasing (VVTC), there is 1% overlapping in fuel consumption reduction. Our technology-cost model has taken this factor into account.

cost curves are upper estimate: b_3 = 85936 and b_4 = –2177, mean: b_3 = 34121 and b_4 = –847, and lower estimate: b_3 = 16699 and b_4 = –639. For the simulation study in Section 4.3, we use the upper estimate cost curve as a base case since the mean and lower estimates may both optimistic and underestimate the costs of fuel-saving technology[63].

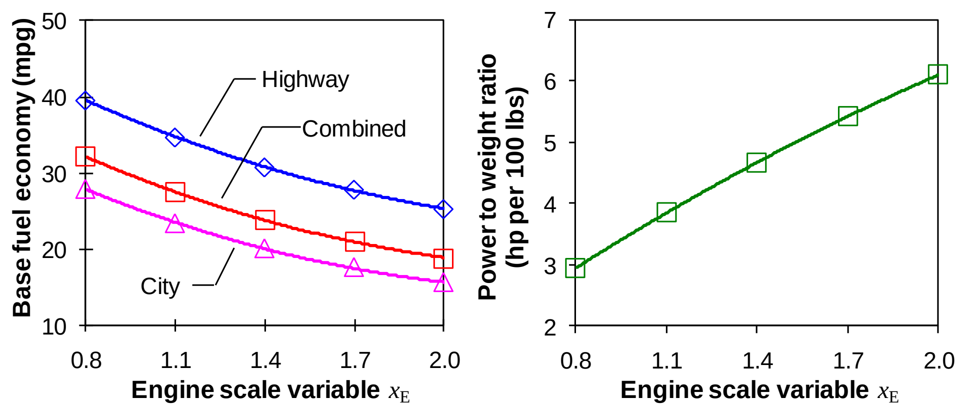

Figure 6.5 Meta-model of vehicle fuel economy simulations

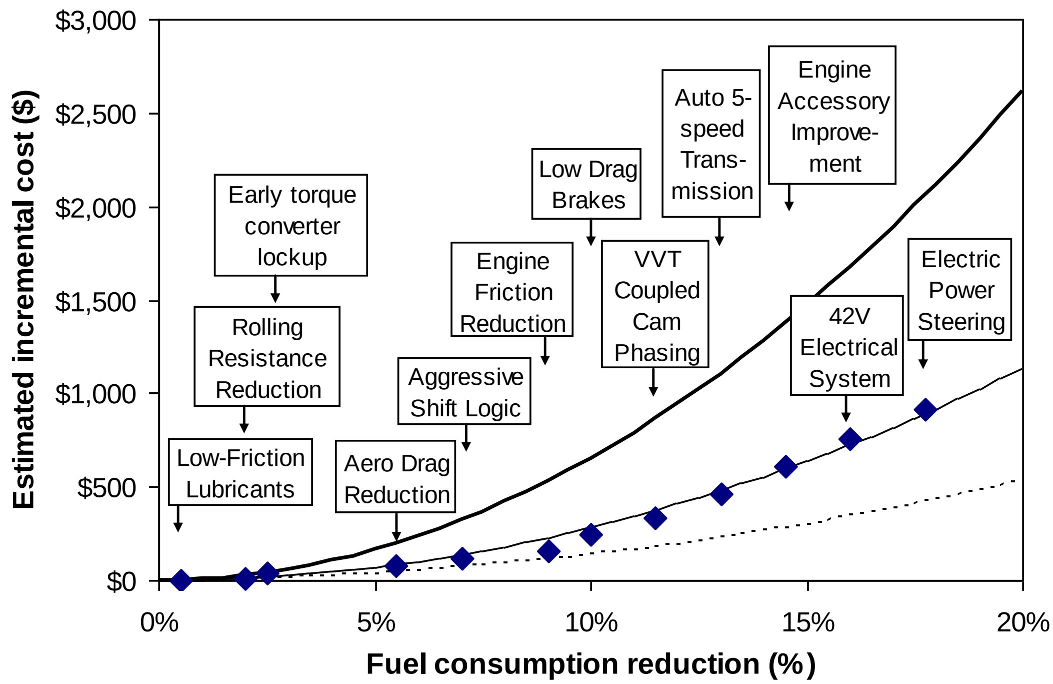

Figure 6.6 Cumulative technology cost versus fuel consumption improvement

[63] We also examined the medium cost curve and found that firms fully implement the maximum technology (20% reduction) in the case.

6.4.2 Demand Side Modeling

For automotive market demand modeling, we estimate market demand based on Ward's Auto 2005-2007 sales data using a mixed logit specification in order to account for consumer preference heterogeneity (Train, 2003). We consider four random coefficients: manufacturer suggested retail price (MSRP)[64] (unit: \$10,000), operation cost (unit: cent per mile), power-to-weight ratio (horsepower per 100 lbs), and footprint (100 square-feet). The base vehicle type is a domestic mid-size vehicle. There are eight dummy variables included for distinguishing different vehicle types. The utility u_{ij} for vehicle j and consumer i under the mixed logit framework is

$$
\begin{aligned}
u_{ij} &= v_{ij} + \varepsilon_{ij} \\
&= \left(\mu_{\mathrm{P}} + \sigma_{\mathrm{P}}\Phi_{\mathrm{P}i}\right) p_j + \left(\mu_{\mathrm{C}} + \sigma_{\mathrm{C}}\Phi_{\mathrm{C}i}\right)\gamma z_{\mathrm{C}j} + \left(\mu_{\mathrm{H}} + \sigma_{\mathrm{H}}\Phi_{\mathrm{H}i}\right) z_{\mathrm{H}j} \\
&\quad + \left(\mu_{\mathrm{S}} + \sigma_{\mathrm{S}}\Phi_{\mathrm{S}i}\right) z_{\mathrm{S}j} + \beta_{\mathrm{2S}} z_{\mathrm{2S}} + \beta_{\mathrm{SC}} z_{\mathrm{SC}} + \beta_{\mathrm{CP}} z_{\mathrm{CP}} + \beta_{\mathrm{LG}} z_{\mathrm{LG}} \\
&\quad + \beta_{\mathrm{LX}} z_{\mathrm{LX}} + \beta_{\mathrm{SP}} z_{\mathrm{SP}} + \beta_{\mathrm{IM}} z_{\mathrm{IM}} + \beta_{\mathrm{HY}} z_{\mathrm{HY}} + \varepsilon_{ij}
\end{aligned}
\tag{6.15}
$$

where v_{ij} is observable utility, ε_{ij} is the unobservable random utility component, μ is the mean coefficient, σ is the standard deviation and Φ is an IID normal distribution. The subscripts P, C, H and S represent price, operation cost, horsepower-to-weight ratio and vehicle size (footprint), respectively. The remaining terms z_{2S}, z_{SC}, z_{CP}, z_{LG}, z_{LX}, z_{SP}, z_{IM} and z_{HY} are binary variables for two-seater, subcompact, compact, large, luxury, sports, imported and hybrid vehicles, respectively, and the betas are corresponding coefficients. Assuming ε_{ij} as Gumbel distribution, the mixed logit choice probability for vehicle j becomes (Train, 2003):

$$
s_j = \int_{\boldsymbol{\Phi}} \frac{\exp\left(v_{j|\boldsymbol{\Phi}}\right)}{\sum_{k\in K}\sum_{j'\in J_k}\exp\left(v_{j'|\boldsymbol{\Phi}}\right)} f_{\Phi}\left(\boldsymbol{\Phi}\right) d\boldsymbol{\Phi} \approx \frac{1}{R}\sum_{r=1}^{R}\frac{\exp\left(v_j^r\right)}{\sum_{k\in K}\sum_{j'\in J_k}\exp\left(v_{j'}^r\right)}
\tag{6.16}
$$

[64] Use of MSRP as a proxy for transaction price is a potential source of error; however, transaction price varies by consumer, and the data is unavailable.

where $f_\Phi(\Phi)$ is the probability density function of the set of distribution Φ. Eq. (6.16) shows that numerical simulation is required to estimate mixed logit probability since no closed-form expression is available for integration. We use 1000 random normal draws (R=1000) and the maximum likelihood method for our mixed logit estimation.

The mixed logit estimation results for the 2007 automotive demand are shown in the first column of Table 6.3. While the mean coefficients of price and operation cost imply that consumers generally prefer lower purchase price and operation cost, there is significant heterogeneity in the degree of importance placed on the attributes. The positive coefficients of power-to-weight ratio (a proxy for acceleration performance) and footprint with small deviations represent consistent preferences for cars with faster acceleration and larger size. The negative coefficients for two-seater and subcompact and the positive coefficient for large cars match our expectation of people's preferences for car class. One exception is that compact vehicle has a slightly higher utility than mid-size. Since vehicle classes are taken into account in the estimation, the footprint preference implies spacious cars are preferred in every vehicle class. The last four coefficients show that luxury, sports and hybrid vehicles are appreciated by consumers, whereas imported vehicles are less preferred, all else being equal.

We further carried out two mixed logit estimations for 2005-2006 automotive sales data in order to observe potential consumer preference changes.[65] Estimation results for 2006 and 2005 are shown in the second and third column, respectively, in Table 6.3. Figure 6.7 shows the coefficient differences in graphic bars. Noticeable preference changes in 2005-2007 are found in car size and hybrid vehicle. The coefficients for compact car and hybrid variables are negative in the 2005 model and are positive in the 2006 and 2007 models. The coefficient changes match the

[65] All prices are converted into 2007 dollars using Consumer Price Index (BLS, 2008).

observed increasing popularity and market penetration of hybrid electric vehicles in the U.S. auto market (Maynard, 2007).

We tested the predicted market shares of midsize vehicle segment for each year using three sets of demand coefficients separately. The results are compared in Figure 6.8. It can be seen that using the same year coefficients produces better predicted results to the observed market shares. However, all prediction errors are within 5%. Specifically, the errors for the predicted 2006-2007 market shares using 2007 and 2006 coefficients are within 2 %. These results test the robustness of the demand predictions using the 2007 demand coefficients.[66] Although price endogeneity is not considered in this estimation[67], the mixed logit coefficients are able to provide reliable demand predictions for the vehicle design responses simulations in this case study.

[66] We assume static consumer preferences here. While dynamic discrete choice modeling can capture consumer taste variations across time, the potential implications would not be in the scope of this study. Furthermore, the market share predictions using static estimation for the midsize car segment show only small deviations from observed market data. The static estimation is able to serve a purpose to this CAFE study.

[67] The BLP method (Berry et al., 1995) is an estimation approach to analyze aggregate market data and also account for price endogeneity. The approach is a combination of random-coefficient logit model, instrumental variables, generalized method of moment (GMM) and a fixed-point iteration algorithm, which has been popular in econometrics and marketing science community (Nevo, 2000; Sudhir, 2001; Petrin, 2002; Besanko et al., 2003; Berry et al., 2004). The BLP method is not used in our estimation because of our concerns about instrumental variable selection and validation. While excluding instruments may lead to potential bias, weak instruments may lead to inconsistent estimation results and weak identification leads to non-normal distributions in GMM statistics (Bound et al., 1993; Bound et al., 1995; Stock et al., 2002).

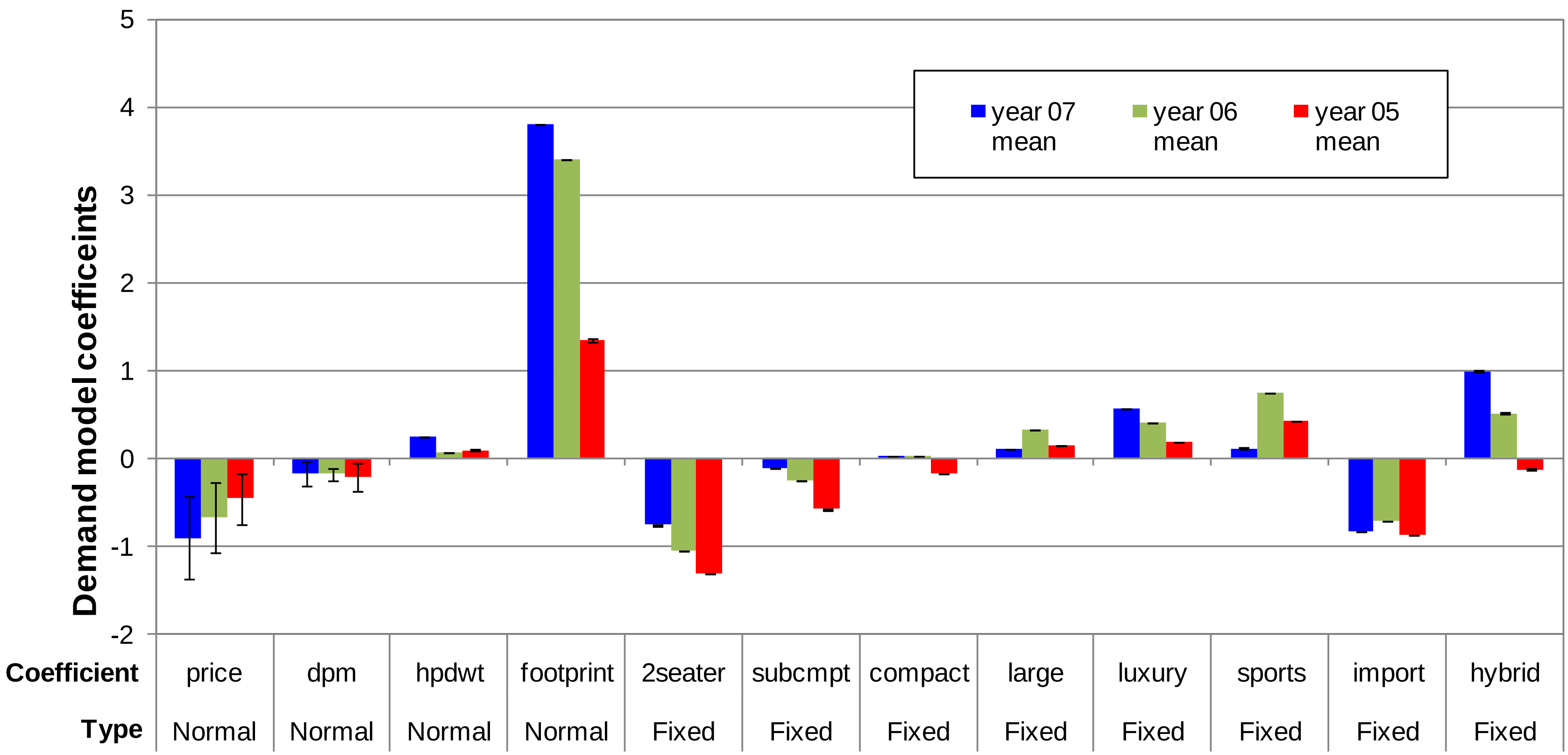

Note: The bars of the normal coefficients represent means of their distributions, and the corresponding error bars are the standard deviation of the coefficient distribution. The error bars of the fixed coefficients represent standard errors in maximum likelihood estiamtion.

Figure 6.7 The coefficients of mixed logit demand model on the US 2005-2007 automotive sales data

Table 6.3 Mixed logit estimation coefficients for the 2005-2007 US auto sales data

Coefficient	2007	2006	2005
Price*	–0.911 (0.002) [0.468] (0.001)	–0.677 (0.001) [0.397] (0.0007)	–0.467 (0.001) [0.300] (0.0007)
Operation cost*	–0.181 (0.0004) [0.145] (0.001)	–0.185 (0.0004) [0.072] (0.002)	–0.213 (0.0005) [0.155] (0.001)
Power/Weight*	0.242 (0.001) [0.004] (0.001)	0.060 (0.0005) [0.004] (0.002)	0.086 (0.0005) [0.010] (0.001)
Footprint*	3.803 (0.010) [0.002] (0.012)	3.403 (0.009) [0.003] (0.011)	1.341 (0.009) [0.017] (0.012)
Two-seater	–0.765 (0.004)	–1.062 (0.004)	–1.319 (0.003)
Subcompact	–0.124 (0.002)	–0.264 (0.002)	–0.587 (0.002)
Compact	0.025 (0.001)	0.022 (0.001)	–0.183 (0.001)
Large	0.097 (0.001)	0.325 (0.001)	0.139 (0.001)
Luxury	0.557 (0.002)	0.408 (0.002)	0.178 (0.002)
Sports	0.111 (0.003)	0.745 (0.003)	0.419 (0.002)
Import	–0.830 (0.001)	–0.717 (0.001)	–0.878 (0.001)
Hybrid	0.990 (0.006)	0.507 (0.006)	–0.129 (0.006)
Log-likelihood	-3.53×10^{7}	-3.72×10^{7}	-3.83×10^{7}

* Random coefficient in the mixed logit model: the value in square brackets is the standard deviation of random coefficient and the value in round brackets is standard error.

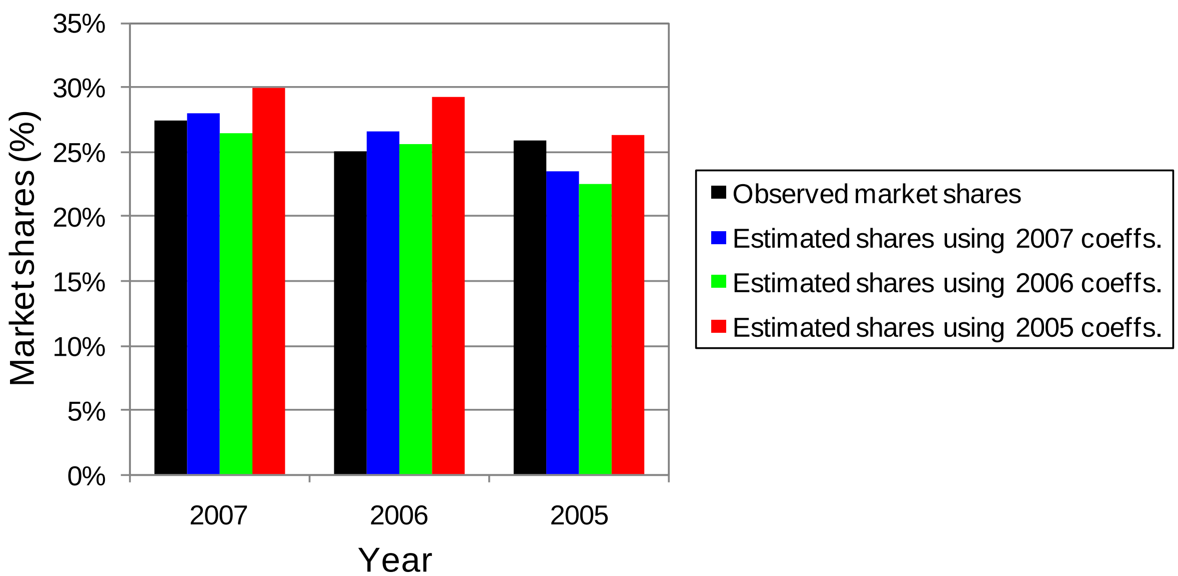

Figure 6.8 Comparison of estimated market shares using different demand coefficients

We further estimate the vehicle class own- and cross-elasticities of price by increasing all vehicle prices by 1% in the corresponding segment and observing the change in predicted demand for the 2007 data. The price elasticity matrix is shown in Table 6.4. The mid-size and compact vehicle segments have lower own-elasticities than other vehicle segments. Furthermore, the price variation of mid-size vehicle has stronger cross-demand influence than other vehicle segments. The demand for sports cars and two-seaters are strongly correlated. The only hybrid vehicle in our 2007 sales data is the Toyota Prius. It can be seen that the price of the hybrid vehicle, as a unique vehicle segment, has less influence on the demand for other vehicles in the market. Since mid-size vehicle is our main focus in the study, we further verify the attribute elasticities of regular domestic mid-size vehicle. The elasticity values with respect to price, operation cost and power-to-weight ratio are –1.194, –1.349 and 0.870, respectively. The result indicates that operation cost has a higher elasticity than price and power-to-weight ratio.

Table 6.4 Elasticities of demand for row segment evaluated by price variations in column segments

Segment	1	2	3	4	5	6	7	8
1 Two-seater	–1.986	0.034	0.036	0.037	0.034	–0.065	–0.774	0.032
2 Subcompact	0.113	–1.543	0.187	0.175	0.154	–0.073	–0.790	0.164
3 Compact	0.316	0.494	–1.119	0.491	0.424	–0.179	0.135	0.490
4 Mid-size	0.536	0.745	0.794	–1.125	0.679	–0.363	0.634	–1.227
5 Large	0.264	0.362	0.382	0.374	–1.607	–0.090	0.330	0.298
6 Luxury	–0.588	0.015	0.060	–0.027	0.010	–1.768	–0.114	0.277
7 Sports	–1.948	–0.322	0.052	0.090	0.085	–0.047	–1.904	0.069
8 Hybrid	0.026	0.042	0.048	–0.062	0.032	0.025	0.027	–1.844

6.5 Results and Discussions

By integrating the demand estimation results in Section 4.2 with the vehicle design model in Section 4.1, the manufacturer's vehicle design decisions are solved using the framework proposed in Section 3 with the FOC equations provided in Appendix B.4. For the base case study, we use a gasoline price γ = \$2.50 per gallon and a CAFE penalty of \$55 per mpg per car. We simulate 10 generic domestic manufacturers competing in the market. The fuel economy design responses to various CAFE standards are shown in Figure 6.9. The solid line represents the result of the base case under different levels of CAFE fuel economy standards. For the 2007 passenger car standard 27.5 mpg, the manufacturer's fuel economy responses are not binding with CAFE regulation. The 34.6 mpg in region 1 matches the general trend of the passenger car fuel economy at 2007-2008 levels in Figure 6.1, where manufacturers are designing cars with higher fuel efficiency than the regulatory level. The situation implies that automakers' vehicle design decisions are direct responses to market demand and consumer preferences. Thus CAFE regulation is inactive. The CAFE-binding range (region 2) is between 34.6 and 36.5 mpg. When the regulatory standard rises beyond 36.5 mpg, the optimal equilibrium response is to ignore further increases and pass the CAFE penalty cost along to consumers (region 3).

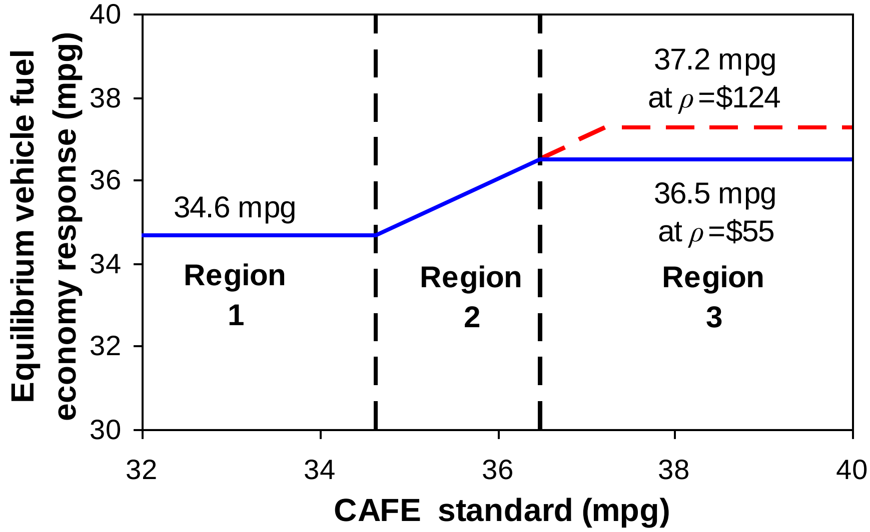

Figure 6.9 Design responses to various fuel economy regulatory levels

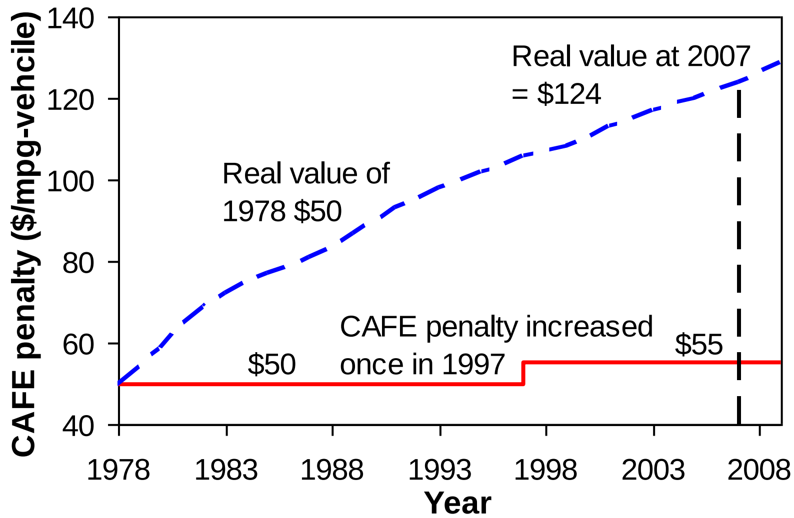

Figure 6.10 CAFE penalty level and inflation-adjusted value of $50 in 1978

We then verify the design responses at different levels of CAFE penalty. Figure 6.10 shows the history of the CAFE penalty compared to the inflation-adjusted value of the original $50 penalty set in 1978 using Gross Domestic Product (GDP) price index adjustment (BEA, 2008). Clearly the CAFE penalty has lagged below inflation. We verify the vehicle design response at the higher penalty $124 level, and the result is shown as a dashed line in Figure 6.9. The higher CAFE penalty extends the window of region 2.

Figure 6.11 shows a contour plot of Nash responses for a range of CAFE regulatory fuel economy standards and penalty values. The structural effect of two CAFE regulatory parameters to firm's vehicle design responses is visible: In region 1, when the CAFE standard is less than 34.6 mpg, manufacturer design responses are not affected by the CAFE standard or penalty. In region 2, fuel economy design responses are only affected by the CAFE standard but not the CAFE penalty parameter. In region 3, fuel economy design response is function of the CAFE penalty but not the CAFE standard, and the border between region 2 and region 3 depends on both the CAFE standard and the CAFE penalty. There are several useful implications of our observations. When firms are binding with the CAFE regulation (region 2), changing mpg standard as a policy tool to urge automakers to improve their fuel economy is effective. However, changes in regulatory standards may not be useful when firms have no incentive to follow the standard (region 1 and region 3). Moreover, when firms violate the CAFE regulation (region 3), increasing the penalty can increase firms' fuel economy responses, but the improvement may be modest: we find that a $100 increase in penalty would cause a fuel economy increase less than 1 mpg.[68]

[68] Additional costs observed by the firm, such as public relations or litigation cost for violation, would extend the effective region of CAFE policy. In practice, domestic automakers hold a policy to treat CAFE as a constraint, due in part to fear of shareholder reaction.

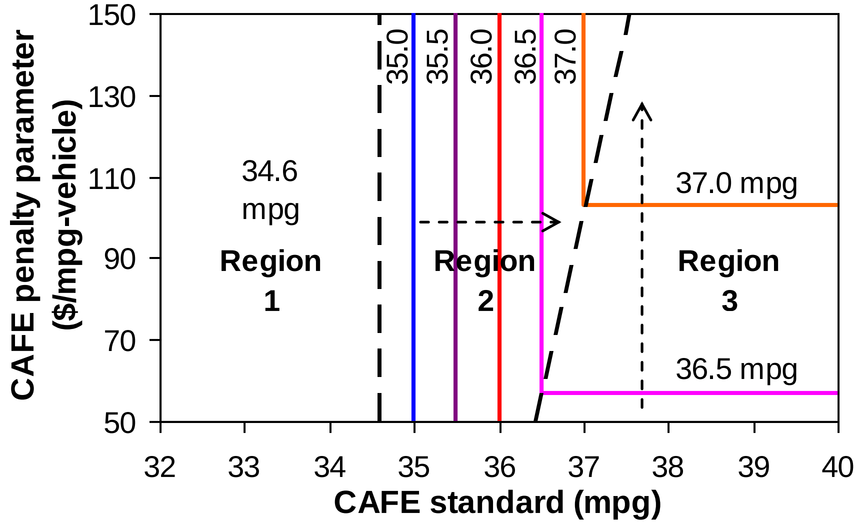

Figure 6.11 Vehicle fuel economy responses under various fuel economy standards and penalty levels

We further analyze vehicle fuel economy responses under different gasoline prices and a fixed CAFE penalty of $55 per vehicle per mpg. We tested the fuel economy response by using two gasoline price levels, $4.20 per gallon and $1.60 per gallon. The former is the highest weekly retail gas price during 2007-2008 and the later is the lowest (EIA, 2009).[69] The analysis results in Figure 6.12 show that gasoline price variations offset the entire fuel economy response curve significantly: high fuel prices shift the Nash design responses upward, while low fuel prices shift the response curves to a lower fuel economy region. At high fuel price level, we find that automakers reduce their engine sizes to the lower bound and implement more fuel-saving technology. On the other hand, lower fuel prices create incentives for automakers to design vehicles with more powerful engines and fewer technology options implemented.[70]

[69] Our demand model assumes that consumer preference is for operating cost, rather than fuel economy, and that preference for operating cost does not vary with fuel price.

[70] The equilibrium framework predicts static long run responses and does not account for responses to short run fuel price volatility or uncertainty.

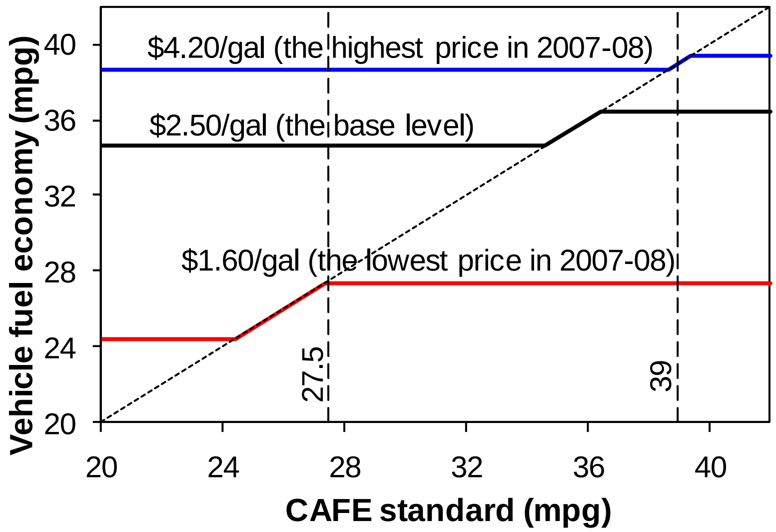

Figure 6.12 Vehicle fuel economy responses under various gasoline prices

The response curves are relatively sensitive to fuel price (because of consumer demand for low operating cost) compared to CAFE standards, despite the fact that CAFE standards more directly address fuel economy (Vlasic, 2008). Thus policies that influence gasoline prices, such as fuel taxes or carbon taxes[71], may encourage greater vehicle fuel economy improvement than adjusting the CAFE standard if prices are sufficiently high. Indeed, historical data on CAFE (Figure 6.1) shows that manufacturers have moved ahead of the CAFE standard in recent years with higher fuel prices.

We also examine the penalty amount required for the Obama administration's new fuel efficiency target 39 mpg on passenger cars. Our simulation model shows that a high penalty up to $255 would be needed for reaching the target if gasoline price remains at the base level of $2.50 per gallon. In contrast, without CAFE regulations, the target can be reached with a

[71] The average life cycle GHG emissions of gasoline is about 11.3 kg-CO_2-eq per gallon (Wang et al., 2007). Thus $10/tonne of carbon tax would result in gasoline cost increase in 11 cents. For the base gas price at $2.5/gal, a high carbon tax $168/tonne would be needed to make retail gasoline price equivalent to $4.40/gal. At that price level, the average fuel economy for midsize cars would reach Obama's target 39 mpg without CAFE regulation.

gasoline price \$4.40 per gallon. The required increase in CAFE penalty is significantly higher than the 72% increment in gasoline price. Furthermore, at such a high fuel economy level, the equilibrium vehicle design solutions have the smallest engine size at lower bound, and more fuel-saving technology options are implemented (18% fuel-saving), which are close to our model limits of midsize conventional vehicle. The result implies that automakers should have more sales shift towards small vehicles, such as compact or subcompact cars and have more advanced technology implementations, such as alternative fuel vehicle, hybrids and plug-in hybrids, when facing the arriving high fuel economy requirements.

6.6 Conclusions

We pose an oligopoly model of automaker responses to CAFE standards where vehicles are viewed as differentiated products. We find that Nash vehicle design responses to CAFE standards follow a distinctive pattern under general demand, cost, and performance functions and single-vehicle firms: Firms ignore low CAFE standards, treat moderate CAFE standards as binding, and violate high CAFE standards, where the point and amount of violation depends on the penalty for violation, and increases of the CAFE standard beyond the violation point are ineffective. While the original penalty for CAFE violation set in 1978 has not been adjusted for inflation, other factors, such as public and government relations costs for violation of CAFE standards, may contribute to extending the range of effective CAFE standards.

Our case study results show that for current models of automotive demand, cost, and performance, vehicle fuel economy responses are more sensitive to fuel prices than to CAFE standards with the ranges examined, and fuel prices address driving patterns in addition to vehicle design. This result may partly support prior conclusions in the literature that Pigovian gasoline taxes are a lower cost option than CAFE policy for reducing gasoline consumption. The effects on vehicle design caused by the increases in CAFE standards set by the Obama administration to a combined 35.5 mpg by 2016 will depend on the path of gasoline prices and the penalties set for violation of CAFE standards. Responding to stricter fuel efficiency standards, such as the European and California corporate average standards on CO_2 emissions per mile, will likely require both a shift to smaller, lighter vehicles and inclusion of alternative technologies, such as cellulosic-based ethanol vehicles, hybrid electric vehicles, and plug-in hybrid electric vehicles (Lave et al., 2000).

CHAPTER 7. CONCLUSIONS

7.1 Summary

The series of studies in this dissertation proposed integrated models of product design, consumer choice, market competition and environmental regulation to examine the implications in design decisions and public policy. The answers to the three questions proposed in the beginning of this thesis are summarized in follows with primary assumptions stated explicitly:

1. How does market competition affect product design decisions?

The investigation for answering this question was conducted in Chapter 2 and 3. The following assumptions were made for developing the models in the chapters: (1) the market is described as a non-cooperative oligopolistic game with complete information and a fixed number of firms (no entry and exit); (2) firms are generic with identical decision-spaces, no technological change, identical cost structures, no differences in intellectual property rights, and negligible brand effects; (3) firms make price and design decisions for seeking profit maximization, and the market outcome is described by Nash equilibrium; (4) focal firm designs a set of differentiated products that will enter a market with existing products sold by competitors; (5) in the short-run case, competitors are Nash price setters with fixed product design; (6) in the long-run case, competitors change both price and design in response to focal firm's new product entry; (7) market demand is described by a random-utility discrete-choice model with time invariant consumer preference coefficients; and (8) price and design decision variables are continuous, and each firm's profit function is differentiable.

In Chapter 2, optimization models were presented using the theory of mathematical programs of equilibrium constraints (MPEC) to account for competitor reactions under Nash and Stackelberg price competition. The case studies showed that the proposed formulations are able to find equilibrium solution with shorter computational time and better convergence accuracy than the prior methods. The results indicated that the Stackelberg approach outperforms Nash by anticipating competitors' pricing reactions, and exclusion of competitor reaction results in overestimation in market performance and suboptimal solutions. In Chapter 3, a long-run competition model was proposed to determine design and pricing decisions at market equilibrium. The model was utilized to examine the influence of two market modeling factors: (1) channel structure for manufacturer-retailer interactions; and (2) demand modeling for consumer preference heterogeneity. The mathematical analysis proved that design decisions become independent of market factors, including competition and channel structure, if demand modeling is linear logit with heterogeneous preferences ignored.

In summary, the answer to the first research question is that an optimal product design that would perform well in the current market may perform poorly under market competition. When consumer preference heterogeneity in the market demand is not pronounced, designers may treat preference variations as noise and perform design tasks independent of market competition. On the other hand, if heterogeneity in demand is significant, ignoring consumer taste variations can lead to a design decision disengaged from market systems and result in suboptimal solutions.

2. What are the design and policy implications of plug-in hybrid technology?

To answer this question, a life cycle analysis model for PHEV economic and environmental performance was developed in Chapter 4, and an optimization model for social objectives was proposed in Chapter 5. The primary assumptions for the PHEV optimization model include (1) vehicles are designed and allocated optimally to drivers via a dictated assignment for best social benefits; (2) each driver has a constant daily driving distance over the vehicle life; (3) the US NHTS weighted driving data are described using the exponential distribution function; and (4) vehicle performances are measured using EPA UDDS driving cycle simulation, and PHEV is assumed one full charge per day. The major parameters and their uncertainty test ranges are: PHEV lithium-ion battery pack cost \$400/kWh (high \$1000/kWh and low \$250/kWh), HEV NiMH battery pack cost \$600/kWh (high \$700/kWh and low \$440/kWh), retail gasoline price \$3.30/gal (high \$6.00/gal and low \$1.50/gal), retail electricity price \$0.11/kWh (high \$0.30/kWh and low \$0.06/kWh), carbon allowance price \$0 to \$100 per CO_2-eq-ton, and market discount rate 0% to 10%.

Based on the analysis results, several critical factors affecting PHEV performance were identified: (1) Battery weight: When more batteries are added to a PHEV to increase electrical travel range, the electrical and fuel efficiencies are decreased due to additional weights. According to the simulation analysis in Chapter 4, the impact of battery weight to PHEV performance is visible but less influential than the following factors. (2) Distance between charges: While it is commonly known that PHEVs can best utilize electric mode capability when the driver' charging patterns match the battery capacity, this study pointed out that small-capacity PHEVs with frequent charges can outperform large PHEVs on life cycle cost. It is worth noting that an increase in gas price, a decrease in electricity price, or a decrease in battery cost would make PHEV less costly for a wide range of drivers, and vice versa. (3) Specific energy: Battery technology that increases specific energy would not affect net cost and GHG emissions significantly. The result suggested that research on reducing battery cost would be more effective than that of improving specific energy. (4) Battery degradation and replacement: Since PHEVs rely on large batteries storing electrical energy, battery replacement would make PHEVs less cost-competitive. The study in Chapter 5 showed that recent lithium iron phosphate ($LiFeO_4$) battery technology allows designers to utilize maximum energy capacity in the battery without nonlinearly degrading the battery life. This finding implies that greater all-electrical range (AER) can be achieved by smaller battery pack, and policy to subsidize battery cost on AER may be more effective than on capacity. (5) Carbon allowance price: Carbon allowance policy should be advantageous to PHEVs because of less lifecycle GHG emissions. However, the analysis results indicated that carbon policy with current U.S. grid mix has limited effect to improve the economic performance of PHEVs. If renewable energy in the source mix of the grid became significant, the carbon policy would create cost-saving incentives for PHEVs.

In summary, the study in Chapter 4 investigated which *individual drivers save most* on fuel, GHGs, and cost. Chapter 5 conducted an extensive PHEV optimization study with focusing on *which drivers make most impacts* on social objectives with accounting for battery degradation and replacement. The optimal solutions indicated different social objectives result in alternative optimal vehicle options. Large-capacity and medium-capacity PHEVs are the vehicle options to reduce petroleum consumption and lifecycle GHG emissions, respectively. The mix of PHEV with smaller battery capacity and ordinary hybrid electrical vehicle (HEV) for longer travel has lowest total cost. While each objective has distinctive vehicle choice, small-to-medium capacity

PHEVs with frequent charges have implications on overall benefits to designers, consumers and policy planners.

3. How does CAFE policy affect vehicle design decisions in a competitive market?

A long-run competition model of automaker responses to CAFE standards was proposed in Chapter 6 to investigate this question. The following assumptions are made in developing the model: (1) market competition is modeled as static and non-cooperative game with complete information, and market solution is defined by Nash equilibrium; (2) firms have identical design capability and fuel-saving technologies without branding and patenting advantages, and no firm enters and exits during the competition; (3) market demand is described by discrete choice model simulation with static consumer preferences which are estimated from market or survey data; (4) CAFE regulations and gasoline prices are considered exogenous factors in the model.

A unique three-region pattern of Nash equilibrium vehicle design responses were identified under oligopoly of single-vehicle firms with generic demand model and design functions: (1) firms ignore low CAFE standards; (2) firms follow moderate CAFE standards; (3) firms violate high CAFE standards - firms stop to response to increased standards, and the amount of violation depends on the penalty parameter in the CAFE regulations. The case study results for midsize vehicle powertrain design using current market data and fuel-efficiency technologies showed that automakers' design responses are more sensitive to gas prices than to CAFE standards under the ranges examined. Overall, when U.S. government, California state and European Union have raised fuel economy standards for the future years, automakers' vehicle design decisions for pursuing maximum profit will not solely be controlled by fuel-economy threshold but depend on gas prices, fuel-efficiency technology costs, and violation penalties.

7.2 Summary of Contributions

The contributions of this dissertation are summarized in follows:

1. Two optimization formulations were proposed to solve the problems of new product design under Nash and Stackelberg price competitions. In a game-theoretic framework, the case studies demonstrated that profit overestimation can be avoided by taking market competition into account and the proposed formulation has superior computational performances to the prior methods in the literature.
2. Under the context of Nash equilibrium, the effects of consumer preference heterogeneity in the market-design equilibrium problems were identified. The analysis demonstration showed that treating consumer taste variations as noise (logit) can lead to design-market decoupling in the problems of design for market systems. Taste heterogeneity in demand model links design decisions to market systems and results in differentiated designs in different channel structures.
3. The PHEV life cycle cost analysis showed that small-capacity plug-in hybrid vehicles have good potential to save cost and reduce greenhouse gas emissions if the drivers charge battery frequently. Carbon allowance policy accompanying with renewable energy sources may provide cost-saving incentives to consumers and thus assist market penetration of PHEVs.
4. Optimal PHEV design and allocation for different social objectives showed that (1) larger capacity PHEVs are best for reducing petroleum consumption; (2) medium capacity

PHEVs are best for reducing GHG emissions; and (3) allocations of PHEV-HEV are best for saving lifecycle cost when PHEVs for short to medium distance travel are charged frequently and HEVs are used for long distance travel.

5. The PHEV optimization study showed that cost-minimized PHEVs and HEVs have close economic performances. Over the driver-allocation range up to 200 daily travel miles, PHEVs are part of a least-cost solution as gasoline price is above $3 per gal, retail electricity price is below $0.14 per kWh, battery capacity cost is below $460 per kWh, or discount rate is below 7%.
6. The study results indicated that the recently developed lithium iron phosphate ($LiFePO_4$) battery technology has important implication to optimal PHEV designs: instead of limiting battery capacity in use for reserving battery life, designers should optimally utilize full battery capacity and replace batteries as needed.
7. The unique patterns of Nash-profit-seeking automakers' optimal design responses under CAFE regulations and market competition are identified. Firms' fuel efficiency design decisions at Nash equilibrium may fail to response to higher CAFE fuel standards if violation penalty is not further increased. The case study results showed that design decisions are more sensitive to gasoline prices than CAFE standards.

7.3 Open Questions

There are still many open questions beyond the scope of this dissertation and worthy of future investigation. In Chapter 2 and 3, uncertainty in design for market systems is a research direction that requires verifications. In a framework of design and market, there are at least two uncertainty sources: (1) uncertainties in engineering system (e.g. distributions in design parameters), and (2) uncertainties in market systems (e.g. consumer preference heterogeneity). The potential research questions include: How do market demand uncertainties propagate into final design decisions? What are the potential interacting effects between two types of uncertainties? How do different channel structures affect the robustness of optimal design solutions? These factors may alter the design implications in designers' optimal decisions.

In the market competition models in Chapter 3 and 6, symmetric equilibria were found even if consumer preference heterogeneity (standard deviations in random coefficients) was significant. Such result implies that potential artifacts may still exist in the heterogeneity modeling of well-known mixed (random-coefficient) logit models, which has been considered a solution to eliminate IIA properties in the logit model family. The answer to this question is not found in the marketing or econometric literature as yet, and awaiting more research effort to resolve.

For the PHEV analysis and design in Chapter 4 and 5, there are still many influential factors and possible implications to be examined. First, the scope of the study was confined to all-electric PHEVs, whereas blended-mode PHEVs can make use of the gasoline engine during CD-mode to allow additional control flexibility and smaller motors and battery packs. Analysis of blended-mode PHEVs requires further examination of the control strategy variables. Second, the study assumed fixed Li-ion battery technology and constant battery capacity cost for all PHEV designs. In practice, different hybrid systems may require different battery designs, such as thin electrode design (high cost) for high power and thick electrode design (low cost) for high capacity applications. Future investigation for the technical feasibility of heterogeneous battery designs is required. Third, infrastructure advancements, such as automatic charging connections installed in garages or designated public parking spaces, may help to ensure frequent charging and increase the number of drivers for whom PHEVs are competitive. However, the tradeoff in the costs of the smart charging devices may alter the economic implications of PHEVs. Finally, the benefits of PHEVs can only be effective when substantial market penetration occurs. However, market penetration of new vehicle technology is difficult to be estimated since consumer preferences on unique features of PHEVs are unknown. A possible approach is to examine the relative importance to consumers of attributes such as purchase cost, operating cost, fuel economy, performance, reliability, perceived sustainability and charging requirements. This may help designers and policy makers on which vehicles may emerge as successful in the competitive marketplace.

The CAFE policy study in Chapter 6 has several limitations that provide opportunities for future work: First, the assumption of a single vehicle design per producer helps to produce closed-form results and general conclusions; however, it restricts the ability to predict sales shifts from one vehicle type to another and instead presumes that firms respond only through redesign. The role of consumer heterogeneity and differences in firm brand and cost structures must be better understood in order to predict product line design response in equilibrium. Second, attribute-based CAFE standards will imply different incentives for vehicle responses than single-target standards. Further study of attribute-based standards is warranted. Third, non-regulation-fee costs for CAFE violation could be incorporated to examine the general effect and the effect when some firms observe higher costs than others. We see opportunity for a range of potential follow-up studies examining transportation policy while accounting for the effects of differentiated vehicle design, consumer responses to differentiated products, and technical tradeoffs in the ability to achieve vehicle attributes that are competitive in the regulated marketplace.

In the end, this dissertation has accomplished only a small portion of the research tasks in the domain of design decisions for market system and public policy by posing integrated models, offering solution strategies, and examining practical implications. When a number of questions are still awaiting exploration, it is the author's hope that the findings from this study can provide fundamental knowledge for the future research.

BIBLIOGRAPHY

Ahmad, S., D. L. Greene. 2005. Effect of fuel economy on automobile safety - A reexamination. *Transportation Research Record.* **1941** 1-7.

Amjad, S., S. Neelakrishnan, R. Rudramoorthy. 2010. Review of design considerations and technological challenges for successful development and deployment of plug-in hybrid electric vehicles. *Renewable and Sustainable Energy Reviews.* **14**(3) 1104-1110.

Anderson, S. P., A. De Palma, J. F. Thisse. 1992. *Discrete Choice Theory of Product Differentiation*. Cambridge, Mass, MIT Press.

Anitescu, M. 2000. On solving mathematical programs with complementarity constraints as nonlinear programs. Mathematics and Computer Science Division, Argonne National Laboratory.

Argonne National Laboratory. 2008. Powertrain Systems Analysis Toolkit (PSAT).

Austin, D., T. Dinan. 2005. Clearing the air: The costs and consequences of higher CAFE standards and increased gasoline taxes. *Journal of Environmental Economics and Management.* **50**(3) 562-582.

AVL. 2004. *ADVISOR 2004 User Guide*, AVL North America, Inc.

Axsen, J., A. Burke, K. Kurani. 2008. Batteries for Plug-in Hybrid Electric Vehicles (PHEVs): Goals and the State of Technology circa 2008. Institute of Transportation Studies, University of California. http://pubs.its.ucdavis.edu/publication_detail.php?id=1169

Bazaraa, M. S., C. M. Shetty. 1979. *Nonlinear Programming: Theory and Algorithms*. New York, Wiley.

BEA. 2008. National Economic Accounts Data. Bureau of Economic Analysis, U.S. Department of Commerce.

Berry, S., J. Levinsohn, A. Pakes. 1995. Automobile Prices in Market Equilibrium. *Econometrica.* **63**(4) 841-890.

Berry, S., J. Levinsohn, A. Pakes. 2004. Differentiated products demand systems from a combination of micro and macro data: The new car market. *Journal of Political Economy.* **112**(1) 68-105.

Berry, S. T. 1992. Estimation of a model of entry in the airline industry. *Econometrica.* **60**(4) 889-917.

Besanko, D., J. P. Dube, S. Gupta. 2003. Competitive price discrimination strategies in a vertical channel using aggregate retail data. *Management Science.* **49**(9) 1121-1138.

Besanko, D., S. Gupta, D. Jain. 1998. Logit demand estimation under competitive pricing behavior: An equilibrium framework. *Management Science.* **44**(11) 1533-1547.

Besharati, B., L. Luo, S. Azarm, P. K. Kannan. 2006. Multi-objective single product robust optimization: An integrated design and marketing approach. *Journal of Mechanical Design.* **128**(4) 884-892.

Biller, S., J. Swann. 2006. Pricing for environmental compliance in the auto industry. *Interfaces.* **36**(2) 118-125.

BLS. 2008. Consumer price index history table. Bureau of Labor Statistics, U.S. Department of Labor. http://www.bls.gov/cpi/#data

BLS. 2009. Producer Price Indexes. Bureau of Labor Statistics, U.S. Department of Labor. http://www.bls.gov/ppi/

Bonami, P., L. T. Biegler, A. R. Conna, G. Cornuejols, I. E. Grossmann, C. D. Laird, J. Lee, A. Lodi, F. Margot, N. Sawaya, A. Wachter. 2008. An algorithmic framework for convex mixed integer nonlinear programs. *Discrete Optimization.* **5**(2) 186-204.

Bound, J., D. A. Jaeger, R. Baker. 1993. The cure can be worse than the disease: A cautionary tale regarding instrument variables. NBER Technical Working Paper No. 137.

Bound, J., D. A. Jaeger, R. M. Baker. 1995. Problems with Instrumental Variables Estimation When the Correlation between the Instruments and the Endogenous Explanatory Variable Is Weak. *Journal of the American Statistical Association.* **90**(430) 443-450.

Boyd, J. H., R. E. Mellman. 1980. The Effect of Fuel-Economy Standards on the United-States Automotive Market: An Hedonic Demand Analysis. *Transportation Research Part A: Policy and Practice.* **14**(5-6) 367-378.

Bradley, T. H., A. A. Frank. 2009. Design, demonstrations and sustainability impact assessments for plug-in hybrid electric vehicles. *Renewable and Sustainable Energy Reviews.* **13** 115-128.

Broder, J. M. 2009. Obama to Toughen Rules on Emissions and Mileage. *The New York Times*.

Brooker, A., M. Thornton, J. Rugh. 2010. Technology Improvement Pathways to Cost-Effective Vehicle Electrification. *SAE 2010 World Congress*. Detroit, Michigan preprint.

Brownstone, D., D. S. Bunch, K. Train. 2000. Joint mixed logit models of stated and revealed preferences for alternative-fuel vehicles. *Transportation Research Part B: Methodological.* **34**(5) 315-338.

Brownstone, D., K. Train. 1999. Forecasting new product penetration with flexible substitution patterns. *Journal of Econometrics.* **89**(1-2) 109-129.

BTS. 2003. National Household Travel Survey 2001. U.S. Department of Transportation, Bureau of Transportation Statistics.

BTS. 2010. National Household Travel Survey 2009. U.S. Department of Transportation, Bureau of Transportation Statistics.

Bunch, D. S., M. Bradley, T. F. Golob, R. Kitamura, G. P. Occhiuzzo. 1993. Demand for clean-fuel vehicles in California: A discrete-choice stated preference pilot project. *Transportation Research Part A: Policy and Practice.* **27**(3) 237-253.

Bunkley, N. 2008. Plug-In Hybrid From G.M. Is Nearly Ready for Testing. *The New York Times*.

Burke, A. F. 2007. Batteries and ultracapacitors for electric, hybrid, and fuel cell vehicles. *Proceedings of the IEEE.* **95**(4) 806-820.

California Code. 2008. *Health and Safety Code for Manufacturers and Dealers: Section 43211*.

Cagan, J., C. M. Vogel. 2002. *Creating Breakthrough Products: Innovation from Product Planning to Program Approval*. Upper Saddle River, NJ, Prentice Hall.

California Air Resources Board. 2004. *California Code of Regulations, Title 13 Sections 1900 and 1961: Low-Emission Vehicle Program*.

Chernick, H., A. Reschovsky. 1997. Who pays the gasoline tax? *National Tax Journal.* **50**(2) 233-259.

Cherry, B. 2009, Electric Schedule E-9: Experimental residential time-of-use service for low emission vehicle customers. Pacific Gas and Electric Company. Retrieved Jan. 1, 2010, http://www.pge.com/tariffs/tm2/pdf/ELEC_SCHEDS_E-9.pdf.

Choi, S. C. 1991. Price competition in a channel structure with a common retailer. *Marketing Science.* **10**(4) 271-296.

Choi, S. C., W. S. Desarbo. 1993. Game theoretic derivations of competitive strategies in conjoint analysis. *Marketing Letters.* **4**(4) 337-348.

Choi, S. C., W. S. Desarbo, P. T. Harker. 1990. Product Positioning under Price Competition. *Management Science.* **36**(2) 175-199.

Choi, S. C., W. S. Desarbo, P. T. Harker. 1992. A Numerical Approach to Deriving Long-Run Equilibrium Solutions in Spatial Positioning Models. *Management Science.* **38**(1) 75-86.

Choo, S., P. L. Mokhtarian. 2004. What type of vehicle do people drive? The role of attitude and lifestyle in influencing vehicle type choice. *Transportation Research Part a-Policy and Practice.* **38**(3) 201-222.

Coughlan, A. T. 2001. *Marketing Channels*. Upper Saddle River, N.J., Prentice Hall.

Crandall, R. W., J. D. Graham. 1989. The effect of fuel economy standards on automobile safety. *Journal of Law & Economics.* **32**(1) 97-118.

Crandall, R. W., H. K. Gruenspecht, T. E. Keeler, L. B. Lave. 1986. *Regulating the Automobile*. Washington, D.C., Brookings Institution.

de la Torre, S., A. J. Conejo, S. A. Gabriel, Y. Shim, R. Garcia-Bertrand. 2007. Application of a new Benders decomposition method for DC-MPECs to the bidding strategy of a power producer. *Trans-Atlantic INFRADAY*. College Park, Maryland, USA.

Decker, C. S., M. E. Wohar. 2007. Determinants of state diesel fuel excise tax rates: the political economy of fuel taxation in the United States. *Annals of Regional Science.* **41**(1) 171-188.

Dieter, G., L. C. Schmidt. 2008. *Engineering Design*. New York, NY, McGraw-Hill.

Dirkse, S. P., M. C. Ferris. 1995. MCPLIB: A Collection of Nonlinear Mixed Complementarity Problems. *Optimization Methods and Software.* **5** 319-345.

Duvall, M. 2004. Advanced batteries for electric-drive vehicles. Electric Power Research Institute.

EIA. 2008. Annual Energy Review 2007. U.S. Department of Energy http://www.eia.doe.gov/emeu/aer/elect.html

EIA. 2008. Monthly Energy Review May 2008, U.S. Department of Energy.

EIA. 2009. Average Retail Price of Electricity to Ultimate Customers: Total by End-Use Sector. Energy Information Administration, U.S. Department of Energy. http://www.eia.doe.gov/cneaf/electricity/epm/table5_3.html

EIA. 2009. Electric Power Annual 2007. Energy Information Administration, U.S. Department of Energy. http://www.eia.doe.gov/cneaf/electricity/epa/epa.pdf

EIA. 2009. Energy market and economic impacts of H.R. 2454, the American Clean Energy and Security Act of 2009. Energy Information Administration, U.S. Department of Energy. http://www.eia.doe.gov/oiaf/servicerpt/hr2454/pdf/sroiaf%282009%2905.pdf

EIA. 2009. The U.S. Weekly Retail Gasoline and Diesel Prices. Energy Information Administration, U.S. Department of Energy. http://tonto.eia.doe.gov/dnav/pet/pet_pri_gnd_dcus_nus_a.htm

EPA. 1996. Federal Test Procedure Revisions, Environmental Protection Agency.

EPA. 2004. Fuel Economy and Emissions Programs. U.S. Environmental Protection Agency.

EPA. 2005. Emission facts: Average carbon dioxide emissions resulting from gasoline and diesel fuel. U.S. Environmental Protection Agency. http://www.epa.gov/OMS/climate/420f05001.htm

EPA. 2005. Emission Facts: Greenhouse Gas Emissions from a Typical Passenger Vehicle.

EPA. 2006. Emission Durability Procedures and Component Durability Procedures for New Light-Duty Vehicles, Light-Duty Trucks and Heavy-Duty Vehicles; Final Rule and Proposed Rule. U.S. Environmental Protection Agency.

EPA. 2006. Inventory of U.S. Greenhouse Gas Emissions and Sinks: 1990-2004, U.S. Environmental Protection Agency, Washington, DC.

U.S. Environmental Protection Agency. 2007. *Code of Federal Regulations. Title 40 Part 86: Control of emissions from new and in-use highway vehicles and engines*.

U.S. Environmental Protection Agency. 2007. *Code of Federal Regulations. Title 40 Part 600: Fuel Economy of Motor Vehicles*.

EPA. 2009. Executive Summary: EPA's Waiver Decision on California's Greenhouse Gas Emission Standards for New Motor Vehicles. U.S. Environmental Protection Agency. http://www.epa.gov/otaq/climate/ghgwaiverexecutivesummary.pdf

EPRI. 2001. Comparing the benefits and impacts of hybrid electric vehicle options. Electric Power Research Institute.

EPRI. 2007. Environmental assessment of plug-in hybrid electric vehicles. Volume 1: Nationwide greenhouse gas emissions. Electric Power Research Institute.

Espey, M., S. Nair. 2005. Automobile Fuel Economy: What Is it Worth? *Contemporary Economic Policy*. **23**(3) 317-323.

European Commission. 2007. Results of the review of the Community Strategy to reduce CO2 emissions from passenger cars and light-commercial vehicles. COM(2007)19 SEC(2007)60&61. European Commission.

European Parliament. 2005. Winning the Battle Against Global Climate Change. European Parliament.

European Parliament. 2008. Emission performance standards for new passenger cars: Resolution 17 December, 2008. European Parliament.

Facchinei, F., J.-S. Pang. 2003. *Finite-dimensional variational inequalities and complementarity problems*. New York, Springer.

Ferris, M. C., T. S. Munson. 2000. Complementarity problems in GAMS and the PATH solver. *Journal of Economic Dynamics & Control.* **24**(2) 165-188.

Ferris, M. C., J. S. Pang. 1997. Engineering and economic applications of complementarity problems. *Siam Review.* **39**(4) 669-713.

Fischer, C., W. Harrington, I. W. H. Parry. 2007. Should automobile fuel economy standards be tightened? *Energy Journal.* **28**(4) 1-29.

Frank, A. A. 2007. Plug-in hybrid vehicles for a sustainable future. *American Scientist.* **95**(2) 158-165.

Friedman, J. W. 1986. *Game theory with applications to economics*. New York, Oxford University Press.

Fudenberg, D., J. Tirole. 1991. *Game theory*. Cambridge, Mass., MIT Press.

US Government Accountability Office. 1990. *The Inflation Adjustment Act codified at 28 U.S.C. 2461 note amended in 1996 (Pub. L. 104-134, Sec. 31001, 110 Stat. 1321-373).*

GAO. 2007. Reforming fuel economy standards could help reduce oil consumption by cars and light trucks, and other options could complement these standards. US Government Accountability Office,. http://www.gao.gov/new.items/d07921.pdf

Gerard, D., L. Lave. 2003. The economics of CAFE reconsidered: a response to CAFE critics and a case for fuel economy standards. AEI-Brookings Joint Center.

Gerard, D., L. Lave. 2004. CAFE Increases: Missing the Elephant in the Living Room. AEI-Brookings Joint Center.

gm-volt.com. 2009. Latest Chevy Volt battery pack and generator details and clarifications. DOI:

Godek, P. E. 1997. The Regulation of Fuel Economy and the Demand for "Light Trucks" *Journal of Law and Economics.* **40**(2) 495-509.

Goldberg, P. K. 1995. Product Differentiation and Oligopoly in International Markets - the Case of the United-States Automobile-Industry. *Econometrica.* **63**(4) 891-951.

Goldberg, P. K. 1998. The effects of the Corporate Average Fuel Efficiency Standards in the US. *Journal of Industrial Economics.* **46**(1) 1-33.

Gonder, J., T. Markel, A. Simpson, M. Thornton. 2007. Using GPS travel data to assess the real world driving energy use of PHEVs. *Transportation Research Board Annual Meeting*. Washington, D.C.

Greene, D. L., J. DeCicco. 2000. Engineering-economic analyses of automotive fuel economy potential in the United States. *Annual Review of Energy and the Environment.* **25** 477-535.

Greene, D. L., J. L. Hopson. 2003. An Analysis of Alternative Forms of Automotive Fuel Economy Standards for the United States. *Transportation Research Record.* **1842** 20-28.

Greene, W. H. 2003. *Econometric analysis*. Upper Saddle River, N.J., Prentice Hall.

Gupta, S., R. Loulou. 1998. Process innovation, product differentiation, and channel structure: Strategic incentives in a duopoly. *Marketing Science.* **17**(4) 301-316.

Hammar, H., A. Lofgren, T. Sterner. 2004. Political economy obstacles to fuel taxation. *Energy Journal.* **25**(3) 1-17.

Hanson, W., K. Martin. 1996. Optimizing multinomial logit profit functions. *Management Science.* **42**(7) 992-1003.

Harker, P. T. 1984. A Variational Inequality Approach for the Determination of Oligopolistic Market Equilibrium. *Mathematical Programming.* **30**(1) 105-111.

Harker, P. T., S. C. Choi. 1991. A Penalty-Function Approach for Mathematical Programs with Variational Inequality Constraints. *Information and Decision Technologies.* **17**(1) 41-50.

Horsky, D., P. Nelson. 1992. New Brand Positioning and Pricing in an Oligopolistic Market. *Marketing Science.* **11**(2) 133-153.

Inderwildi, O., C. Carey, G. Santos, X. Yan, H. Behrendt, A. Holdway, L. Maconi, N. Owen, T. Shirvani, A. Teytelboym. 2010. Future of Mobility Roadmap: Ways to Reduce Emissions While Keeping Mobile. Smith School of Enterprise and the Environment, University of Oxford.

Ingene, C. A., M. E. Parry. 2004. *Mathematical models of distribution channels*. New York, Kluwer Academic Publishers.

IPCC. 2001. *Climate Change 2001: The Scientific Basis: Contribution of Working Group I to the Third Assessment Report of the Intergovernmental Panel on Climate Change*. New York, Cambridge University Press.

Jacobsen, M. R. 2008. Evaluating U.S. Fuel Economy Standards in a Model with Producer and Household Heterogeneity. San Diego, CA, University of California.

Jeuland, A. P., S. M. Shugan. 1983. Managing Channel Profits. *Marketing Science.* **2**(3) 239-272.

Kalhammer, F. R., B. M. Kopf, D. H. Swan, V. P. Roan, M. P. Walsh. 2007. Status and Prospects for Zero Emissions Vehicle Technology. http://www.arb.ca.gov/msprog/zevprog/zevreview/zev_panel_report.pdf

Kammen, D. M., D. Lemoine, S. M. Arons, H. Hummel. 2008. Evaluating the Cost-Effectiveness of Greenhouse Gas Emission Reductions from Deploying Plug-in Hybrid Electric Vehicles. Brookings-Google Plug-in Hybrid Summit.

Karden, E., S. Ploumen, B. Fricke, T. Miller, K. Snyder. 2007. Energy storage devices for future hybrid electric vehicles. *Journal of Power Sources.* **168**(1) 2-11.

Kelly, K. J., M. Mihalic, M. Zolot. 2002. Battery Usage and Thermal Performance of the Toyota Prius and Honda Insight for Various Chassis Dynamometer Test Procedures. *17th Annual Battery Conference on Applications and Advances*. Long Beach, California.

Kleit, A. N. 1990. The Effect of Annual Changes in Automobile Fuel-Economy Standards. *Journal of Regulatory Economics.* **2**(2) 151-172.

Kleit, A. N. 2004. Impacts of long-range increases in the fuel economy (CAFE) standard. *Economic Inquiry.* **42**(2) 279-294.

Kolstad, C. 2000. *Environmental Economics*. New York, Oxford University Press.

Konnov, I. 2007. *Equilibrium models and variational inequalities*. Amsterdam ; Boston, Elsevier.

Kromer, M. A., J. B. Heywood. 2009. A comparative assessment of electric propulsion systems in the 2030 US light-duty vehicle fleet. *SAE International Journal of Engines.* **1**(1) 372-391.

Kwoka, J. E., Jr. 1983. The Limits of Market-Oriented Regulatory Techniques: The Case of Automotive Fuel Economy. *The Quarterly Journal of Economics.* **97** 695-704.

Kyoto Protocol. 1997. Kyoto Protocol to the United Nations Framework Convention on Climate Change. Kyoto Protocol.

Labbe, M., P. Marcotte, G. Savard. 1998. A bilevel model of taxation and its application to optimal highway pricing. *Management Science.* **44**(12) 1608-1622.

Lave, L., H. Maclean, C. Hendrickson, R. Lankey. 2000. Life-cycle analysis of alternative automobile fuel/propulsion technologies. *Environmental Science & Technology.* **34**(17) 3598-3605.

Lee, E., R. Staelin. 1997. Vertical strategic interaction: Implications for channel pricing strategy. *Marketing Science.* **16**(3) 185-207.

Lemoine, D. M. 2008. Valuing Plug-In Hybrid Electric Vehicles Battery Capacity using a Real Options Framework. University of California, Berkeley.

Lemoine, D. M., D. M. Kammen, A. E. Farrell. 2008. An innovation and policy agenda for commercially competitive plug-in hybrid electric vehicles. *Environmental Research Letters.* **3** 014003.

Lesser, J. A., D. Dodds, R. O. Zerbe. 1997. *Environmental economics and policy*. Reading, Mass., Addison-Wesley.

Lewis, K., W. Chen, L. Schmidt. 2006. *Decision Making in Engineering Design*. New York, ASME Press.

Lewis, K., F. Mistree. 1998. Collaborative, sequential, and isolated decisions in design. *Journal of Mechanical Design.* **120**(4) 643-652.

Li, H., S. Azarm. 2000. Product design selection under uncertainty and with competitive advantage. *Journal of Mechanical Design.* **122**(4) 411-418.

Lipman, T. E., M. A. Delucchi. 2006. A retail and lifecycle cost analysis of hybrid electric vehicles. *Transportation Research Part D-Transport and Environment.* **11**(2) 115-132.

Lou, Z. Q., J. S. Pang, D. Ralph. 1996. *Mathematical Programs with Equilibrium Constraints*. New York, Cambridge University Press.

Luo, L., P. K. Kannan, B. Besharati, S. Azarm. 2005. Design of robust new products under variability: Marketing meets design. *Journal of Product Innovation Management.* **22**(2) 177-192.

Luo, L., P. K. Kannan, B. T. Ratchford. 2007. New Product Development under Channel Acceptance. *Marketing Science.* **26**(2) 149-163.

MacLean, H. L., L. B. Lave. 2003. Evaluating automobile fuel/propulsion system technologies. *Progress in Energy and Combustion Science.* **29**(1) 1-69.

Markel, T., A. Brooker, J. Gonder, M. O'Keefe, A. Simpson, M. Thornton. 2006. Plug-In Hybrid Vehicle Analysis. National Renewable Energy Laboratory.

Markel, T., A. Simpson. 2006. Plug-In Hybrid Electric Vehicle Energy Storage System Design. *Advanced Automotive Battery Conference*. Baltimore, Maryland.

Mas-Colell, A., M. D. Whinston, J. R. Green. 1995. *Microeconomic Theory*, Oxford University Press.

Maynard, M. 2007. Toyota to Increase Imports to Meet Demand for Prius. *The New York Times*.

Mazzeo, M. J. 2002. Product choice and oligopoly market structure. *Rand Journal of Economics.* **33**(2) 221-242.

McFadden, D., K. Train. 2000. Mixed MNL Models of Discrete Response. *Journal of Applied Econometrics.* **15**(5) 447-470.

McGuire, T. W., R. Staelin. 1983. An Industry Equilibrium Analysis of Downstream Vertical Integration. *Marketing Science.* **2**(2) 161-191.

Michalek, J. J. 2005. Preference Coordination in Engineering Design Decision-Making. Ann Arbor, MI., PhD Dissertation, University of Michigan.

Michalek, J. J. 2008. Design for market systems: Integrating social, economic, and physical sciences to engineer product success. *Mechanical Engineering: The Magazine of ASME*. **130** 32-36.

Michalek, J. J., O. Ceryan, P. Y. Papalambros, Y. Koren. 2006. Balancing Marketing and Manufacturing Objectives in Product Line Design. *ASME Journal of Mechanical Design.* **128**(6) 1196-1204.

Michalek, J. J., F. M. Feinberg, P. Y. Papalambros. 2005. Linking marketing and engineering product design decisions via analytical target cascading. *Journal of Product Innovation Management.* **22**(1) 42-62.

Michalek, J. J., P. Y. Papalambros, S. J. Skerlos. 2004. A study of fuel efficiency and emission policy impact on optimal vehicle design decisions. *ASME Journal of Mechanical Design.* **126**(6) 1062-1070.

Moawad, A., G. Singh, S. Hagspiel, M. Fellah, A. Rousseau. 2009. Impact of Real World Drive Cycles on PHEV Fuel Efficiency and Cost for Different Powertrain and Battery Characteristics. *The 24th International Electric Vehicle Symposium and Exposition (EVS-24)*. Stavanger, Norway.

Morrow, W. R., S. J. Skerlos. 2009. Fixed-Point Approaches to Computing Bertrand-Nash Equilibrium Prices Under Mixed Logit Demand. *Operations Research, in review.*

Nagurney, A. 1993. *Network Economics: A Variational Inequality Approach*. Boston, MA., Kluwer Academic Publishers.

Naughton, K. 2008, July 02, 2008 Assaulted Batteries. *Newsweek*, http://www.newsweek.com/id/138808.

Nevo, A. 2000. A practitioner's guide to estimation of random-coefficients logit models of demand. *Journal of Economics & Management Strategy.* **9**(4) 513-548.

U.S. Department of Transportation. 2006. *Code of Federal Regulations, Title 49, Chapter 329: Automotive Fuel Economy*.

U.S. Department of Transportation. 2006. *Code of Federal Regulations. Title 49, Part 571: Federal Motor Vehicle Safety Standards*.

NHTSA. 2008. Average Fuel Economy Standards Passenger Cars and Light Trucks Model Years 2011-2015. National Highway Traffic Safety Administration.

NHTSA. 2009. Average Fuel Economy Standards Passenger Cars and Light Trucks Model Year 2011: Final Rule. National Highway Traffic Safety Administration.

NHTSA. 2009. Summary of CAFE Fines Collected (Updated Jan. 2009). U.S. Department of Transportation, National Highway Traffic Safety Administration.

NRC. 2009. Hidden Costs of Energy: Unpriced Consequences of Energy Production and Use. National Research Council.

Orsborn, S., J. Cagan, P. Boatwright. 2009. Quantifying Aesthetic Form Preference in a Utility Function. *Journal of Mechanical Design.* **131**(6) -.

Papalambros, P. Y., D. J. Wilde. 2000. *Principles of Optimal Design: Modeling and Computation*. New York, Cambridge University Press.

Pesaran, A., T. Markel, H. Tataria, D. Howell. 2007. Battery requirements for plug-in hybrid electric vehicles - Analysis and Rationale. *The 23th International Electric Vehicle Symposium*. Anaheim, CA.

Peterson, S. B. 2009. Pittsburgh, PA, Carnegie Mellon University, Department of Engineering and Public Policy.

Peterson, S. B., J. Apt, J. F. Whitacre. 2010. Lithium-ion battery cell degradation resulting from realistic vehicle and vehicle-to-grid utilization. *Journal of Power Sources.* **195**(8) 2385–2392.

Peterson, S. B., J. F. Whitacre, J. Apt. 2010. The economics of using plug-in hybrid electric vehicle battery packs for grid storage. *Journal of Power Sources.* **195**(8) 2377-2384.

Petrin, A. 2002. Quantifying the benefits of new products: The case of the minivan. *Journal of Political Economy.* **110**(4) 705-729.

Plassmann, H., J. O'Doherty, B. Shiv, A. Rangel. 2008. Marketing actions can modulate neural representations of experienced pleasantness. *Proceedings of the National Academy of Sciences of the United States of America.* **105**(3) 1050-1054.

Porter, R. 1999. *Economics at the Wheel: The Costs of Cars and Drivers*, Academic Press.

Ralph, D., S. J. Wright. 2004. Some properties of regularization and penalization schemes for MPECs. *Optimization Methods & Software.* **19**(5) 527-556.

Reynolds, C., M. Kandlikar. 2007. How hybrid-electric vehicles are different from conventional vehicles: the effect of weight and power on fuel consumption. *Environmental Research Letters.* **2**(1) 014003.

Rhim, H., L. G. Cooper. 2005. Assessing potential threats to incumbent brands: New product positioning under price competition in a multisegmented market. *International Journal of Research in Marketing.* **22**(2) 159-182.

Romm, J. 2006. The car and fuel of the future. *Energy Policy.* **34**(17) 2609-2614.

Samaras, C., K. Meisterling. 2008. Life cycle assessment of greenhouse gas emissions from plug-in hybrid vehicles: Implications for policy. *Environmental Science & Technology.* **42**(9) 3170-3176.

Scaparra, M. P., R. L. Church. 2008. A bilevel mixed-integer program for critical infrastructure protection planning. *Computers & Operations Research.* **35**(6) 1905-1923.

Scheel, H., S. Scholtes. 2000. Mathematical programs with complementarity constraints: Stationarity, optimality, and sensitivity. *Mathematics of Operations Research.* **25**(1) 1-22.

Scott, M. J., M. Kintner-Meyer, D. B. Elliott, W. M. Warwick. 2007. Impacts assessment of plug-in hybrid vehicles on electric utilities and regional U.S. power grids, Part 2: Economic assessment, Pacific Northwest National Laboratory.

Shiau, C.-S., J. J. Michalek. 2007. A game-theoretic approach to finding market equilibria for automotive design under environmental regulation. *ASME International Design Engineering Technical Conferences*. Las Vegas, NV.

Shiau, C.-S. N., N. Kaushal, S. B. Peterson, J. J. Michalek. 2010. Optimal plug-in hybrid electric vehicle design and allocation for minimum net cost, petroleum consumption and greenhouse gas emissions. *ASME Journal of Mechanical Design.* In review.

Shiau, C.-S. N., C. Samaras, R. Hauffe, J. J. Michalek. 2009. Impact of battery weight and charging patterns on the economic and environmental benefits of plug-in hybrid vehicles. *Energy Policy.* **37**(7) 2653-2663.

Shiau, C. S. N., J. J. Michalek. 2009. Optimal product design under price competition. *ASME Journal of Mechanical Design.* **131**(7) 071003.

Shiau, C. S. N., J. J. Michalek. 2009. Should designers worry about market systems? *ASME Journal of Mechanical Design.* **131**(1) 011011.

Shiau, C. S. N., J. J. Michalek, C. T. Hendrickson. 2009. A structural analysis of vehicle design responses to Corporate Average Fuel Economy policy. *Transportation Research Part A: Policy and Practice.* **43**(9-10) 814-828.

Simpson, A. 2006. Cost-benefit analysis of plug-in hybrid electric vehicle technology. *The 22nd International Electric Vehicle Symposium*. Yokohama, Japan.

Sioshansi, R., P. Denholm. 2009. Emissions Impacts and Benefits of Plug-In Hybrid Electric Vehicles and Vehicle-to-Grid Services. *Environmental Science & Technology*. **43**(4) 1199-1204.

Small, K. A., K. Van Dender. 2007. Fuel efficiency and motor vehicle travel: The declining rebound effect. *Energy Journal.* **28**(1) 25-51.

Stock, J. H., J. H. Wright, M. Yogo. 2002. A survey of weak instruments and weak identification in generalized method of moments. *Journal of Business & Economic Statistics.* **20**(4) 518-529.

Stockman, A. C. 1996. *Introduction to microeconomics*. Fort Worth, Dryden Press.

Sudhir, K. 2001. Competitive pricing behavior in the auto market: A structural analysis. *Marketing Science.* **20**(1) 42-60.

Sudhir, K. 2001. Structural analysis of manufacturer pricing in the presence of a strategic retailer. *Marketing Science.* **20**(3) 244-264.

Tawarmalani, M., N. V. Sahinidis. 2004. Global optimization of mixed-integer nonlinear programs: A theoretical and computational study. *Mathematical Programming.* **99**(3) 563-591.

The While House. 2009. President Obama Announces National Fuel Efficiency Policy. Washington, DC.

Tirole, J. 1988. *The theory of industrial organization*. Cambridge, Mass., MIT Press.

Toyota. 2009. 2010 Prius Plug-in Hybrid Makes North American Debut at Los Angeles Auto Show. DOI:

Train, K. E. 1980. A structured logit model of auto ownership and mode choice. *Review of Economic Studies.* **47**(2) 357-370.

Train, K. E. 2003. *Discrete Choice Methods with Simulation*. New York, Cambridge University Press.

Train, K. E., C. Winston. 2007. Vehicle choice behavior and the declining market share of US automakers. *International Economic Review.* **48**(4) 1469-1496.

Ullman, D. G. 1992. *The Mechanical Design Process*. New York, McGraw-Hill.

Uri, N. D., R. Boyd. 1989. The potential benefits and costs of an increase in US gasoline tax. *Energy Policy.* **17**(4) 356-369.

US Bureau of Labor Statistics. 2010, Inflation calcualtor. http://www.bls.gov/data/inflation_calculator.htm.

1975. *Energy Policy and Conservation Act of 1975*.

2007. *Energy Independence and Security Act of 2007*.

2008. *American Recovery and Reinvestment Act of 2009*.

USABC. 2008. Plug-in HEV Battery Goals, United States Council for Automotive Research.

Viswanathan, J., I. E. Grossmann. 1990. A Combined Penalty-Function and Outer-Approximation Method for Minlp Optimization. *Computers & Chemical Engineering*. **14**(7) 769-782.

Vlasic, B. 2008. As Gas Costs Soar, Buyers Flock to Small Cars. *The New York Times*.

Wang, M., Y. Wu, A. Elgowainy. 2007. GREET 1.7 fuel-cycle model for transportation fuels and vehicle technologies. Argonne National Laboratory.

Wassenaar, H. J., W. Chen. 2003. An approach to decision-based design with discrete choice analysis for demand modeling. *Journal of Mechanical Design.* **125**(3) 490-497.

Wassenaar, H. J., W. Chen, J. Cheng, A. Sudjianto. 2005. Enhancing discrete choice demand modeling for decision-based design. *Journal of Mechanical Design.* **127**(4) 514-523.

Weber, C. L., P. Jaramillo, J. Marriott, C. Samaras. 2010. Life Cycle Assessment and Grid Electricity: What Do We Know and What Can We Know? *Environmental Science and Technology*. **44**(6) 1895–1901

Whitacre, J. F. 2009. The economics and science of materials for lithium ion batteries and PEM fuel cells. *Science, in review.*

Williams, N., S. Azarm, P. K. Kannan. 2008. Engineering product design optimization for retail channel acceptance. *ASME Journal of Mechanical Design.* **130**(6) 061401-10.

Ye, J. J., D. L. Zhu, Q. J. Zhu. 1997. Exact penalization and necessary optimality conditions for generalized bilevel programming problems. *Siam Journal on Optimization.* **7**(2) 481-507.

Yun, J. M. 2002. Offsetting behavior effects of the corporate average fuel economy standards. *Economic Inquiry.* **40**(2) 260-270.

Zervas, E., C. Lazarou. 2008. Influence of European passenger cars weight to exhaust CO2 emissions. *Energy Policy*. **36**(1) 248-257.

APPENDIX A. LAGRANGIAN FOC METHOD

This appendix presents a solution approach using general NLP solvers to find Nash equilibria in oligopolistic competition problems. We call this approach Lagrangian FOC method since it is a combination of FOC equilibrium equation and Lagrange formulation. This method is used in solving the market competition problems in Chapter 2, 3 and 6.

Several approaches to compute Nash equilibrium can be found in the literature, including the relaxation methods (Harker, 1984; Nagurney, 1993), the projection method (Nagurney, 1993), the nonlinear complementarity problem (NCP) approach (Facchinei and Pang, 2003), the combined-gradient fixed-point method (Morrow and Skerlos, 2009), and the ordinary FOC method (Friedman, 1986). The relaxation methods, which are developed based on the variational inequality theory, can be divided into relaxation parallel and relaxation serial approaches. The former formulates each firm's optimization with competitors' best responses concurrently (in parallel within each round) (Harker, 1984; Choi et al., 1990; Nagurney, 1993), and the latter models that each firm is optimized in turn while holding all other firms fixed and the process is repeated sequentially over all firms until convergence (in sequential rounds) (Nagurney, 1993; Michalek et al., 2004). The relaxation methods are straightforward and easy to be programmed (merely adding external loop to single optimization), but it can be computationally expensive, especially when the number of firms' in the game is large or each sub-optimization task is complex. The method may fail to converge, which is demonstrated in the weight scale case study in Chapter 2. The projection method, another variational inequality based approach, does not require an internal optimization loop and is computationally efficient, but it may not always converge (Konnov, 2007). The NCP method is a powerful tool to solve equilibrium problems (Ferris and Pang, 1997). However, it requires specialized solver and complementarity reformulation (Ferris and Munson, 2000), which can be an issue for designers who are not familiar with complementarity conditions to implement. The fixed-point iteration method also requires derivations for the specific fixed-point equations (Morrow and Skerlos, 2009). The characteristics of these solution approaches are summarized in Table A.1.

We select the FOC method as our primary Nash price solution tool for several reasons. First, its solution process does not require iterative optimization loops. Second, the method only requires first-order derivatives of the profit function with respect to the decision variables, and no further reformulation is needed. FOC equations can be derived analytically or obtained by numerical differentiation. Third, the system of FOC equations can be solved by general-purpose NLP algorithms, and no special solver is required.

Table A.1 Numerical approaches to computing Nash equilibrium

Solution approach	FOC information	Solver	External iteration loop
Relaxation parallel	Optional	NLP solver	Yes
Relaxation series	Optional	NLP solver	Yes
Projection method	Required	None	None
Fixed-point iteration	Required	None	None
Nonlinear complementarity problem	Required	NCP solver	None
Lagrangian FOC method	**Required**	**NLP solver**	**None**

The fundamental concept of Lagrangian FOC method is necessary condition of Nash equilibrium. The mathematical expression of Nash equilibrium is given by (Fudenberg and Tirole, 1991):

$$\Pi_k\left(\mathbf{x}_1^*,\ldots,\mathbf{x}_j^*,\ldots,\mathbf{x}_J^*\right)\geq\Pi_k\left(\mathbf{x}_1^*,\ldots,\mathbf{x}_j,\ldots,\mathbf{x}_J^*\right)\quad\forall j\in J_k,\ \forall k\in K \tag{A.1}$$

$\mathbf{x}_j$ is the design variables of product j of firm k and the * denotes the decisions at Nash equilibrium. This formulation states that no unilateral change to a single firm's design decision can result in higher profit for that firm than its Nash decisions, or, alternatively, each firm is responding optimally to the decisions of the others. Assuming no variable bounds and other constraints, the FOC formulation for profit maximization with respect to decision variables $\mathbf{x}$ can be expressed as (Friedman, 1986):

$$\begin{aligned}&\text{Find }\mathbf{X}^*\text{ such that }\frac{\partial\Pi_k}{\partial\mathbf{x}_k}=0;\ \forall k\\&\text{where }\mathbf{X}^*=[\mathbf{x}_1^*\cdots\mathbf{x}_k^*\cdots\mathbf{x}_K^*]\end{aligned} \tag{A.2}$$

where Π_k is the profit of firm k, $\mathbf{x}_k$ is the variable vector of product k and $\mathbf{X}$ is variable vector of all K firms. When equation constraints $\mathbf{h}(\mathbf{x}_k)=\mathbf{0}$ and inequality constraints $\mathbf{g}(\mathbf{x}_k)\leq\mathbf{0}$ are given in the model, the Lagrange function L for each firm k becomes

$$L_k=\Pi_k-\boldsymbol{\lambda}_k^T\mathbf{h}\left(\mathbf{x}_k\right)-\boldsymbol{\mu}_k^T\mathbf{g}\left(\mathbf{x}_k\right) \tag{A.3}$$

where $\boldsymbol{\lambda}_k$ and $\boldsymbol{\mu}_k$ are the vectors of Lagrange multipliers for $\mathbf{h}$ and $\mathbf{g}$, respectively. The first-order necessary Karush-Kuhn-Tucker (KKT) conditions for a Nash equilibrium in a general constrained formulation can be expressed in Lagrangian formulation as a set of system equations with inequality conditions (Papalambros and Wilde, 2000):

$$\begin{aligned}
&\nabla_{\mathbf{x}_k} L_k = \nabla_{\mathbf{x}_k} \Pi_k - \boldsymbol{\lambda}_k{}^T \nabla_{\mathbf{x}_k} \mathbf{h}(\mathbf{x}_k) - \boldsymbol{\mu}_k{}^T \nabla_{\mathbf{x}_k} \mathbf{g}(\mathbf{x}_k) = \mathbf{0} \\
&\boldsymbol{\mu}_k{}^T \mathbf{g}(\mathbf{x}_k) = 0; \quad \boldsymbol{\mu}_k \geq \mathbf{0}; \\
&\mathbf{h}(\mathbf{x}_k) = \mathbf{0}; \quad \mathbf{g}(\mathbf{x}_k) \leq \mathbf{0}; \quad \forall k
\end{aligned} \tag{A.4}$$

The above formulation is a general NLP form with a dummy objective. The solutions found by Eq. (A.4) satisfy the Nash necessary conditions but may not fulfill sufficient conditions. If the profit function is concave with respect to price, the first-order conditions are sufficient (Friedman, 1986). For a non-cooperative game with complete information, a Nash equilibrium exists if: (1) strategy set is nonempty, compact and convex for each player; (2) payoff function is defined, continuous and bounded; and (3) each individual payoff function is concave with respect to individual strategy (Friedman, 1986). Specifically, Anderson et al. (1992) proved that there exists a unique price equilibrium under logit demand when the profit function is strictly quasi-concave. However, in the case of nonconcavity, the solutions found by the proposed method must be verified using the Nash equilibrium definition (Eq. (A.1)) post hoc.

APPENDIX B. EQUATIONS FOR EQUILIBRIUM NECESSARY CONDITIONS

This appendix provides the detailed derivations for the Nash equilibrium FOC equations under different logit demand model forms, including ideal point logit model (Section B.1), latent class model with multiple market segments (Section B.2), and mixed logit model (Section B.3). For the mixed logit FOC equations in Section B.3 are derived with respect to design variables, wholesale price and retail margin for the channel structure study in Chapter 3 specifically. In Section B.4, the discrete conditions of the mixed logit FOC equations are prepared for the CAFE policy study in Chapter 6.

B.1 FOC Equations with Ideal Point Logit Model

The utility function of an ideal-point logit model is given by

$$v_{ij} = -\left(\sum_{n=1}^{N} \beta_i \left(z_{nj} - \theta_{in} \right)^2 + \overline{\beta}_i p_j + b_i \right) \quad \forall i, j \tag{B.1}$$

where z_{nj} is the value of product attribute n on product j, θ_{in} is consumer i's desired value for attribute n, β_i is consumer i's sensitivity of utility to deviation from the ideal point, $\overline{\beta}_i$ is consumer i's sensitivity of utility to price, and b_i is a constant utility term estimated from consumer i. The first-order derivatives of utility function with respect to price p_j and product attribute z_{nj} are:

$$\frac{\partial v_{ij}}{\partial p_j} = -\overline{\beta}_i; \quad \frac{\partial v_{ij}}{\partial z_{nj}} = -2\beta_i \left(z_{nj} - \theta_{in} \right) \tag{B.2}$$

The first-order derivative of logit choice probability with respect to price and design are

$$\frac{\partial s_{ij}}{\partial p_j} = \left(\chi \frac{\partial v_{ij}}{\partial p_j} \right) s_{ij} - s_{ij} \left(\chi \frac{\partial v_{ij}}{\partial p_j} \right) s_{ij} = -\chi \overline{\beta}_i s_{ij} \left(1 - s_{ij} \right) \tag{B.3}$$

$$\frac{\partial s_{ij}}{\partial z_{nj}} = \left(\chi \frac{\partial v_{ij}}{\partial z_{nj}} \right) s_{ij} - s_{ij} \left(\chi \frac{\partial v_{ij}}{\partial z_{nj}} \right) s_{ij} = -2 \chi \beta_i \left(z_{nj} - \theta_{in} \right) s_{ij} \left(1 - s_{ij} \right) \tag{B.4}$$

Therefore the FOC equation for profit maximization with respect to price p_j is

$$\begin{aligned} \frac{\partial \Pi_k}{\partial p_j} &= \frac{Q}{I} \sum_{i=1}^{I} \frac{\partial s_{ij}}{\partial p_j} \left(p_j - c_j \right) + s_{ij} \\ &= \frac{Q}{I} \sum_{i=1}^{I} s_{ij} \left[-\chi \overline{\beta}_i \left(1 - s_{ij} \right) \left(p_j - c_j \right) + 1 \right] \end{aligned} \tag{B.5}$$

Thus,

$$\frac{\partial \Pi_k}{\partial p_j} = \sum_{i=1}^{I} s_{ij} \left[1 - \chi \overline{\beta}_i \left(1 - s_{ij} \right) \left(p_j - c_j \right) \right] = 0 \quad \forall j \in J_k, k \in K \tag{B.6}$$

Similarly, the FOC equation with respect to design attribute z_{nj} is:

$$\begin{aligned} \frac{\partial \Pi_k}{\partial z_{nj}} &= \frac{Q}{I} \sum_{i=1}^{I} \frac{\partial s_{ij}}{\partial z_{nj}} \left(p_j - c_j \right) - s_{ij} \frac{\partial c_j}{\partial z_{nj}} \\ &= -\frac{Q}{I} \sum_{i=1}^{I} s_{ij} \left[2 \chi \beta_i \left(z_{nj} - \theta_{in} \right) \left(1 - s_{ij} \right) \left(p_j - c_j \right) + \frac{\partial c_j}{\partial z_{nj}} \right] = 0 \\ & \forall j \in J_k, k \in K \end{aligned} \tag{B.7}$$

B.2 FOC Equations with Latent Class Model

We derive the following equations for the general latent class model with multiple market segments. Logit model (one market without segmentation) can be considered as a special case of the general latent class model. We consider that each firm k has one specific brand-product $j \in J_k$. The share of choices for the product j in segment m is

$$s_{mj} = \frac{\exp\left(v_{mj}\right)}{\exp\left(v_{m0}\right) + \sum_{j \in J_k} \exp\left(v_{mj}\right)} \tag{B.8}$$

The first-order derivative of choice probability with respect to price for each segment is

$$\begin{aligned}
\frac{\partial s_{mj}}{\partial p_j} &= \frac{\partial v_{mj}}{\partial p_j} s_{mj}\left(1 - s_{mj}\right) \\
\frac{\partial s_{mj}}{\partial \mathbf{z}_j} &= \frac{\partial v_{mj}}{\partial \mathbf{z}_j} s_{mj}\left(1 - s_{mj}\right) \\
\frac{\partial s_{mj}}{\partial \mathbf{x}_j} &= \frac{\partial v_{mj}}{\partial \mathbf{z}_j} \frac{\partial \mathbf{z}_j}{\partial \mathbf{x}_j} s_{mj}\left(1 - s_{mj}\right)
\end{aligned} \tag{B.9}$$

The profit function of product *j* is

$$\Pi_j = \left(\sum_{m=1}^{M} Q_m s_{mj} \left(p_j - c_j \right) \right) - c_j^{\mathrm{F}} \tag{B.10}$$

The first-order condition equation is

$$\frac{\partial \Pi_j}{\partial p_j} = \left[\sum_{m=1}^{M} Q_m \frac{\partial s_{mj}}{\partial p_j} \left(p_j - c_j \right) + s_{mj} \right] \tag{B.11}$$

$$\frac{\partial \Pi_j}{\partial \mathbf{x}_j} = \sum_{m=1}^{M} Q_m \frac{\partial s_{mj}}{\partial \mathbf{z}_j} \frac{\partial \mathbf{z}_j}{\partial \mathbf{x}_j} \left(p_j - c_j \right) \tag{B.12}$$

Therefore, the necessary conditions for Nash equilibrium are

$$\begin{aligned}
\frac{\partial \Pi_j}{\partial p_j} &= \left[\sum_{m=1}^{M} Q_m \frac{\partial s_{mj}}{\partial p_j} \left(p_j - c_j \right) + s_{mj} \right] \\
&= \sum_{m=1}^{M} Q_m s_{mj} \left[\frac{\partial v_{mj}}{\partial p_j} \left(1 - s_{mj}\right)\left(p_j - c_j \right) + 1 \right] = 0
\end{aligned} \tag{B.13}$$

$$
\begin{aligned}
\frac{\partial \Pi_j}{\partial \mathbf{x}_j} &= \sum_{m=1}^{M} Q_m \frac{\partial s_{mj}}{\partial \mathbf{z}_j} \frac{\partial \mathbf{z}_j}{\partial \mathbf{x}_j} \left(p_j - c_j \right) \\
&= \sum_{m=1}^{M} Q_m \frac{\partial v_{mj}}{\partial \mathbf{z}_j} \frac{\partial \mathbf{z}_j}{\partial \mathbf{x}_j} s_j \left(1_j - s_j \right) \left(p_j - c_j \right) = \mathbf{0}
\end{aligned} \tag{B.14}
$$

For the weight scale problem, the utility in each segment is fit with fourth order polynomial:

$$
\begin{aligned}
\bar{\psi}_{mj} &= \bar{a}_{4m} p_j^4 + \bar{a}_{3m} p_j^3 + \bar{a}_{2m} p_j^2 + \bar{a}_{1m} p_j + \bar{a}_{0m} \\
\psi_{nmj} &= a_{4mn} z_{nj}^4 + a_{3mn} z_{nj}^3 + a_{2mn} z_{nj}^2 + a_{1mn} z_{nj} + a_{0mn}
\end{aligned} \tag{B.15}
$$

Therefore, the equilibrium equation becomes

$$
\frac{\partial \Pi_j}{\partial p_j} = \sum_{m=1}^{M} Q_m s_{mj} \left[\left(4\bar{a}_{4m} p_j^3 + 3\bar{a}_{3m} p_j^2 + 2\bar{a}_{2m} p_j + \bar{a}_{1m} \right) \left(1 - s_{mj} \right) \left(p_j - c_j \right) + 1 \right] = 0 \tag{B.16}
$$

$$
\frac{\partial \Pi_j}{\partial \mathbf{x}_j} = \sum_{m=1}^{M} Q_m \left[\sum_{n=1}^{N} \left(4a_{4mn} z_{nj}^3 + 3a_{3mn} z_{nj}^2 + 2a_{2mn} z_{nj} + a_{1mn} \right) \frac{\partial z_{nj}}{\partial \mathbf{x}_j} \right] s_j \left(1_j - s_j \right) \left(p_j - c_j \right) = \mathbf{0} \tag{B.17}
$$

For the angle grinder problem in the third case study, the part-worth price utility is interpolated with quadratic function. Thus the first-order condition for price decision is given by

$$
\frac{\partial \Pi_j}{\partial p_j} = \sum_{m=1}^{M} Q_m s_{mj} \left[\left(2\bar{a}_{2m} p_j + \bar{a}_{1m} \right) \left(1 - s_{mj} \right) \left(p_j - c_j \right) + 1 \right] = 0 \tag{B.18}
$$

B.3 FOC Equations with Mixed Logit Model and Channel Structure

This appendix provides the derivation details of the FOC equations for manufacturer's wholesale price and design decisions, and retailer's margin decisions under multiple common retailers (MCR) scenario. The manufacturing profit function for manufacturer *k* in the MCR scenario is

$$\Pi_k^{\mathrm{M}} = \left[\sum_{t \in T} \sum_{j \in J_k} q_{jt} \left(w_{jt} - c_j \right) - c_j^{\mathrm{F}} \right] \tag{B.19}$$

And the profit function for retailer t in the MCR scenario is given by

$$\prod_t^{\mathrm{R}} = \sum_{k \in K} \sum_{j \in J_k} q_{jt} m_{jt} \tag{B.20}$$

Wholesale Price FOC Equation: From the manufacturer profit function, the total profit of manufacturer k is the sum of product $j \in J_k$ and all other products $j' \in \{J_k/j\}$:

$$\begin{aligned}
\Pi_k^{\mathrm{M}} &= \Pi_{jt}^{\mathrm{M}} + \sum_{\substack{t' \in T \\ t' \neq t}} \Pi_{jt'}^{\mathrm{M}} + \sum_{\substack{j' \in J_k \\ j' \neq j}} \sum_{\bar{t} \in T} \Pi_{j'\bar{t}}^{\mathrm{M}} \\
&= \left(q_{jt} \left(w_{jt} - c_{jt} \right) + \sum_{\substack{t' \in T \\ t' \neq t}} q_{jt'} \left(w_{jt'} - c_{jt'} \right) \right) - c_j^{\mathrm{F}} + \sum_{\substack{j' \in J_k \\ j' \neq j}} \left[\left(\sum_{\bar{t} \in T} q_{j'\bar{t}} \left(w_{j'\bar{t}} - c_{j'\bar{t}} \right) \right) - c_{j'}^{\mathrm{F}} \right] \\
&\forall t, k, j \in J_k
\end{aligned} \tag{B.21}$$

The reaction function of product price with respect to wholesale price is

$$\frac{\partial p_{jt}}{\partial w_{jt}} = \frac{\partial \left(w_{jt} + m_{jt} \right)}{\partial w_{jt}} = 1 + \frac{\partial w_{jt}}{\partial m_{jt}} = 1 \tag{B.22}$$

The marginal changes of market share with respect to wholesale price are

$$\begin{aligned}
\frac{\partial s_{ijt}}{\partial w_{jt}} &= \frac{\partial s_{ijt}}{\partial p_{jt}} \frac{\partial p_{jt}}{\partial w_{jt}} = \frac{\partial v_{ijt}}{\partial p_{jt}} s_{ijt} \left(1 - s_{ijt} \right) \\
\left. \frac{\partial s_{ijt'}}{\partial w_{jt}} \right|_{t' \neq t} &= \frac{\partial s_{ijt'}}{\partial p_{jt}} \frac{\partial p_{jt}}{\partial w_{jt}} = -\frac{\partial v_{ijt}}{\partial p_{jt}} s_{ijt} s_{ijt'} \\
\left. \frac{\partial s_{ij't}}{\partial w_{jt}} \right|_{j' \neq j} &= \frac{\partial s_{ij't}}{\partial p_{jt}} \frac{\partial p_{jt}}{\partial w_{jt}} = -\frac{\partial v_{ijt}}{\partial p_{jt}} s_{ijt} s_{ij't}
\end{aligned} \tag{B.23}$$

Take the derivative with respect to w_{jt}:

$$
\begin{aligned}
\frac{\partial \Pi_k^{\mathrm{M}}}{\partial w_{jt}} &= \frac{\partial \Pi_j^{\mathrm{M}}}{\partial w_{jt}} + \sum_{\substack{j' \in J_k \\ j' \neq j}} \frac{\partial \Pi_{j'}^{\mathrm{M}}}{\partial w_{jt}} \\
&= \left[\frac{\partial q_{jt}}{\partial w_{jt}} \left(w_{jt} - c_j \right) + q_{jt} \right] + \sum_{\substack{t' \in T \\ t' \neq t}} \left[\frac{\partial q_{jt'}}{\partial w_{jt}} \left(w_{jt'} - c_j \right) \right] + \sum_{\substack{j' \in J_k \\ j' \neq j}} \left[\sum_{t' \in T} \frac{\partial q_{j't'}}{\partial w_{jt}} \left(w_{j't'} - c_{j'} \right) \right] \\
&= Q \int_{\boldsymbol{\beta}} \left[\frac{\partial s_{jt|\boldsymbol{\beta}}}{\partial w_{jt}} \left(w_{jt} - c_j \right) + s_{jt|\boldsymbol{\beta}} \right] + \sum_{\substack{t' \in T \\ t' \neq t}} \left[\frac{\partial s_{jt'|\boldsymbol{\beta}}}{\partial w_{jt}} \left(w_{jt'} - c_j \right) \right] \\
&\qquad + \sum_{\substack{j' \in J_k \\ j' \neq j}} \left[\sum_{t' \in T} \frac{\partial s_{j't'|\boldsymbol{\beta}}}{\partial w_{jt}} \left(w_{j't'} - c_{j'} \right) \right] f_{\beta}(\boldsymbol{\beta}) d\boldsymbol{\beta} \\
&= Q \int_{\boldsymbol{\beta}} \left[\frac{\partial v_{jt|\boldsymbol{\beta}}}{\partial p_{jt}} s_{jt|\boldsymbol{\beta}} \left(1 - s_{jt} \right) \left(w_{jt} - c_j \right) + s_{jt|\boldsymbol{\beta}} \right] - Q \sum_{\substack{t' \in T \\ t' \neq t}} \left[\frac{\partial v_{jt|\boldsymbol{\beta}}}{\partial p_{jt}} s_{jt|\boldsymbol{\beta}} s_{jt'|\boldsymbol{\beta}} \left(w_{jt'} - c_j \right) \right] \\
&\qquad \sum_{\substack{j' \in J_k \\ j' \neq j}} \sum_{t' \in T} \left[\frac{\partial v_{jt|\boldsymbol{\beta}}}{\partial p_{jt}} s_{jt|\boldsymbol{\beta}} s_{j't'|\boldsymbol{\beta}} \left(w_{j't'} - c_{j'} \right) \right] f_{\beta}(\boldsymbol{\beta}) d\boldsymbol{\beta}
\end{aligned}
\tag{B.24}
$$

The above expression can be simplified as

$$
\frac{\partial \Pi_k^{\mathrm{M}}}{\partial w_{jt}} = \int_{\boldsymbol{\beta}} s_{jt|\boldsymbol{\beta}} \left[\frac{\partial v_{jt|\boldsymbol{\beta}}}{\partial p_{jt}} \left(\left(w_{jt} - c_j \right) - \sum_{j' \in J_k} \sum_{t' \in T} s_{j't'|\boldsymbol{\beta}} \left(w_{j't'} - c_{j'} \right) \right) + 1 \right] f_{\beta}(\boldsymbol{\beta}) d\boldsymbol{\beta} = 0 \tag{B.25}
$$

Design Variable FOC Equation: From the manufacturer profit function, the total profit of manufacturer k is the sum of product $j \in J_k$ and all other products $j' \in \{J_k/j\}$:

$$
\begin{aligned}
\Pi_k^{\mathrm{M}} &= \sum_{t \in T} \Pi_{jt}^{\mathrm{M}} + \sum_{\substack{j' \in J_k \\ j' \neq j}} \sum_{t \in T} \Pi_{j't}^{\mathrm{M}} \\
&= \left(\sum_{t \in T} q_{jt} \left(w_{jt} - c_j \right) \right) - c_j^{\mathrm{F}} + \sum_{\substack{j' \in J_k \\ j' \neq j}} \left[\left(\sum_{t \in T} q_{j't} \left(w_{j't} - c_{j'} \right) \right) - c_{j'}^{\mathrm{F}} \right] \\
&\forall t, k, j \in J_k
\end{aligned}
\tag{B.26}
$$

The marginal change in market share with respect to design variables are

$$\frac{\partial s_{ijt}}{\partial \mathbf{x}_j} = s_{ijt}\frac{\partial v_{ijt}}{\partial \mathbf{x}_j}\left(1-\sum_{\bar{t}\in T} s_{ij\bar{t}}\right)$$
$$\left.\frac{\partial s_{ij't}}{\partial \mathbf{x}_j}\right|_{j'\neq j} = -s_{ij't}\frac{\partial v_{ijt}}{\partial \mathbf{x}_j}\sum_{\bar{t}\in T} s_{ij\bar{t}} \tag{B.27}$$

Take the derivative of retailer profit with respect to $\mathbf{x}_j$:

$$\begin{aligned}
\frac{\partial \Pi_k^{\mathrm{M}}}{\partial \mathbf{x}_j} &= \sum_{t\in T}\left[\frac{\partial q_{jt}}{\partial \mathbf{x}_j}\left(w_{jt}-c_j\right)-q_{jt}\frac{\partial c_j}{\partial \mathbf{x}_j}\right]+\sum_{\substack{j'\in J_k\\ j'\neq j}}\sum_{t\in T}\left[\frac{\partial q_{j't}}{\partial \mathbf{x}_j}\left(w_{j't}-c_{j'}\right)-q_{j't}\frac{\partial c_{j'}}{\partial \mathbf{x}_j}\right]\\
&= Q\sum_{t\in T}\int_{\boldsymbol{\beta}}\left[s_{jt|\boldsymbol{\beta}}\frac{\partial v_{jt|\boldsymbol{\beta}}}{\partial \mathbf{x}_j}\left(1-\sum_{\bar{t}\in T} s_{j\bar{t}|\boldsymbol{\beta}}\right)(w_{jt}-c_j)-s_{jt|\boldsymbol{\beta}}\frac{\partial c_j}{\partial \mathbf{x}_j}\right] f_\beta(\boldsymbol{\beta})d\boldsymbol{\beta}\\
&\quad -Q\sum_{\substack{j'\in J_k\\ j'\neq j}}\sum_{t\in T}\int_{\boldsymbol{\beta}}\left[s_{j't|\boldsymbol{\beta}}\frac{\partial v_{jt|\boldsymbol{\beta}}}{\partial \mathbf{x}_j}\sum_{\bar{t}\in T} s_{j\bar{t}|\boldsymbol{\beta}}(w_{j't}-c_{j'})\right] f_\beta(\boldsymbol{\beta})d\boldsymbol{\beta}\\
&= Q\int_{\boldsymbol{\beta}}\sum_{t\in T} s_{jt|\boldsymbol{\beta}}\left[\frac{\partial v_{jt|\boldsymbol{\beta}}}{\partial \mathbf{x}_j}(w_{jt}-c_j)-\frac{\partial c_j}{\partial \mathbf{x}_j}\right]-\sum_{j'\in J_k}\sum_{t\in T} s_{j't|\boldsymbol{\beta}}\left[\frac{\partial v_{jt|\boldsymbol{\beta}}}{\partial \mathbf{x}_j}\left(\sum_{\bar{t}\in T} s_{j\bar{t}|\boldsymbol{\beta}}\right)(w_{j't}-c_{j'})\right] f_\beta(\boldsymbol{\beta})d\boldsymbol{\beta}
\end{aligned} \tag{B.28}$$

The above expression can be simplified as

$$\begin{aligned}
\frac{\partial \Pi_k^{\mathrm{M}}}{\partial \mathbf{x}_j} = Q\int_{\boldsymbol{\beta}}\sum_{t\in T}&\left[\left(\frac{\partial v_{jt|\boldsymbol{\beta}}}{\partial \mathbf{z}_j}\frac{\partial \mathbf{z}_j}{\partial \mathbf{x}_j}\right)\left(s_{jt|\boldsymbol{\beta}}(w_{jt}-c_j)-\left(\sum_{\bar{t}\in T} s_{j\bar{t}|\boldsymbol{\beta}}\right)\left(\sum_{j'\in J_k} s_{j't|\boldsymbol{\beta}}(w_{j't}-c_{j'})\right)\right)-s_{jt|\boldsymbol{\beta}}\frac{\partial c_j}{\partial \mathbf{x}_j}\right]\\
& f_\beta(\boldsymbol{\beta})d\boldsymbol{\beta}=0\\
\forall t,k,j\in J_k &
\end{aligned} \tag{B.29}$$

If design constraints present in the model, Lagrange formulation needs to be imposed into the above FOC equation (Appendix A):

$$\begin{aligned}
\frac{\partial L_k}{\partial \mathbf{x}_j} = \int_{\boldsymbol{\beta}}\sum_{t\in T}&\left[\left(\frac{\partial v_{jt|\boldsymbol{\beta}}}{\partial \mathbf{z}_j}\frac{\partial \mathbf{z}_j}{\partial \mathbf{x}_j}\right)\left(s_{jt|\boldsymbol{\beta}}(w_{jt}-c_j)-\left(\sum_{\bar{t}\in T} s_{j\bar{t}|\boldsymbol{\beta}}\right)\left(\sum_{j'\in J_k} s_{j't|\boldsymbol{\beta}}(w_{j't}-c_{j'})\right)\right)\right.\\
&\left.-s_{jt|\boldsymbol{\beta}}\frac{\partial c_j}{\partial \mathbf{x}_j}\right] f_\beta(\boldsymbol{\beta})d\boldsymbol{\beta}-\boldsymbol{\lambda}_j^T\frac{\partial \mathbf{h}_j}{\partial \mathbf{x}_j}-\boldsymbol{\mu}_j^T\frac{\partial \mathbf{g}_j}{\partial \mathbf{x}_j}=\mathbf{0} \qquad \forall k,t,j\in J_k
\end{aligned} \tag{B.30}$$

The additional equations for completing the Karush-Kuhn-Tucker conditions, $\mathbf{h}=\mathbf{0}$, $\mathbf{g}\leq\mathbf{0}$, $\boldsymbol{\mu}^T\mathbf{g}=0$, must be included in the system and solved simultaneously.

Retail Margin FOC Equation: Starting from the retailer profit function, the total profit of common retailer t can be separated into three parts: 1) profit of the specific product j from manufacturer k; 2) the sum of profits from other products of manufacturer k; and 3) the sum of profits from all other manufacturers' products.

$$\Pi_t^{\mathrm{R}} = \sum_{k\in K}\sum_{j\in J_k}\Pi_{jt}^{\mathrm{R}} = \Pi_{jt}^{\mathrm{R}} + \sum_{\substack{j'\in J_k\\ j'\neq j}}\Pi_{j't}^{\mathrm{R}} + \sum_{\substack{k'\in K\\ k'\neq k}}\sum_{j''\in J_{k'}}\Pi_{j''t}^{\mathrm{R}} \qquad \forall t,k, j\in J_{kt} \tag{B.31}$$

In the Nash game, manufacturer's wholesale price decision is made under a fixed retailer's retail margin decision:

$$\begin{aligned}
&\frac{\partial p_{jk}}{\partial m_{jk}} = \frac{\partial\left(w_{jk}+m_{jk}\right)}{\partial m_{jk}} = \frac{\partial w_{jk}}{\partial m_{jk}}+1=1\\
&\frac{\partial s_{ijk}}{\partial m_{jt}} = \frac{\partial s_{ijk}}{\partial p_{jt}}\frac{\partial p_{jt}}{\partial m_{jt}} = \frac{\partial v_{ijt}}{\partial p_{jt}} s_{ijt}\left(1-s_{ijt}\right)\\
&\left.\frac{\partial s_{ij't}}{\partial m_{jt}}\right|_{j'\neq j} = \frac{\partial s_{ij't}}{\partial p_{jt}}\frac{\partial p_{jt}}{\partial m_{jt}} = -\frac{\partial v_{ijt}}{\partial p_{jt}} s_{ijt}s_{ij't}\\
&\left.\frac{\partial s_{ijt'}}{\partial m_{jt}}\right|_{t'\neq t} = \frac{\partial s_{ijt'}}{\partial p_{jt}}\frac{\partial p_{jt}}{\partial m_{jt}} = -\frac{\partial v_{ijt}}{\partial p_{jt}} s_{ijt}s_{ijt'}
\end{aligned} \tag{B.32}$$

Take the derivative of retailer profit with respect to m_{jt}:

$$
\begin{aligned}
\frac{\partial \Pi_t^{\mathrm{R}}}{\partial m_{jt}} &= \frac{\partial \Pi_j^{\mathrm{R}}}{\partial m_{jt}} + \sum_{\substack{j' \in J_k \\ j' \neq j}} \frac{\partial \Pi_{j'}^{\mathrm{R}}}{\partial m_{jt}} + \sum_{\substack{k' \in K \\ k' \neq k}} \sum_{j'' \in J_{k'}} \frac{\partial \Pi_{j''}^{\mathrm{R}}}{\partial m_{jt}} \\
&= \left[\frac{\partial q_{jt}}{\partial m_{jt}} m_{jt} + q_{jt} \right] + \left[\sum_{\substack{j' \in J_k \\ j' \neq j}} \frac{\partial q_{j't}}{\partial m_{jt}} m_{j't} \right] + \left[\sum_{\substack{k' \in K \\ k' \neq k}} \sum_{j'' \in J_{k'}} \frac{\partial q_{j''t}}{\partial m_{jt}} m_{j''t} \right] \\
&= Q \int_{\boldsymbol{\beta}} \left[\frac{\partial s_{jt|\boldsymbol{\beta}}}{\partial m_{jt}} m_{jt} + s_{jt|\boldsymbol{\beta}} \right] + \left[\sum_{\substack{j' \in J_k \\ j' \neq j}} \frac{\partial s_{j't|\boldsymbol{\beta}}}{\partial m_{jt}} m_{j't} \right] + \left[\sum_{\substack{k' \in K \\ k' \neq k}} \sum_{j'' \in J_{k'}} \frac{\partial s_{j''t|\boldsymbol{\beta}}}{\partial m_{jt}} m_{j''t} \right] f_\beta(\boldsymbol{\beta}) d\boldsymbol{\beta} \\
&= Q \int_{\boldsymbol{\beta}} \left[\frac{\partial v_{jt|\boldsymbol{\beta}}}{\partial p_{jt}} s_{jt|\boldsymbol{\beta}} \left(1 - s_{jt|\boldsymbol{\beta}}\right) m_{jt} + s_{jt|\boldsymbol{\beta}} \right] - Q \left[\sum_{\substack{j' \in J_k \\ j' \neq j}} \frac{\partial v_{jt|\boldsymbol{\beta}}}{\partial p_{jt}} s_{jt|\boldsymbol{\beta}} s_{j't|\boldsymbol{\beta}} m_{j't} \right] \\
&\qquad - Q \left[\sum_{\substack{k' \in K \\ k' \neq k}} \sum_{j'' \in J_{k'}} \frac{\partial v_{jt|\boldsymbol{\beta}}}{\partial p_{jt}} s_{jt|\boldsymbol{\beta}} s_{j''t|\boldsymbol{\beta}} m_{j''t} \right] f_\beta(\boldsymbol{\beta}) d\boldsymbol{\beta} \\
&= Q \int_{\boldsymbol{\beta}} \left[\frac{\partial v_{jt|\boldsymbol{\beta}}}{\partial p_{jt}} s_{jt|\boldsymbol{\beta}} m_{jt} + s_{jt|\boldsymbol{\beta}} \right] - \left[\sum_{k' \in K} \sum_{j' \in J_{k'}} \frac{\partial v_{jt|\boldsymbol{\beta}}}{\partial p_{jt}} s_{jt|\boldsymbol{\beta}} s_{j't|\boldsymbol{\beta}} m_{j't} \right] f_\beta(\boldsymbol{\beta}) d\boldsymbol{\beta}
\end{aligned} \tag{B.33}
$$

The above expression can be simplified as

$$
\frac{\partial \Pi_t^{\mathrm{R}}}{\partial m_{jt}} = \int_{\boldsymbol{\beta}} s_{jt|\boldsymbol{\beta}} \left[\frac{\partial v_{jt|\boldsymbol{\beta}}}{\partial p_{jt}} \left(m_{jt} - \sum_{k' \in K} \sum_{j' \in J_{k'}} s_{j't|\boldsymbol{\beta}} m_{j't} \right) + 1 \right] f_\beta(\boldsymbol{\beta}) d\boldsymbol{\beta} = 0 \tag{B.34}
$$

$$\forall k, t, j \in J_k$$

B.4 FOC Equations with Mixed Logit Model and CAFE Regulations

This appendix provides the design and pricing FOC equations for the three discrete cases under the CAFE regulation:

Case 1 (surpassing the CAFE standard):

The price solution with mixed logit demand function is expressed as

$$\int_{\boldsymbol{\beta}} s_{j|\boldsymbol{\beta}} \left(\frac{\partial v_{j|\boldsymbol{\beta}}}{\partial p_j} \left(1 - s_{j|\boldsymbol{\beta}}\right)\left(p_j - c_j\right) + 1 \right) f_\beta\left(\beta\right) d\boldsymbol{\beta} = 0 \tag{B.35}$$

The design FOC equation with mixed logit demand function is

$$\int_{\boldsymbol{\beta}} s_{j|\boldsymbol{\beta}} \left(\left(\frac{\partial v_{j|\boldsymbol{\beta}}}{\partial \mathbf{z}_j} \right)^T \left(\frac{\partial \mathbf{z}_j}{\partial x_{nj}} \right) \left(1 - s_{j|\boldsymbol{\beta}}\right)\left(p_j - c_j\right) - \frac{\partial c_j}{\partial x_{nj}} \right) f_\beta\left(\beta\right) d\boldsymbol{\beta} = 0 \tag{B.36}$$

Case 2 (Equal to CAFE standard):

The price FOC equation is

$$\int_{\boldsymbol{\beta}} s_{j|\boldsymbol{\beta}} \left(\frac{\partial v_{j|\boldsymbol{\beta}}}{\partial p_j} \left(1 - s_{j|\boldsymbol{\beta}}\right)\left(p_j - c_j\right) + 1 \right) f_\beta\left(\beta\right) d\boldsymbol{\beta} = 0 \tag{B.37}$$

The design solution is the inverse function of vehicle fuel economy equal to mpg standard κ:

$$\mathbf{x}_j = f_{\mathrm{F}}^{-1}\left(\kappa\right) \tag{B.38}$$

Case 3 (Violating the standard):

The price solution equation is

$$\int_{\boldsymbol{\beta}} s_{j|\boldsymbol{\beta}} \left(\frac{\partial v_{j|\boldsymbol{\beta}}}{\partial p_j} \left(1 - s_{j|\boldsymbol{\beta}}\right)\left(p_j - c_j - \rho\delta_j\right) + 1 \right) f_\beta\left(\beta\right) d\boldsymbol{\beta} = 0 \tag{B.39}$$

The design FOC equation is

$$\int_{\boldsymbol{\beta}} s_{j|\boldsymbol{\beta}} \left(\left(\frac{\partial v_{j|\boldsymbol{\beta}}}{\partial \mathbf{z}_j} \right)^T \left(\frac{\partial \mathbf{z}_j}{\partial x_{nj}} \right) \left(1 - s_{j|\boldsymbol{\beta}}\right)\left(p_j - c_j - \rho\delta_j\right) + \rho \frac{\partial z_{\mathrm{F}j}}{\partial x_{nj}} - \frac{\partial c_j}{\partial x_{nj}} \right) f_\beta\left(\beta\right) d\boldsymbol{\beta} = \mathbf{0} \tag{B.40}$$